SUSTAINABLE AIRPORTS: GREEN ENERGY SOLUTIONS TO ACHIEVE CARBON NEUTRALITY

THESIS SUBMITTED FOR THE DEGREE OF

DOCTOR OF PHILOSOPHY

MOHAMMED ALRUWAILI

SCHOOL OF ENGINEERING

CARDIFF UNIVERSITY

December, 2022

CONTENTS

LIST OF FIGURES

LIST OF TABLES

LIST OF PUBLICATION

Journal Papers:

1. **M. Alruwaili** and L. Cipcigan, "Airport electrified ground support equipment for providing ancillary services to the grid," Electr. Power Syst. Res., vol. 211, p. 108242, Oct. 2022, doi: 10.1016/j.epsr.2022.108242.

2. **M. Alruwaili** and L. Cipcigan, "Optimal Annual Operational Cost of a Hybrid Renewable-Based Microgrid to Increase the Power Resilience of a Critical Facility," Energies, vol. 15, no. 21, p. 8040, Oct. 2022, doi: 10.3390/en15218040.

Papers Presented in Conferences:

1. **M. Alruwaili** and L. Cipcigan, "Optimal Grid-Connected Hybrid Renewable Energy System for a Civilian Airport," in 2022 IEEE International Conference on Environment and Electrical Engineering and 2022 IEEE Industrial and Commercial Power Systems Europe (EEEIC / I&CPS Europe), Jun. 2022, pp. 1–6. doi: 10.1109/EEEIC/ICPSEurope54979.2022.9854755.

2. **M. Alruwaili** and L. Cipcigan, "Optimal Size of PV Grid Connected to Low-Voltage Network in Saudi Arabia," in 2019 54th International Universities Power Engineering Conference (UPEC), Sep. 2019, pp. 1–5. doi: 10.1109/UPEC.2019.8893552.

Submitted Journal Papers:

1. **M. Alruwaili** and L. Cipcigan, "Reducing The Impact of Electric Ground Support Equipment Charging on Airport Distribution Power Transformer," Springer, Electrical Engineering. (Submitted on 27-12-2021)

DECLARATION

This thesis is the result of my own independent work, except where otherwise stated, and the views expressed are my own. Other sources are acknowledged by explicit references. The thesis has not been edited by a third party beyond what is permitted by Cardiff University's Use of Third Party Editors by Research Degree Students Procedure.

Signed……(candidate) Date ……..……

STATEMENT 1

This thesis is being submitted in partial fulfilment of the requirements for the degree of PhD.

Signed……(candidate) Date ……..……

STATEMENT 2

This work has not been submitted in substance for any other degree or award at this or any other university or place of learning, nor is it being submitted concurrently for any other degree or award (outside of any formal collaboration agreement between the University and a partner organisation).

Signed……(candidate) Date ……..……

STATEMENT 3

I hereby give consent for my thesis, if accepted, to be available in the University's Open Access repository (or, where approved, to be available in the University's library and for inter-library loan), and for the title and summary to be made available to outside organisations, subject to the expiry of a University-approved bar on access if applicable.

Signed……(candidate) Date ……..……

ABSTRACT

The decarbonisation of the aviation sector to cut its contribution to climate change due to various emission sources and the high cost of the proposed green solutions is a challenging goal. As the backbone of the aviation industry, airports have been under pressure to cut their direct and indirect emissions. This thesis investigates the feasibility of innovative solutions to boost the adaptation of green energy technologies for achieving carbon neutrality and sustainable airports.

The reduction of indirect airport emissions related to electricity purchases by deploying renewable energy resources is investigated in this thesis. As a hard-to-abate sector, green hydrogen is expected to play a key role in the aviation industry on the road to carbon neutrality. As such, the economic benefits of a hybrid, renewable-based system are analysed. The novelty of this work is that no existing studies utilise HOMER Pro for the techno-economic evaluation of airport microgrids. The results show that the use of on-site green hydrogen production using solar PV by deploying a small power-to-hydrogen-to-power system provides cost-effective benefits.

Electricity is the primary artery of the airport transition towards carbon neutrality. Hence, the adaptation of microgrids to enhance airport power resilience is modelled considering a civilian airport with an uptake level of electric ground support equipment (EGSE) under different power outage criteria. This research proposes an optimisation model to find the optimal economic dispatch of a resilient microgrid. This novel work evaluates the resiliency of airport microgrids by employing XENDEE, which has not been previously studied. Very few studies in the literature have been conducted on the topic of airport microgrids. The results show that the resilient microgrid can sustain up to 1 day of power outages and offer annual operating cost savings of 20–22%.

As the uptake level of EGSE is expected to increase in the near future, its potential benefits should be explored at different levels of networks, including the national grid, distribution, and customer. An optimisation algorithm is developed to demonstrate EGSE benefits at the end-user level by flattening the airport load profile using airport electricity demand and flight schedule data. This type of work has not been previously presented. The results show that an EGSE fleet with vehicle-to-building (V2B) capability enhances the load factor to 79% and improves the valley-to-peak ratio to 45%.

The grid-level benefits of EGSE with vehicle-to-grid (V2G) capability to participate in the future energy market are also explored. As such, an optimisation model for EGSE frequency response provision through an aggregator is developed using passenger flight schedules and ancillary service market data. This novel method, which has not been previously presented, allows EGSE owners and aggregators to participate in ancillary services markets and make profits. The results show that an EGSE aggregator can make $4,700/day by providing frequency regulation services.

The additional load from EGSE fleet charging in the low-voltage distribution network is accommodated by distribution transformers. The dynamic loading of the distribution transformers that power an airport is introduced to mitigate the impact of the EGSE charging requirements on the transformer's lifetime. The dynamic model is formulated to optimise the EGSE fleet charging using the IEC 60076-7 thermal loading guide and flight schedule data. The key benefits of transformer dynamic loading to distribution networks and airport operators are the enhancement of transformer loading to minimise EGSE impact, allowing for higher levels of EGSE uptake. This novel approach has not previously been presented in the existing literature. The results show that the transformer dynamic loading approach reduces the EGSE charging impact by 50% for the simulated cases.

To my parents, my wonderful wife, and my lovely son.

ACKNOWLEDGEMENTS

First and foremost, I would like to praise Allah the Almighty for His blessing given to me during my study and in completing this thesis.

Furthermore, I would like to express my deepest gratitude to my PhD supervisor, Prof. Liana Cipcigan, for her continuous trust and support during my PhD endeavour, which would not have been possible without her countless hours of support. It is a privilege and an unforgettable experience to work with her. Her vast knowledge, expertise, and valuable advice helped me overcome countless barriers and challenges, which refined my knowledge and my scientific research skills. I also extend my thanks to my second supervisor, Prof. Jun Liang, for his help and advice.

I am thankful to all my colleagues and friends in the Smart Grids and EV group for their support and advice. I am also grateful to the Northern Border University, which has funded my PhD study. I would not have been able to pursue postgraduate studies at Cardiff University without this financial support.

Most importantly, I am extremely grateful to my beloved parents (Turki and Zalah), my lovely wife (Eman), and my son (Abdulrahman), who have consistently supported and stood with me through this journey to overcome all challenges and finish my degree. I am grateful for the many sacrifices they have made daily to see that I complete my PhD. To my treasured wife: without your love, understanding, and support, this thesis could not be possible.

NOMENCLATURE

Abbreviations

AC	Alternating Current
ACE	Aviation Carbon Exchange
ACI	Airports Council International
ACR	Area Control Error
ACRP	Airport Cooperative Research Program
AGC	Automatic Generator Control
AOC	Annual Operational Cost
APS	Announced Pledges Scenario
BAU	Business as Usual
CNG	Compressed Natural Gas
CO_2	Carbon Dioxide
CORSA	Carbon Offsetting and Reduction Scheme for International Aviation
DC	Direct Current
DER	Distributed Energy Resources
DL	Dynamic Loading
DR	Demand Response
DSM	Demand Side Management
DSO	Distribution System Operators
EC	European Commission
EENS	Expected Energy Not Served
EGSE	Electric Ground Support Equipment
EPA	Environmental Protection Agency
EPR	Energy Research Partnership
ESS	Energy Storages Systems
ETS	Emissions Trading System
EU	European Union
EV	Electric Vehicle
FC	Fuel Cell
FCEGSE	Fuel Cell Electric Ground Support Equipment
FCR	Frequency Containment Reserves
FRR	Frequency Restoration Reserves

G2V	Grid-to-Vehicle
GHG	Greenhouse Gases
GHI	Global Solar Irradiance
GPU	Ground Power Unit
GSE	Ground Support Equipment
HEGSE	Hybrid Electric Ground Support Equipment
HLLI	High Load Plus Low Solar Irradiance
HOMER	Hybrid Optimisation Model for Multiple Energy Resources
HRES	Hybrid Renewable Energy System
HST	Hot-Spot Temperature
IATA	International Air Transport Association
IC	Internal Combustion
ICAO	International Civil Aviation Organisation
IEA	International Energy Agency
IEC	International Electrotechnical Commission
IEEE	Institute of Electrical and Electronic Engineers
LCC	Life Cycle Cost
LCOE	Levelised Cost of Energy
LF	Load Factor
LFP	Lithium Ferro Phosphate
LLHI	Low Load Plus High Irradiance
LOL	Loss of Life
LOLP	Loss of Load Probability
LPG	Liquefied Petroleum Gas
LPHI	Low Probability High Impact
LV	Low Voltage
MG	Microgrid
MILP	Mixed-Integer Linear Programming
MINLP	Mixed-Integer Non-linear Programming
MPC	Model Predictive Control
NOx	Nitrogen Oxides
NPC	Net Present Cost
NPV	Net Present Value
NZE	Net Zero Emissions

O&M	Operation and Maintenance
P2H2P	Power-to-Hydrogen-to-Power
PCA	Preconditioned Air Unit
PCC	Point of Common Coupling
PEM	Polymer Electrolyte Membrane
PHEGSE	Plug-In Hybrid Electric Ground Support Equipment
PJM	Pennsylvania, New Jersey, and Maryland Interconnection Area
PLR	Peak Load Reduction
PV	Photovoltaic
RES	Renewable Energy Sources
RoC	Rate of Change
RR	Replacement Reserves
SAIDI	System Average Interruption Duration Index
SDR	Seve Ballesteros-Santander
SOC	State of Charge
SP	Scottish Power
TSO	Transmission System Operator
U.S.	United States
UK	United Kingdom
V/P	Valley-Peak Ratio
V2B	Vehicle-to-Building
V2G	Vehicle-to-Grid
VALE	Voluntary Airport Low Emissions Grants Program
VFP	Valley Filling Promotion
$	United States Dollar

Symbols

A_{EGSE}	Number of available EGSE
ANN	Annualised investment rate
ava	EGSE availability binary variable
C_{DER}	Purchasing and operating cost of DERs ($)
C_{NPC}	Net present cost ($)
C_{ch}	Aggregator charging cost ($)
C_{deg}	Aggregator degradation cost ($)

C_{fuel}	Fuel cost ($)
C_{grid}	Energy cost ($)
C_{PV}	Capacity rating of solar PV array (kW)
C_{resi}	Lost load cost ($)
CA_{inv}	Annualised capital cost ($)
CA_{rep}	Replacement cost ($)
Cd	Demand price ($/kW)
CRF	Capital return factor
D_{PV}	Solar PV derating factor (%)
DC	Lost demand (kWh)
E^{ch}	Regulation down dispatched energy (kWh)
E^{dis}	Regulation up dispatched energy (kWh)
E_A	EGSE consumption per turnaround event (kWh)
E_{def}	Annual served deferrable load (kWh/yr)
E_{pr}	Annual served electric load (kWh/yr)
E_r	EGSE required energy (kWh)
E_{sell}	Annual energy sales (kWh/yr)
EM	Charging or discharging binary variable
ESS^i	Energy storage input (kWh)
ESS^l	Energy storage losses (kWh)
ESS^o	Energy storage output (kWh)
ESS_c	Energy storage capacity (kWh)
FP	Purchased fuel (litre)
$G_{T,STC}$	Incident solar radiation under standard test conditions (kW/m^2)
G_T	Incident solar radiation (kW/m^2)
$H_{2\,con}$	FC hydrogen consumption (kg)
H_{out}	Produced hydrogen (kg)
Hr	Hot-spot to top-oil at rated current (K)
If	Fixed cost ($)
IR	Interest rate (%)
Iv	Variable cost ($)
K	Transformer load factor
k_{11}	Thermal model constant

k_{21}	Thermal model constant
k_{22}	Thermal model constant
L	Total loss of life
LD	Departing and landing flights
N_{life}	Project lifetime (yrs)
NO_t	Number of required EGSE
n_A	Number of turnaround events
OM	Operating and maintenance cost ($)
OT	Top-oil temperature (°C)
P	Available regulation down capacity (kW)
P^-	Available regulation up capacity (kW)
P^{ch}	EGSE charging power (kW)
P^{dis}	EGSE discharging power (kW)
P_{in}	Input power (kW)
P^{tch}	EGSE fleet total charging power (kW)
P^{tdis}	EGSE fleet total discharging power (kW)
P_{PV}	Solar PV array power output (kW)
P_n	FC nominal power (kWh)
P_{out}	Output power (kW)
P_{rate}^{max}	Charger maximum rate (kW)
P_{rate}^{min}	Charger minimum rate (kW)
Pch_l	Minimum charging power rate (kW)
Pch_m	Maximum charging power rate (kW)
$Pdis_l$	Minimum discharging power rate (kW)
$Pdis_m$	Maximum discharging power rate (kW)
PN	Purchased diesel generators
PR	Regulation up capacity prediction (kW)
PR^-	Regulation down capacity prediction (kW)
PT	Capacity of purchased technologies (kW)
PVn	Solar PV normalised performance
Px	Sellback price ($/kWh)
pd	Capacity price of regulation down ($/kW-h)
pu	Capacity price of regulation up ($/kW-h)

Q_h	Hydrogen higher heating value
R	Ratio of load losses to no-load losses at rated current
R_{com}	Component lifetime (yr)
R_{rem}	Component remaining life (yr)
Rd	Available capacity of the regulation down (kW)
Rd_{od}	Offered regulation down capacity (kW)
Res	Reserved time factor
Ru	Available capacity of the regulation up (kW)
Ru_{od}	Offered regulation up capacity (kW)
Rx	Top-oil temperature rise at rated losses (K)
r_{sales}	Exported energy income ($)
S	Exported energy (kWh)
SOC	State of charge (%)
SOC_{max}	Maximum state of charge (%)
SOC_{min}	Minimum state of charge (%)
SG	Capacity of diesel generator (kW)
T_{AC}	Annualised cost ($/year)
$T_{c,STC}$	Temperature of PV cell at standard test conditions (25℃)
T_c	Temperature of PV cell (℃)
TH	Hot-spot to top-oil rise (K)
t_{du}	Required time to dispatch energy for regulation up (h)
t_{dw}	Required time to dispatch energy for regulation down (h)
tF	Required time to return from aeroplane (min)
tS	Required time to serve aeroplane (min)
tR	Required time to arrive to aeroplane (min)
U	EGSE unavailability binary variable
Uf	Utility fixed monthly cost ($)
V	Transformer aging rate
Vf	Fuel price ($/litre)
Vl	Price of lost energy ($/kWh)
Vu	Energy tariff ($/kWh)
x	Oil exponent
y	Winding exponent
Z	Airport demand (kW)

α	Temperature coefficient (%/℃)
α_u	Regulation up average dispatched to contract ratio
α_w	Regulation down average dispatched to contract ratio
α_{FC}	Hydrogen consumption curve coefficient (kg/kWh)
β_{FC}	Hydrogen consumption curve coefficient (kg/kWh)
β_t	Energy price ($/kWh)
η_{PEM}	Efficiency of hydrogen conversion
η_{ch}	Storage charging efficiency (%)
η_{dis}	Storage discharging efficiency (%)
θ_h	Hot-spot temperature (°C)
θ_a	Ambient temperature (°C)
τ_o	Average oil time constant (min)
τ_w	Winding time constant (min)
φ	Battery degradation cost ($/kWh)
$\emptyset_{ch}$	Charging rate (kW)
$\emptyset_{dis}$	Discharging rate (kW)

Units

h	Hours
K	Kelvin
kg	Kilogram
kW	Kilowatt
kWh	Kilowatt hour
min	Minutes
MW	Megawatt
MWh	Megawatt hour
yr	Years
°C	Degree celsius

Chapter 1
Introduction

Today, airports have a significant role in connecting the world. Thousands of commercial airports operate globally, enabling the swift, safe, and convenient transportation of passengers and goods [1]. In 2019, more than 4.5 billion passengers and more than 61 million tonnes of air freight were transferred via around 3,760 commercial airports worldwide [2]–[4]. In just over two decades, the number of people flying around the world has tripled [5]. The effects of the COVID-19 pandemic became apparent between April and May 2020, when air traffic fell by more than 75% and global passenger volumes were approximately two-thirds lower than in 2019 [5]. However, the annual number of air passengers is projected to almost double by 2037, reaching about 8.2 billion [6].

1.1 Emissions

Aviation is considered a convenient and fast travel option. However, it is also recognised as one of the most carbon-intensive sectors and, at the same time, one of the most difficult to decarbonise, accounting for 12% of all transport CO_2 emissions and 2% of global carbon emissions [7]. In 2018, aviation generated around 3% of the total U.S. CO_2 emissions and around 9% of GHG emissions from the U.S. transportation sector [8]. In the same year, aviation emissions accounted for 7% of UK GHG emissions, which were 88% higher than 1990 levels [9]. The share of domestic and international aviation emissions in the UK increased to roughly 8% in 2019 [10]. Globally, passenger flights accounted for almost 85% of commercial aviation CO_2 emissions in 2018 and 2019, as shown in Figure 1-1 [11].

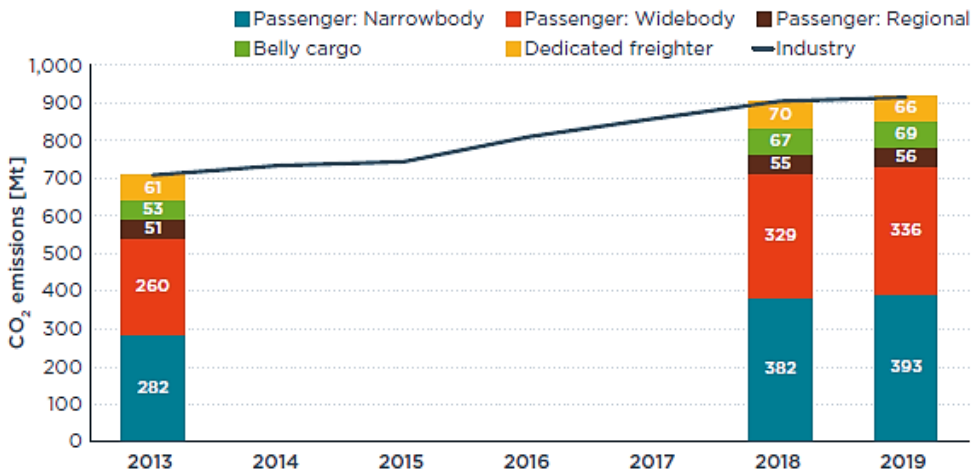

Figure 1-1 CO_2 emissions breakdown per operations and aircraft type worldwide [11].

Furthermore, commercial international aviation CO_2 emissions are expected to triple by 2050 if current demand remains unchanged [7], [12]. According to the International Energy Agency (IEA), CO_2 emissions increased steadily from 2009 to 2019 [5]; 2020 is excluded from recent statistics due to COVID-19. In the Announced Pledges Scenario (APS), which considers the most recent announced targets to achieve zero emissions by 2050, efforts still lag behind stated goals, and CO_2 emissions are expected to increase to about 1,150 $MtCO_2$ by 2030 globally. In contrast, in the Net Zero Emissions by 2050 Scenario (NZE), global CO_2 emissions are projected to decrease to about 780 $MtCO_2$ by 2030, which is near the 2012 emissions level.

Global efforts to reduce aviation sector emissions to achieve carbon neutrality have various ambitious plans, which can be categorised into two primary categories: short- and long-term plans. In terms of the former, the International Air Transport Association (IATA) has adopted a voluntary and immediate carbon offsetting programme to reduce CO_2 emissions and achieve the ambitious target by 2050 [13]. Airlines and passengers can contribute to the offsetting programme by neutralising their proportion of CO_2 emissions by investing in other emissions reduction projects. The offsetting programme is integrated via over 30 web-sales engines or through a third-party offset provider. Moreover, emissions unit trading is implemented on a global and regional basis. Globally, in 2020, the Carbon Offsetting and Reduction Scheme for International Aviation (CORSA) approved the first emission unit [14] which can be exchanged via a centralised market such as the IATA Aviation Carbon Exchange (ACE) [15]. Regionally, the European Union (EU) Emissions Trading System (EU ETS) is seen as a key tool to limit GHG [16]. The EU ETS is the first international emission trading system covering commercial aviation within the European Economic Area. Similarly, the China ETS, Korea ETS (K-ETS), and New Zealand ETS include domestic flights [17], [18].

Long-term zero-emission aviation plans are set to achieve a carbon-free sector in most cases by 2050. Recent plan to decarbonise UK aviation [19] set a commitment to net-zero emissions by 2050 through some interim decarbonisation targets, such as a 15% reduction in net emissions relative to 2019 by 2030 and a 40% reduction by 2040. Moreover, the European Commission (EC) announced Flight Path 2050, which aims to reduce aviation CO_2 emissions by 75% and NOx emissions by 90% by 2050 [20]. Furthermore, all ground support equipment (GSE) must comprise emission-free

vehicles. Although zero-emission aeroplanes are essential to achieving clean aviation, the use of electricity or hydrogen to power commercial aeroplanes faces many barriers. However, small pure electric aircraft, such as those with two to nine seats, have successfully made short journeys [21]–[23].

In an airport ecosystem, pollution springs from various sources, classified as one of three scopes according to the Airports Council International Europe (ACI EUROPE), which is responsible for the well-known certification programme Airport Carbon Accreditation. This institution-endorsed programme independently assesses and recognises airports efforts to reduce carbon emissions. The three scopes of airport emissions sources are as follows [24]:

Scope 1: The airport's **direct GHG emissions**, which come from sources it owns or controls. Examples include GSE, airport-owned power plants that burn fossil fuels, and de-icing substances.

Scope 2: The airport's **indirect GHG emissions** relate to the purchase of electricity to supply, such as airport air conditioning and lighting.

Scope 3: The airport's **indirect GHG emissions** relate to other sources, such as shuttle buses, passenger vehicles arriving or departing the airport, aircraft-released gases, and GSE not owned by the airport.

This thesis focuses on enabling technologies to reduce GHG emissions within scopes 1 and 2 by utilising airport microgrids, an aspect that few existing studies have discussed. Additionally, it identifies the potential benefits of electrifying GSE to decrease GSE-related emissions, as identified within scopes 1 or 3, an aspect not previously explored.

1.2 Thesis Objectives

The thesis aims to answer the following research question: how can green energy technologies be promoted to reduce direct and indirect airport emissions to achieve carbon neutrality consistent with airport sustainability initiatives? As such, the key objective of this thesis is to investigate the feasibility of green energy solutions to achieve carbon neutrality within airports in the most economic manner. Two primary sub-goals are addressed: the reinforcement of renewable DER penetration and the smart charging management of the EGSE fleet to help achieve sustainable airports. To this end, the following objectives are established:

i. The techno-economic evaluation of renewable distributed energy resources (DERs) that can be installed within the airport's geographical area. The proposed renewable energy-based hybrid systems include an evaluation of on-site green hydrogen production.
ii. The assessment of an airport microgrid's optimal and economic dispatch to leverage resilience benefits. The resilience benefits are evaluated under various outage scenarios, considering the value of lost load and including the EGSE fleet in the developed resilient microgrid.
iii. The development of an algorithm to schedule the EGSE charging and discharging to flatten the airport load curve. The developed algorithm aims to provide a methodology to shave peak and fill valleys of an airport load demand with the help of EGSE.
iv. The development of an algorithm for EGSE to provide ancillary services to the grid through an aggregator. The model is formulated to maximise the aggregator's profits.
v. The design of a detailed thermal model of the distribution transformer and develop a dynamic charging model for EGSE. The developed algorithm seeks to mitigate the impact of EGSE's daily charging requirements without affecting the transformer's expected normal lifetime.

1.3 Thesis Structure

This thesis contains nine chapters. Chapter 1 introduces the research problem and states the research aim and objectives. Chapter 2 presents a summary of the literature used to inform and direct the modelling work. Chapter 3 reviews the modelling methods and tools available to promote the integration of distributed energy resources and microgrids. Chapter 4 discusses the economic benefits of integrating renewable distributed energy resources within airports. Chapter 5 evaluates airport microgrids to enhance an airport's electrical power resiliency and reduce electricity operational costs. Chapter 6 presents an optimisation model to utilise the EGSE fleet to flatten the airport load curve by providing peak shaving and valley filling. Chapter 7 introduces a methodology for EGSE to provide ancillary services to the grid through an aggregator. Chapter 8 presents a dynamic loading model of distribution transformers, considering the transformer's thermal characteristics and the charging EGSE fleet's daily needs to maintain the transformer's lifetime. Finally, chapter 9 provides a summary discussion

of the key findings, identifies the limitations of the work, and makes recommendations for stakeholders in the aviation sector, policymakers, and others who provide engineering services to the sector. Appendix A contains the developed scripts for chapters 6, 7, and 8.

Chapter 2
Literature Review

2.1 Brief Background of Airport Engineering

In the present era, various transport types, including land, water, and air, have distinct, specific infrastructures. Airports serve as the primary infrastructure for air transport, facilitating the take-off and landing of aircraft. They enable the boarding of passengers and the loading and unloading of cargo. Airports hold a critical position in the world economy, providing essential connectivity for regions and citizens. They significantly contribute to economic expansion and generate thousands of jobs at local, regional, and national scales. "Airport" is defined according to the International Civil Aviation Organisation (ICAO) as "*a defined area on land or water including any buildings, installations and equipment intended to be used either wholly or in part for the arrival, departure and surface movement of aircraft*" [25].

Several aviation organisations have standardised airports design, such as ICAO Annex 14 [25]; air traffic management, such as (EU) 2017/373 [26]; and environmental management, such as ISO 14001 [27]. These documents cover wide-ranging topics, including obstruction limitations at airports, specific details on facilities, and electrical and energy facilities. Airports are typically classified based on the volume of passenger traffic they handle annually. The exact categories can vary by country or organisation. The European Airports Council International (ACI EUROPE) classifies commercial airports using the airport connectivity index, as shown in Table 2-1 [28]. The classification of commercial airports by type of activity used by the Federal Aviation Administration (FAA) in the United States is shown in Table 2-2 [29].

Table 2-1 Airport connectivity index.

Type	Characteristics
MAJORS	Top 5 busiest airports in Europe
GROUP 1	Airports welcoming over 25 million passengers per year
GROUP 2	Airports welcoming between 10 and 25 million passengers per year
GROUP 3	Airports welcoming between 5 and 10 million passengers per year
GROUP 4	Airports welcoming below 5 million passengers per year

Table 2-2 Airport Classification Criteria by the Federal Aviation Administration.

Type	Characteristics
Large Hub	Handle 1% or more of the country's annual passenger enplanements, typically as the largest and busiest airports in major cities
Medium Hub	Handle between 0.25% and 1% of the nation's passenger enplanements each year, usually located in small cities or serving as secondary airports in large metropolitan areas
Small Hub	Account for between 0.05% and 0.25% of the nation's annual passenger enplanements
Non-hub	Have more than 10,000 passengers annually, but account for less than 0.05% of the nation's total passenger enplanements

Conventionally, airports are divided into two primary areas of activity from an operational perspective: landside and airside [30]. All processes related to passengers are done on landside, such as passenger movements, car parking, and baggage facilities. Common structures and areas such as terminal buildings and vehicle parking are present on the landside of airports. Conversely, all operations related to aircraft are performed on airside, such as aircraft apron, aircraft fuelling, air navigation, and cargo loading and unloading. These operations are done with the help of specially designed vehicles known as ground support equipment. Common buildings and areas such as control towers, firefighting buildings, hangars, power station buildings, cargo terminals, meteorological areas, aircraft movement areas, and radio navigation systems are present on the airside of airports.

The key building on the landside of an airport is the terminal building, which acts as the connection point between airside and landside transportation. Airport terminal buildings typically use more energy than other airport structures due to their specific functions and operations. In particular, the heating, ventilation, and air conditioning systems consume substantial energy, contributing significantly to the yearly total energy usage in terminal buildings, especially in extreme weather conditions [31]. Additionally, terminal buildings contain several critical loads, such as data centres, security monitoring systems including cameras, sensors, computers, information and communication systems, and airline systems. On the airside, several critical loads and buildings are located, such as runway lights, meteorological equipment, and the control tower, which consists of air and radio navigation systems, computers, and information and communication systems.

2.2 Ground Support Equipment

The ground handling process comprises a number of highly specialised tasks that require highly trained personnel and complex technological equipment known as ground support equipment (GSE) [32]. Ground handling is the term used to describe the various services provided to aeroplanes on the ground while they are parked in an airport apron [32]. Ground support equipment is designed to support aircraft operations on the ground between flights or maintenance operations [33]. Different providers are in charge of airport ground handling operations, including airport operators, airlines, and third-party agents.

Unlike road cars, fewer public statistics are available for GSE. The GSE global market was estimated at $13 billion in 2019 and is expected to increase to around $22 billion by 2027 [34]. In the U.S., the total number of GSE vehicles was estimated in 2012 at around 108,000 [35]. The electric based GSE (EGSE) share was estimated globally at around 10% in 2013, while the majority are fossil fuel based [36]. In 2016, Delta Airlines successfully converted around 15,000 units of GSE, or 15% of their fleet, to electric based GSE [37].

According to the U.S. Environmental Protection Agency (EPA), GSE are typically categorised into two types of mobile sources:

- **On-road GSE,** which can travel on public roads, such as crew vans, and cabin service trucks.
- **Non-road GSE,** which are not able to be on public roads, only within the airport apron, such as baggage tractors, belt loaders, and push-back tractors [38].

Moreover, non-road GSE are further classified into the following:

- Compression-ignition engines, which are traditionally powered by diesel.
- Park-ignition engines that are typically powered by gasoline.

In the U.S., about 35% of GSE fleets are powered by diesel, 40% have gasoline engines, and the rest have alternative types of fuel [35]. Some examples of the alternative fuels, other than diesel and gasoline, used to power low- or zero-emission GSE are compressed natural gas (CNG), methanol, liquefied petroleum gas (LPG), biodiesel, hydrogen, and electricity.

2.2.1 Electric GSE

Electric GSE (EGSE) refers to the broad category of vehicles and equipment that service aircraft and use electric motors for their motion. They use rechargeable batteries (i.e., lead-acid and lithium-ion), or stored chemicals such as hydrogen to derive the required power and can be classified into sub-types based on technology similar to road EVs, including battery EGSE, plug-in hybrid EGSE, hybrid EGSE, and fuel cell EGSE.

Battery EGSE, also known as fully electric, all-electric, or pure electric, refers to vehicles that are solely powered by electric motors and do not have a secondary source such as internal combustion (IC) engines. These vehicles exclusively use energy stored in their rechargeable battery packs. Their battery-electric charging needs are only supplied by the grid. Battery EGSE (BEGSE) is considered zero-emission vehicles. Some types of EGSE are fully electric and commercially mature, such as the Ranger 15E loader [39], Commander 15i E loader [40], and TLD JET-16 baggage tractor [41]. Plug-in hybrid EGSE (PHEGSE) is powered by a combination of an electric motor and an IC engine, which work together to provide power to the vehicle. The EGSE is equipped with a small rechargeable battery to power the electric motor, which is usually used for movements and partial EGSE duties. The batteries of PHEGSE have the capability to charge either via the IC engine or from the electric network. An example of PHEGSE is Vestergaard Elephant® BETA de-icer [42].

Hybrid EGSE (HEGSE) is equipped with a battery to power an electric motor charged only by the IC engine. They use the electric battery for limited range at low speeds and then switch to an IC engine (diesel or gasoline). Furthermore, hybrid vehicles are divided into four technology sub-classes: full HEV, parallel full HEV, series-parallel full HEV, and complex full HEV [43]. Some commercial examples of HEGSE aircraft tow tractors are JBT LEKTRO [44] and Volk HFZ 40 N [45], and the HEGSE ground power unit is AERO JetGo 800AL-RJ [46]. Similar to BEGSE, the fuel cell EGSE (FCEGSE) is exclusively powered by an electric motor. However, FCEGSE is powered by hydrogen, which can be either stored on board or produced via the electrolysis process [47]. Compared to the battery based EGSE, the FCEGSE has longer ranges and faster refuelling. Fuel cell EGSE is still an immature technology since storing hydrogen on board remains a challenge in terms of weight, volume, kinetics, safety, and cost [47]. One example of FCEGSE prototypes is the Mulag

Comet 4FC baggage tractor [48]. Only BEGSE and PHEGSE, which use electricity from the electric power grid to charge their batteries, are included in this thesis. The term EGSE refers to BEGSE and PHEGSE unless otherwise stated.

2.2.2 Non-road GSE

Non-road GSE is mainly operated on the airside to provide services to aircraft with a generic sequence optimised by the ground service provider based on aircraft type [49]. Ground support equipment vehicles are being used in large numbers at airports because they play such a key role in increasing operational speed. Common GSE types include aircraft push-back units, baggage tractors, belt loaders, container loaders, pre-conditioned air units, ground power units, and boarding stairs [38].

Aircraft push-back units, also known as aircraft tractors, are used to push back the aeroplane from the gate to the aircraft movement area, such as a taxiway, or to tow the aircraft to another location, such as a maintenance hangar. They are used when the aeroplane is not operating under its own engine power. Push-back tractors are divided into two categories: towbars, which are linked to an aircraft nose wheel in traditional tugs, and towbar-less tractors, which lift up the nose wheel and elevate it off the ground before moving.

A baggage tractor is used to tow a train of baggage carts or cargo between the aircraft and the airport facilities. They are one of the most common GSE vehicles used in airports. A belt loader is used to load and unload baggage and cargo between the aeroplane baggage and cargo compartments and the baggage and cargo carts. A container loader, used to load and unload cargo containers, pallets, and other payloads into and off the aeroplane, is a highly specialised unit equipped with pneumatics and rollers to assist in the horizontal and vertical movement of payloads capable of lifting tens of tonnes.

A pre-conditioned air unit (PCA) provides cooled or heated air to parked aircraft when their primary engines and auxiliary power units are off. It can be portable, providing service for remote parked aircraft, or installed with a fixed gate bridge. The ground power unit (GPU) is used to supply electricity to the aircraft electrical system when the aircraft is on the ground. It functions to supply the 400 Hz aircraft electrical system and can be either a fixed unit that draws power from the electricity grid or a mobile unit that generates on-site electrical power. Boarding stairs are used for boarding and

deplaning at remote aircraft parking stands or during the unavailability of the jet bridge. In this thesis, four types of non-road EGSE are considered in the following analysis chapters, due to the availability of mature commercial models, as detailed in Table 2-3 [41], [50], [51].

Table 2-3 EGSE models.

Type	Model	Battery
Aircraft push-back	Challenger 280e	96V-875Ah
Container loader	CHAMP70We	80V-810Ah
Baggage tractor	TLD Jet-16	80V-620Ah
Belt loader	CBL-150E	48V-500Ah

2.2.3 Turnaround Event

Once the aircraft is landed, various operations occur to prepare it before taking off again. The turnaround event includes all actions completed by GSE while servicing the plane between landing and departure. As such, from the EGSE perspective, the turnaround event is defined as the EGSE leaving its parking slot to serve an aircraft and returning to the same spot after finishing the required work [32]. Given the unavailability of real data, it is assumed in this thesis that EGSE of the same type has an equal energy requirement to perform a turnaround event. However, in reality, the energy consumption may vary. Additionally, the charging process is assumed to be linear to express battery SOC in terms of energy. Handling time is strictly standardised in the aviation industry [32] and varies based on the aeroplane model ranging from about 20 min to several hours. However, flights delay or cancellations can impact the handling time planning. In this thesis, such an impact is not considered since it is another field of research related to flight scheduling and prediction. Figure 2-1 presents the individual activities of a turnaround event for a Boeing 747.

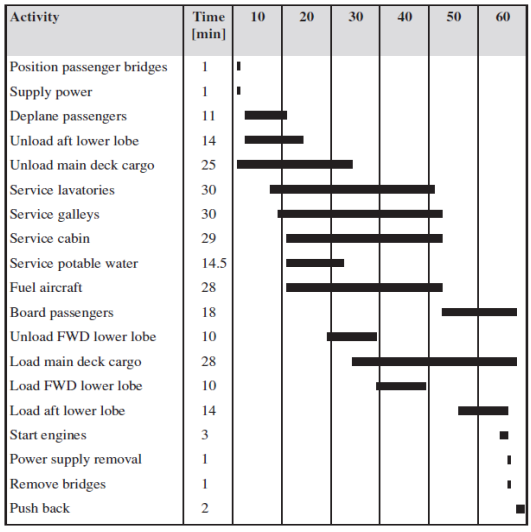

Figure 2-1 Boeing 747 turnaround [32]**.**

2.3 Airports Sustainability

In a more general scientific context, "Sustainability is equivalent to continuum, or the ability to continue a course without termination" [52]. In the same context and from an aviation perspective, sustainability is a long-term strategy to tackle the challenges and ensure a cleaner, quieter, and smarter future for the aviation industry [53]. Two primary priorities generally exist for achieving sustainable aviation: the use of sustainable aviation fuels and the development of sustainable airports. Sustainable aviation fuel is focused on producing fuel from sustainable feedstocks that is very similar in chemistry to traditional fossil jet fuel and has fewer emissions [54]. Airport sustainability development includes, in most cases, four pillars, as shown in Figure 2-2.

Figure 2-2 Airport sustainability pillars [55]**.**

These pillars, which align with the United Nations Sustainable Development Goals (UN SDG) and are widely implemented by airport operators, include various categories to be adopted for a typical sustainability plan, such as energy, climate, air quality, noise, water, waste, human supporting, employability, and engagement. A sustainability plan for an airport can be found as a stand-alone plan or as part of a standard airport master plan. Today, almost all leading airports worldwide have sustainable plans.

Airport efforts to tackle emissions in scopes 1 and 2 are addressed in their sustainability strategies, while strategies to reduce emissions in scope 3 associated with third-party operations are published separately. Table 2-4 shows strategies to achieve carbon neutrality resulting from GSE and energy consumption at some global airports and third-party ground handling agents.

Table 2-4 Airports sustainability objectives.

Airport	GSE	Electricity-Buildings
Heathrow (LHR) [56]	***Current*** *on-road* 27% EGSE, 20% hybrid EGSE *non-road (Third-party)* 15% EGSE ***Future*** 100% electric by 2030	71kWp installed rooftop PV 100% renewable purchased Improve energy efficiency (e.g., LED lightbulbs) 0% emission by mid of 2030s
Denver (DEN) [57]	***Current*** *on-road (out of 1,681 total fleet*) 2 electric (buses), 19 hybrid vehicles, 4 CNG buses, 97 CNG light duty vehicles ***Future*** Adding electric PCA and GPU	About 10 MW aggregated PV installed on-site Additional 18.6 MW on-site PV Improve energy efficiency to reduce energy usage by 20% Install ESS to provide 1 hr back-up power for train system
San Francisco (SFO) [58], [59]	***Current*** *on-road & non-road* 34% electric ***Future*** 100% by 2040	About 4 MW aggregated PV installed on-site 100% renewable purchased Additional PV and ESS
Agent	**GSE**	
Swissport [60]	***Current*** *non-road* 15.3% EGSE & hybrid EGSE ***Future*** 50% by 2025	
Dnata [61]	***Current*** *on-road & non-road* 15% electric ***Future*** Unavailable	
Menzies aviation [62], [63].	***Current*** Fully electrified at Amsterdam Schiphol Airport, Gothenburg-Landvetter Airport and Oslo Airport ***Future*** Carbon neutral by 2033	

Due to their complex operations, which comprise numerous energy-intensive facilities, airports exert a substantial impact on energy consumption and, consequently, the environment. As such, it is critical to implement energy conservation and efficiency policies at airports. The primary objectives of these policies for airports are enhancing competitiveness, ensuring a stable energy supply, and promoting sustainability.

Recently, energy conservation and efficiency policies have been implemented by airport owners and operators as one of their pillars to align airport operations with sustainability. A key step towards energy conservation at airports is the introduction of energy management systems capable of monitoring and regulating energy use across a wide range of facilities, extending from terminal buildings to runway lights. Advanced technologies can provide real-time information on energy consumption, thereby enabling airport management to make informed decisions about where and how to reduce energy use. Energy conservation involves reducing energy usage, potentially by downgrading the quality of services provided, such as by lowering the heating thermostat setting [31], while, energy efficiency involves using less energy to perform the same task or produce the same result without compromising comfort or safety [64].

A vital focus is the heating, ventilation, and air conditioning systems within terminal buildings, which are amongst the most significant contributors to energy consumption. The incorporation of efficient heating, ventilation, and air conditioning systems, the use of natural ventilation, and the optimisation of the operations of these systems can result in substantial energy savings. The implementation of automated systems to control temperature and lighting based on occupancy can also help minimise energy waste. A further area is the investment in energy-efficient lighting for both terminal buildings and airfields, such as LED technology, which is more efficient and has a longer lifespan than traditional lighting solutions [65].

The European research project CASCADE evaluated the most important measures for reducing energy consumption at European airports [66], including enhancements in management systems and energy facilities, the adoption of renewable energy technologies or combined heat and power plants, the introduction of new operational and maintenance procedures to improve and optimise equipment energy efficiency, and upgrades in heating, ventilation, and air conditioning and lighting systems.

2.4 Distributed Energy Resources

Traditionally, end-use electricity is generated by large power plants fuelled by fossil fuels such as coal or gas and delivered through a centralised grid. However, modern networks have changed to more decentralised grids with the help of advanced technology such as distributed energy resources (DERs), adding new energy generation technologies and bi-directional power flow. Distributed energy resources

are small-scale energy-generating units, controllable loads, and energy storage technologies that produce and supply energy on customer sites [67], whose generating capacity can be sized based on particular needs, typically with less than 10 MW [67] comprising small distributed generation (DGs) units, each usually less than 5 MW [68]. There are different technologies of DERs, including renewable and non-renewable generation, such as solar PV, wind turbines, microturbines, natural gas turbines, fuel cells, diesel generators, and energy storage systems (ESS). In this thesis, the following DER technologies are included: solar PV, fuel cell (FC), energy storage system (ESS), electric vehicle (EGSE) and back-up diesel generator.

Over the last few decades, renewable energy resources such as solar PV, wind turbines, and green hydrogen fuel cells have been widely implemented. The share of renewable energy generation capacity is rapidly increasing to accomplish the net-zero emission objective by 2050. Figure 2-3 shows the newly installed capacity added to the grid between 2001 and 2020 globally. The additional renewable capacity in the last 5 yrs was higher than fossil fuel and nuclear combined. The increment in renewable share was driven by solar PV, where 127 GW added in 2020 accounted for 50% of the added renewable capacity [69].

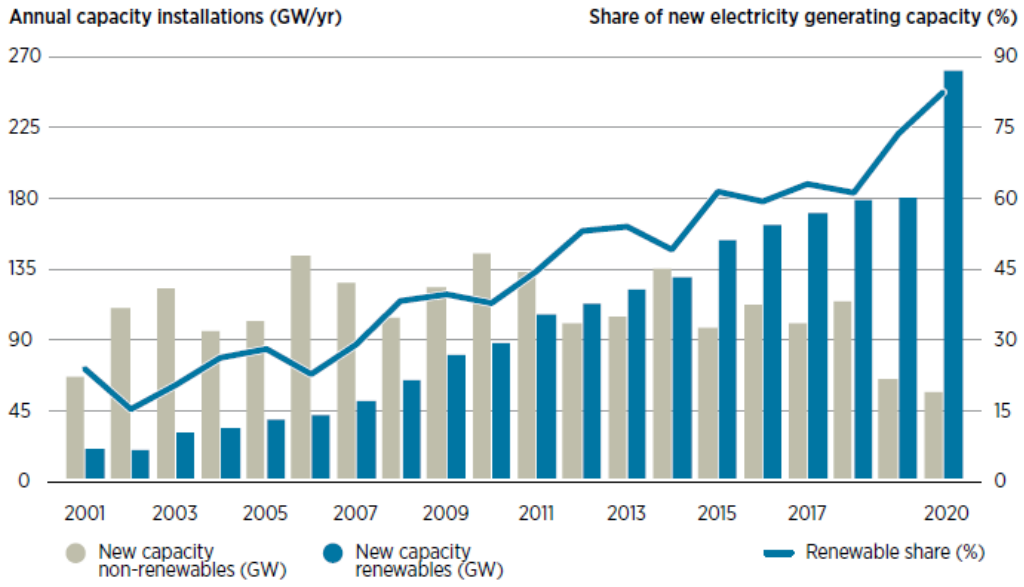

Figure 2-3 Global share of new electricity capacity [69]**.**

The selection of renewable energy technologies is typically influenced by each airport's unique technical and economic factors, such as geographical location, local climate, existing infrastructure, and local energy market dynamics. Wind turbines, for example, can provide a significant source of energy, especially for airports located in

windy areas. However, their placement must be carefully considered due to potential interference with radar systems and flight paths. This concern is documented by the Federal Aviation Administration [70] and other organisations, such as Sandia National Laboratories [71] and the National Academies of Sciences and Engineering [72], which provide guidelines on wind turbine installations near airports. The technologies that are available for the transition to sustainable airports are reviewed in the following sections, with an emphasis on solar energy, power-to-hydrogen-to-power systems, and microgrids.

2.4.1 Solar Energy

The quantity of sunlight reaching the earth's surface in just 90 min is sufficient to handle the global energy demand for an entire year. Solar technologies convert sunlight into electrical energy through two primary types: photovoltaics (PV) and concentrating solar-thermal power (CSP) [73], [74]. Various sectors are leveraging solar technologies to diversify their energy portfolios, increase efficiency, and achieve cost savings. Energy producers and utilities use solar photovoltaic and concentrated solar power systems to generate electricity on a large scale, powering both metropolitan areas and smaller communities.

From the perspective of airport operators and policy regulators, solar PV technology is seen as a key player in sustainable airports. In the U.S., about 22% of public airports have deployed solar PV [75]. The Voluntary Airport Low Emissions Grants Programme (VALE) is the prime mover towards greener airports; in 2019 more than 131 projects to cut CO_2 emissions at 59 airports were funded by VALE [76]. Moreover, Cochin International Airport successfully installed a 12 MW solar power plant, which provides 100% of the airport's electricity needs [77]. As a part of their environmental flight path plan, a 2 MW solar farm at Cardiff Airport is to be installed and is anticipated to cut 20,508 metric tonnes of carbon emissions over 25 yrs [78]. Substantial efforts have been put into investigating the integration of solar PV within airport infrastructure, taking advantage of the vast available land and rooftop space [79], [80]. This renewable technology has proven to be reliable and sustainable, providing substantial energy output and contributing to the decarbonisation efforts of the aviation industry. However, to optimise energy generation, reduce reliance on the grid, and enhance resilience, it is important to explore the integration of a mix of

renewable sources along with solar PV. The solar PV array power output is given in Equation (2.1) [81].

$$P_{PV} = C_{PV} \times D_{PV}\left(G_T / G_{T,STC}\right) \times \left[(1+\alpha) \times \left(T_c - T_{c,STC}\right)\right] \quad (2.1)$$

where C_{PV} represents the capacity rating of solar PV array in kW, and D_{PV} denotes the PV derating factor in %. G_T and $G_{T,STC}$ stands for incident solar radiation in the current time step in kW/m^2, and the incident radiation under standard test conditions 1kW/ m^2, respectively. α is the temperature coefficient of power in %/℃, T_c is the temperature of PV cell in the current time step in ℃, and $T_{c,STC}$ represents the PV cell temperature in ℃ at standard test conditions 25℃. The solar PV panel total losses, or derating factor, considered in this thesis include soiling, mismatch, wiring, shading, light-induced degradation, connections, availability, and nameplate rating [82].

2.4.2 Power-to-Hydrogen-to-Power System

A power-to-hydrogen-to-power system (P2H2P) converts electricity produced by renewable energy to hydrogen by employing electrolysis technology. The hydrogen is then stored for later use and converted back into power using a fuel cell [83], [84]. This process allows for the storage of surplus renewable energy, helping to balance supply and demand, smooth out the intermittent nature of renewable generation, and provide power when it is most needed. The ability to store and later use this otherwise wasted energy is a major advantage in efforts to transition towards a more sustainable and resilient energy system. The utilisation of the P2H2P system for on-site green hydrogen production and usage is based on three primary components: the electrolyser, hydrogen storage tank, and fuel cell.

2.4.2.1 Fuel Cell

A hydrogen fuel cell (FC) can play a significant role in the energy strategies of airports, helping to provide both resilience and sustainability. Hydrogen is increasingly being recognised as a potentially crucial element in the aviation sector's transition towards electrification and sustainability. Hydrogen fuel cells can be used in a variety of applications within the airport. For example, they could provide power for buildings and facilities, reducing reliance on the grid and lowering carbon emissions. They can also be used to power ground support equipment, such as tugs, belt loaders, and

baggage tractors, which are traditionally powered by fossil fuels. Moreover, fuel cells provide high-quality power, and their scalability makes them suitable for any size of airport. They can be used as a stand-alone system or in combination with other DER technologies to create a more resilient and flexible energy system. However, the use of hydrogen fuel cells presents some challenges. The infrastructure for producing, storing, and distributing hydrogen is still being developed, and the cost of fuel cells and hydrogen can be high. Despite their limitations, advances in technology and an increasing focus on renewable energy are expected to decrease these barriers.

The fuel cell is one of the most attractive energy devices because of its high efficiency in extracting power from fuel [85]. The FC is capable of converting various types of fuels, such as hydrogen and natural gas, into electric power. The three primary FC technologies are (1) the polymer electrolyte membrane (PEM) FC, (2) alkaline FC, and (3) solid oxide FC. In this thesis, the PEM FC is used because of its low operating temperature, fast response to load changes, and fast start-up. Figure 2-4 shows the primary structure of the PEM FC.

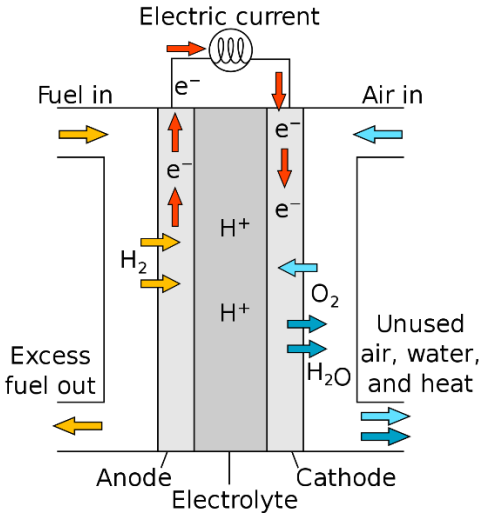

Figure 2-4 PEM FC structure [86]**.**

Typically, an FC reverses the electrolysis process to produce electricity by combining oxygen and hydrogen. The emissions out of this process are only water and heat, as expressed in Equation (2.2), where H_2 and O_2 are hydrogen and oxygen molecules, respectively [87].

$$\begin{aligned} at\ anode\text{:}\ \ H_2 &\rightarrow 2H^+ + 2e^- \\ at\ cathode\text{:}\ 4H^+ + 4e^- + O_2 &\rightarrow 2H_2O \end{aligned} \tag{2.2}$$

At the anode, the hydrogen is oxidised, releasing protons and electrons. At the cathode, the proton and electron are combined with oxygen to produce water. The PEM FC hydrogen consumption is calculated using Equation (2.3).

$$H_{2\,con} = \alpha_{FC} P_n + \beta_{FC} P_{out} \tag{2.3}$$

where α_{FC} and β_{FC} are hydrogen consumption curve coefficients in kg/kW, P_n is the FC nominal power in kW, and P_{out} is the FC output power in kW.

2.4.2.2 Electrolyser

An electrolyser is used to split water into oxygen and hydrogen, where hydrogen can be used as FC fuel. The splitting process is called water electrolysis, which is the result of the passage of a DC current through water [88]. Electrolysers consist of an anode and a cathode separated by an electrolyte, as shown in Figure 2-5.

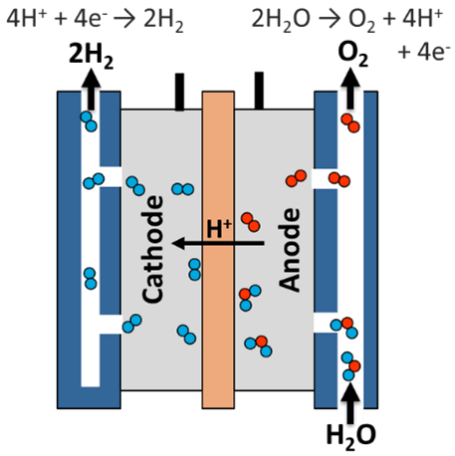

Figure 2-5 Electrolyser structure [88]**.**

Hydrogen ions mix with electrons from the external circuit at the cathode to generate hydrogen gas. Electrolysers can range in size from small to large based on the desired application and have three primary technologies: (1) polymer electrolyte membrane (PEM) electrolysers, (2) alkaline electrolysers, and (3) solid oxide electrolysers. In this thesis, the PEM electrolyser is used since it has several advantages in renewable energy scenarios, such as lower cost, simplicity, smaller size, and highly pure hydrogen production [89]. The hydrogen is produced by the electrolyser utilising electricity via the electrolysis process, as given in Equation (2.4).

$$H_2O \rightarrow O_2 + 2H_2 \tag{2.4}$$

The hydrogen produced by the PEM electrolyser is calculated as Equation (2.5) [84].

$$H_{out} = (P_{in} \times \eta_{PEM}) \times {}^{1}/_{Q_h} \quad (2.5)$$

where H_{out} is the produced hydrogen in kg, P_{in} is the input energy in kWh, η_{PEM} is the efficiency of hydrogen conversion in %, and Q_h is the hydrogen higher heating value in kWh/kg.

2.4.2.3 Hydrogen Storage Tank

The hydrogen storage unit is a key component that enables the FC and electrolyser to operate on site. The hydrogen storage technologies are categorised into physical- and material-based [90]. The former include storing hydrogen as compressed gas, cold or cryo-compressed hydrogen, and liquid hydrogen, whereas the latter include storing hydrogen based on chemical sorption/chemisorption and physical sorption/physisorption. In this chapter, a compressed gas hydrogen tank is used.

The use of DERs has expanded globally for several reasons, including the cost reduction of renewable-based DGs, especially solar PV, government incentives and policies to promote renewable technologies, emission reduction, resiliency, and energy security [91]. However, due to the rapid integration of DERs, the electricity grid is facing various challenges, including network stability, power quality, and protection coordination [92]–[94]. Microgrids and demand-side management are gaining attention as potential solutions to address such challenges.

2.5 Microgrids

A microgrid (MG) is an aggregation of interconnected DERs that include generation systems, storage, and loads, all within well-defined electrical boundaries [95]. An microgrid has the capability to connect to and disconnect from the grid as necessary and is controlled and managed locally [95]. It is connected and disconnected from the grid at the point of common coupling (PCC) where the associated requirements of PCC are applied according to standards, such as IEEE Standard 1547.4-2011 [96]. Technical specifications and performance requirements, such as voltage and frequency regulation, islanding, abnormal conditions of operation, and power quality, are addressed in these requirements.

In 2019, the total installed capacity of MGs globally was around 3.5 GW [97]. The microgrids capacity is anticipated to increase to reach nearly 20 GW by 2028, with an

annual growth rate of about 21%. Global MGs implementation is led by the Asia Pacific region and North America, as seen in Figure 2-6.

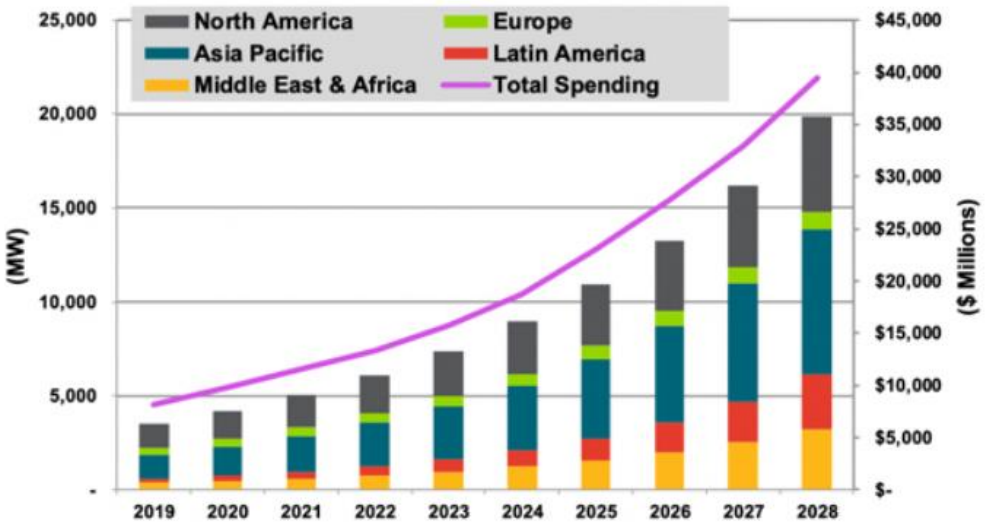

Figure 2-6 Global annual MG capacity 2019-2028 [98]**.**

As a part of aviation sustainability plans, few airports are adapting MGs within airport premises due to a lack of standards to design and develop airport MGs. The microgrids implementation for airports has the opportunity to increase power reliability and resiliency while reducing operational costs and GHG emissions [99]. In an airport setting, microgrids provide an extra layer of energy security, ensuring essential operations continue seamlessly even during larger grid disruptions. Some airports have taken some steps toward executing a big vision. For example, a 20 MW MG consisting of five natural gas generators and about 10,000 solar PV panels has been constructed at Pittsburgh International Airport [100]. The microgrid serves all airport facilities, which have had 14 MW of peak demand since July 2021.

Solar PV is a widely adapted energy source for powering airports, despite the availability of other renewable options. Cochin International Airport successfully installed a 12 MW solar power plant, which provides 100% of the airport's electricity needs [77]. Minneapolis-St. Paul International Airport's renewable system has 3 MW of PV that provides about 20% of the terminal's electricity needs [77]. To date, the majority of MG have been deployed to campuses, rural and remote areas, and military bases. However, airports are particularly well-suited to microgrids due to their high, round-the-clock energy demand and the critical need for reliable power [99]. Essential services, such as air traffic control, security systems, runway lighting, and passenger services, cannot afford power interruptions. Microgrids can provide continuous power

to these critical systems, either by providing back-up during a grid outage or by forming the primary power source. The implementation of airport microgrids involves various steps, including assessing energy consumption and designing and sizing possible DERs to be installed.

2.5.1 Microgrid Design

Microgrids are becoming popular power systems for enabling renewable DERs at the distribution level. Designing an MG involves numerous objectives, usually consisting of economic and operational performance, such as load modelling, generation modelling, component sizing, and defining the control approach [101]. Three types of MG exist based on their nature of structure, which are AC, DC, and hybrid (AC/DC), as seen in Figure 2-7 [102].

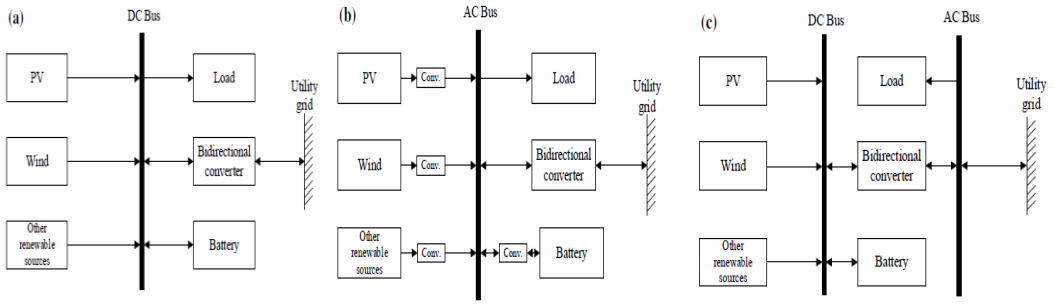

Figure 2-7 Category of MG based on structure a) DC, b) AC, c) hybrid [102]**.**

Designing a microgrid for an airport involves several steps and considerations to ensure that the system is efficient, reliable, and capable of meeting the airport's unique energy needs. These steps involve performing an energy audit, choosing energy sources, designing the control system, and determining the physical layout [99]. The energy audit involves analysing airport energy consumption patterns, peak load times, and the energy requirements of critical systems to inform the size and capacity of the microgrid and help determine the most effective mix of energy sources. The choice of energy sources is influenced by a variety of factors, including local climate, availability of renewable resources, space constraints, and sustainability goals.

Standardising the design of airport microgrids is not achievable due to numerous variations that affect optimal system sizing and configuration [99]. Factors such as electricity and natural gas prices, available solar resources, airport operational needs, peak times, passenger levels, local climate, accessibility to incentives and grants, local construction costs, the goals of the airport management, site-specific limitations,

geographical remoteness, and the consideration of modifying existing structures or constructing new ones are all case-specific details. Different combinations of these details can lead to vastly diverse systems, each designed to meet the unique technical, financial, and sustainability goals of an airport microgrid. Given that airport microgrid designs are distinctive and that it is challenging to establish universal principles or best practice guidelines, the industry could greatly benefit from sharing case studies that utilise various software packages available on the market [103]. Hence, in this thesis, the economic benefits of the hybrid structure airport microgrid are introduced in chapter 4, while the improvement of resilience is discussed in chapter 5, using commercial modelling tools.

2.5.2 Sizing of Microgrid

Microgrid sizing is a complex decision-making problem that requires defining the optimal mix of generation and storage components. Renewable DERs such as wind turbines and solar PV are highly intermittent energy sources. Thus, the use of hybrid renewable energy systems (HRES) offers a more reliable and emission-free system. The term “hybrid” in this research refers to the use of two or more energy-generating sources. Moreover, location criteria of a served site, such as available resources and area, play a significant role in determining the possibility of implementing multiple renewable sources. The most common HRES arrangements are wind-PV, wind-PV-hydrogen fuel cell (FC), and PV-hydrogen FC. The latter is deemed an HRES if hydrogen is produced using zero-emission energy sources; this process is called green hydrogen production. The production of hydrogen via the electrolysis of water is one way to store renewable energy.

2.6 Economic Performance

The MG sizing problem is traditionally modelled with the objective of finding an optimal system to reduce costs and increase system reliability [101], [104]–[106]. This is also known as techno-economic analysis. The problem is solved by deploying various tools (i.e., analytical methods, probabilistic methodology, artificial intelligence, and software modelling). The approach to the financial analysis uses the output derived from the various MG configurations to facilitate a comparison of the technical advantages and prospective financial returns. Investment check techniques are used to optimally select, size, and dispatch the ultimate MG components, including net present cost (NPC), levelised cost of energy (LCOE), and payback period.

Net Present Cost

Net present cost (NPC), or life-cycle cost, serves as a crucial economic evaluation tool, offering a comprehensive view of a project's financial feasibility over its operational life. This financial index accounts for various costs associated with project development and operation, including initial investment, operational, and maintenance expenses. In terms of microgrids, NPC is the present value of all the costs the system incurs over its lifetime minus the present value of all the revenue it earns over its lifetime. Costs include capital costs, replacement costs, operating and maintenance (O&M) costs, fuel costs, emissions penalties, and the cost of buying power from the grid. Revenues include salvage value and grid sales revenue. The total net present cost in terms of total annual cost is determined using Equation (2.6) [107], [81].

$$C_{NPC} = T_{AC}/CRF(IR, N_{life}) \tag{2.6}$$

where C_{NPC} is the total net present cost in \$, T_{AC} is the total annualised cost \$/yr, and CRF is the capital return factor, IR is the annual interest rate in %, and N_{life} is the project lifetime in years. The annualised cost T_{AC} and capital return factor CRF are calculated using Equations (2.7) and (2.8), respectively.

$$T_{AC} = CA_{inv} + CA_{rep} + OM + C_{fuel} \tag{2.7}$$

$$CRF\big(IR, N_{life}\big) = \frac{IR(1+IR)^{N_{life}}}{[(1+IR)^{N_{life}} - 1]} \tag{2.8}$$

where CA_{inv} is the annualised capital cost in \$, CA_{rep} is the replacement cost in \$, OM is the operating and maintenance cost in \$, and C_{fuel} is the fuel cost in \$.

Levelised Cost of Energy

The levelised cost of energy (LCOE) is a measure often used in the power generation sector that represents the average total cost to build and operate a power-generating asset over its lifetime divided by the total energy output of the asset over that lifetime. It is often used to compare the cost effectiveness of different energy generation sources, including fossil fuels, such as coal and gas, as well as renewable sources, such as wind and solar. To compare different microgrid configurations and sizes, the LCOE is calculated as the average cost per kWh of useful electrical energy produced by the system, as given in Equation (2.9) [107], [81].

$$\text{LCOE} = \frac{T_{AC}}{E_{pr} + E_{def} + E_{sell}} \tag{2.9}$$

where E_{pr} is the primary electric load served per year in kWh/yr, E_{def} is the total served deferrable load per year in kWh/yr, and E_{sell} is the total amount of energy sales to the grid per year in kWh/yr.

Payback Period

The payback period method is a simple and widely used financial analysis tool that calculates the length of time it takes for an investment to recoup its initial cost out of the cash inflows that it generates. However, one major limitation of the payback method is that it does not consider the time value of money, which is a key concept in finance that states that money today is worth more than money in the future. Additionally, the pattern of cash flow can yield contradictory outcomes, particularly in situations where positive cash flows only materialise in the latter stages of a project [108]. Nevertheless, the payback period serves as an indicator of risk, rendering this approach appropriate for projects necessitating minimal investments, such as microgrids at airports.

Amortisation Rate

An amortisation rate, as described in Equation (2.10), where lif_t is the technology lifetime in years, and IR is the annual interest rate in %, converts the up-front purchase cost of DERs into an equivalent annual cost [109]–[111]. This allows for a more direct comparison with operational costs, offering a comprehensive understanding of the financial impact of the technology. Furthermore, it determines the present value of the technology, considering the interest rate, and the lifespan of the technology, which together represent the financial implication of the technology over its operational life.

$$ANN_t = \frac{IR}{1 - \frac{1}{(1 + IR)^{lif_t}}} \tag{2.10}$$

A limited number of publications have considered grid-connected HRES implementation within airport geosystems. An online tool funded by ACRP was introduced to expand airport MG implementation [112]. The toolkit itself is a web-based resource designed to educate airport stakeholders about the capabilities of microgrids, including case studies and tools for effective implementation [113]. The

work in [114] explored the economic benefits of an airport DC MG consisting of solar PV, batteries, EVs, an electric auxiliary power unit (APU), and a mobile hydrogen fuel cell. The proposed model was formulated as a mixed-integer linear programming problem (MILP). The objective of an MG is to reduce airport annual costs, including investment, operation, and emission costs, over the project life-cycle. However, the hydrogen fuel cell is only considered to provide power for remote-stand aircraft rather than the whole electric load. Moreover, major cost savings derive from selling the oxygen that is produced along with hydrogen, which increases PV capacity significantly.

In [115], a mobile energy storage system was developed to reduce the usage of conventional APUs in airports. Lithium-ion battery packs and a power conversion system were combined to design the mobile storage system, and a scheduling model was implemented for a proposed DC/AC microgrid. The objective was formulated to maximise the environmental and economic benefits of the airport operator. However, the use of on-site renewable generation technologies was not considered, assuming that renewable energy is always supplied by a third party.

As such, the primary aim of this part of the thesis is to investigate the economic benefits of grid-connected HRES integration, including green hydrogen production and use locally. The economic benefits of green hydrogen are investigated, since the aviation sector sees green hydrogen as the key enabler of sector decarbonisation.

2.7 Resilience Performance

The globe's efforts to mitigate environmentally harmful emissions have shifted the electricity system towards decarbonisation and decentralisation, which has increased the trend to rely on electrified technologies. Thus, the dependency on electricity is a key factor for various sectors, as seen in Figure 2-8. In these sectors, electricity is becoming vital because continuous power delivery is lifesaving and goes beyond monetary value.

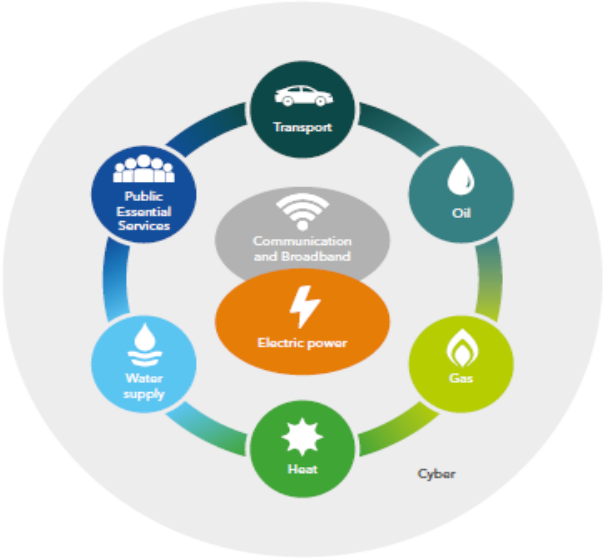

Figure 2-8 Key systems dependent on electricity[116]**.**

The transportation sector, including aviation, is being transformed into a partially electrified sector, particularly GSE, to cut sector GHG emissions. In addition, electricity has always been a major artery for airports that have high power consumption to ensure continuous operation [117],[118]. However, power outages have increased around the world recently as a result of natural events and cyber-attacks, highlighting the significance of power network resilience. Additionally, the power grid is outdated in most countries. For example, in the U.S., 60% of the grid is beyond its lifespan [119]. Traditionally, airport transportation and energy infrastructure operations are assessed based on economics, safety, environmental, reliability, and resilience.

In terms of power systems, no universally accepted definition of power system resilience exist; this term can refer to various definitions in the literature [120]–[123]. However, the definition of term resilience by U.S. Presidential Policy Directive 21 [124] is widely used: ‘‘*the ability to prepare for and adapt to changing conditions and withstand and recover rapidly from disruptions. Resilience includes the ability to withstand and recover from deliberate attacks, accidents, or naturally occurring threats or incidents*’’. Moreover, in 2011, the UK Cabinet Office defined resilience as “*Resilience is the ability of assets, networks and systems to anticipate, absorb, adapt to and / or rapidly recover from a disruptive event*” [125]. The UK Energy Research Partnership (EPR) gives a recent definition for resilience: “*the ability to withstand and reduce the magnitude and/or duration of disruptive events, which includes the capability to anticipate, absorb, adapt to, and/or rapidly recover from such*

events" [116]. From these definitions, a resilient electricity grid includes four components: fault tolerance, fast response, recovery, and reliability [126]. These characteristics are employed not only at the utility grid level but also in critical infrastructure. As critical infrastructure, airports require a reliable and resilient independent energy infrastructure to minimise the impact of power outages [127]–[129]. Microgrids have the potential to enhance resilience locally with the rapid increment of power outages related to extreme natural disasters such as wildfires and severe storms.

The extent of intense and frequent extreme events caused by climate change has increased weather-related power interruptions over the past few years, reinforcing the need for resilient electric infrastructure [130]. Traditionally, these extreme weather-related events are known as low probability, high impact events (LPHI). Between 2003 and 2012, the weather was responsible for 80% of major outages in the U.S., costing between $20 and $55 billion annually [131]. In addition, in 2017, five major weather-related power blackouts caused power interruptions to over one million consumers per event globally [132]. Power resilience enhancement strategies can be categorised into two parts: long-term strategies, such as upgrading transmission and/or distribution, and short-term strategies, such as the implantation of microgrids [132].

The ability of microgrids to operate under both grid-connected and off-grid conditions has the advantage of providing energy during normal operation and in case of grid outages over traditional back-up generators, which only operate during emergencies [133], [134]. Moreover, the use of only fossil fuel generators as back-up systems to supply critical loads is unreliable for long outages due to fuel supply and storage and a long turn-off period, which negatively impact generators lifetime [135]. Electricity is the primary mover of airport operations, and the consequences of energy interruption include flight delays, long layovers, cargo operations retardation, economic losses, and a limited ability to provide emergency support [136]. In 2017, a nearly 11 hr power outage at the busiest airport globally, Hartsfield-Jackson Atlanta International Airport, caused more than 1,000 flight cancellations and about $50 million in revenue losses [136], [137]. In 2016, a failure of power delivery lasted for about 5 h at a Delta airline facility, causing more than 1,500 flight cancellations and a total loss of around $150 million [138], [139].

Various studies have been conducted to boost the resiliency of the power grid against extreme events, including resilience analysis [132], [140], [141], catastrophic event modelling [142], [143], and resilience planning [144], [145]. The importance of grid-connected microgrids in enhancing the resilience of power systems has received little attention in previous studies, while microgrid techno-economic assessment, sizing and dispatching, and the resilience benefits of off-grid DER systems have been widely researched in many studies [146]–[150]. Research efforts related to airport microgrids are the least explored amongst all sectors, with only a single study to date examining the resiliency benefits [151]. In [152], the resiliency of an airport microgrid was evaluated under different outage scenarios. The study compared the life-cycle cost (LCC) of different resilience configurations with business as usual and evaluated the added benefits of microgrids during power outages. The results show that over the project lifetime, the proposed solar PV, lithium-ion batteries, and diesel generator system provided on average more than $70,000 cost savings and a survivability of around 700 h. To this end, work in Chapter 5 focuses primarily on the optimal and economic benefits associated with MG to leverage resilience benefits during different grid outages. Additionally, a microgrid economic dispatch is performed under various power outage conditions for comparison and to verify resilient microgrid performance.

2.8 Electric GSE Impact on Power Grid

The deployment of electrically powered technologies into airport systems is an important development towards aviation electrification. Typically, the phrase “electrification” refers to a move from fossil fuel-based technology to ones that run on electricity. The emerging of EGSE can provide many environmental benefits, such as reducing airport local emissions sources, and economic benefits, such as reducing operational costs [36]. However, similar to road EVs, the large penetration of EGSE may introduce additional challenges for airport and system operators, including but not limited to distribution transformer overloading, higher peak demand, increased network losses, and voltage variation [153]. Charging rate and time are the primary driving factors behind these challenges [154].

Electric ground support equipment can be treated as aggregated batteries, which can be turned into a profit source by, for example, participating in the ancillary service market. Hence, the concept of smart charging is deployed in this thesis as a key idea to mitigate negative impacts and boost positive opportunities. Smart charging refers to

adapting the charging cycle of EGSE to both the conditions of the power system and the needs of the vehicle fleet [155]. The potential influence of EGSE on the electricity system, environment, and economy is depicted in Figure 2-9 [156].

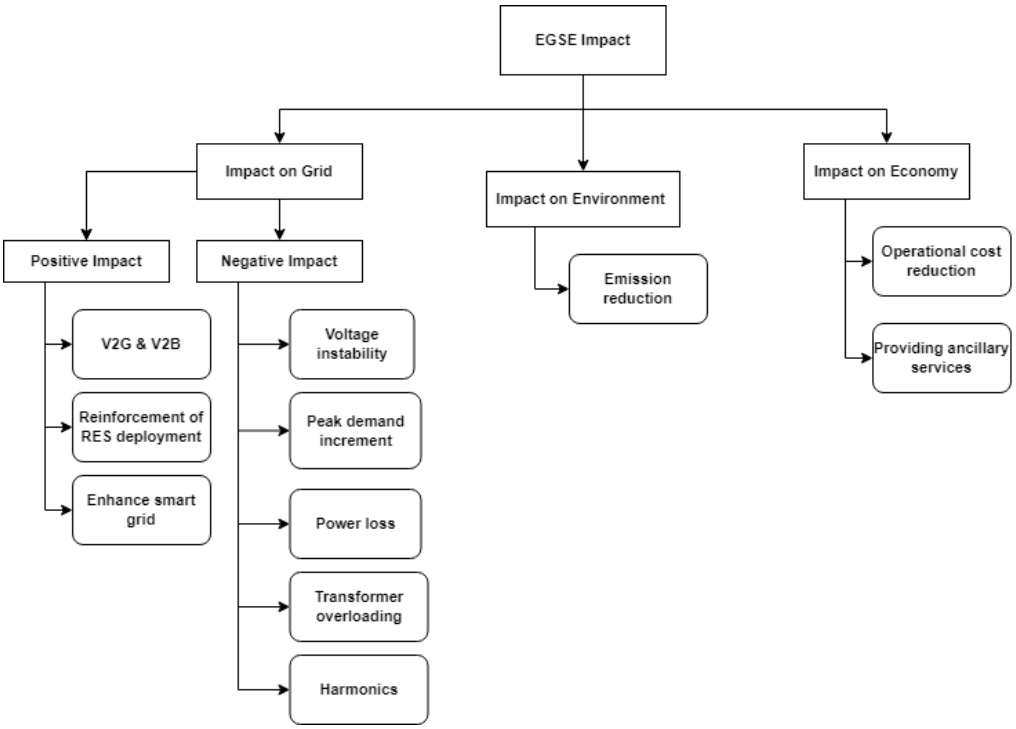

Figure 2-9 EGSE potential impact.

2.9 Demand Side Management

Demand-side management (DSM) is described as changes to the demand-side energy consumption pattern to improve electrical energy system efficiency and operations [157]. This term is used by utility companies and system operators to describe solutions that allow them to control energy use on the customer side and is divided into two categories in the literature [158]:

(i) Energy efficiency is a concept that focuses on the use of high-efficiency technologies to reduce the energy required for the provision of services or products.

(ii) Demand response (DR) refers to changes in energy demand by end-use customers in reaction to changing power pricing or incentives and provides more flexible control.

In addition, DR includes various programmes based on the given monetary amount, which are incentive-based and price- or time-based programmes. Figure 2-10 shows

the common DR programmes that are offered to both commercial and residential consumers, which offer a cost-effective solution when compared with network upgrades to mitigate grid challenges.

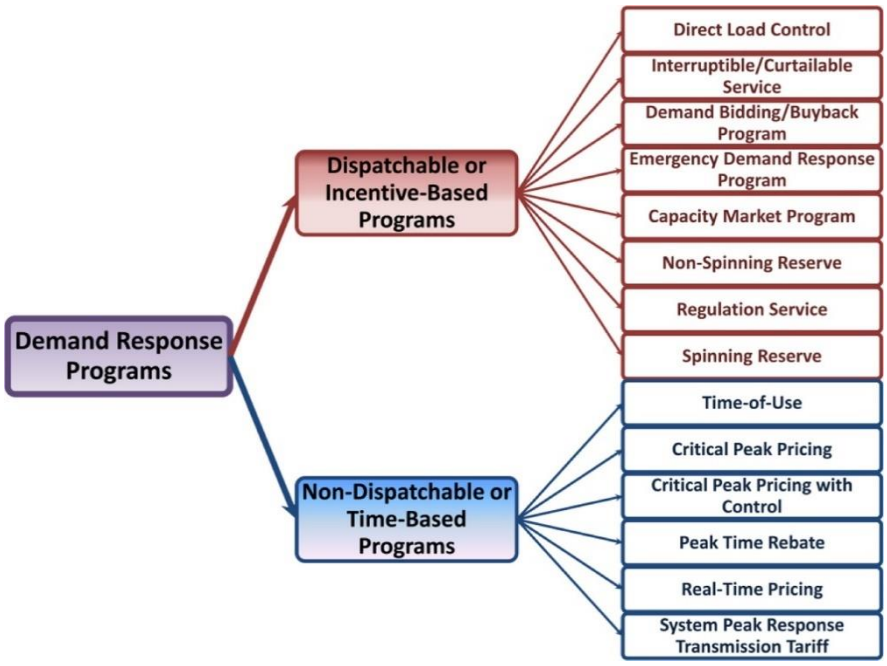

Figure 2-10 DR programmes [159]**.**

2.10 Electric Vehicles as Flexibility Sources

Power system flexibility can be defined as the ability of the system to mitigate changes in demand and supply to maintain power system stability and deliver reliable service to consumers [160]. Traditionally, large conventional power stations are responsible for providing flexibility to the power system by adjusting generator power output because the generated electric energy cannot be stored easily. However, the power system has recently seen a massive transformation with the increasing share of DER and the continued shutting down of large coal and thermal stations. This transformation has spurred the need to explore new flexible sources to overcome the daily operating challenges of the system.

One new source of flexibility can be obtained by integrating DR and energy storage. Since DR refers to the ability of electricity consumers to adjust their energy usage in response to changing prices or incentives, aggregated energy storage can help balance the grid by responding to DR programmes. Electric vehicles (EV), including road EVs and non-road EVs (EGSE), can act as a source of flexibility in the form of energy

storage because they have a large battery capacity that can be charged and discharged as needed. Utilities and grid operators can help mitigate the negative impact of high shares of fluctuating DER on the grid using DR with road EVs, and EGSE as flexible distribution energy storage sources. Distributed energy resources, such as solar panels and wind turbines, are a growing source of electricity generation, but they can be unpredictable and intermittent due to changes in weather conditions. By using EVs as a way to store excess energy from DERs, utilities and grid operators can smooth out fluctuations in supply and demand and help maintain a stable and reliable power grid. Together, DR and the use of aggregated EVs as distribution energy storage sources can help improve the efficiency and reliability of the electricity grid and reduce the need for expensive grid upgrades or additional power plants.

Primarily, EVs were developed and used to reduce CO_2 emissions in road transport. However, EVs, as a battery on wheels, are capable of storing surplus energy via the grid-to-vehicle (G2V) charging mode and releasing the stored energy in EV batteries in discharging mode (i) back to the grid via vehicle-to-grid (V2G), (ii) to the building via vehicle-to-building (V2B), or (iii) to home via vehicle-to-home (V2H).

Similar to road EVs, EGSE can discharge the stored energy in its batteries through V2G and V2B modes using bidirectional chargers. However, the installation cost of bidirectional chargers is not considered in this thesis. If EGSE charging and discharging is managed properly, both utilities and EGSE owners can benefit from these devices' modes of operation. The V2H mode of operation is excluded in the case of EGSE, which does not operate at the home level.

2.10.1 V2G In Energy System

The V2G system was trialled to manage the impact of EVs on the power grid [161]. The concept of V2G is that EVs can charge during off-peak hours and discharge power into the electric grid when power is required via a bi-directional power charger [162]. As such, both the power grid and the EV owners, who become active rather than passive customers, could make profits while the EVs are not in use [163]. The charging and discharging processes of EVs should be optimally controlled to reduce negative impacts on the power system [164]. As such, V2G is a proper technology that quickly responds to mitigate the fluctuation in the grid rather than conventional technologies since EVs are treated as a controllable load. Subject to the availability of the hardware

required for the bi-directional power flows that contains an appropriate smart controller, the vehicle's batteries via V2G can be used as an energy buffer for balancing services. Electric vehicles, or in this study, EGSE fleets, can form an aggregated surplus of energy that can flow back to the grid to provide supportive tasks such as ancillary services (e.g., frequency and voltage regulation), peak clipping, valley filling, and spinning reserve.

2.10.1.1 Ancillary Services

The ancillary service market provides flexible solutions to the power grid to overcome many challenges facing the transmission system operator (TSO) regarding reliable power grid operation. Conventionally, bulk generators primarily manage the transmission system's frequency and voltage by delivering some advanced services. However, the rapid implantation of renewable DER has specifically accelerated the decommissioning of synchronous generators. The majority of renewable DERs are intermittent, converter dominated, non-rotational masses, which poses stability and reliability challenges for grid operators [165]. Currently, the ancillary services used to ensure system balance, security and quality are provided by synchronous generators. However, renewable DERs have the potential to provide multiple ancillary services. Figure 2-11 gives a short overview of various ancillary services provided by renewable DERs.

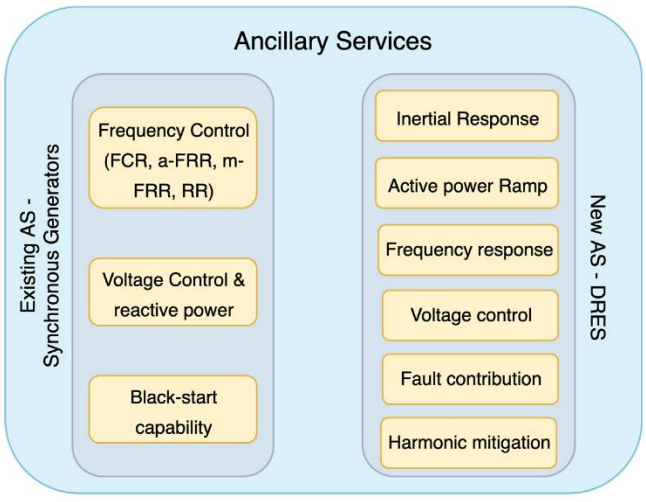

Figure 2-11 Renewable DERs and synchronous generators ancillary services [165]**.**

The most common and available ancillary services in the existing global markets include frequency response, voltage support, inertia, black start, and reserve power

[166]–[168]. Such services can be provided wholly or partially based on renewable DER technology. In the context of this thesis, the focus is on frequency response since it can be provided by EGSE. To the author's best knowledge, such a study has not been done before.

2.10.1.2 Frequency Response (Regulation)

Frequency regulation service is utilised by the TSO to maintain the balance between generation and consumption. Generally, the frequency regulation ancillary service market is designed based on bidding and contracting structures to provide frequency control [169]. The electricity system operator offers frequency control requirements for bidding in the auction for spinning and non-spinning reserves, and then the winning bidder must respond upon call. Two types of frequency regulation services are considered in this thesis:

(i) Regulation up occurs when the system frequency is below the reference frequency, and this can be done by discharging the EGSE's battery or lowering their charging level.
(ii) Regulation down occurs when the system frequency is over the reference frequency, and this can be done by increasing EGSE's charging power rate.

In addition, power grid balance is maintained by three types of control reserves [168]:

(i) Primary reserve: This type is usually activated instantly in the controlled region to prevent additional frequency drops. It has a very quick response and takes between 0–30 s to activate.
(ii) Secondary reserve: A signal is sent automatically and continually to activate this type of response. It follows the primary reserve, and participants must react between 30 s and 15 min. This type is suitable for EGSE's participation considering aggregator control.
(iii) Tertiary reserve: If the secondary reserve cannot maintain frequency fluctuation after 15 min, the tertiary reserve is manually activated by the system operator to restore frequency, typically during a significant incident.

The changes in the traditional vertical power system paradigm unbundled the power system into generating units, ESO, TSO, and distribution system operators (DSO). For transparent and cost-effective energy trading, electricity markets have been established.

Through the liberalisation of the electricity markets, certain services linked to power generation, transmission, and distribution were separated. The power system has recently seen a massive transformation, and the decarbonisation of the electricity system requires investment in low-carbon energy sources, resulting in an increased share of distributed energy resources (DER). A need exists for emerging technologies to provide flexibility through ancillary services [170] because of reductions in the operating hours of conventional large-scale fossil fuel generators including various services related to power system characteristics such as frequency control, voltage control, congestion management, black start, and loss compensation [166], [171], [172]. The frequency control market is more commercialised globally since it is related to active power supply, which can be promptly priced [173], whereas, for example, the voltage control market is linked with reactive power, which has local influence and is difficult to trade [173], [174].

No unified universal market structure exists for frequency control in most countries. However, the common feature is that the frequency control ancillary service market is designed based on bidding and contracting structures [169], [173]. In addition, the frequency control ancillary service nomenclature and functionality differ locally and globally. For example, in the U.S., frequency control ancillary services are termed regulations and reserves for Pennsylvania, New Jersey, and Maryland Interconnection area (PJM) [175], regulations for New York Independent System Operator (ISO) [166], and regulation up, regulation down, spinning reserve and non-spinning reserve for California ISO [176]. In addition, frequency control ancillary services in Australia include contingency and regulation [177]. In European Union countries, frequency control services are known as frequency containment reserves (FCR; i.e., primary control), frequency restoration reserves (FRR; i.e., secondary control), and replacement reserves (RR; i.e., slow tertiary control) [170], [178], [179].

The FCR, or primary control, is the first type of control that automatically responds within seconds to a frequency deviation following a disruption. The available reserve of active power is used to cover the mismatch between generation and demand and stabilise the system frequency within seconds [168], [180]. Later, the FRR is activated to set the system frequency back to its nominal value. The active power reserve available is used to restore power balance between control areas. The area control error (ACE) is reduced to zero by restoring unscheduled power flow between different areas

to its original values by the automatic generator control (AGC), which increases or decreases the set points of active power of various regulation resources, including the EV fleet, to provide the required response to minimise ACE. The minimisation of ACE includes signals for frequency regulation up and down.

Regulation up is required when the system frequency is below the reference frequency, which can be done by discharging the EV's battery, whereas regulation down is required when the system frequency is above the reference frequency, which can be done by increasing the EV charging power rate. The FRR requirements are established based on day ahead or real time (1 h in advance). In addition, the FRR activation starts after a few seconds (typically 30 s) and lasts for a few minutes (typically 15 min) to make FCR available for any other system disturbance and can be either automatic or manual [180], [181]. Finally, the RR, or tertiary control, is manually activated to restore and support the required level of FRR for further system disturbance using the available active power reserve.

Ancillary services such as frequency and voltage regulation are provided through an aggregator that interacts between the electricity market and aggregated EVs [182]. The aggregator interacts between the EV owner and electricity market to ensure the available power capacity is ready when needed by the market operator. Many studies have been conducted to find the best participation strategies for EV aggregators in the ancillary services market. These studies aim to optimise the charging strategy for optimal bidding in the electricity market.

In [173], a secondary frequency response through an aggregator model was developed, which considered the EV user preference. An optimal scheduling strategy using V2G was applied to optimise the energy and provide ancillary services [161] (e.g., load regulation and spinning reserves). An algorithm was developed to be used by an aggregator to maximise profits by providing ancillary services. The study also considered the unexpected EV departures during the contracted period of providing ancillary services. In addition, in [183], the use of the plug-in electric vehicle to provide frequency response services based on a real-time greedy index was introduced. The proposed method transforms the multi-dimensional problem of optimal dispatch into a one-dimensional problem while satisfying the optimal solution. A day-ahead optimisation formulation to minimise the cost of operation of an electric vehicle fleet participating in the regulation market was developed in [184]. A hierarchical control

system that optimises the charging, market bidding, and response to the system operator was developed to minimise the operation cost and maximise the regulation services revenue.

2.10.2 V2B in Localised Energy Systems

The rapid growth of EV usage today and in the foreseeable future is leading EVs to charge in various locations. As such, their batteries can be aggregated as a large storage system, allowing for demand peak reduction as well as charging or discharging as needed. Similar to V2G, the concept of V2B allows energy to flow bidirectionally between EVs and buildings [185]. Electric vehicles can be aggregated and the surplus power discharged to one or a group of buildings locally with V2B technology. The promising technology of V2B has received more attention lately, with some trials seen globally, like at The Alliance Centre [186]. This project is one of the first V2B projects in North America that enables buildings to draw power from a Nissan LEAF fleet for heating/cooling loads. However, for the wide deployment of V2B technology, additional infrastructure, policy support, and proper building energy management system software is still required [187].

From the perspective of building operators, various benefits can be obtained by enabling V2B technology, including the following [188]–[190]:

- Electricity bill cost reduction, by taking advantage of charging EV fleets during off-peak periods and then delivering energy back to buildings during peak hours;
- Peak reduction and its associated peak demand cost, especially for large end-users;
- Increased renewable distributed generators, since EVs can play the role of energy storage batteries;
- The receipt of a share of the building's cost savings by EV owners in exchange for the use of their battery; and
- The potential for the EV fleet to be employed as a back-up system to power buildings' critical loads during unexpected outages.

In this context, the work in chapter 6 of this thesis focuses on exploring the opportunity for buildings to draw power from EGSE fleet batteries, aiming to reduce peak demand. Energy usage reduction is included in airport sustainability plans. In China, for example, civil aviation consumes around 8% of the total transportation energy

consumption [191]. In Spain in 2019, airports consumed about 0.95 TWh of electricity, which is equal to 0.4% of the country's overall electricity consumption [192], [193].

Vehicle-to-building enables EVs to play a role in the modern energy system but is restricted within buildings by, for example, adding extra energy storage, emergency back-up energy, and demand peak shaving. An efficient charging/discharging system and a smart building energy management system are combined through the V2B concept [194]. The technology of V2B has enabled electric vehicles to support the electricity network and even participate in ancillary services to make profits. The extended literature review found that airport electrification's impact on airport demand and providing DR programmes is less investigated in the literature. The impact of utilising electric EGSE, especially a pre-conditioned air unit and a ground power unit, is studied in [195], while the authors of another study [196] propose an energy exchange model by using road EVs in long-term airport parking lots equipped with V2G and different charging levels, and another study [197] proposed smart charging and flight schedule modifications to reduce peak electricity demand by implementing hybrid electric aircraft. In [198], airport demand forecasting for DR services based on flight schedules was introduced. As such, in this thesis, the airport electrical demand peak shaving and valley filling optimisation problem using EGSE is addressed using a mixed-integer linear programming optimisation problem (MILP) approach.

2.11 Mitigation of EGSE Integration Impact in Low Voltage Distribution Networks

The impact of EVs on low-voltage distribution networks was broadly investigated in the literature, including (e.g., voltage unbalance, transformer overloading, cable thermal overload, peak demand growth, and electrical losses) [199]–[202]. Moreover, many studies have been devoted to quantifying and mitigating the impact of road EVs on transformer overloading and lifespan because transformers are amongst the most expensive and critical pieces of equipment in the power network. However, conspicuously absent from these investigations is an examination of the potential effects of non-road EVs, specifically EGSE. This research gap in the existing literature emphasises the need for further research. As delineated in section 2.7, the integration of EGSE can potentially pose significant challenges to the power grid infrastructure and its constituent elements. It is thus imperative to thoroughly assess and address

these challenges when considering the transition from a conventional GSE fleet to an electrically powered one.

Traditionally, transformers are designed to sustain a certain amount of marginal overloading. However, the uncontrolled charging of EVs and EGSE could lead to the overloading of the transformer, which could result in transformer failure or a shorter lifetime. According to IEC Standard 60076-7:2018, when a transformer's loading exceeds the nameplate rating and/or the ambient temperature exceeds the design ambient temperature, there is a degree of risk and accelerated ageing [203]. The risks are classified into general effects, emergency short-time loading effects, and emergency long-time loading effects. The general effects encompass, for instance, abnormal temperature escalation in winding, cables, and oil, as well as heightened stress on components such as bushings, tap-changers, and cable-end connections. The short-time loading effects include the formulation of gas bubbles in oil, the expansion and overflow of oil in the conservator, and the temporary deterioration of mechanical abilities. Finally, the long-time loading effects include a reduction in transformer lifetime due to acceleration of conductor mechanical property deterioration, an increment in tap-changer contact resistance, and brittleness in the gasket materials.

The expected future deployment rate of EGSE is significant, which requires innovative methods to smartly manage their potential impact on the distribution/transmission systems. One major challenge relates to the potential overloading of transformers. The power transformers are crucial and expensive equipment, so unexpected damage, unplanned outages, and accelerated ageing have a great negative impact on the grid in terms of reliability and cost. Traditionally, power transformers are upgraded to a higher capacity to contain any additional load. However, the power transformers can be loaded above their nameplate rating without causing damage if the loading process is effectively planned. As such, dynamic loading is one potential solution that can defer the pros and cons of transformer upgrading without risking the transformer's lifetime.

Researchers' efforts are increasing to identify and propose solutions to limit EV charging's impact on transformer lifetime. These solutions are conducted to avoid or delay the need for substantial reinforcement investment associated with EV deployment. Various approaches are used to implement smart charging or charging control to alleviate transformer overloading, including optimisation, heuristic search, time-of-use pricing, and risk assessment. Although EV charging impact on power

transformers is widely studied in the literature [199], [204]–[207], to the author's best knowledge, such a study considering non-road EVs, especially EGSE impact, has not been done before. As such, the work presented in chapter 8 aims to fill the gap by developing a mixed-integer non-linear programming optimisation problem (MINLP) considering the EGSE fleet data, which will help to mitigate the power transformer ageing and the need for transformer size upgrades.

2.11.1 Transformer Thermal Modelling

The IEC 60076-7 regulation established the operation of the oil-immersed transformers under varying loads and ambient temperatures [203], and suggests guidance for power transformer operation and loading with respect to operating temperature and thermal ageing. It proposes an appropriate approach for the operator to load the transformer above the rated capacity. The transformer's age mainly depends on the winding insulation's life. Thus, the insulation degradation is calculated based on the IEC 60076-7 recommended model, which considers the insulation temperature a controllable parameter. The transformer's relative ageing rate is determined by Equation (2.11).

$$V_{(n)} = e^{\left(\frac{15000}{383} - \frac{15000}{\theta_{h(n)}+273}\right)} \tag{2.11}$$

where $V_{(n)}$ is transformer ageing rate for thermally upgraded paper insulation at the n^{th} time step, and $\theta_{h(n)}$ is the hot-spot temperature at the n^{th} time-step in °C. The transformer lifetime relies on the insulation deterioration rate $V_{(n)}$, which is very sensitive to hot-spot temperature θ_h or insulation temperature. Table 2-5 shows the transformer ageing rate due to different hot-spot temperatures (HST) [203]. At reference HST temperature 110°C, the ageing rate is equal to 1 and is increasing when HST is above the reference temperature, and vice versa. The ageing rate of 1 represents 24 h. The normal insulation life of a thermally upgraded insulation paper transformer is 180,000 h, or 20.5 yrs [203].

Table 2-5 Aging rates due to different hot-spot temperatures.

θ_h (°C)	V
80	0.036
92	0.145
104	0.536
110	1
122	3.29
134	10.1
140	17.2

Figure 2-12 provides a basic depiction of temperature distribution inside the transformer winding [208].

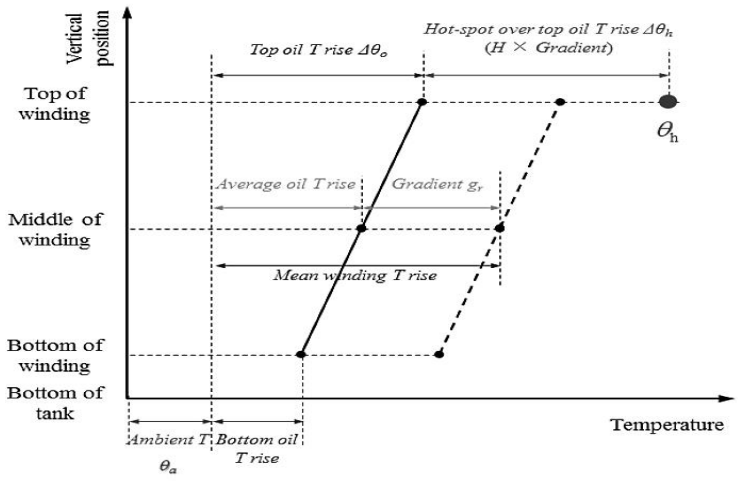

Figure 2-12 Transformer thermal model [208]**.**

As seen in Figure 2-12, the oil temperature surrounding windings rises from bottom to top in a linear pattern, where the hottest point (HST θ_h) is the summation of ambient temperature θ_a, hot-spot to top-oil gradient TH, and top-oil temperature OT. There are two ways to obtain HST as a function of time under varying ambient temperature and loading factor:

1- Exponential equation model, which is ideal for a load variation based on a step function; and
2- Difference equation model, which is appropriate for arbitrary time-varying transformer loading and time-varying ambient temperature.

In this chapter, the difference model is used due to time-varying criteria. The difference model is represented by the block diagram shown in Figure 2-13 [203].

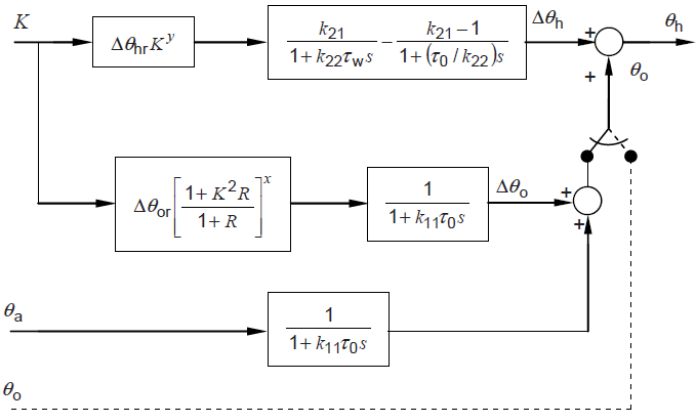

Figure 2-13 Differential equations block diagram [203]**.**

The difference model inputs are load factor K and ambient temperature θ_a, whereas the model output is HST θ_h. According to IEC 60076-7 guideline, the differential model equations in Figure 2-13 can be simplified and converted to difference equation solution where the solution is quite straightforward [203]. The hot-spot temperature rise is obtained by using the difference model for arbitrarily loading and is given by Equation (2.12).

$$\theta_{h(n)} = OT_{(n)} + TH_{(n)} \tag{2.12}$$

where $OT_{(n)}$ is the top-oil temperature at considered load at the n^{th} time step in °C, and $\mathrm{TH}_{(n)}$ is the hot-spot to top-oil gradient at considered load at the n^{th} time step in K. The difference equation for hot-spot temperature rise $\Delta TH_{(n)}$ is given by Equation (2.13). The subsequent Equations (2.14) to (2.19) calculate the different components of hot-spot temperature rise.

$$TH_{(n)} = \Delta M1_{(n)} - \Delta M2_{(n)} \tag{2.13}$$

$$\Delta M1_{(n)} = \Delta M1_{(n-1)} + dM1_{(n)} \tag{2.14}$$

$$\Delta M2_{(n)} = \Delta M2_{(n-1)} + dM2_{(n)} \tag{2.15}$$

$$dM1_{(n)} = f1 \cdot (k_{21} \times Hr \times K^y - \Delta M1) \tag{2.16}$$

$$f1 = \frac{Dt}{k_{22} \times \tau_w} \tag{2.17}$$

$$dM2_{(n)} = f2 \cdot [(k_{21} - 1) \times Hr \times K^y - \Delta M2] \tag{2.18}$$

$$f2 = \frac{Dt}{(1/k_{22}) \times \tau_o} \tag{2.19}$$

where d is the difference operator, Dt is the considered time step in min, k_{22} and k_{21} are the thermal model constants, Hr is the hot-spot to top-oil gradient at rated current in K, τ_w is the winding time constant in min, τ_o is the average oil time constant in min, y is the winding exponent, and K is load factor. The top-oil temperature $OT_{(n)}$ at considered load is given in Equation (2.20). The difference in $OT_{(n)}$ that corresponds to each time step *Dt* is calculated using Equations (2.21), (2.22), and (2.23).

$$OT_{(n)} = OT_{(n-1)} + dOT_{(n)} \tag{2.20}$$

$$dOT_{(n)} = f3 \cdot \left[(f4 \times Rx) - (OT_{(n-1)} - \theta_a) \right] \tag{2.21}$$

$$f3 = \frac{Dt}{k_{11} \times \tau_0} \tag{2.22}$$

$$f4 = \left(\frac{1 + K^2 \times R}{1 + R} \right)^x \tag{2.23}$$

where k_{11} is the thermal model constant, R is the ratio of load losses to no-load losses at rated current, x is the oil exponent, Rx is the top-oil temperature rise in steady state at rated losses in *K*, and θ_a is the ambient temperature in °C. The transformer total loss of life *L* at the n^{th} time step is given by Equation (2.24), where $L_{(n)}$ is the total loss of life (LOL) over the considered period in hour. The corresponding loss of life to time step *Dt* is given by Equation (2.25).

$$L_{(n)} = L_{(n-1)} + dL_{(n)} \tag{2.24}$$

$$dL_{(n)} = V_{(n)} \times Dt \tag{2.25}$$

2.12 Summary of Key Findings

In this chapter, a review of literature on the topics of airport engineering and classification, ground support operation and equipment, airport sustainability, distributed energy resources, and microgrids, as well as the potential benefits and impacts of electric ground support equipment on different levels of the electricity grid, has been presented. The purpose of the chapter is to identify the gaps and open issues that must be addressed in the future to promote clean technologies and achieve airport sustainability. The key findings are listed as follows:

i. The electrification of airports and ground support equipment is highly significant in terms of carbon reduction and the use of renewable energy as a

key enabler. However, given that each airport is unique, the electrification process will require careful planning depending on each airport's specific characteristics, such as its size, location, available resources, energy demand, and local energy regulations.

ii. The installation of microgrids within the airport ecosystem was found to be underutilised in many applications. Given the relative novelty of airport microgrid studies, the number of relevant research papers was found to be limited.

iii. Wind turbine installation inside or near airports is challenging due to possible interference with radar systems and flight paths.

iv. The replacement of conventional ground support equipment with zero-emission ground support equipment is still lagging. However, exploring the potential benefits of using electric ground support equipment in airports rather than only emission and operation cost reductions could accelerate their implementation rate.

v. The flexibility and ancillary services that electric ground support equipment can provide at various levels of power systems were found to be unexplored. Given the relatively new concept of ground support equipment electrification, no relevant research papers were found.

vi. The potential impact of uncontrolled charging of electric ground support equipment on power system components must be properly recognised and examined.

In the subsequent chapters, the integration of airport microgrids is assessed, considering both economic and resiliency benefits. The use of electric ground support equipment fleets to flatten the airport load curve and their participation in ancillary services are assessed. Finally, reducing the uncontrolled charging impact on power system components is introduced.

Chapter 3
Modelling Approaches and Tools

3.1 Introduction

The motivation of this work is to review the modelling methods and tools available to facilitate the integration of distributed energy resources, which supports the net-zero transition. This chapter postulates that the appropriate combination of modelling methods and software address the challenge of emerging renewable distributed energy resources to secure sustainable development. The decision about employing renewable distributed energy resources involves optimising various aspects, such as resource types, sizes, location, and economic factors. Currently, numerous modelling tools are available to analyse the benefits of distributed energy resources, including techno-economic analysis and emission reduction. These tools employ various optimisation approaches, such as linear programming, mixed-integer linear programming, non-linear programming, and mixed-integer non-linear programming.

3.2 Optimisation Modelling

Optimisation modelling is defined as the process of developing a mathematical model of a real-world system or process with the goal of finding the optimal solution to a problem [209]. This can involve minimising or maximising a given objective, subject to certain constraints. Optimisation models typically involve variables that represent quantities that can be adjusted or controlled in order to achieve the desired outcome and constraints that describe the limitations or requirements of the system. These variables, called decision variables, represent the choices that can be made in the optimisation problem, and their values are usually unknown or uncertain at the beginning of the optimisation process. While constraints are limitations or boundaries that are imposed on the solution to an optimisation problem and express the relationship between decision variables and other parameters, the constraints can be expressed in terms of equality (=) or inequality (greater than or equal to ≥, and less than or equal to ≤).

Optimisation modelling has wide applications in various fields, such as engineering, economics, computer science, and operations research, and various techniques are used to find the optimal solution to a given problem, each suitable for different types

of problems. In general, these methods are categorised into two primary parts, including the following [210], [211]:

- Mathematical/numerical methods, such as linear programming (LP), non-linear programming (NP), mixed-integer linear programming (MILP), mixed-integer non-linear programming (MINLP), quadratic programming (QP), Mixed-integer quadratic programming (MIQP), dynamic programming (DP), and geometric programming (GP).
- Artificial intelligence methods, such as neural networks, genetic algorithms, particle swarm optimisation, evolutionary computation, and fuzzy logic.

3.2.1 Mixed-Integer Linear Programming Approach

The MILP combines the principles of linear programming with the ability to include integer variables in the model [212], [213]. It involves formulating the problem as a linear mathematical model in which the objective function and the constraints are expressed as linear equations or inequalities. The model also includes integer variables, which represent discrete decision variables that can only take on integer values (e.g., 0, 1, 2, etc.). The MILP models are used to solve a wide range of optimisation problems, including resource allocation, scheduling, and design problems. The MILP problem objective function can be expressed as Equation (3.1) and is subject to various equality and inequality constraints as Equations (3.2) to (3.12) [212].

$$minmise \quad f = \sum_{t,k,i} x_{t,k,i} + \sum_{t,k,i} y_{t,k,i} \tag{3.1}$$

Subject to

$$p^{min} \leq x_{t,k,i} \leq p^{max} \tag{3.2}$$

$$p^{min} \leq y_{t,k,i} \leq p^{max} \tag{3.3}$$

$$x_{t,k,i} \leq P^{x}_{t,k,i} \tag{3.4}$$

$$y_{t,k,i} \leq P^{y}_{t,k,i} \tag{3.5}$$

$$x_{t,k,i} \leq p^{max} * a_{t,k,i} \tag{3.6}$$

$$P^{x}_{t,k,i} - x_{t,k,i} \leq p^{max} * (1 - a_{t,k,i}) \tag{3.7}$$

$$y_{t,k,i} \leq p^{max} * a_{t,k,i} \tag{3.8}$$

$$P^{y}_{t,k,i} - y_{t,k,i} \leq p^{max} * (1 - a_{t,k,i}) \tag{3.9}$$

$$b_{t,k,i} * p^{min} \leq P^{x}_{t,k,i} \leq p^{max} * b_{t,k,i} \quad (3.10)$$

$$(1 - b_{t,k,i}) * p^{min} \leq P^{y}_{t,k,i} \leq p^{max} * (1 - b_{t,k,i}) \quad (3.11)$$

$$a_{t,k,i}\ and\ \ b_{t,k,i} \in \{0,1\} \quad (3.12)$$

where $x_{t,k,i}$, $y_{t,k,i}$ are unknown decision variables which represent the choices of the optimisation problem and can take any value between defined boundaries p^{max} and p^{min}; $a_{t,k,i}$ and $b_{t,k,i}$ are binary variables; $P^{x}_{t,k,i}$ and $P^{y}_{t,k,i}$ are auxiliary variables that are introduced to avoid the non-linearity of objective function resulting from multiplying decision variables by binary variables. The MILP model is then solved using specialised algorithms to find the optimal solution that maximises or minimises the objective function subject to the given constraints. Some of the most commonly used algorithms include the following:

- **Branch and bound**: This is a systematic search algorithm that explores the solution space by dividing it into smaller sub-problems and solving them one by one. The algorithm starts with a continuous relaxation of the MILP problem and then progressively adds integer constraints until the optimal solution is found.
- **Cutting plane**: This is an iterative algorithm that generates linear inequalities called cut planes to tighten the feasible region of the MILP problem. The algorithm starts with a continuous relaxation of the problem and then adds the cut planes to the model until the optimal solution is found.
- **Gomory cuts**: This is a variant of the cutting-plane algorithm that generates a special type of cut plane called Gomory cuts. These cuts are based on the properties of the optimal solution to the continuous relaxation of the MILP problem and are particularly effective at tightening the feasible region of the problem.
- **Linear programming (LP) relaxation**: This is a method that involves solving the continuous relaxation of the MILP problem using a standard LP solver. The solution to the continuous relaxation is then rounded to the nearest integer value to obtain a feasible integer solution to the MILP problem.
- **Branch and cut**: This is a hybrid algorithm that combines the branch-and-bound method with the cutting-plane method. The algorithm starts with a continuous relaxation of the MILP problem and then adds cut planes and integer constraints to the model until the optimal solution is found.

The MILP approach has many advantages, including the following:

- It can tackle various optimisation problems, including problems with multiple objectives, multiple constraints, and discrete variables.
- It can handle both continuous and discrete variables, which can be used to solve problems that involve both types of variables, such as scheduling problems.
- It can identify the optimal solution to a problem rather than an approximation solution because it employs linear programming techniques.
- It can handle problems with a large number of variables and constraints, making it a useful tool for solving real-world optimisation problems.
- It can handle both hard constraints, which must be satisfied in any solution, and soft constraints, which can be violated to some extent in order to improve the overall solution.

However, The MILP has some limitations, including the following:

- It can take a significant amount of time to find the optimal solution depending on the size and complexity of the problem, which makes MILP a time-sensitive problem.
- It can require a great deal of memory and processing power to solve large problems.
- It can get stuck in local optima, which are sub-optimal solutions that are not necessarily the best overall solution.
- It can only be used to solve optimisation problems with linear objective functions and linear constraints; it cannot be used to solve problems with non-linear objective functions or constraints.

3.2.2 Mixed-Integer Non-linear Programming Approach

The MINLP is a sub-field of mathematical and numerical optimisation that deals with optimisation problems that involve both continuous and integer variables, as well as non-linear constraints and objectives. A key challenge in solving MINLP and MILP problems is the presence of both continuous and integer variables. However, in the MINLP, non-linear constraints and objectives further complicate the optimisation process, as they may introduce other mathematical challenges. The objective function of the MINLP problem can take on different forms, including linear or non-linear expressions such as the exponential function presented in Equation (3.13). The

problem is subject to various constraints, which can be expressed as either linear or non-linear equations in the form of equality and inequality, as represented by Equations (3.14) to (3.22) [214].

$$minmise \quad f = e^{1/m_t} \tag{3.13}$$

Subject to

$$m_t = \sum_{t,k,i} x_{t,k,i} \ * \ a_{t,k,i} \tag{3.14}$$

$$y_{t,k,i} = y_{t-1,k,i} + m_{t,k,i} * a_{t,k,i} - w_{t,k,i} * b_{t,k,i} \tag{3.15}$$

$$p^{min} \leq x_{t,k,i} \leq p^{max} \tag{3.16}$$

$$Y^{min} \leq y_{t,k,i} \leq Y^{max} \tag{3.17}$$

$$m_t \ \leq M^{max} \tag{3.18}$$

$$\sum a_{t,k,i} = A_{t,k,i} \tag{3.19}$$

$$\sum b_{t,k,i} = B_{t,k,i} \tag{3.20}$$

$$a_{t,k,i} + \ b_{t,k,i} \leq 1 \tag{3.21}$$

$$a_{t,k,i} \ and \ \ b_{t,k,i} \ \in \{0,1\} \tag{3.22}$$

where $m_{t,k,i}$ and $y_{t,k,i}$ are functions of the unknown decision variable $x_{t,k,i}$ which represent the choices of the optimisation problem and can take any value between defined boundaries p^{max} and p^{min} for $x_{t,k,i}$ and Y^{max} and Y^{min} for $y_{t,k,i}$. Several algorithms can be used to solve the MINLP problems, including the following:

- **Global optimisation algorithms**: These algorithms aim to find the global optimal solution to MINLP problems by exploring the entire feasible region. Examples include branch-and-bound, cutting-plane methods, and evolutionary algorithms.
- **Heuristics**: These algorithms aim to find good solutions quickly by using simple and efficient search procedures. Examples include simulated annealing, tabu search, and genetic algorithms.
- **Interior point methods**: These algorithms use the interior of the feasible region to find the optimal solution. They rely on the Karush-Kuhn-Tucker (KKT) conditions to solve non-linear optimisation problems.
- **Sequential quadratic programming (SQP) methods**: These algorithms are iterative methods that use quadratic approximations to solve non-linear

optimisation problems. They can be used to solve MINLP problems by incorporating integer variables into the optimisation process.

- **Outer approximation methods**: These algorithms iteratively solve a sequence of linear programming (LP) problems to approximate the optimal solution to the MINLP problem.

The MINLP approach has many advantages, including the following:

- It can be used to solve a variety of optimisation problems, including problems with multiple objectives, multiple constraints, and both continuous and discrete variables.
- Since it can handle both continuous and discrete variables, it can be used to solve problems that involve both types of variables, such as scheduling problems.
- It can handle problems with complex, non-linear objective functions and constraints.
- It can handle both hard and soft constraints.

However, The MINLP approach has some limitations, including the following:

- Usually, MINLP problems are computationally intensive and time consuming because of the non-linearity of the objective functions or constraints.
- In some cases, large or complex problems can be difficult to solve because the solution process can involve finding the optimal solution to a sequence of non-linear sub-problems.
- In some cases, an initial guess or starting point is required, which can have a significant impact on the final solution.
- solvers of MINLP can depend on the choice of solver parameters, such as tolerances or convergence criteria, which can result in poor performance or even failure to find a solution.
- It can sometimes fail to converge on a solution, either because the problem is too difficult or because the algorithm gets stuck in a local optimum.

Various solvers are available on the market that can solve different types of numerical optimisation methods. Table 3-1 shows the capability of different solvers to solve different types of optimisation problems [215].

Table 3-1 Comparison of different solvers in terms of problem type.

Solver	Developer	LP	CP	MIP	MILP	MIQP	NLP
CPLEX	IBM	✓	✓	✓	✓	✓	✓
XPRESS	FICO	✓	✓	✓	✓	✓	✓
GUROBI	GUROBI	✓	✓	✓	✓	✓	×
KNITRO	Ziena Opt. Inc	✓	×	×	×	×	✓
GLPK	GNU project	✓	×	✓	×	×	×
Lindo	Lindo Systems Inc.	✓	×	✓	✓	✓	✓
MOSEK	Mosek Aps	✓	×	✓	✓	×	×

Optimisation solvers are generally classified in terms of licencing into paid ones, such as CPLEX, GUROBI, and XPRESS, and open-source ones, such as Lindo and GLPK. However, GUROBI offers a free academic licence. Choosing a specific solver mainly depends on the problem type, programming language, and performance benchmarks. The solver GUROBI is known for its fast solution times, often outperforming other solvers such as CPLEX and XPRESS in many problem instances. Additionally, the solver is compatible with many programming languages and environments such as Python, MATLAB, and Java [216]. Various solvers can solve MINLP optimisation problems, such as XPRESS and Lindo. However, a limited number of solvers are able to solve non-convex MINLP, such as COIN-OR Couenne, a C++-based open-source solver established in 2006 by IBM and Carnegie Mellon University as part of a joint effort to develop algorithms for solving MINLP problems [217]. It is designed to find globally optimal solutions for convex and non-convex optimisation problems with continuous and discrete variables. Finally, in this thesis, the proposed optimisation models in chapters 5, 6, and 7 are solved using the branch-and-bound approach, since the used solvers, GUROBI and COIN-OR Couenne, are adopting this approach to solve MILP and MINLP optimisation problems [216], [217].

3.3 Microgrid Modelling Tools

Microgrids design and development involve a multi-step process that requires comprehensive analysis, resource planning, and a comprehensive knowledge of microgrid operation. To achieve specific goals and objectives, microgrids are designed with a particular purpose in mind, which requires a detailed planning and execution process that involves conceptualising the microgrid purpose, planning its parameters such as load profile and DER costs, conducting a techno-economic analysis, conducting a power system analysis, constructing the microgrid network with a desired

control system, and the microgrid operating [218] The techno-economic analysis to optimally sizing the microgrid is delivered by several methods, including analytical methods, probabilistic methodology, artificial intelligence, and software modelling. Microgrid modelling tools are frequently utilised in the techno-economic and power system analysis stages to ensure cost effectiveness, optimal placement of DERs, and stable operation of the microgrids. In addition, some microgrid modelling software enables the analysis of microgrids reliability and resilience during unexpected events or contingencies. Effective microgrid design software requires both techno-economic and power system analysis capabilities. However, few of the existing microgrid design tools have the capability of power system analysis. Table 3-2 shows a comparison of some common microgrid modelling software.

Table 3-2 Microgrid modelling tools comparison.

Features	HOMER Pro	XENDEE	SAM	REopt	DER-VET
Simulation	✓	✓	✓	✓	✓
Optimisation	✓	✓	×	✓	✓
Resiliency	×	✓	×	✓	✓
Sensitivity analysis	✓	✓	✓	×	✓
Ancillary services	×	✓	×	×	✓
Web-based	×	✓	×	✓	×
Complete reporting	✓	✓	✓	✓	×
Utility rates modelling	✓	✓	✓	✓	✓
Incentives	×	✓	✓	✓	✓
Conventional generation (e.g., diesel, and coal)	✓	✓	✓	✓	✓
Free – open source	×	×	✓	✓	✓
Beginner software	×	×	✓	✓	×
Advanced software	✓	✓	✓	×	✓
Short circuit analysis	×	✓	×	×	×
Power flow modelling	×	✓	×	×	×
Residential and commercial (behind the meter)	✓	✓	✓	✓	✓
Residential and commercial (front of the meter)	✓	✓	✓	✓	×
Power purchase agreement	✓	✓	✓	×	×
Solar PV	✓	✓	✓	✓	✓
Wind turbine	✓	✓	✓	✓	✓
Battery storage	✓	✓	✓	✓	✓
Thermal storage	✓	✓	×	✓	✓
Fuel cells	✓	✓	✓	×	×
EV charging	×	✓	×	×	✓
Hydropower	✓	✓	×	×	×
Geothermal	×	×	✓	✓	×
Biomass	✓	✓	✓	×	×
References	[81], [103]	[219]	[220]	[221]	[222]

The Hybrid Optimisation of Multiple Energy Resources (HOMER Pro) by HOMER Energy is the global standard for optimum microgrid design, with simulation, optimisation, and sensitivity analysis as tools. The software is widely used as a sizing tool in the literature [83], [105], [106], [223], where a series of simulations are performed to find the optimal HRES size that has the lowest net present cost. The tool evaluates different suitable combinations considering the cost and availability of energy resources [81]. Simulation, optimisation, and sensitivity analysis are the three primary functions of HOMER Pro. In the simulation process, the performance of a proposed system configuration includes energy balance calculations for each hour of

the year. The electric and thermal demands are satisfied in each time step by the system component's energy output, and the energy flow of each component is obtained. In addition, the battery charging and discharging processes for each time step are calculated in this stage. For each considered system configuration, HOMER Pro defines whether the proposed system is feasible and then calculates the project life-cycle cost over the considered period for feasible systems. In the optimisation process, HOMER Pro simulates a variety of system configurations to find the one that best meets the technical limitations while also being the most cost effective over the project lifetime. The objective function of HOMER Pro is to identify the optimal system configuration that minimises the total net present cost of the system while meeting the required energy demands and technical constraints.

The user can choose between two primary optimisation algorithms to find the lowest life-cycle cost: (1) grid search algorithm, which simulates all feasible configurations within a defined search space; and (2) HOMER Optimiser, which is a proprietary derivative-free algorithm. Finally, to evaluate the changes in the input, HOMER Pro repeats the analysis according to user-defined uncertainties in the sensitivity process, such as the change in the average annual wind speed, fuel and technology prices change in future, and discount rate change. The full process of HOMER Pro is shown in Figure 3-1, where the relation between simulation, optimisation, and sensitivity is shown in the analysis [224]. As seen in the oval shape, the optimisation process surrounds the simulation process, which indicates that out of all possible combinations in the simulation process, the optimal configuration is obtained in the optimisation process based on user preferences. Similarly, the sensitivity process surrounds the optimisation process, which indicates that each single sensitivity analysis consists of multiple optimisation processes.

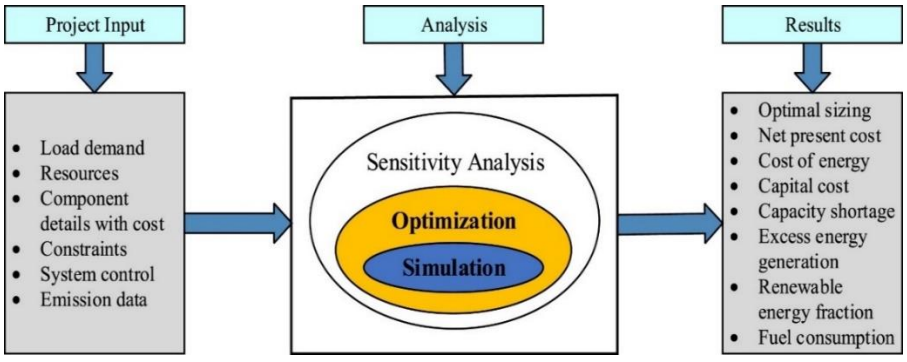

Figure 3-1 HOMER Pro workflow [224]**.**

The tool is popular, user-friendly software for modelling, simulating, and optimising microgrids and distributed energy resources. Its strengths include a comprehensive library of components, optimisation capabilities, sensitivity analysis, scalability, and robust reporting features. However, it has limitations, such as simplified electrical modelling, limited representation of grid constraints, usage of average monthly solar data rather than hourly data, and being proprietary software, which may restrict customisation and accessibility. Despite its limitations, HOMER Pro is still a valuable tool for designing and optimising hybrid renewable energy systems. It has been shown to provide results that are in close proximity to actual results, and it is widely used by engineers and researchers around the world [218], [103].

The state-of-the-art XENDEE cloud-based optimisation engine platform by XENDEE Corporation optimally selects, sizes, and dispatches microgrid DERs considering economic and physical constraints over a defined project length [219]. The platform combines the Distribution System Simulator (OpenDSS) software to perform power system analysis and the Distributed Energy Resources Customer Adoption Model (DER-CAM) to perform techno-economic analysis. The XENDEE scripts can be modified to simulate DERs such as inverter characteristics, second-to-second to yearly timelines for small- or large-scale PV integration, power flow analysis, microgrid project management, motor-starting analysis, short circuit analysis, one-line diagram design, and scenarios with higher levels of penetration that require analysis of feeder loading and grid impact. The XENDEE simulates input data sets such as load using full-scale time-series (8,760 data points for hourly resolution or 35,040 for 15 min resolution) and a down-sampling peak-preserving approach where hourly demand data are reduced into three types of profiles for each month, including typical weekday, peak day, and weekend day [225], [226]. Each day type is constructed with an hourly resolution of 24 h.

The objective function of XENDEE software is to identify the optimal design and configuration of distributed energy resources and microgrid systems that minimise the total life-cycle cost while meeting the required energy demands, reliability, and resilience objectives, as well as adhering to any technical, environmental, and regulatory constraints. The optimisation problem is formulated using MILP and, in some cases, MINLP approaches [219]. These mathematical programming techniques enable the software to model discrete decisions, such as the choice of equipment and

its sizing, as well as continuous variables, such as the amount of energy generated, stored, or consumed. Two different dispatch strategies during outages can be simulated by XENDEE [219]. Multi-day discharge, which is suitable for long-duration outages (usually 24 h and over) is used to ensure that battery discharge has sufficient energy over multiple days, whereas a conservative dispatch strategy, called the end-of-day recharge, is considered during less than 24 h outages. The battery should recharge to pre-outage level by the end of the day to avoid battery oversizing. The platform is used to manage over $3 billion in microgrid projects in various critical and non-critical projects such as army bases, companies, universities, and rural areas, which ensures its validity [227], [228]. The full process of XENDEE is shown in Figure 3-2.

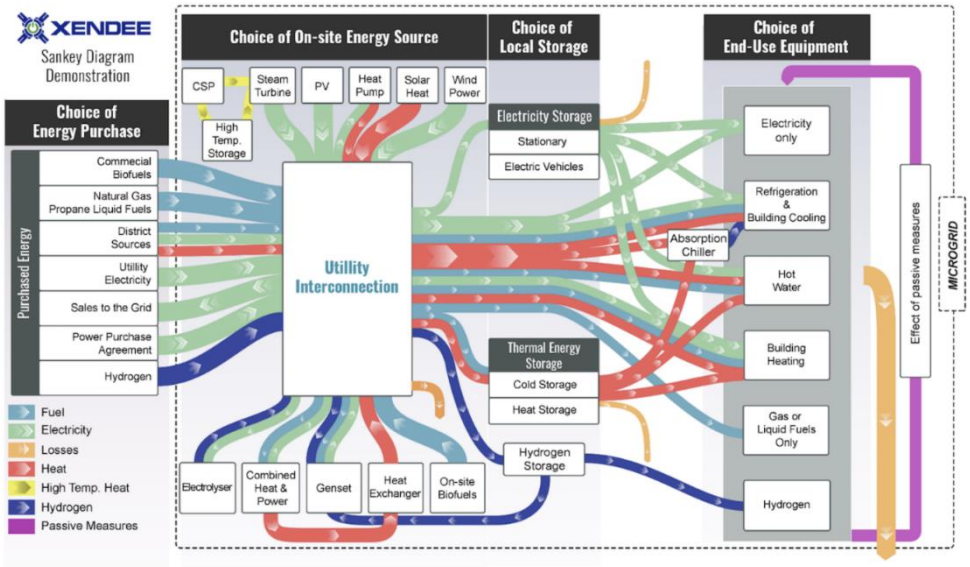

Figure 3-2 Sankey diagram for XENDEE workflow [226]**.**

The tool's key advantages include comprehensive capabilities, which combine power system analysis and techno-economic assessment; customisability, where users can modify tool scripts to simulate diverse DER aspects; and advanced optimisation techniques, which include both MILP and MINLP based on the required objective. It also includes a wide range of distributed energy resources and EV modelling. A recent update has expanded the distributed energy resources simulation to include additional technologies such as fuel cells and green hydrogen production. Additionally, other strengths include scalability from small residential systems to large commercial or industrial installations, detailed input data handling, and a proven track record in managing various microgrid projects. However, XENDEE is an advanced proprietary

tool that requires intensive learning, subscription fees, and internet access. Despite its limitations, the platform is still a robust tool for designing and optimising microgrids.

Renewable Energy Integration and Optimisation (REopt) by the National Renewable Energy Laboratory (NREL) is a techno-economic tool for optimising energy systems for microgrids, buildings, campuses, and communities. The tool is used to optimise the integration and operation of behind-the-meter energy assets. The tool uses time-series data sets from 1 min to hourly resolution, in which energy balances and operational constraints are ensured at each time step [221]. The REopt minimises the project life-cycle cost of energy using a single year, assuming constant production and consumption overall years of the desired analysis period. It can model both grid-connected and island microgrid operation modes. The optimisation problem aims to minimise the life-cycle cost using the MILP approach [221].

The System Adviser Model (SAM) is a free techno-economic software model that facilitates decision-making for people in the renewable energy industry [220]. The tool offers a consistent framework for examining and contrasting power system expenses and performance across various solar technologies and markets. This ranges from photovoltaic systems for residential and commercial sectors to concentrated solar power and sizeable photovoltaic systems for utility markets. The tool combines an hourly simulation model with performance, cost, and finance models to calculate energy output, energy costs, and cash flows. The Distributed Energy Resources Value Estimation Tool (DER-VET) offers a complimentary, publicly available, open-source platform for determining, comprehending, and optimising the value of distributed energy resources by considering their technical strengths and limitations [222]. The tool utilises load information and other site-specific data to simultaneously optimise the sizing of distributed energy resources in conjunction with optimising their dispatch. The dispatch optimisation incorporates time-series data on customer and system electric loads and energy and ancillary service prices in either hourly, 15 min, 10 min, or 5 min resolution. The optimisation problem aims to maximise the economic benefits using the MILP approach [222].

3.4 Summary of Key Findings

The aim of this chapter has been to review the modelling methods and tools available to promote the integration of distributed energy resources and microgrids, which can support the transition to sustainable energy. The purpose of the study is to determine

the best modelling approaches and tools to be used in this thesis. The key findings are listed as follows:

i. The optimisation modelling technique will vary based on the objective function and constraint formulation. The use of binary integers in the optimisation problem formulation will increase the amount of time it takes to find the optimal solution, but they are necessary to be used to formulate the EGSE availability status.
ii. Solver choice will vary depending on optimisation problem formulation, programming language, and performance benchmarking. However, this must be carefully chosen for MINLP due to the lack of available solvers that can solve non-convex MINLP optimisation problems.
iii. Modelling tools for distributed energy resources and microgrids are essential for economic analysis. However, in some cases, careful planning may be required depending on the desired analysis and the types of distributed energy resources involved.
iv. The ancillary services that distributed energy resources can deliver need to be widely included within modelling tools. This could be a key enabler in developing the growth of distributed energy resources and demand response.
v. The electrification of transportation plays a pivotal role in the mitigation of carbon emissions. However, the modelling of EV charging is not included in the distributed energy resource modelling tools.

In chapters 4 and 5, the modelling tools used to analyse the integration of distributed energy resources at airports are conducted using HOMER Pro, due to its capability to model power-to-hydrogen-to-power systems, and XENDEE, due to its capabilities to model resiliency and EGSE charging. In chapters 6 and 7, the solver package GUROBI is used to tackle the MILP because it has a high performance for solving such types of optimisation problems compared to other solvers. Additionally, it is compatible with many languages, such as MATLAB, and is freely available to academia. Finally, chapter 8 utilises the open-source package COIN-OR Couenne due to its capability in handling MINLP problems.

Chapter 4

A Techno-Economic of Distributed Energy Resources at a Civilian Airport Using HOMER Pro

4.1 Introduction

The objective of this chapter is to investigate the possibility of implementing HRES within the airport geosystem. This chapter introduces a techno-economic assessment of different sizes of grid-connected HRES to meet airport electrical loads. A comparison was made with respect to using different solar PV, hydrogen FC, and battery storage system sizes. The HRES economic evaluation is made with the help of the HOMER Pro analysis tool. As opposed to previous studies [105], [106], [223], the work in this chapter evaluates HRES, including solar PV and hydrogen FC, as a grid-connected system, considering the available areas to optimally install commercial sizes of PV and hydrogen FC at airport premises. In addition, compared to [114], where hydrogen FC is only used to supply aircraft remote stands, this chapter assesses the on-site production of green hydrogen to supply the whole electrical load.

4.2 Methodology for the Proposed Hybrid System

The proposed grid-connected HRES model to serve an airport load consists of solar PV, lithium ferro phosphate (LFP) batteries, hydrogen FC, an electrolyser, and a hydrogen tank, as shown in Figure 4-1. The HOMER Pro package is used to design and evaluate the proposed HRES. The energy is generated on-site by solar PV and hydrogen FC.

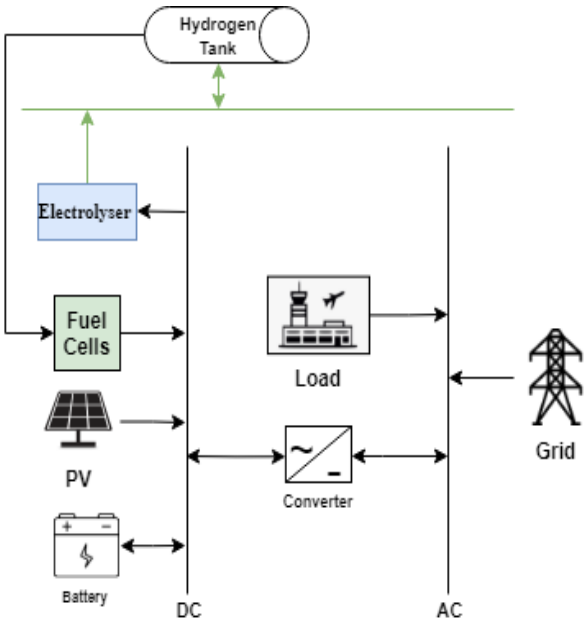

Figure 4-1 Proposed HRES configuration.

In addition, the energy flow is bi-directional, where energy can be imported and exported from/to the grid. The electrical load is supplied by the grid utility when distributed energy resources (DERs) have insufficient power output to supply the load. Whereas the excess energy produced by DERs is either locally stored or sent back to the grid. Moreover, LFP batteries and hydrogen are used to store energy, which increases the HRES reliability. The proposed methodology is shown in Figure 4-2.

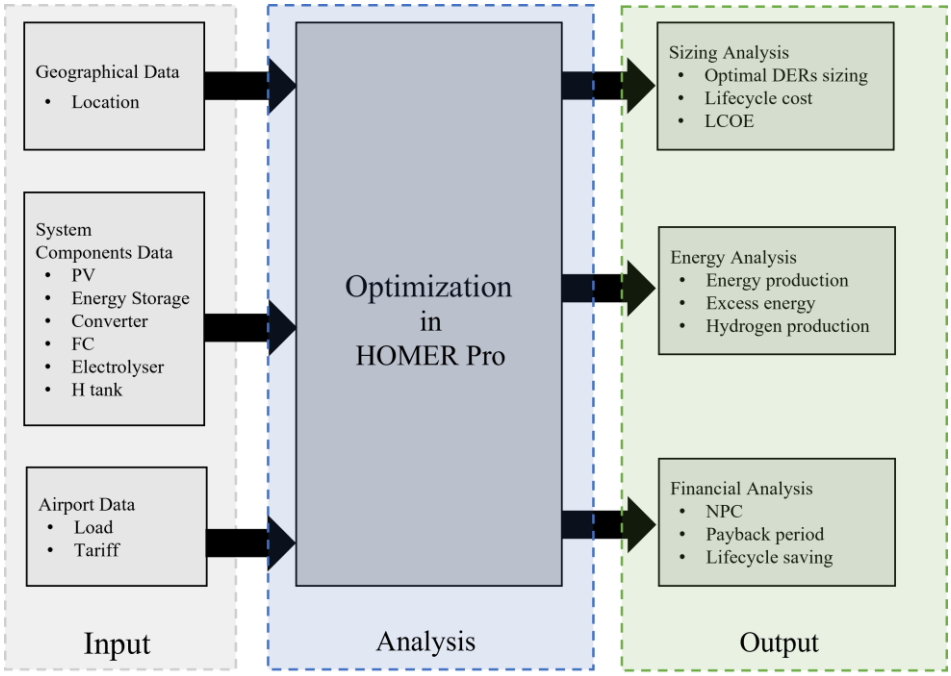

Figure 4-2 HRES sizing and dispatching methodology.

In the modelling tool HOMER Pro, airport location was entered as a parameter. Based on this location, the software then automatically generated the corresponding solar irradiance and temperature data from its integrated databases. The technical and economic data for the proposed HRES components were inputted into the software. This includes technical data such as nominal voltage, losses, efficiency, nominal operating cell temperature, and fuel curves of fuel cells, as well as economic data such as capital, replacement, and O&M costs, and component lifetimes. Finally, the airport electric load and tariff data were fed to the software.

In the second stage, HOMER Pro optimises different possible HRES configurations and sizes with the aim of minimising the net present cost [81]. In each step, HOMER Pro dispatches the power-producing components of the system to serve the total electrical load. The output of the optimisation process includes various feasible HRES configurations ranked according to lowest net present cost. Additionally, feasible

systems are compared with the base case using various economic indicators, such as the levelised cost of energy and payback period. The results for each viable system also encompass the yearly dispatch of the component, along with the corresponding costs and savings.

4.3 Case Study: Seve Ballesteros-Santander Airport

The Seve Ballesteros–Santander (SDR) airport data was used to investigate the monetary value of the proposed HRES using HOMER Pro Version 3.14.5 on a desktop computer with a 64-bit Windows 10 operating system, an Intel® Core™ i7 CPU @ 3.4GHz, and 16 GB of RAM. The airport was selected for this study due to the public availability of its load data online. The SDR is a medium-sized airport because between 0.3–0.4% of the country's annual passenger enplanements use the airport each year [229]. It is located in the north of Spain and has a total annual consumption of 3GWh/yr [230]. The peak load is 637 kW. Figure 4-3 displays the airport hourly load profile for 2015, which was inputted into the software as a parameter. The airport has more than 90,000 m^2 of shade-free area between the terminal and taxiway, which is enough to install up to 10 MWp of PV. The simulated airport monthly average global solar irradiance (GHI) and temperature are shown in Figure 4-4.

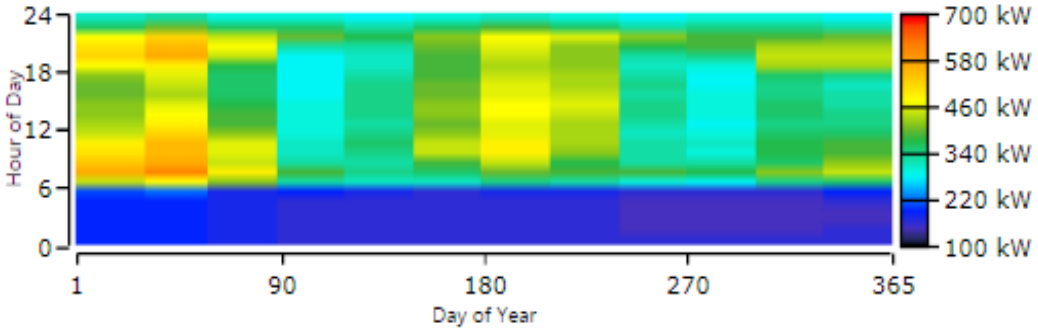

Figure 4-3 Airport hourly electrical demand [230]**.**

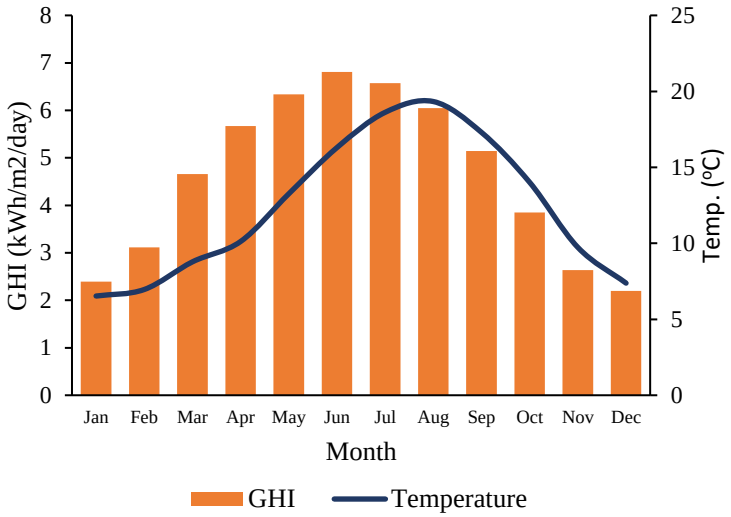

Figure 4-4 Airport average GHI and temperature.

The electricity tariff is shown in Table 4-1 [231]. The U.S. dollar is used here since it is a standard global currency. In addition, the simulated PV size varies from 10kW to 10MW. Fuel cells and electrolysers capacity sizes range from 50–750kW. The battery and converter are optimally sized by HOMER to satisfy the HRES configuration. Hydrogen tank size changes between 10–1,000kg. The project lifetime, discount rate, and inflation rate are 25 yrs, 8%, and 2%, respectively [89], [232], [233]. The techno-economic parameters of HRES components are shown in Table 4-2.

Table 4-1 Electricity tariff.

Time	Consumption Rate $/kWh	Demand Rate $/kW/month	Sellback Rate $/kWh
00:00-7:00 & 22:00-23:00	0.15	1.44	
8:00-9:00 & 14:00-17:00	0.17	2.5	0.05
9:00-13:00 & 18:00-21:00	0.19	2.95	

Table 4-2 Technical and cost parameters of components.

Component	Capital Cost	Replacement Cost	O&M Cost	Efficiency	lifetime	Ref.
PV	887$/kW	887$/kW	8$/kW/yr	17.7%	25yrs	[89]
FC	3,000$/kW	3,000$/kW	0.02$/kW/yr	50%	60,000h	[89], [223]
Electrolyser	1,500$/kW	1,500$/kW	20$/kW/yr	80%	15yrs	[89], [233]
H Tank	1,100$/kg	1,100$/kg	20$/kg/yr	-	25yrs	[89], [223]
Converter	180$/kW	180$/kW	7$/kW/yr	98%	15yrs	[223]
Batteries	690$/kWh	690$/kWh	10$/kW/yr	98%	10yrs	[89]

In the present methodology, the variations of load demand within weekdays of each month have not been considered as the available dataset of the airport only contained the average monthly load demand on an hourly basis. The software does not consider the variations in voltage and current fluctuations from the supply side. Instead, it only considers the power output as a whole. This means that HOMER Pro may not be able to provide accurate results for systems that are connected to a grid with significant voltage and current fluctuations. As a result, the analysis yields an approximate outcome rather than an exact one. Although HOMER has its constraints, it can still generate numerous in-depth theoretical outcomes that closely resemble real-world results. As a globally popular tool for such analyses, HOMER has been employed in this study.

4.4 Results and Analysis

This chapter proposes grid-tied HRES consisting of PV/hydrogen FC to power a civilian airport. Different feasible combinations of sizes are identified and compared based on NPC and LCOE. Table 4-3 lists the sets of feasible HRES during the 25yr project lifetime, comparing the current situation of the airport connected to the primary grid (grid-only). The NPC and LCOE in the case of grid-only are $7.16 million and $0.19, respectively.

Table 4-3 HRES components.

Component	Hybrid Renewable Energy System			
	HRES1	**HRES2**	**HRES3**	**HRES4**
PV (MW)	1.1	1.4	1.2	2.2
FC (kW)	50	50	100	100
Electrolyser (kW)	50	50	100	100
H tank (kg)	20	20	70	50
LFP-battery (kWh)	-	20	-	-
Converter (kW)	670	715	652	710
NPC (million$)	6.3	6.4	7.3	7.4
LCOE ($/kWh)	0.15	0.14	0.19	0.19
Electricity Production (MWh/yr)	3,392	3,624	3,707	4,600

Table 4-3 demonstrates the optimal HRES is the HRES1 configuration, which comprises 1.1MW of PV panels and 50kW of FC. The NPC of the HRES1 configuration is reduced by about $0.8 million compared with the grid-only base case. The optimal hybrid system payback period is 10.8 yrs. Moreover, the NPC of HRES2 is $6.4 million, and the payback period is 12 yrs. The net present cost increase for

HRES3 is higher than the grid-only base case by about $0.2 million. The same case is seen in HRES4, where NPC rises by $0.3 million.

Figures 4-5 show the cost of HRES components. The major costs are related to PV installation and O&M costs. Fuel cell replacement cost is zero, which indicates that FC operates less than its lifetime in all HRES.

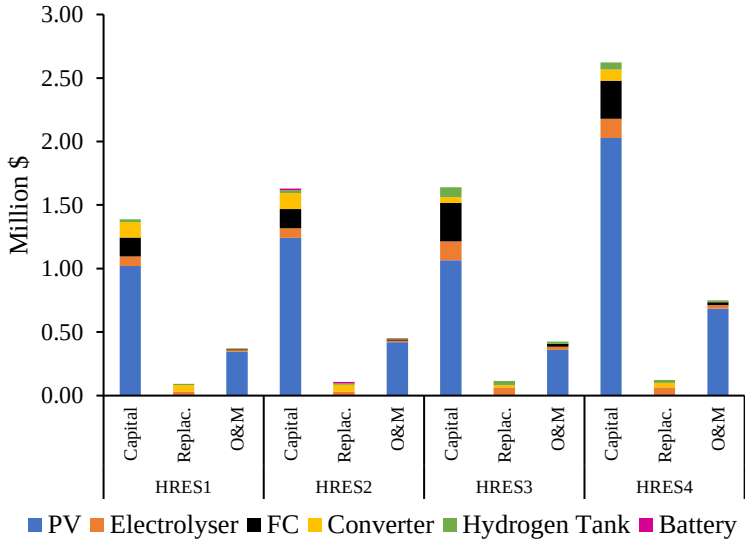

Figure 4-5 Costs of HRESs components.

Figures 4-6 show the yearly electricity production by sources of HRES. In the optimal HRES1, the generated electricity by PV represents 42% and grid purchasing is 57.3%. While FC generates about 0.7% of HRES1's total yearly production. Furthermore, the FC production is slightly increased to 0.8% in the HRES2 configuration. Solar PV production is about 48% while the grid provides 51.2% of electricity. In the case of HRES3, PV and FC generate about 40% and 1.8% of renewable energy, respectively. PV and FC generate about 62% and 2% of the total electricity produced in the case of HRES4, respectively.

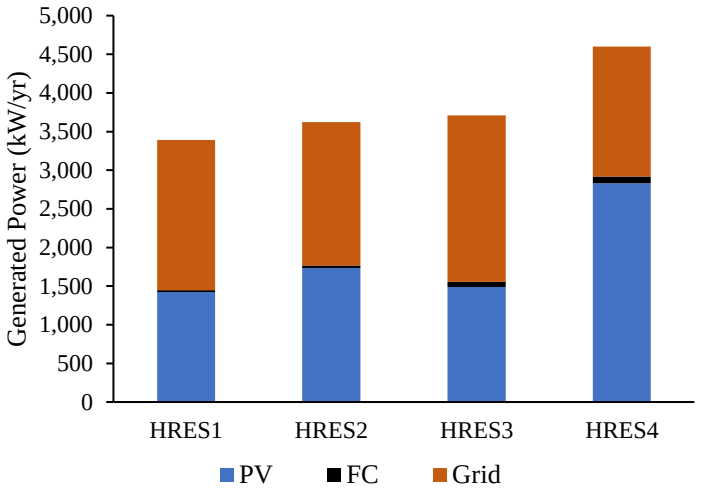

Figure 4-6 Electricity sources of HRESs.

Annually produced on-site green hydrogen is shown in Figures 4-7. Hydrogen is produced by an electrolyser, which is 100% powered by solar PV. In HRES1, the electrolyser consumes about 74MWh/yr to produce about 1,500kg of hydrogen/yr, while in HRES2, the electrolyser consumes around 91.4MWh/yr to generate about 1,850kg of hydrogen. The electrolyser requires about 203.8MWh/yr of input energy to generate about 4,100kg of hydrogen in HRES3. The highest amount of hydrogen produced is around 5,000kg in HRES4, which requires nearly 248MWh/yr of input energy.

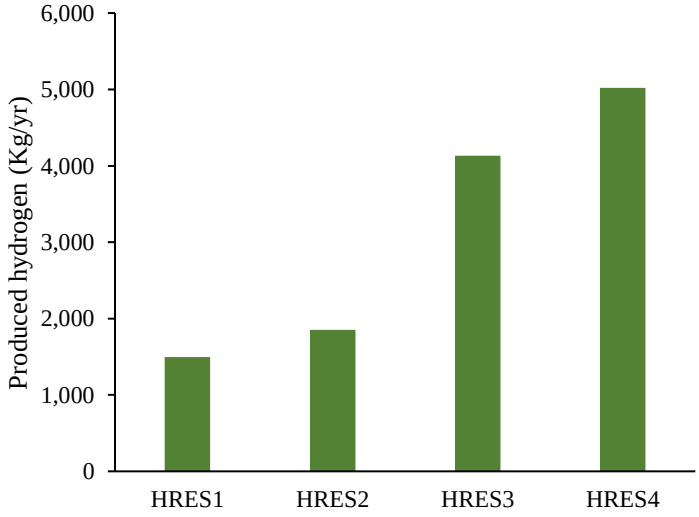

Figure 4-7 Amount of hydrogen produced.

Figures 4-8 to 4-12 illustrate the power output and input from the components of the optimal system, HRES1. The airport load is predominantly powered by solar PV during daylight hours, producing surplus energy that is fed back into the grid and is fully supplied by the grid during night-time hours.

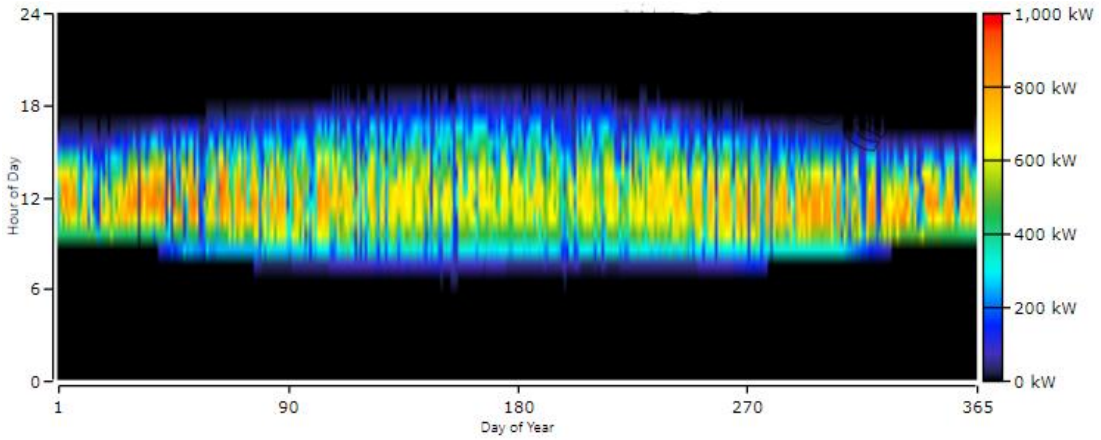

Figure 4-8 Solar PV hourly output power.

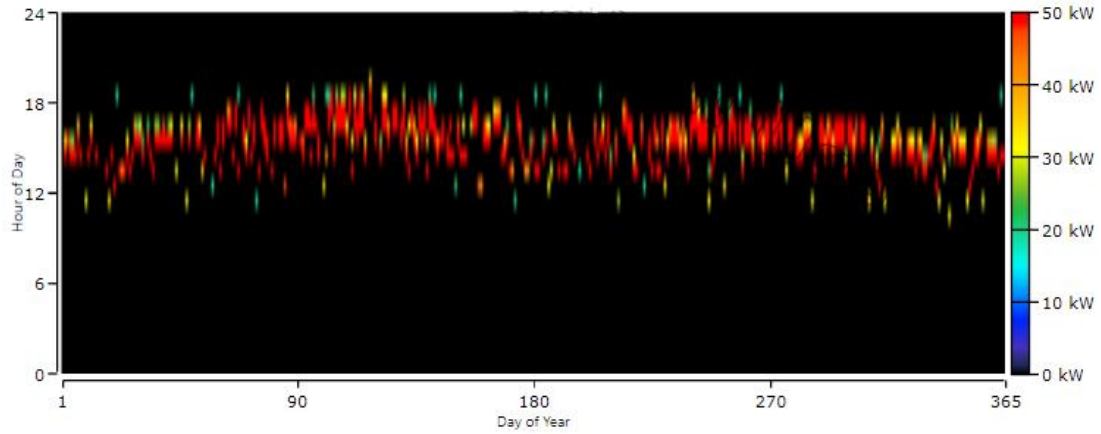

Figure 4-9 Fuel cells hourly output power.

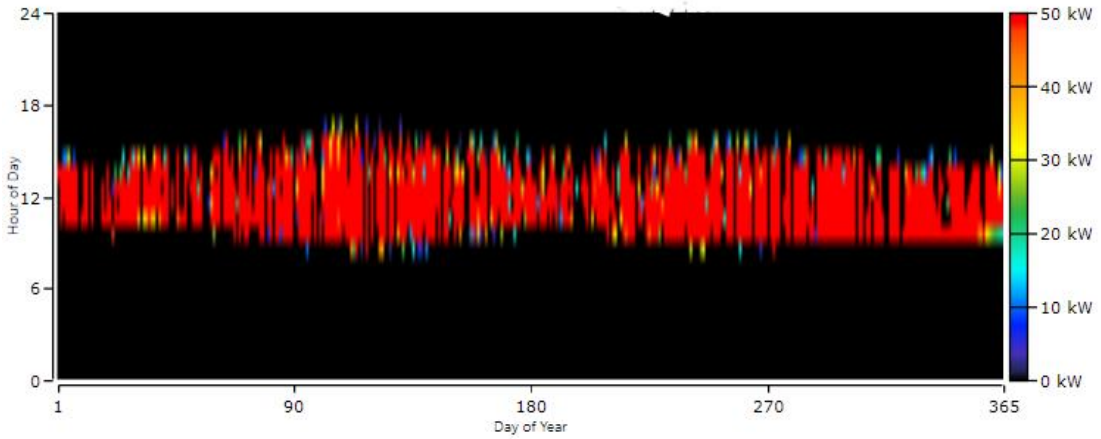

Figure 4-10 Electrolyser hourly input power.

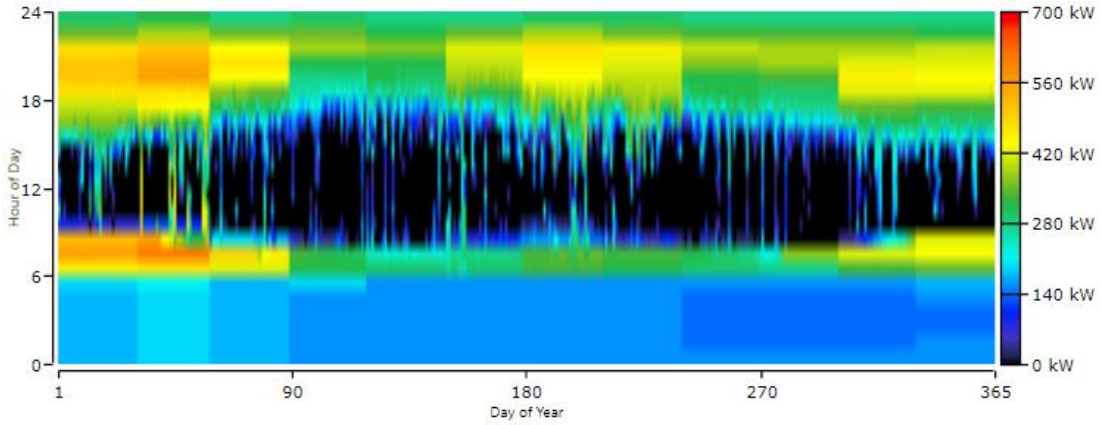

Figure 4-11 Electricity purchased from grid.

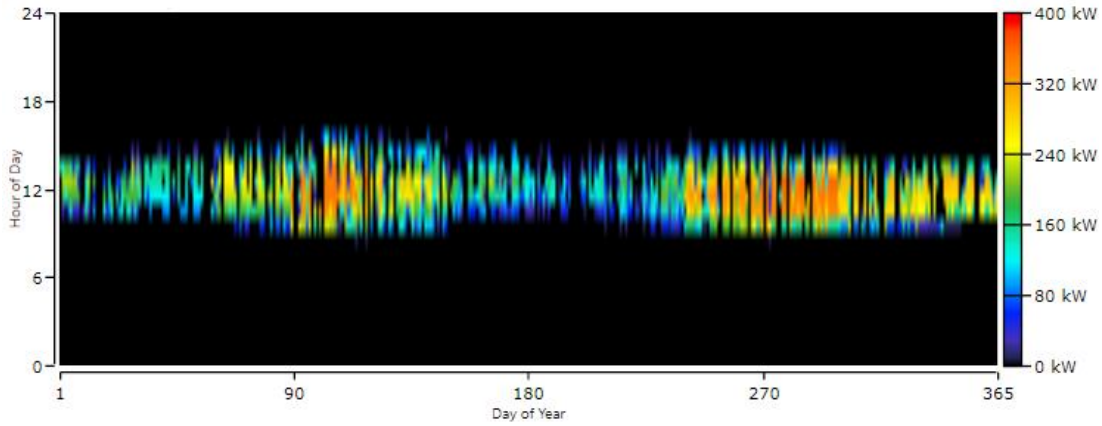

Figure 4-12 Electricity sold to grid.

4.4.1 Emissions Abatement and Financial Savings

The environmental impact of power generation and consumption is a critical consideration in the design of sustainable airports. Given the carbon emission factor of 190gCO_2eq/kWh in Spain [234], [235], the airport contributes to 569,100kg/yr of CO_2 emissions in the base-case scenario. Through the implementation of the first hybrid renewable energy system configuration (HRES1), a substantial reduction of around 35% in these emissions is achieved, bringing them down to 369,382kg/yr. This reduction corresponds to potential annual savings of approximately $19,570 through the European Union Emissions Trading System (EU ETS), given the average emissions allowance price of $98 per metric tonne of carbon [236]. A further reduction in emissions to 353,201kg/yr, which represents an overall reduction of approximately 38% from the base case, is facilitated by the second configuration, HRES2. This configuration could potentially lead to even greater annual savings of around $21,158 under the EU ETS.

4.4.2 Sensitivity Analysis

Understanding the dynamics of an HRES necessitates a thorough examination of how variations in the availability and cost parameters of different renewable energy resources impact the system within the given geographic area. In this study, sensitivity analysis has been applied to the optimal energy mix, specifically HRES1. This analysis considers changes in variables, such as capital expenditure for fuel cells, the electrolyser, and hydrogen storage, as well as fluctuations in energy prices. This selection of variables is primarily motivated by the fact that the costs of green hydrogen production are projected to decline in the foreseeable future. This projected decline is due to ongoing research and development and impending government policies designed to encourage its use [237]. Additionally, energy prices are known to fluctuate and escalate in response to global crises, as evidenced by the recent unprecedented energy crisis in Europe [238].

Table 4-4 shows the impact of different projected cost reductions for FC, electrolysers, and hydrogen storage on system economics. Both the NPC and LCOE consistently exhibit a rising trend as the costs of system components incrementally increase. The minimum of $6.20 million and the lowest LCOE of $0.1479 are observed when the costs of system components fall to 50% of their current values. The highest NPC and LCOE are observed when all system component costs are at their full current values. Reducing the capital costs of all green hydrogen system components by 50% results in a reduction in the LCOE of about 2.07%.

The influence of energy price increments on NPC and LCOE for the HRES1 system is detailed in Table 4-5. Notably, the base case NPC is $7.16 million, indicating that the HRES maintains cost effectiveness when energy prices remain constant, as represented by a lower NPC of $6.31 million and an LCOE of $0.151. However, any escalation in energy prices has a dramatic impact on the system's economics. A 75% increase in energy prices, for instance, results in an NPC of $9.45 million and an LCOE of $0.226, surpassing the base case NPC and thus suggesting a reduction in system cost effectiveness.

Table 4-4 Effect of capital costs change on system economics.

FC Cost Reduction (%)	Electrolyser Cost Reduction (%)	H-Tank Cost Reduction (%)	NPC (million $)	LCOE ($)
50	50	50	6.20	0.1479
50	50	25	6.21	0.1481
50	50	0	6.21	0.1482
25	50	50	6.21	0.1487
25	50	25	6.22	0.1489
25	50	0	6.22	0.1491
0	50	50	6.24	0.1494
0	50	25	6.25	0.1496
0	50	0	6.25	0.1498
50	25	50	6.22	0.1485
50	25	25	6.23	0.1487
50	25	0	6.24	0.1488
25	25	50	6.23	0.1493
25	25	25	6.24	0.1495
25	25	0	6.25	0.1497
0	25	50	6.26	0.15
0	25	25	6.27	0.1502
0	25	0	6.28	0.1504
50	0	50	6.25	0.1491
50	0	25	6.26	0.1493
50	0	0	6.26	0.1494
25	0	50	6.26	0.1499
25	0	25	6.27	0.1501
25	0	0	6.27	0.1503
0	0	50	6.29	0.1506
0	0	25	6.30	0.1508
0	0	0	6.31	0.151

Table 4-5 Effect of energy prices change on system economics.

Energy prices increment %	NPC (million $)	LCOE ($)
0%	6.31	0.151
25%	7.35	0.176
50%	8.40	0.201
75%	9.45	0.226

4.5 Discussion

The benefits of using hydrogen FC along with solar PV as a grid-connected HRES to supply airport electricity needs are cost effective to a certain limit. As Table 4-3 reveals, the results show that increasing the size of the FC, electrolyser, and hydrogen tank to increase production of on-site green hydrogen is a costly option. Even with the

availability of large solar PV sizes, the cost remains high due to the high initial cost and short life of hydrogen FC. Broadly speaking, the incorporation of a moderately sized PV system with a supporting FC provided optimal results. This resulted in a lower NPC, indicating the potential for considerable savings in long-term project life cycles. These savings, coupled with promising payback periods, suggest that such configurations could offer a cost-effective means of transitioning towards renewable energy infrastructure in airports. The primary costs associated with these hybrid systems were found to stem from PV installation and operation and maintenance (O&M), rather than FC-related costs. This indicates that a strategic blend of solar PV and hydrogen FC technology could help balance up-front costs and system longevity.

The implementation of an HRES can substantially decrease emissions, leading to a considerable reduction in environmental impact. As seen in the case study, the use of such systems can result in up to a 35% reduction in CO_2 emissions compared to conventional energy sources. This decrease not only helps in achieving environmental sustainability goals but also brings about financial benefits. Savings are potentially attainable through emission trading systems, as these systems often reward lowering emissions with economic incentives. Hence, the use of HRES can effectively help balance both environmental and economic concerns at large-scale facilities. The financial performance of an HRES is connected to the capital expenditure associated with its components, such as fuel cells, electrolysers, and hydrogen storage, along with the volatility of energy prices. Specifically, a notable decrease in these costs by 50% could result in a corresponding reduction in LCOE, thereby bolstering the economic feasibility of the system. Conversely, energy price escalations could significantly impact the system's cost effectiveness. As such, stability in energy prices is pivotal for maintaining an advantageous NPC and LCOE. The economic viability of an HRES is consequently predicated on an intricate interplay between component costs and energy market dynamics.

On-site green hydrogen production, wholly powered by solar PV, also introduces an important dimension of energy resilience. Even with a relatively low contribution to the total energy output, the generated hydrogen could be stored and used when needed and could serve as a reliable energy source during periods of high demand or low solar output. Additionally, green hydrogen shows promising results in replacing the need for electrochemical energy storage systems such as lithium-ion batteries. However,

this study's findings are subject to certain limitations, one of which being the lack of actual operational data or independently calculated data for comparison and validation of the results obtained from HOMER Pro. This restricts the study's ability to test the accuracy of the model against real-world performance. As such, while the results are promising, they should be interpreted with caution. While HOMER Pro is a widely accepted and used tool for modelling renewable energy systems, it should be noted that its predictions are based on theoretical calculations and assumed conditions, which may not perfectly align with actual system performance. Future studies could benefit from the availability of actual performance data or independently calculated results to enhance the validation of the model.

The research underscores the potential for renewable energy systems to provide a cost-effective, resilient, and sustainable energy supply for civilian airports. Despite the limitations, the study provides valuable insights for policymakers and stakeholders interested in promoting renewable energy infrastructure. Future research, equipped with actual performance data, will further enhance the validity and applicability of these findings. These findings have implications for the broader goal of reducing greenhouse gas emissions and enhancing energy security. Airports adopting such systems stand to not only make significant economic savings but also contribute meaningfully to sustainability goals. This research also highlights the importance of continued investment in data collection and validation, which are crucial for accurately assessing the feasibility and impact of renewable energy systems in the future.

4.6 Summary of Key Findings

The aim of this study was to conduct techno-economic assessments of a grid-connected hybrid renewable energy system (HRES) designed to power a civilian airport electrical load. Seve Ballesteros–Santander airport's annual electric load profile was used to evaluate the feasibility of the proposed HRES. The simulation was conducted using the HOMER Pro package. The key findings are listed as follows:

i- The analysis of the proposed HRES indicates that renewable energy sources can meet the electrical energy demand of a civilian airport. In fact, it has the potential to reduce electricity costs and direct and indirect emissions related to electricity purchases.

ii- Despite the availability of large solar PV sizes, producing green hydrogen at airports remains expensive, making the combination of small fuel cells

and solar PV a more cost-effective approach for reducing airport total electricity costs.

iii- The consideration of green hydrogen as a storage medium replaced the need for lithium batteries and reduced the HRES's total costs.

iv- The implementation of HRES can reduce emissions, leading to notable environmental and financial benefits, thereby effectively addressing both sustainability and economic concerns in large-scale facilities.

v- The economic viability of HRES hinges on the interplay between component costs, such as those for fuel cells, electrolysers, and hydrogen storage, and energy market dynamics, indicating that reductions in component costs and stability in energy prices can significantly enhance the system's cost-effectiveness.

vi- This study demonstrates that HRES can serve as a sustainable alternative to traditional energy sources for powering airports. This approach can help airports move towards achieving their sustainability goals by reducing energy consumption and emissions.

The findings reached were based on specific airport locations, sizes, and energy tariffs. Overall, the utilisation of HRES resulted in a reduction in airport electricity costs for the considered parameters. However, future investigations are recommended to examine further small, medium, and large civilian airports in different locations.

Chapter 5
Evaluating the Microgrids Resilience to Meet Airport Operational Requirements Using XENDEE

5.1 Introduction

The economic loss due to power outages within airports is significant, which emphasises the need for a robust back-up power system. Hence, this chapter proposes a technical and economic evaluation of an airport grid-connected microgrid consisting of PV, an energy storage system, and a diesel generator to enhance airport power resilience under different power interruption scenarios. A modified mixed-integer linear programming scheme is introduced to minimise the total annual operating cost of the proposed resilient system. The optimal resilient microgrid components sizing and dispatching are investigated as follows:

- with and without a monetary assigned value for resilience as a service;
- in terms of the capability to sustain power outages during solar PV performance changing; and
- with load increment from electric ground support equipment deployment.

5.2 Methodology and Optimisation Formulation

5.2.1 Methodology

The modelling software XENDEE is used to model and evaluate the resiliency of microgrids at airports. The microgrid DER components include solar PV, an energy storage system, an EGSE fleet, and a back-up diesel generator. The proposed methodology is shown in Figure 5-1.

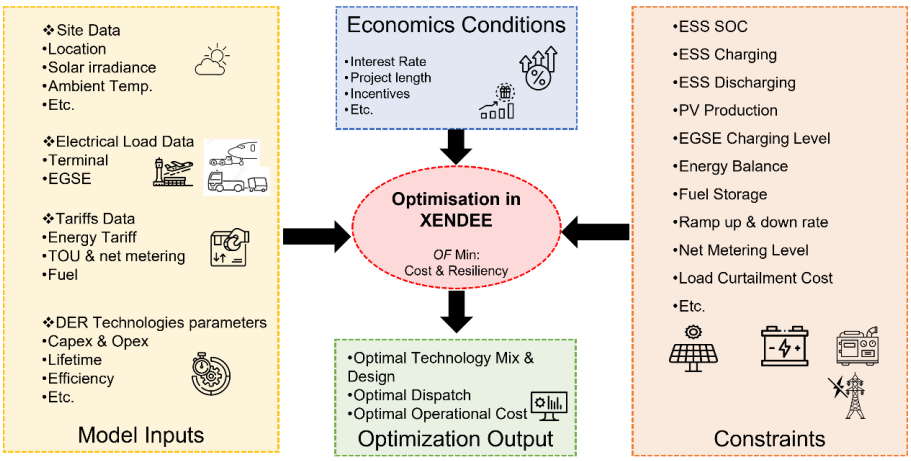

Figure 5-1 Microgrid resiliency evaluation methodology.

In the modelling tool XENDEE, the airport location was entered as a parameter. Based on this location, the software then automatically generated the corresponding solar irradiance and temperature data from its integrated databases. The technical and economic data for the proposed microgrid components were inputted into the software. This includes technical data, such as nominal voltage, losses, efficiency, and nominal operating cell temperature, as well as economic data, such as capital, replacement, and O&M costs, fuel prices, lost load costs, and component lifetimes. Additionally, the airport electric load, EGSE daily energy needs, and tariff data were fed to the software. The project lifetime, interest rate, incentives, and inflation rate were fed to the tool.

The optimisation is subjected to various constraints, including operational, economic, and an energy balance constraint, where at every time step, the demand must equal the sum of the electricity purchased and the electricity produced or consumed by technology. Constraints of DERs, such as energy storage system minimum and maximum state of charge, energy storage and charging and discharging levels, generator ramp up and down rate, fuel limits, and EGSE charging level, were considered. The energy balance was considered to be satisfied during various simulated outages. The objective function is modelled to minimise annual operational costs and associated costs with resiliency to satisfy the required energy at the critical load level. The output of the optimisation process includes the optimal DER mix and economic dispatch that satisfy airport energy needs during normal operations and grid outages. Finally, the annual operational cost of the optimal microgrid is compared with the business as usual case for various outage scenarios to show the benefits of resilient airport microgrids.

In this section, modelling is used to explore various scenarios, including the following:

i. Normal Operation: This scenario sizes and dispatches the microgrid strictly from an economic perspective, overlooking the value of resilience.
ii. Outage Criteria: This scenario assesses the optimal sizing and dispatching of a resilient microgrid under different outage criteria. These outages are characterised by varying starting times, durations, and critical load levels.
    a. Outage starting times: This sub-scenario considers grid outages that occur at different hours of the day.
    b. Outage durations: This sub-scenario acknowledges the variability and unpredictability of weather-related outage durations and investigates

the cost implications of enhancing microgrid resilience to withstand them.

c. Critical load levels: This scenario examines the need to meet various critical load levels during grid outages, which may fluctuate due to reasons such as airport operation expansion or passenger number growth.

iii. Solar PV Performance Changes: This scenario looks into the sizing and dispatching of a resilient microgrid during periods of decreased solar PV power output during outages.

iv. Load Management: This scenario considers the value of lost loads.

5.2.2 Optimisation Formulation

The optimisation problem is modelled using a modified mixed-integer linear programming based on the XENDEE platform [219]. The objective function in Equation (5.1) aims to minimise the total operational cost of microgrid, where C_{grid} indicates the purchased energy and demand cost in \$, C_{DER} represents purchasing and operating cost of DERs in \$, C_{fuel} refers to fuel cost in \$, C_{resi} refers to lost load cost in \$, and r_{sales} donates energy exporting income in \$ [109].

$$\min C: C_{grid} + C_{DER} + C_{fuel} + C_{resi} - r_{sales} \tag{5.1}$$

Equations (5.2), (4.3), (4.4), (4.5), and (5.6) represent the objective function components in terms of decision variables. The first part of Equation (5.2) represents electricity purchasing costs, the second part represents demand costs, and the third part represents electricity generating costs.

$$C_{grid} = \sum_{m} Uf_m + \sum_{m,d,h} Vu_{m,d,h} \cdot U_{m,d,h} \cdot ND_{m,d} + \sum_{p} \max(U_p) \cdot Cd_p + \sum_{m} \left[\sum_{g} PN_g \cdot SG_g + \sum_{k} PT_k \right] \cdot SC_m \tag{5.2}$$

where Uf_m is the utility fixed monthly cost in \$, $Vu_{m,d,h}$ is the utility energy tariff in \$/kWh, $U_{m,d,h}$ is the grid purchased energy in kWh, $ND_{m,d}$ is the number of days in month m, PN_g is the number of purchased diesel generators, Cd_p is the demand price in \$/kW, SG_g is the capacity of diesel generator in kW, PT_k is the capacity of

purchased technologies of type k in kW, and SC_m is the utility standby charge in \$/kW. In addition, $m \in M$ is set of months, $d \in D$ is set of day type, D = {peak, week, weekend}, $h \in H$ is set of hours, $p \in P$ is set of tariff demand period, $g \in G$ is set of diesel generators, $k \in K$ is set of renewable, K = {PV, Batteries}, and $t \in T$ is set of all technologies, T = G ∪ K. Equation (5.3) indicates the annualised purchasing, operating, and variable plus fixed maintenance costs of DER technologies.

$$C_{DER} = \sum_{g} PN_g \cdot SG_g \cdot OM_g + \sum_{k} PT_k \cdot OM_k + \sum_{m,d,h,t} P_{m,d,h,t} \cdot ND_{m,d} \cdot Va_t + \sum_{g} PN_g \cdot Ic_g \cdot ANN_g + \sum_{k} [PT_k \cdot If_k + PT_k \cdot Iv_k] \cdot ANN_k \quad (5.3)$$

where OM indicates the annual O&M cost \$/kW, Va_t represents variable O&M cost of technology t in \$/kWh, and $P_{m,d,h,t}$ represents energy provided by technology t in kWh. Ic_g indicates the capital cost per unit in \$, and ANN represents annualised investment rate of technology. If_k and Iv_k refer to fixed and variable costs of purchased technologies of type k in \$, respectively. The purchased fuel cost and exported energy are calculated using Equations (5.4) and (5.5), respectively.

$$C_{fuel} = \sum_{m,d,h} FP_{m,d,h} \cdot ND_{m,d} \cdot Vf_{m,d,h} \quad (5.4)$$

$$r_{sales} = \sum_{m,d,h} \sum_{t} S_{m,d,h,t} \cdot Px_{m,d,h} \quad (5.5)$$

where $FP_{m,d,h}$ is the purchased fuel in litre, $Vf_{m,d,h}$ is fuel price in \$/litre, $S_{m,d,h,t}$ represents the exported energy by technology t in kWh, and $Px_{m,d,h}$ is the energy sellback price in \$/kWh. In addition, Equation (5.6) describes the cost of lost electrical load during power outages.

$$C_{resi} = \sum_{m,d,h,pr} DC_{m,d,h,pr} \cdot Vl_{pr} \quad (5.6)$$

where $DC_{m,d,h,pr}$ represents the lost demand of level pr in kWh, Vl_{pr} is the value of lost load in \$/kWh, and $pr \in PR$ is set of demand priority, PR = {high critical, low critical, non-critical}. The objective function is subjected to constraints in Equations (5.8), (5.9), and (5.10).

$$L_{m,d,h} + \sum_{t \in T} \left(S_{m,d,h,t} + K_{m,d,h,t} \right) = \sum_{t \in T} P_{m,d,h,t} + U_{m,d,h} \quad (5.8)$$

$$U_{m,d,h} \leq \bar{U}_{m,d,h} * A_{m,d,h} \quad (5.9)$$

$$EPV_{m,d,h} = C_{PV} \cdot PVn_{m,d,h} \quad (5.10)$$

Equation (5.8) manages microgrid energy balance for each time step to ensure total load including energy demand $L_{m,d,h}$ in kWh, energy export $S_{m,d,h,t}$ in kWh, and energy consumed by energy storage system $K_{m,d,h,t}$ in kWh is supplied by utility grid $U_{m,d,h}$ in kWh, and DERs $P_{m,d,h,t}$ in kWh. In addition, Equation (5.9) forces energy purchases from the utility during outages to be zero, where $A_{m,d,h}$ represents grid availability $\in$ [0,1]. Solar PV produced electricity$EPV_{m,d,h}$ in kW is calculated in Equation (5.10), where location, temperature, panels type, and orientation control the solar PV normalised performance $PVn_{m,d,h}$ which multiply by solar PV capacity C_{PV} in kW. The storage system constraints include state of charge SOC, charging and discharging demonstrated in Equations (5.11), (5.12), (5.13), (5.14), and (5.15).

$$SOC_h = SOC_{h-1} + ESS_h^i - ESS_h^o - ESS_h^l \quad (5.11)$$

$$SOC_{min} \leq SOC_h \leq SOC_{max} \quad (5.12)$$

$$ESS_h^i = E_h^{ESSi} * \eta_{ch} \leq ESS_c * \emptyset_{ch} \quad (5.13)$$

$$ESS_h^o = E_h^{ESSo} * \eta_{dis} \leq ESS_c * \emptyset_{dis} \quad (5.14)$$

$$ESS_h^l = SOC_{h-1} * \theta_{ESS} \quad (5.15)$$

where SOC is the energy storage state of charge in kWh; ESS_c is the storage capacity in kWh; SOC_{min} and SOC_{max} are the energy storage minimum and maximum SOC in %; ESS_h^i, ESS_h^o, and ESS_h^l are the storage electricity input, output, and losses in kWh, respectively; $\emptyset_{ch}$ and $\emptyset_{dis}$ are the charging and discharging rate, respectively; and η_{ch} and η_{dis} represent efficiency of storage charging and discharging in %, respectively. The full optimisation model constraints are described in several studies [239]–[241], where only constraints related to this chapter are included. The resilience impact is analysed based on outage characterisation including starting time, date, and duration as well as critical load percentage.

5.3 Case Study: Seve Ballesteros-Santander Airport

The Seve Ballesteros–Santander (SDR) airport facility is selected as a case study to emphasise the resilience enhancement of airports. The airport was selected for this study due to the public availability of its load data online. The airport's average hourly consumption per month in 2015 is illustrated in Figure 5-2 [230]. The projected load in this case study, including critical loads, ranges from 50–100% depending on the simulated outage scenario.

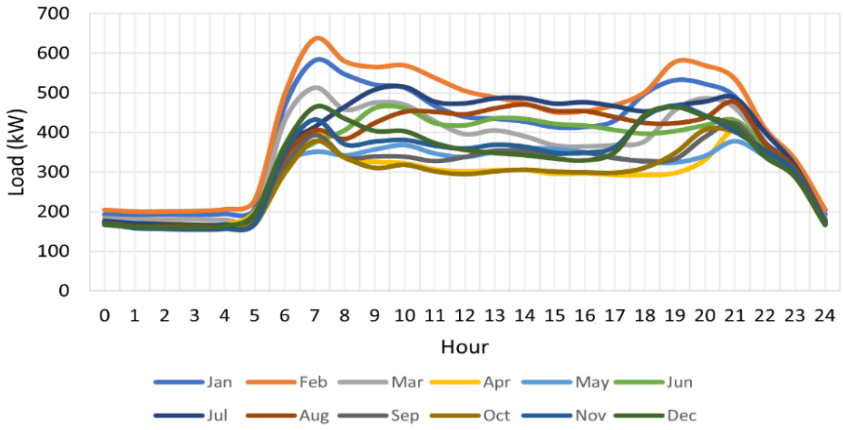

Figure 5-2 Airport average monthly load demand.

The optimum rate tariff from Endesa electric utility company is applied [242] and is shown in Figure 5-3. Note that the energy and demand rates are categorised into six levels, where P6 is the lowest rate and P1 is the highest rate.

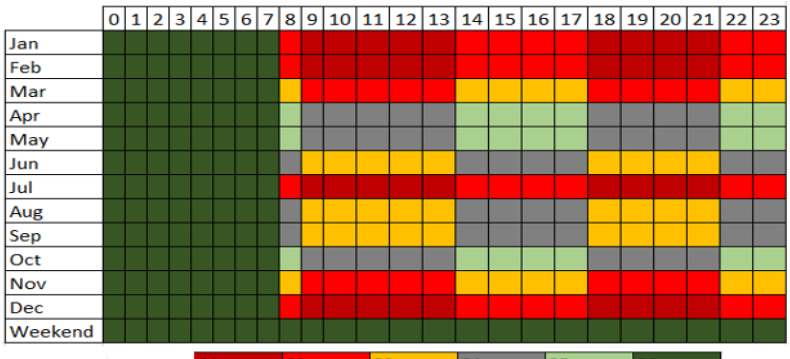

	P1	P2	P3	P4	P5	P6
$/kWh	0.41	0.4	0.38	0.37	0.35	0.34
$/kW	2.33	2.03	1.16	0.93	0.27	0.15

Figure 5-3 Utility tariff.

The solar PV system performance is generated by the PVWatts platform based on the location of the microgrid, creating a 24h daily profile as shown in Figure 5-4 which is expressed as the PV output (kW) per kW installed (kWdc). PVWatts is a web-based platform developed by the National Renewable Energy Laboratory (NREL) that

estimates the grid-connected rooftop or ground-mounted solar PV system's energy production. It uses the weather data from the NREL National Solar Radiation Database (NSRDB) PSM V3 TMY 2020 dataset. Based on the performance data, the solar PV system can generate in each hour a fraction of its installed electrical power capacity. The performance is calculated using various data such as irradiance profile, system losses, inverter and PV technology efficiencies, available space, and array specification (fixed or tracking, roof or ground mounted, tilt angle, and direction).

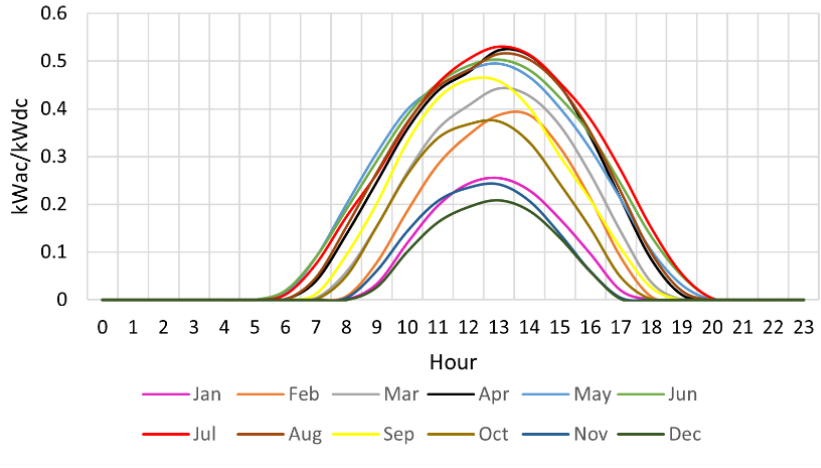

Figure 5-4 Average solar PV performance per month.

In this chapter, the EGSE load is modelled based on the average daily required energy to perform the required tasks in the airport [50], [51]. The used EGSE types are shown in Table 2-3. The aggregated availability of the EGSE fleet to charge is based on the average daily flight schedule [243] where the EGSE fleet has a higher charging probability during low numbers of flights. Figure 5-5 illustrates the aggregated charging availability schedule. Table 5-1 shows the inputs used in the modelling tool.

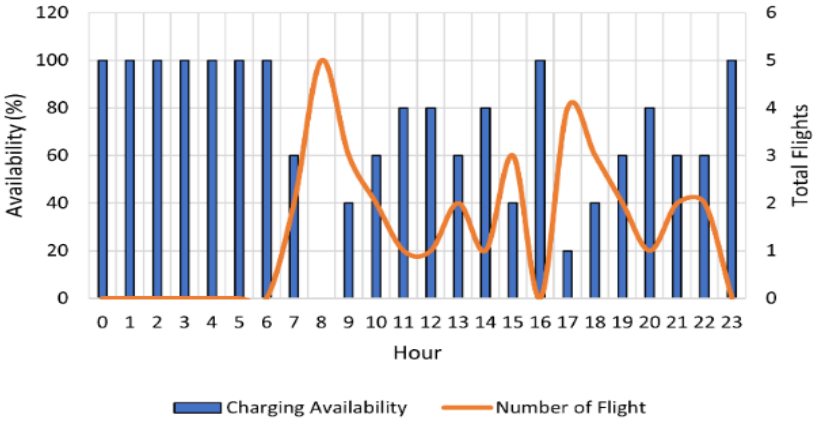

Figure 5-5 Aggregated EGSE fleet charging probability.

Table 5-1 Model techno-economic inputs.

Financial parameters	
Interest rate	6%
Reporting years	25
Incentives (storage and generators)	NA
EGSE charging station parameters	
Load shape	simulated
Rating	154kW
Efficiency	96%
Total available charging energy	2,536kWh
Daily energy need	2,000kWh
Solar PV system	
Purchase cost	1,600 $/kWdc
O&M cost	16 $/kWdc/yr
Lifetime	25 yrs
Available space	90,000 m^2
Panel technology type	standard
Array type	Fixed ground-mounted
MACRS incentives	5
Amount depreciable	100%
Efficiency	15% [82]
System losses	14% [82]
Inverter efficiency	96%
Tilt angle	10°
Pointing	South
Source data	5.2 km away (43.47, −3.81)
Energy storage	
Purchase cost	420 $/kWh
Inverter cost	840 $/kw
O&M cost	10 $/kWh/yr
Lifetime	10 yrs
Max SOC	100%
Min SOC	20%
Emergency min SOC	20%
Charging efficiency	96%
Continuous charging rate	0.1
Discharge efficiency	96%
Continuous discharging rate	0.1
Charge from utility	allowed
MACRS incentives	7 yrs
Amount depreciable	100%
Diesel Generator	
Purchase cost	500 $/kw
O&M	10 $/kW/yr
Lifetime	15
Efficiency	30%
Fuel price	0.8 $/litre
Fuel annual limit	2500 litres
Ramp up rate	0.5 %/min
Ramp down rate	0.5 %/min
Load lost cost – scenario 4	
High critical (30%)	39.7 $/kWh
Low critical (20%)	12.7 $/kWh
Non-critical (50%)	1.3 $/kWh

5.4 Scenario Results and Analysis

5.4.1 Scenario 1: Normal Operation (No Outages)

In this scenario, the sizing and dispatching of the microgrid are conducted from an economic viewpoint without considering the resilience benefits. This scenario serves as the optimal financial base scenario that will be used for comparison with other scenarios. The optimal size configuration of the microgrid includes 2,724kWdc of solar PV and 3,766kWh of storage. Prior to the consideration of a microgrid, in what is referred to as business as usual (BAU) where the airport relies entirely on the utility grid, the annual operational cost (AOC) stood at $1.3833 million. The integration of the microgrid reduces the AOC to $1.0611 million, resulting in a 23.3% reduction. Figure 5-6 presents the optimal power dispatch during this normal operation.

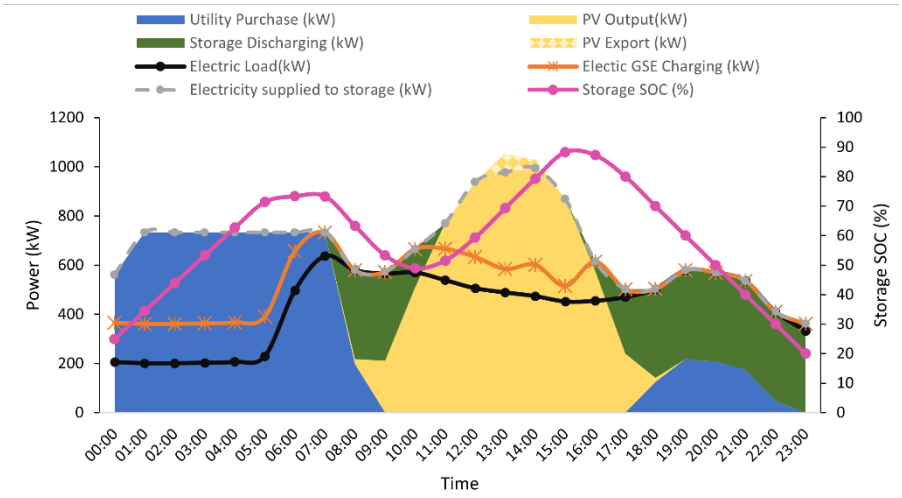

(a)

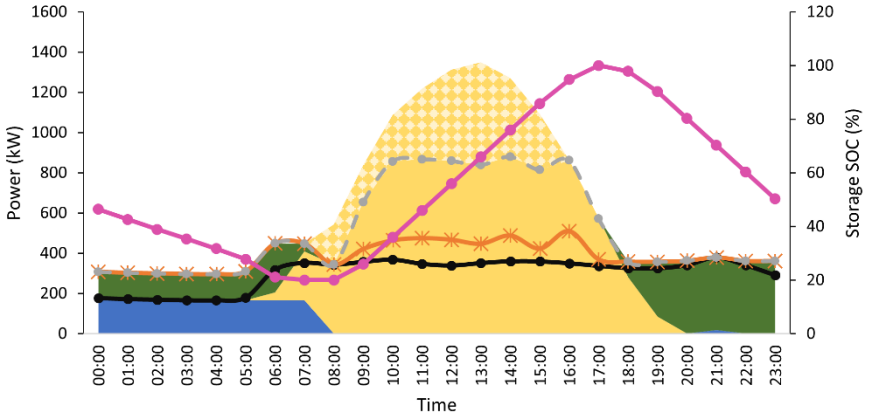

(b)

Figure 5-6 Microgrid energy dispatch during normal operation (a) February, (b) May.

As can be seen from Figure 5-6, the solar PV system is prioritised to serve electrical loads almost entirely during the daytime since PV production and high utility tariffs are matched. However, in February, the storage system is providing energy along with PV between 8:00–10:00 and 16:00 –17:00, when the microgrid load is higher than PV power output, compared to May, where the load is lower than PV power output. Moreover, the storage system is charged via grid in February during the first 7h, which is not the same case in May, where the storage system is mainly charged during the daytime. Note that the system sizing and dispatching would vary under different tariff structures and rates, as well as the net-metering scheme; however, this exceeds the scope of this chapter**.**

5.4.2 Scenario 2: Various Outages Criteria

The design of resilient microgrids is influenced by various factors, including the time when outages begin, their duration, the date they occur, and the level of critical load. Two representative days, one from a peak load season (February) and another from an off-peak load season (May), are considered for analysis. Each day is evaluated across three different outage starting times and three levels of critical load, each with two distinct outage durations. This analysis generates a total of 24 possible outage combinations. The primary results of these comprehensive outage scenarios are detailed in Tables 5-2 and 5-3. It is important to note that each outage is considered an isolated event, occurring only once over the lifetime of the project.

5.4.2.1 Outages Starting Time

Exploring a microgrid's ability to withstand outages that start at various times is crucial, especially during high load plus low solar irradiance (HLLI) and low load plus high irradiance (LLHI) conditions. Airport load and solar data show that in February, the airport sees HLLI conditions, while in May, LLHI conditions are seen. Although September has a lower load than May, it was excluded from consideration due to its lower irradiance. During February, the microgrid is providing both resilience benefits and AOC reduction, which varies from about 20% to 22% compared to BAU, as indicated in Table 5-2. The outage starting time is slightly affecting PV and storage system size in February under the same critical load level and duration. Whereas, in May, the system size is not changing. Figures 5-7 show the power dispatch of different starting times for outages occurring in February under a 50% critical load requirement.

In cases where power outages start at 00:00–7:59 and 16:00–23:59, the critical load is primarily supplied by batteries. In contrast, the battery supplies the load for 1 h at 8:00 before the presence of sunlight, and then the PV provides energy for both the critical load and the battery to charge in the case of 8:00–15:59 outage time. In addition, the storage SOC in the case of 00:00–7:59 (Figure 4-7 a) grid interruption is around 75% to provide enough power to the electrical load before reaching the minimum SOC at the end of the 8 h interruption. While, in the cases of 8:00–15:59 and 16:00–23:59 (Figure 4-7 b and c) batteries SOC at the beginning of the day are at minimum SOC, which leaves more empty capacity to be charged using solar PV. The PV output curtailment level is variable based on outage and operation conditions, which require a proper management scheme. However, this chapter focuses on enhancing resilience from an economic perspective only.

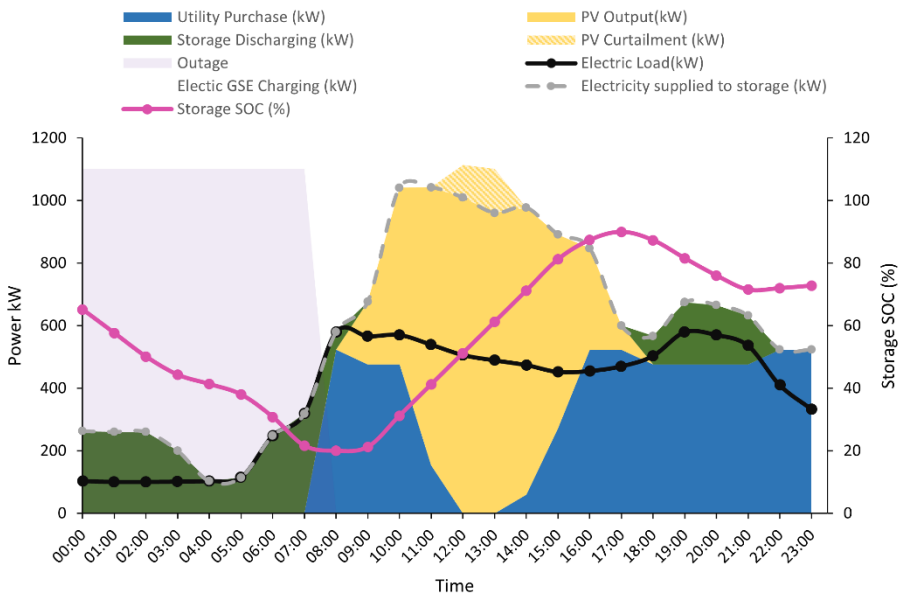

(a)

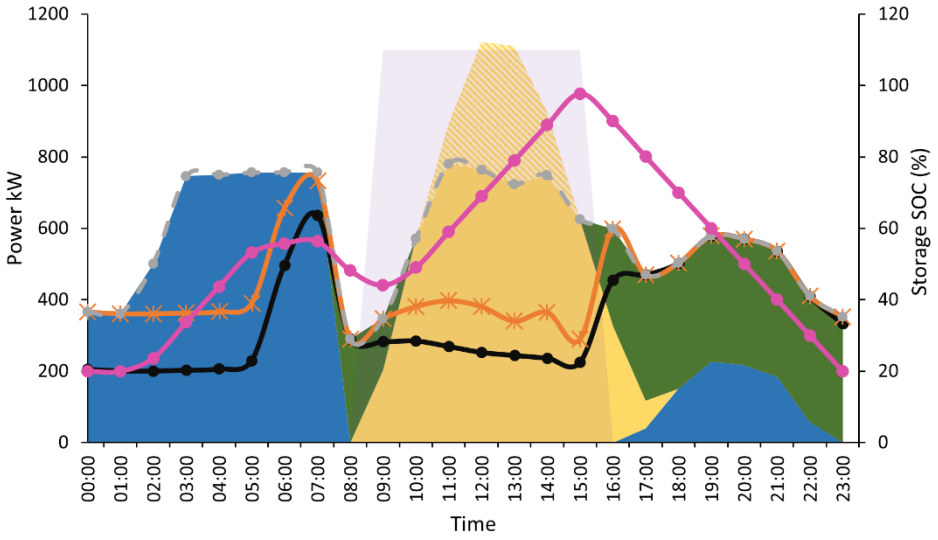

(b)

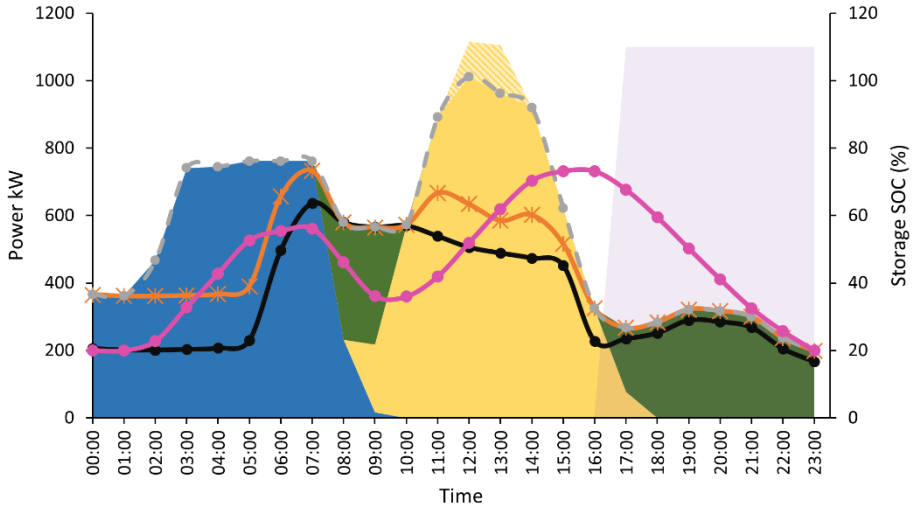

(c)

Figure 5-7 Power dispatch of microgrid DERs under 50% critical load level in February for 8h starting at (a) 00:00-7:59, (b) 8:00-15:59, (c) 16:00-23:59.

5.4.2.2 Critical Load Level

The microgrid's resilience is tested under three critical load levels: 50%, 70% and 100%. In real conditions, 100% critical load is unrealistic; however, this study case is considered for showing the relation between critical load level and microgrid resilience configuration and performance. As presented in Table 5-2, both PV and energy storage system sizes vary specifically during outages in February under different critical load levels for the same outage start time and duration. The PV size varies by about 400kW,

while the storage system difference is up to 1,000kWh. Moreover, a diesel generator would be required in the case of a 100% critical level to ensure continuous energy supply under the simulated outages. The integration of diesel generators results in lower AOC savings.

The system power dispatch under 70% and 100% critical load conditions of an outage starting at 16:00 in February is depicted in Figures 5-8. Figure 5-7 (c) presents the 50% critical load level. Figure 5-8 clearly indicates that the battery system fed the majority of the system load during the outage. The diesel generator operates at near full rated power of 100 kW over the whole outage period in the case of a 100% critical load level. Batteries show the same charging and discharging behaviour under the three modelled levels. The storage system starts the day at the minimum SOC level and charges about 40% during the utility's cheapest tariff to supply the airport peak load at 8:00. The storage system maximum SOC in cases of 50%, 70%, and 100% critical load levels reaches about 80% of rated capacity to ensure the storage system discharges enough energy to return to pre-outage SOC levels because the end-of-day recharge dispatch strategy is applied. In addition, during the daytime and prior to a grid outage, the total load, including airport electrical load, electric ground support equipment, and batteries, is entirely supplied by solar PV. Thus, more cost savings are added by avoiding electricity purchases during high tariff hours. The diesel generator is only needed during an unrealistic 100% critical load level, which implies the benefits of using renewable energy resources to save costs and increase resiliency.

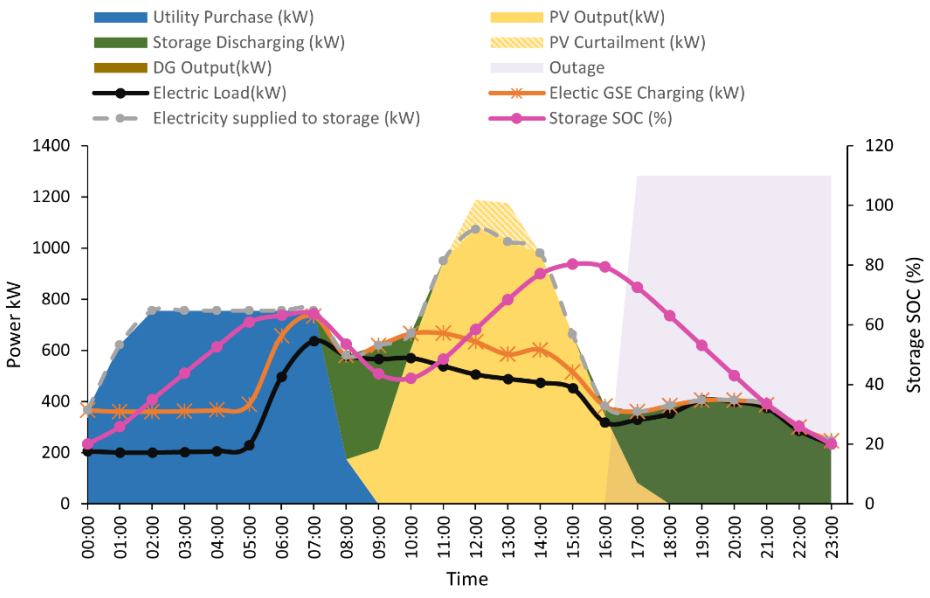

(a)

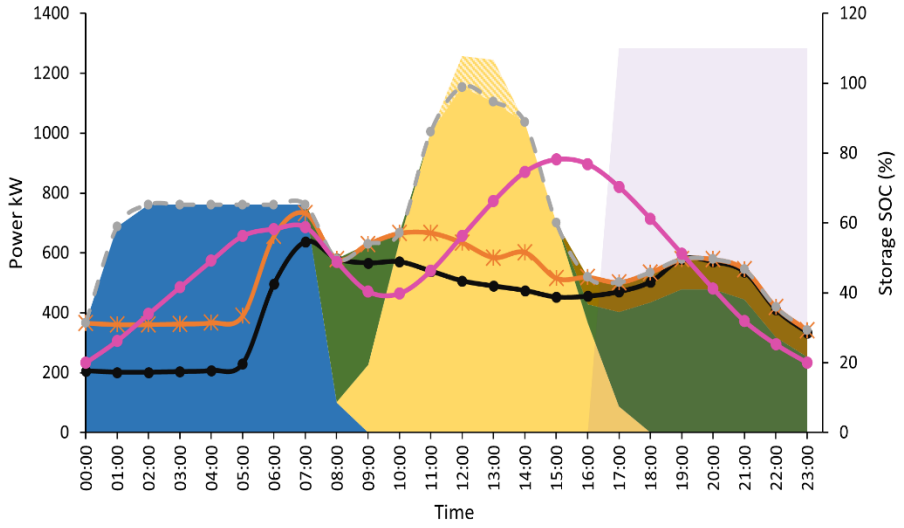

(b)

Figure 5-8 Energy dispatch of DERs during 8h outage starting at 16:00 in February under (a) 70%, and (b) 100% critical load levels.

5.4.2.3 Outage Duration

The duration of a 24h outage is considered alongside the previously discussed 8 h outages. The primary observation is that the optimal resilience system configuration consists of a diesel generator under 24h of power outage for all different situations. The PV and battery sizes are slightly changing in February and May, when outage durations are changing. The change in outage duration reduced the airport AOC savings slightly. Figure 5-9 depicts power dispatch for a 24h outage and 50% critical load in February and May. In February, energy storage and diesel generators fed the microgrid load until PV production started around 9:00. Due to the battery model's maximum charging characteristic, the diesel generator supplies extra power with PV to keep charging constant, as seen in hours 10:00 and 15:00–16:00. Whereas in May, PV and storage are capable of supplying energy through outages.

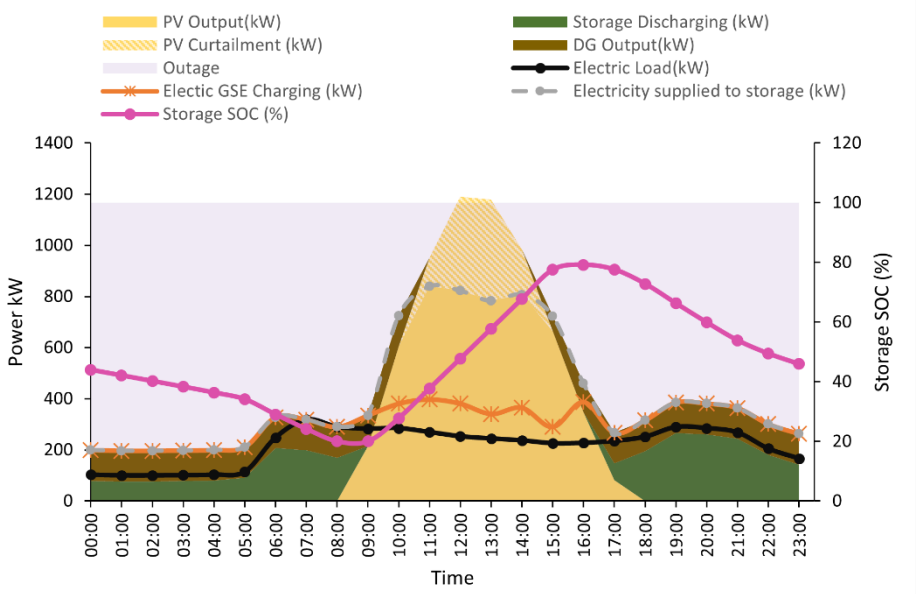

(a)

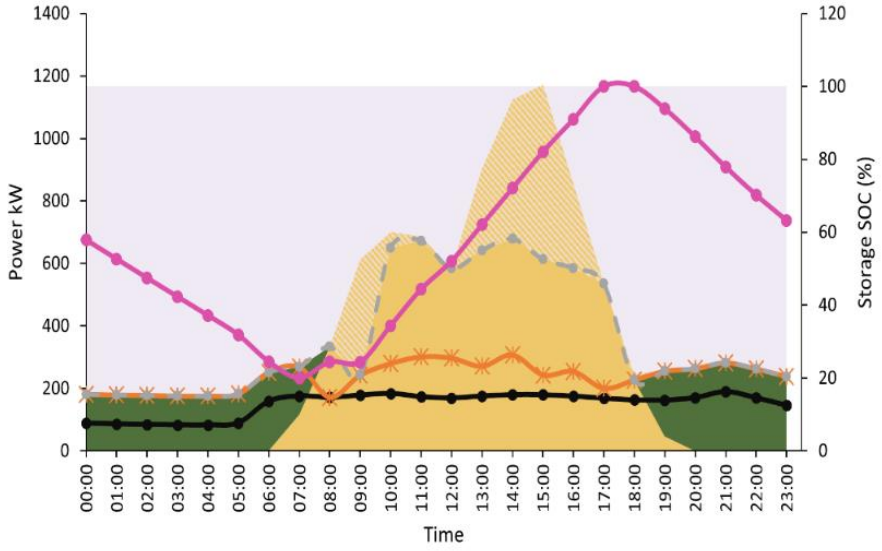

(b)

Figure 5-9 Power dispatch during 24h outage under 50% criticality level in (a)February, and (b)May.

Table 5-2 Key results of scenario 2 in February.

	February											
	50% Critical load				*70% Critical load*				*100% Critical load*			
	Short			*Long*	*Short*			*Long*	*Short*			*Long*
	T1	**T2**	**T3**	**T4**	**T1**	**T2**	**T3**	**T4**	**T1**	**T2**	**T3**	**T4**
PV (kW)	2,483	2,502	2,488	2,654	2,732	2,649	2,649	2,681	2,829	2,834	2,803	2,739
Batteries (kWh)	3,604	3,675	3,625	4,246	4,645	4,219	4,222	4,347	5,073	5,093	4,990	4,520
Generator (kW)	0	0	0	120	0	0	0	200	160	100	100	320
Optimised AOC ($ million)	1.08	1.079	1.079	1.085	1.083	1.079	1.079	1.091.6	1.094	1.089	1.089	1.1
Reduction (%)	21.9	22.0	22	21.5	21.7	21.9	21.9	21.1	20.8	21.2	21.3	20.4

Note: T1 = 00:00-7:59, T2 = 8:00-15:59, T3 = 16:00-23:59, T4 = 00:00-23:59, Short=8h, long=24h, annual operational cost (AOC) of business as usual case is $1.383million.

Table 5-3 Key results of scenario 2 in May.

	May											
	50% Critical load				*70% Critical load*				*100% Critical load*			
	Short			*Long*	*Short*			*Long*	*Short*			*Long*
	T1	**T2**	**T3**	**T4**	**T1**	**T2**	**T3**	**T4**	**T1**	**T2**	**T3**	**T4**
PV (kW)	2,483	2,483	2,483	2,577	2,483	2,483	2,483	2,574	2,483	2,483	2,579	2,700
Batteries (kWh)	3,604	3,604	3,604	3,885	3,604	3,604	3,604	3,885	3,604	3,604	3,948	4,383
Generator (kW)	0	0	0	120	0	0	0	40	0	0	0	100
Optimised AOC ($ million)	1.08	1.08	1.08	1.082	1.081	1.08	1.08	1.086	1.081	1.08	1.081	1.092
Reduction (%)	21.9	21.9	21.9	21.8	21.9	21.9	21.9	21.5	21.8	21.9	21.8	21

Note: T1 = 00:00-7:59, T2 = 8:00-15:59, T3 = 16:00-23:59, T4 = 00:00-23:59, Short=8h, long=24h, annual operational cost (AOC) of business as usual case is $1.383million.

5.4.3 Scenario 3: Solar PV Performance Changes.

Renewable energy resources, including solar PV, have intermittent behaviour related to weather conditions, which most likely matches weather-related outages. This scenario is introduced to investigate how the resilient microgrid is sized and dispatched during a solar PV power output drop. A full-day outage for 50% critical load in February and May is examined under different solar fluctuation conditions. The solar PV power output is assumed to be dropping by 30%, 50%, 80%, and 100% of its original levels. The extreme drop in solar level by 80% and 100% is introduced to represent rare high impact events that can be simulated in different locations. Tables 5-4 and 5-5 summarise the results of modelled PV performance changes in February and May, respectively.

Microgrid PV and storage sizes are slightly decreasing with the increase in solar irradiance. The integration of a diesel generator to support critical loads is increasing when PV drop levels are increasing as well. The system shows a positive annual cost saving in all simulated outages. The resilient system power dispatch under 50% and 80% of PV performance dropping levels is presented in Figure 5-10. In February and

May, the diesel generator ran over the whole outage period. The generator is serving microgrid loads during the night, while during the daytime it is also providing power to support battery charging requirements. The battery is providing more energy during the night with a lower solar drop level (Figure 5-10 a, c) while less energy is supplied with a high drop level (Figure 5-10 b, d). This indicates that receiving more power during an outage from the generator is more profitable than a battery system under high levels of PV output drop.

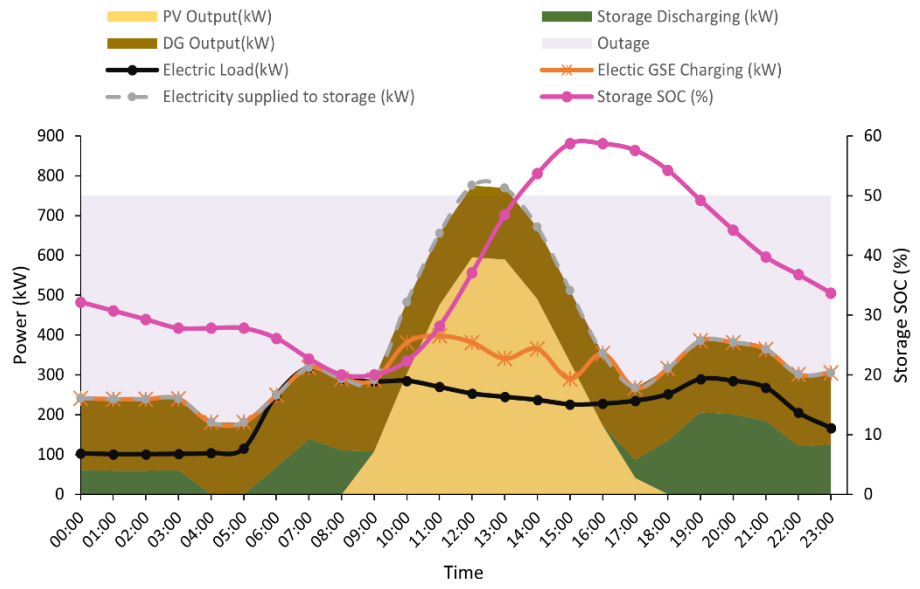

(a)

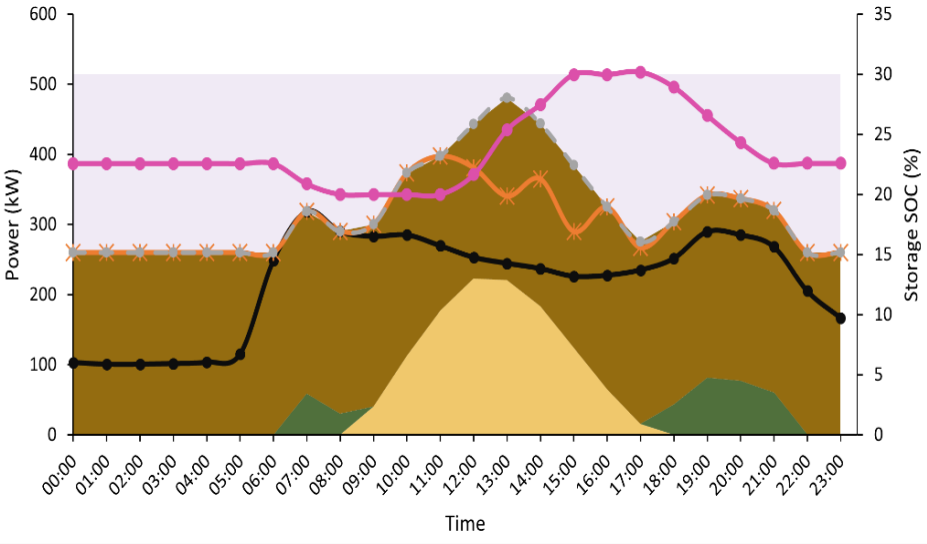

(b)

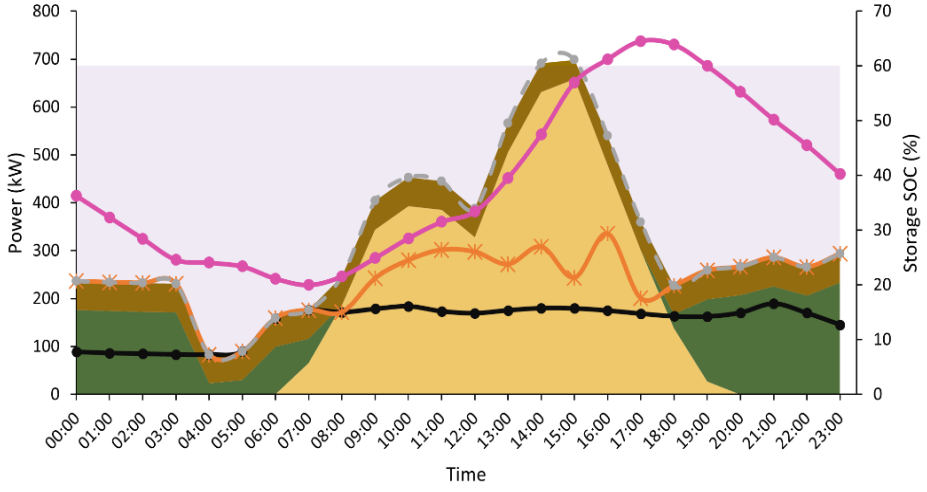

(c)

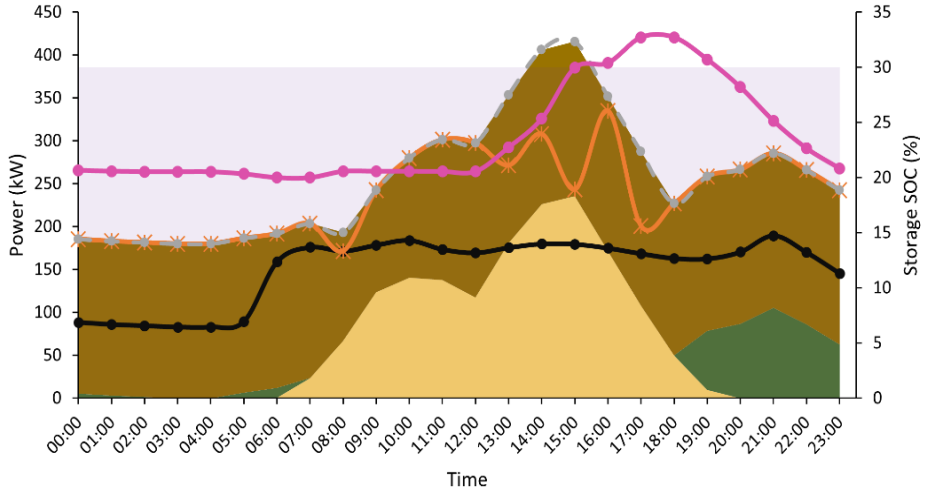

(d)

Figure 5-10 Optimal power dispatch strategies during power outage in February with (a) 50%, and (b) 80% and in May with (c) 50%, and (d) 80% solar performance drop levels.

Table 5-4 Microgrid sizing and economic results for scenario 3 in February.

	February			
Drop level	30%	50%	80%	100%
PV (kW)	2,726	2,655	2,483	2,477
Batteries (kWh)	4,475	4,241	3,604	3,586
Diesel generators	140	180	260	320
Optimised AOC ($ million)	1.088	1.090	1.094	1.098
Reduction (%)	21.3	21.2	20.9	20.6

Note: Annual operational cost (AOC) of business as usual case is $1.383million.

Table 5-5 Microgrid sizing and economic results for scenario 3 in May.

	May			
Drop level	30%	50%	80%	100%
PV (kW)	2,576	2,770	2,480	2,469
Batteries (kWh)	3,937	4,606	3,596	3,554
Diesel generators	20	60	180	240
Optimised AOC ($ million)	1.080	1.085	1.091	1.095
Reduction (%)	21.9	21.5	21.1	20.8

Note: Annual operational cost (AOC) of business as usual case is $1.383million.

5.4.4 Scenario 4: Load Management is Included

In this scenario, a value is assigned to each kWh based on the load criticality level. The airport load is divided into three levels, 30%, 20%, and 50%, representing high critical, low critical, and non-critical loads, respectively. The values of lost load are presented in Table 5-1 [244], [245]. The demand management impact is assessed in February for a 24h blackout. The optimal microgrid sizing according to resilience monetary valuation consists of 2,639kW of PV and 4,167kWh of energy storage. The total AOC is $1.082 million, which results in a 21.8% reduction compared to the BAU AOC of $1.383 million. The optimal microgrid dispatch is demonstrated in Figure 5-11.

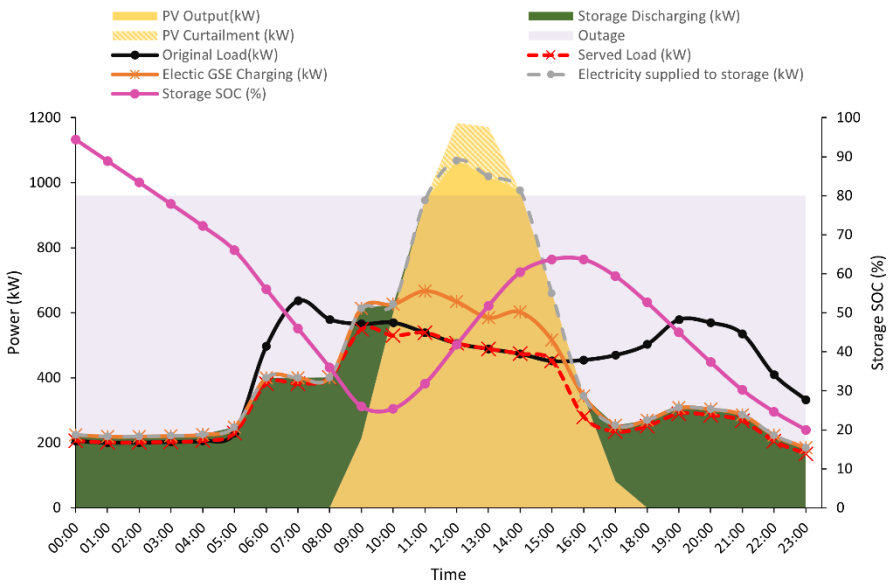

Figure 5-11 Energy dispatch of microgrid considering economic value of resilience.

The total lost load is 3,481kWh over 13h, incurring a total lost cost of $4,526. The shaded load is only a non-critical load where the cost of the unshaded load is low. Moreover, the optimal dispatch considering DR has notable differences. As seen in Figure 5-11, between 11:00–15:00, the load is 100% supplied without loss due to high

PV output. The load is completely supplied by batteries, which are activated between 00:00–5:00. After sunset, the load is supplied by batteries, where the greater part of the non-critical load is reduced, which guarantees continuous supply for high and low critical loads.

It is worth mentioning that the total lost load between 17:00–23:00 is much higher than the lost load between 00:00–8:59. In addition, batteries have around 100% SOC before a blackout and continue to discharge power until solar starts producing power. Between 11:00–15:00, batteries charge again, and SOC reaches around 65% to supply critical loads after sunset.

5.5 Discussion

Airport microgrids have the potential to withstand diverse outages and provide economic benefits. Optimal airport microgrid sizing and dispatch appear to be more influenced by outage duration and the level of critical load than the starting time of the outage. These results, while promising, do rely on certain assumptions about load conditions and should be interpreted with caution due to the inherent variability of real-world power usage and outage situations. Moreover, the study findings underscored the importance of factoring in resilience when planning and operating microgrids for airports.

Adding an economic value to resilience seemed to enhance the system's energy dispatch, reducing curtailment and ensuring both critical and non-critical loads are served more effectively when PV output is high. However, the validation of these findings poses a challenge due to the complexity and variability of real-world conditions as well as the lack of other studies to compare with. Gathering real-time operational data for a specific airport would be beneficial for more accurate modelling and predicting system performance. In this light, it is recommended that future research consider incorporating more detailed, location-specific load and outage data for a more accurate understanding of system performance under diverse conditions. In terms of environmental impact, the integration of hybrid, renewable-based microgrids can contribute to greenhouse gas reduction efforts. By reducing reliance on fossil fuel-based back-up generators and maximising the utilisation of renewable energy sources, carbon emissions can be reduced.

Further recommendations include exploring strategies for reducing overall power demand, such as improving the energy efficiency of airport operations and infrastructure and implementing energy conservation measures. These approaches could complement the deployment of renewable-based microgrids, enhancing their environmental and economic benefits.

5.6 Summary of Key Findings

In this work, a techno-economic hybrid optimisation approach is used to optimise a grid-connected airport microgrid considering resilience to grid interruptions. The proposed model was solved by using a MILP model that aims to minimise the operation cost of the microgrid and is subjected to various constraints. The microgrid was modelled using the load consumption dataset for Seve Ballesteros–Santander airport. The primary findings are as follows:

i- Microgrids deployed in civilian airports will meet the electrical energy demand during power interruptions and lower annual electricity operational costs.
ii- The duration of an outage and the critical load level have a greater impact on system component sizing than the starting time of the outage.
iii- A comparison of power supplies for short outages and long outages shows that renewable sources can power critical loads and reduce costs for less than one-day outages.
iv- Changes in solar PV power output during power outages, such as those caused by weather conditions, can reduce overall cost savings.
v- When the monetary value of critical and non-critical load levels is considered, the served load during the daytime can increase to up to 100%, and annual operational costs can decrease.

The conclusions drawn were derived from considering the unique characteristics of an airport, including location, energy consumption, and energy tariff structure, which were examined using various combinations of power interruptions. However, because it is difficult to validate the results in this study, future studies may involve gathering actual critical load data rather than using a percentage of the overall load and testing it using different outage criteria, input data, and various modelling techniques and software.

Chapter 6
Assessing Airport Activities For Load Flattening Using Electric Ground Support Equipment

6.1 Introduction

In this chapter, a methodology for EGSE to flatten the airport load curve by providing peak shaving and valley filling is presented. The airport electrical load is modelled using a civilian medium-sized airport load profile at peak and off-peak seasons obtained from [230] and different types of EGSE. A mixed-integer linear programming optimisation model is used to optimally manage the EGSE fleet charging and discharging in order to improve airport terminal electrical load shape. The optimisation modelling is conducted to evaluate the impact of controlled EGSE charging and discharging based on flight schedules to flatten the airport load profile. Each gate in the airport usually has different types of GSE that are used during handling operations, but only four GSE types are used in this modelling study [33], [246] including baggage tractor, aircraft push-back, container loader, and belt loader. These four types of non-road GSE were considered in this thesis due to their extensive use in airports and the availability of electric commercial models. The proposed model's performance is assessed based on load factor (*LF*), peak load reduction (*PLR*), valley filling promotion (*VFP*), valley-peak ratio (*V/P*), and load rate of change (*RoC*) indicators.

6.2 Peak Shaving and Valley Filling

Peak load is a delicate factor to consider for both grids and large end-users since, in most cases, it occurs for short periods of time per day. Traditionally, grid operators use conventional approaches, such as using coal or diesel units to supply peak demand, which is not efficient economically or environmentally [247]. For large end-users, exceeding the contracted peak load could increase their energy bills significantly. Thus, load flattening is beneficial for the grid and large end-users. Load flattening refers to reducing the difference between peak load and minimum load by cutting the peak, shifting the peak, and filling load valleys [248]. Load flattening by peak shaving and valley filling is achieved by different strategies, such as the integration of energy storage systems (ESS) and the implementation of V2G [249]. Some examples of benefits for grid operators are power quality improvement, efficient energy utilisation, and more renewable energy integration. Benefits for end-users are cost reduction, back-up systems, and CO_2 reduction [188]. This chapter focuses only on load levelling

from the end-user perspective by adopting EGSE because levelling end-user electricity loads is important to avoid using less efficient peaking generators and reduce production costs per kWh during peak periods, which are ultimately passed on to the end-users.

Airports are large power consumers, where some large airports demand is equivalent to that of a small city [250]. Airport load curves can be flattened by reducing peak load and filling valleys with the integration of airport EGSE with suitable V2B technology, as shown in Figure 6-1. By adjusting the charging and discharging processes of EGSE, the airport load curve can be efficiently levelled. The EGSE's operation is typically associated with the servicing of aeroplanes on the ground [38], where their role to provide peak shaving and valley filling can be predicted in advance.

Figure 6-1 EGSE to building model.

6.3 Methodology for EGSE Peak Shaving and Valley Filling Provision

The primary aim of this work is to provide a methodology to use EGSE to cut airport peak load and fill valleys by controlling charging and discharging processes based on flight schedules. The flowchart of the proposed algorithm for airport load flattening is shown in Figure 6-2. The proposed methodology is shown in Figure 6-3. The developed optimisation model was simulated in CVX MATLAB modelling tool Version 2.1 [251], [252] and solved using GUROBI solver Version 9.5 [216] on a desktop computer with a 64-bit Windows 10 operating system, an Intel® Core™ i7 CPU @ 3.4GHz, and 16 GB of RAM. The modelling tool CVX is a free-of-charge MATLAB-based optimisation modelling tool for constructing and solving various types of optimisation problems, including MILP, that turns MATLAB into a modelling language, allowing constraints and objectives to be specified using standard MATLAB expression syntax.

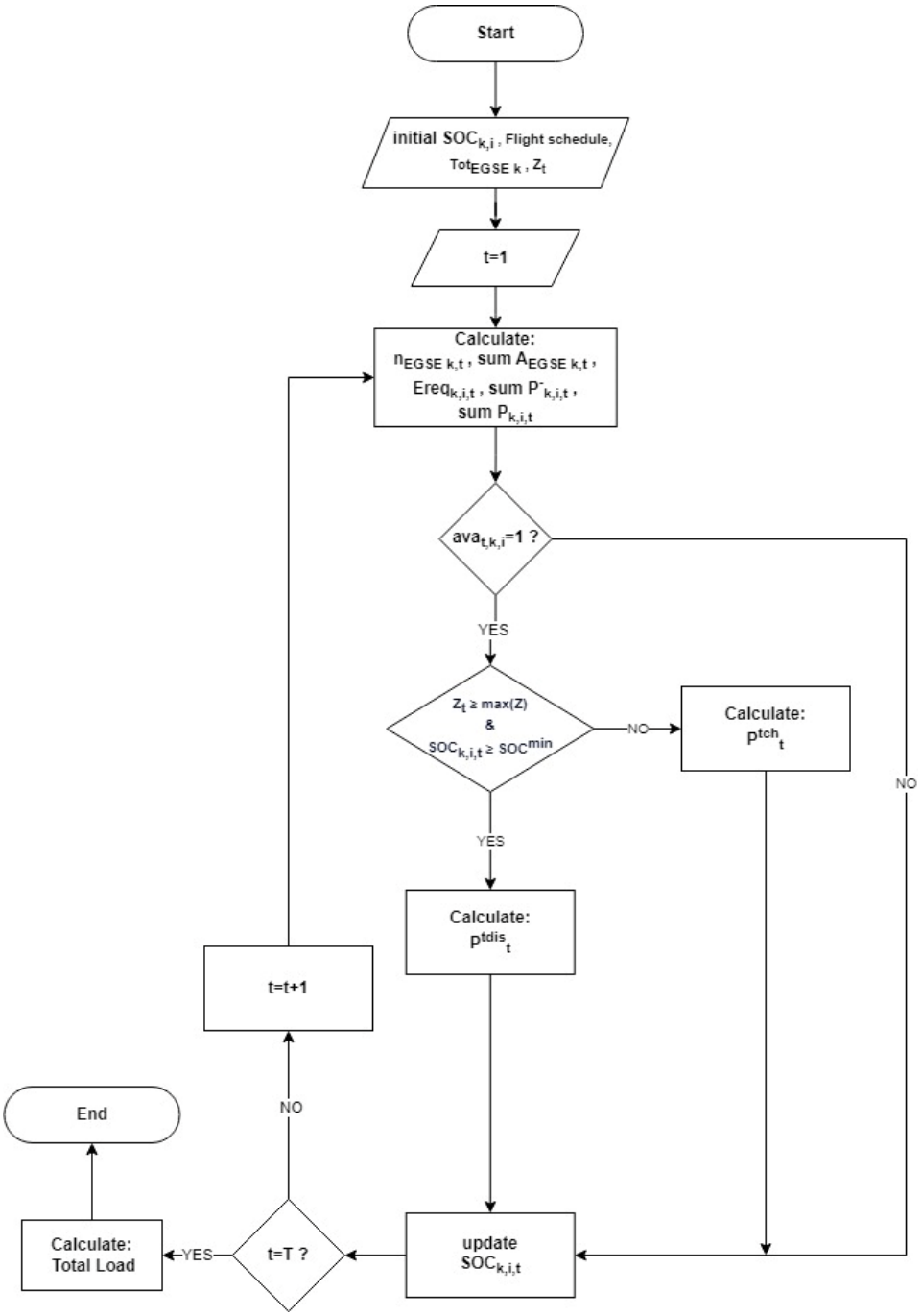

Figure 6-2 Flowchart of the load flattening algorithm.

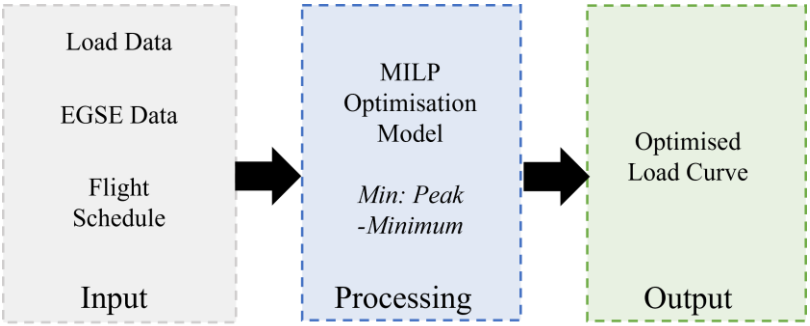

Figure 6-3 Flowchart of the load flatting methodology.

The uncertainty of EGSE availability for V2B can be more predictable since the flight schedule is known in advance. The EGSE charging and discharging cycle is more predictable since it depends on the flight schedule, which is significantly different than EVs, where driver behaviour is the primary factor that affects V2B service. Each EGSE is assigned to perform a turnaround event, which starts when EGSE leaves to serve an aeroplane and ends when the same EGSE return to the same starting spot. Electric ground support equipment vehicles are classified based on their type *K* where $k \in K$ and each type contain a set of EGSE I where $i^{th}\ EGSE \in I$. The proposed GSE scheduling model in [253] is used in this thesis. The required time to perform a turnaround event by $EGSE_{k,i}$ is defined in Equation (6.1).

$$tA_{k,i} = tR_{k,i} + tF_{k,i} + tS_{k,i} \tag{6.1}$$

where $tR_{k,i}$ is the required time of $EGSE_{k,i}$ to arrive to aeroplane in min, $tF_{k,i}$ is the required time of $EGSE_{k,i}$ to return from aeroplane in min, $tS_{k,i}$ is the time that $EGSE_{k,i}$ spend to perform a task in min, and $tA_{k,i}$ is the total turnaround event time in min. The number of hourly turnaround events that each $EGSE_{k,i}$ can perform is described in Equation (6.2).

$$nA_{k,i} = RES \cdot \frac{60}{tA_{k,i}} \tag{6.2}$$

where Res is the reserved time factor for each vehicle in each hour for different works such as driver changes. The number of turnaround events $nA_{k,i}$ is round towards zero since an EGSE can only perform a certain integer number of turnaround events and not a fraction of turnaround events. To serve all aeroplanes on ground during time t, the required number of EGSE of type k is obtained from Equation (6.3). The number of required EGSE ($NO_{t,k}$) is round towards +∞.

$$NO_{t,k} = \frac{LD_t}{nA_{k,i}} \tag{6.3}$$

where LD_t donates the number of departing and landing aircraft at time t. Moreover, the total available EGSE of type k at time t for V2B is calculated as Equation (6.4).

$$AE_{t,k} = Tot_k - NO_{t,k} \tag{6.4}$$

where Tot_k is total number of EGSE of type k. A turnaround event across two consecutive hours is considered since each landing or departing flight is considered separately. For example, flights from 9:00–9:59 are inputs for t=9, and flights from

10:00–10:59 are inputs of t=10. Thus, if a flight lands at 9:50 and departs at 10:20, it counts as two flights: one at t=9 and one at t=10. Electric ground support equipment will be unavailable from 9:00, not from 9:50, and for the next hour, EGSE will be reserved from 10:00 to 10:59, not 10:20. Required energy of $i^{th}\ EGSE$ of type k at time t is obtained from Equation (6.5).

$$Er_{t,k,i} = nA_{k,i} \cdot Ea_{k,i} \tag{6.5}$$

where $Ea_{k,i}$ is required energy to perform a turnaround event of $i^{th}\ EGSE$ of type k in kWh, and $Er_{t,k,i}$ is hourly required energy in kWh. The presence of $EGSE$ of type k during the studied period T is formulated as a binary matrix $ava\{1,0\}^{T\times I}$, where $\forall t \in T\ and\ \forall i \in I$ are with elements defined in Equation (6.6). The $used$ binary matrix is obtained which represents EGSE of type k that serving an aircraft and is unavailable for V2B. U matrix is Boolean not matrix of ava.

$$ava_{t,i} = \begin{cases} 1, & if\ i^{th}\ EGSE \text{ available for V2B at time } t \\ 0, & Otherwise \end{cases} \tag{6.6}$$

Let $P_{k,i}^{ch}$ and $P_{k,i}^{dis}$ denote $i^{th}\ EGSE$ of type k charging and discharging power in kW, respectively, the state of charge (SOC) of $i^{th}\ EGSE$ of type k at time t in kWh is calculated as given in Equation (6.7).

$$SOC_{t,k,i} = SOC_{t-1,k,i} + (P_{t,k,i}^{ch} \times ava_{t,k,i}) - \left(P_{t,k,i}^{dis} \times ava_{t,k,i}\right) - (Er_{t,k,i} \times U_{t,k,i}) \tag{6.7}$$

The total load of airport with the presence of EGSE is expressed in Equation (6.8), where Z_t is the airport electricity demand at time t in kW.

$$Total\ Load = \sum_{t,k,i} Z_t + P_{t,k,i}^{ch} - P_{t,k,i}^{dis} \tag{6.8}$$

6.4 Optimisation Formulation

This chapter proposes an optimisation model that aims to control the charging and discharging processes of EGSE to flatten the airport load profile subjected to various constraints. The objective function is formulated to minimise the maximum load by discharging or adjusting the charging of EGSE batteries to shave the peak and fill the valley of the airport load. While maximising minimal load by increasing charging and decreasing discharging power rates during off-peak would fill load curve valleys, The objective function to minimise the peak-valley difference is given in Equation (6.9).

$$\text{min: } maximal(Total\ Load) - minimal(Total\ Load) \tag{6.9}$$

In addition, the total charging and discharging powers of EGSE are expressed in Equations (6.10) and (6.11), respectively. The airport total load for the same interval is expressed in Equation (6.12).

$$P_t^{tch} = \sum_{t,k,i} P_{t,k,i}^{ch} \times\ ava_{t,k,i} \tag{6.10}$$

$$P_t^{tdis} = \sum_{t,k,i} P_{t,k,i}^{dis} \times\ ava_{t,k,i} \tag{6.11}$$

$$Total\ Load = \sum_{t} Z_t + P_t^{tch} - P_t^{tdis} \tag{6.12}$$

where P_t^{tch} is the EGSE fleet total charging power at time *t* in kW, P_t^{tdis} is the EGSE fleet total discharging power at time *t* in kW, and $ava_{t,k,i}$ is the availability of i^{th} EGSE of type *k* at time *t* for V2B. The objective function in (6.9) is subjected to constraints in subsequent Equations, from (6.13) to (6.18).

$$P_{rate}^{min} \leq P_{t,k,i}^{ch} \leq P_{rate}^{max} \tag{6.13}$$

$$P_{rate}^{min} \leq P_{t,k,i}^{dis} \leq P_{rate}^{max} \tag{6.14}$$

$$\sum_{t,k,i} ava_{t,k,i} = AE_{k,t} \tag{6.15}$$

$$\sum_{t,k,i} U_{t,k,i} = NO_{t,k} \tag{6.16}$$

$$ava_{t,k,i} + U_{t,k,i} = 1 \tag{6.17}$$

$$SOC_{k,i}^{min} \leq SOC_{t,k,i} \leq SOC_{k,i}^{max} \tag{6.18}$$

where $P_{rate}^{min}\ and\ P_{rate}^{max}$ are the minimum and maximum charging and discharging power rate in kW, respectively. $AE_{k,t}$ is the total available EGSE of type *k* at time *t*, and $NO_{t,k}$ is the total EGSE required number of type *k* at time *t*. $SOC_{k,i}^{min}\ and\ SOC_{k,i}^{max}$ are the minimum and maximum EGSE battery state of charge in %, respectively. The constraints in Equations (6.13) and (6.14), are used to limit EGSE battery charging and discharging energy to be within the upper and lower bounds of the charger. The constraint in Equation (6.15) was introduced to ensure the total number of available EGSE for V2B of same type *k* at time *t* is equal to the calculated available number of

V2B in Equation (6.4) based on the flight schedule. The pre-calculated required number of EGSE to serve flights at time *t* in Equation (6.3) is used to define elements of $used$ matrix in Equation (6.16). Equation (6.17) is utilised to ensure i^{th} $EGSE$ of type k at time t is either available for V2B or serving an aeroplane. Constraint in Equation (6.18) controls SOC of i^{th} $EGSE$ of type k at time t to be within the preferable maximum and minimum SOC.

The optimisation model is formulated as mixed-integer linear programming, where the above objectives and constraints are modified to be within the required format. Additional constraints are introduced to linearise Equations (6.10) and (6.11). The charging power limits in Equations (6.13) and (6.14) are extended with constraints in Equations (6.19) to (6.28).

$$P_{rate}^{min} \leq P_{(t,k,i)}^{ach} \leq P_{rate}^{max} \tag{6.19}$$

$$P_{rate}^{min} \leq P_{t,k,i}^{adis} \leq P_{rate}^{max} \tag{6.20}$$

$$P_{t,k,i}^{ach} \leq P_{t,k,i}^{ch} \tag{6.21}$$

$$P_{t,k,i}^{adis} \leq P_{t,k,i}^{dis} \tag{6.22}$$

$$P_{t,k,i}^{ach} \leq P_{rated}^{max} \times ava_{t,k,i} \tag{6.23}$$

$$P_{t,k,i}^{ch} - P_{t,k,i}^{ach} \leq (1 - ava_{t,k,i}) \times P_{rate}^{max} \tag{6.24}$$

$$P_{t,k,i}^{adis} \leq P_{rated}^{max} \times ava_{t,k,i} \tag{6.25}$$

$$P_{t,k,i}^{dis} - P_{t,k,i}^{adis} \leq (1 - ava_{t,k,i}) \times P_{rate}^{max} \tag{6.26}$$

$$EM_{t,k,i} \times P_{rate}^{min} \leq P_{t,k,i}^{ch} \leq EM_{t,k,i} \times P_{rate}^{max} \tag{6.27}$$

$$(1 - EM_{t,k,i}) \times P_{rate}^{min} \leq P_{t,k,i}^{dis} \leq (1 - EM_{t,k,i}) \times P_{rate}^{max} \tag{6.28}$$

where $EM_{t,k,i}$ is a binary variable indicating that i^{th} $EGSE$ of type k at time *t* is either charging or discharging. The total charging power, discharging power, and total load in Equations (6.10), (6.11), and (6.12) are rewritten in Equations (6.29), (6.30), and (6.31), respectively. The electric ground support equipment SOC constraint is also reformulated as Equation (6.32).

$$P_t^{tch} = \sum_{t,k,i} P_{t,k,i}^{ach} \tag{5.29}$$

$$P_t^{tdis} = \sum_{t,k,i} P_{t,k,i}^{adis} \tag{5.30}$$

$$Total\ Load = \sum_{t} Z_t + P_t^{tch} - P_t^{tdis} \tag{6.31}$$

$$SOC_{t,k,i} = SOC_{t-1,k,i} + P_{t,k,i}^{ach} - P_{t,k,i}^{adis} - Er_{t,k,i} \times U_{t,k,i} \tag{6.32}$$

where $P_{t,k,i}^{ach}$, and $P_{t,k,i}^{adis}$ are the available charging and discharging power of i^{th} $EGSE$ of type k at time *t* in kW.

6.5 Case Study: Seve Ballesteros-Santander Airport

In this chapter, the SDR airport, a medium-sized Spanish airport located within the city of Santander's boundaries [243], is considered to validate the proposed model. Usually, airports located in residential areas have limited operating hours to minimise noise impacts on neighbours [254], [255], which has an impact on the airport load pattern. In the case of SDR airport, the airport opens from 6:00–23:30, and air flights are scheduled between 7:30–23:00 [230], [255]. Every day, EGSE is completely off and not in use for approximately 8h, from midnight to early morning. Six aircraft stands are considered in this case study, and each stand is assumed to have an aircraft tractor, a baggage tractor, a container loader, and a belt loader. These EGSE types have been considered because of the availability of an electric commercial model of each type, as shown in Tables 2-3. To preserve the life of the EGSE battery and ensure its capability to perform tasks, the maximum and minimum SOC are set at 90% and 50% of the EGSE battery capacity, respectively, while the initial SOC of the EGSE is randomly distributed due to the absence of real data.

Flight schedule and load data of two representative days in February and September 2015 are considered because SDR airport peak and off-peak seasons occur during winter and autumn, respectively [230], [243]. Hourly landing and departing flight schedules are illustrated in Figure 6-4.

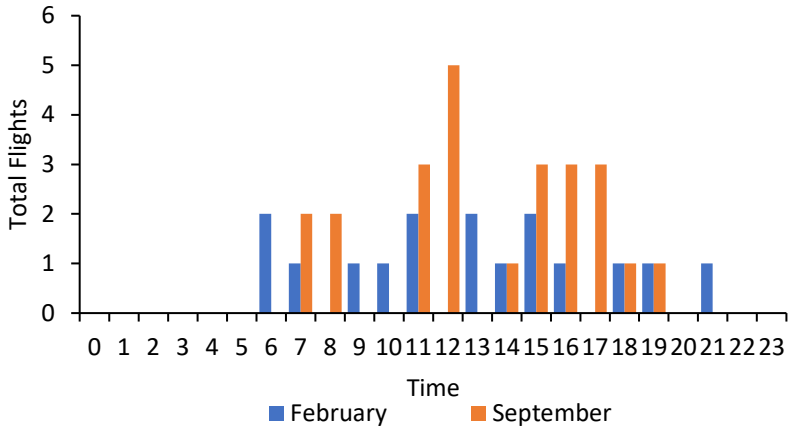

Figure 6-4 Total number of flights per hour.

Average hourly load data of SDR during two representative days in February and September has been used as shown in Figure 6-5 [230].

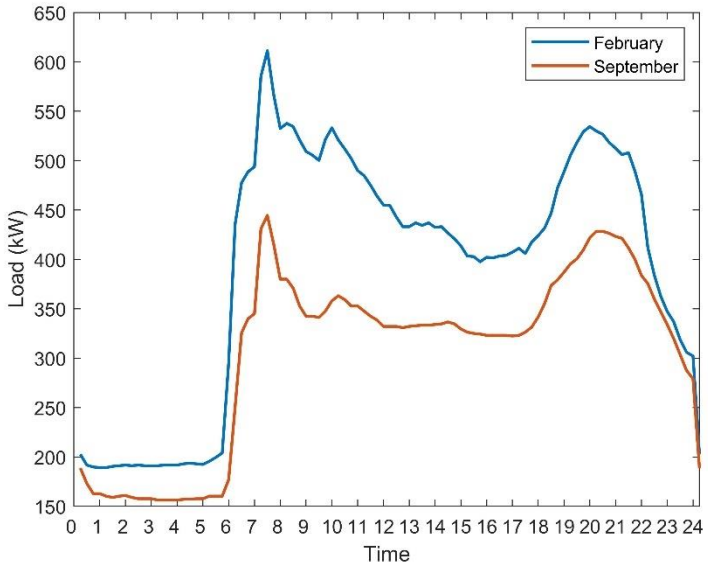

Figure 6-5 Seve-Ballesteros-Santander airport load profile.

The proposed V2B algorithm is evaluated based on various indicators. *LF* represents the SDR airport load factor, and it is calculated as Equation (6.33).

$$LF = \frac{average(\sum_{t=1}^{T} Total\ Load)}{max\ (Total\ Load)} \times 100 \qquad (6.33)$$

where *average (Total Load)* and *max (Total Load)* represent the values of average and maximum total load in kW, including airport and EGSE fleet charging and discharging loads over the studied period, respectively.

The second indicator, *PLR*, assesses to what level the peak value is shaved. The peak load reduction calculation is shown in Equation (6.34). Similarly, *VFP* measures to what extent the minimum value increases, as shown in Equation (6.35).

$$PLR = \frac{max(z) - max\ (total\ load)}{max\ (z)} \times 100 \tag{6.34}$$

$$VFP = \frac{min(total\ load) - min\ (z)}{min\ (z)} \times 100 \tag{6.35}$$

where *max (z)* is the value of airport maximum load in kW, *min (z)* is the value of airport minimum load in kW, and *min (Total Load)* is the minimum value of total load in kW over the studied period. Equation (6.36) is used to calculate *V/P*, which represents the ratio of the lowest load value to the peak load value that occurred during the day. The higher the value, the more the curve is flattening. Rate of change (*RoC*) determines the hourly load change over the studied period, and it is evaluated as Equation (6.37).

$$V/P = \frac{min(total\ load)}{max(total\ load)} \times 100 \tag{6.36}$$

$$RoC = \frac{total\ load_t}{Z_t} \tag{6.37}$$

6.6 Results and Analysis

The proposed methodology to control the EGSE charging and discharging processes is applied to simulate EGSE with V2B access to flatten the airport power demand profile. Two different charging levels are selected as the rated charger power according to the EGSE battery's rated capacity. It is assumed that aircraft tractors and container loaders have access to a 22kW charger, while baggage tractors and belt loaders have access to a 7.6kW charger. The available number of EGSE for V2B is obtained from Equations (6.1)–(6.4), considering the flight schedule presented in Figure 6-4. The available number of EGSE of each type for V2B is shown in Figures 6-6 and 6-7 for February and September 2015, respectively.

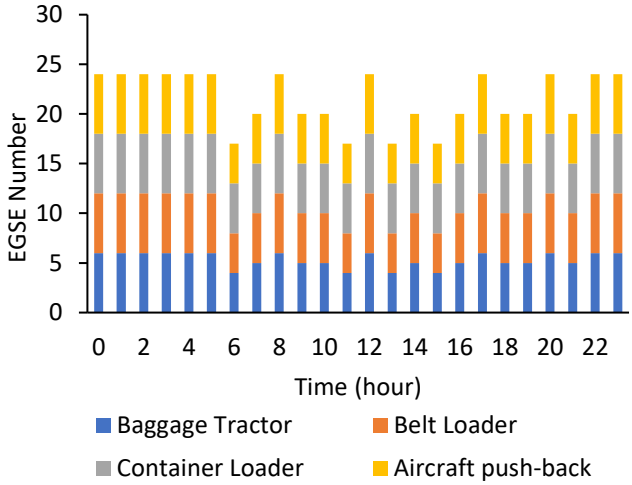

Figure 6-6 Hourly available EGSE in February.

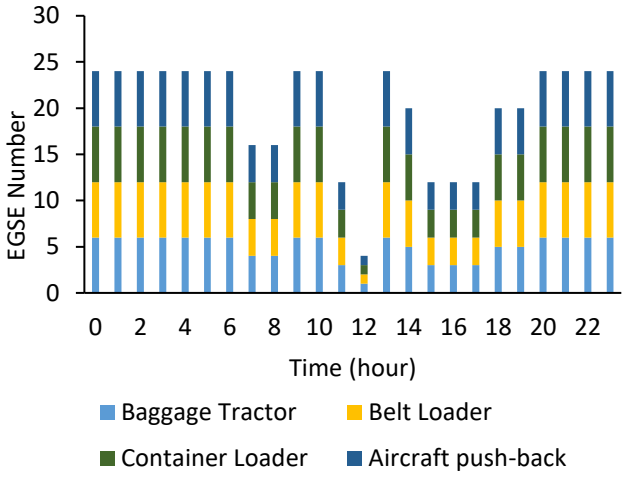

Figure 6-7 Hourly available EGSE in September.

The available number of V2B and the required number to serve aeroplanes are input data to the optimisation algorithm, subject to the constraints presented in Equations (6.15) and (6.16). The EGSE provision to flatten the airport load profile during February is shown in Figure 6-8.

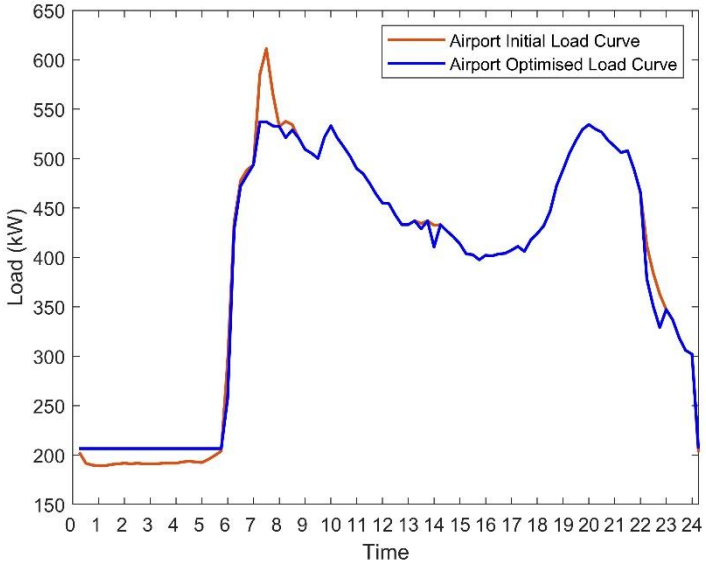

Figure 6-8 Airport power consumption in February.

The airport's original peak load is reduced from 610kW to 537kW in the optimised case. At the same time, the optimised power consumption curve minimum load is increasing after optimisation to 206kW, compared to about 190kW for the airport's original minimum load before smoothing the curve. Compared to the original load curve, EGSE decreases the peak-valley difference from over 420kW to 330kW. Figure 6-9 illustrates the total charging and discharging energy of each type of EGSE in February.

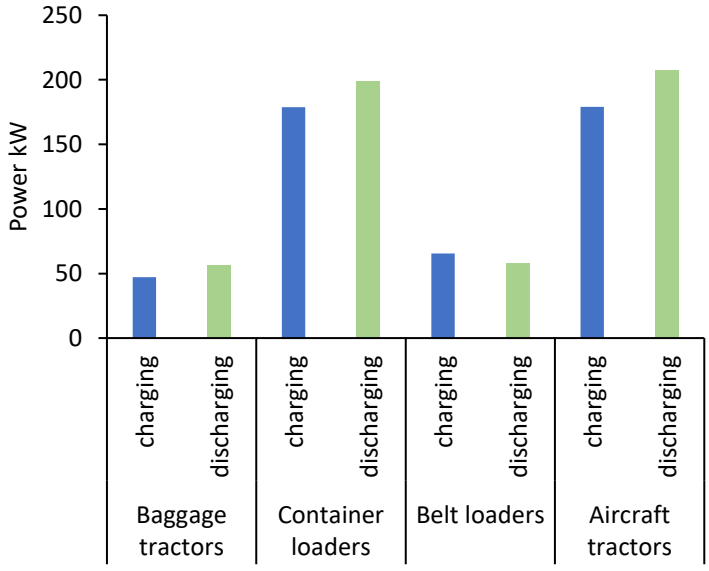

Figure 6-9 EGSE total charging and discharging by type in February.

Container loaders (CL) or aircraft tractors (AT) are used to support the flattening of the SDR power consumption curve more than baggage tractors (BT) and belt

loaders (BL) together. Having a higher battery capacity and higher charging and discharging power allows aircraft tractors and container loaders to contribute more than the other EGSE. The EGSE fleet's final SOC after providing peak shaving and valley filling in February is shown in Figure 6-10. The results clearly show that EGSE's SOC is maintained within limits, and the majority of EGSE's final SOC is higher than the specified minimum.

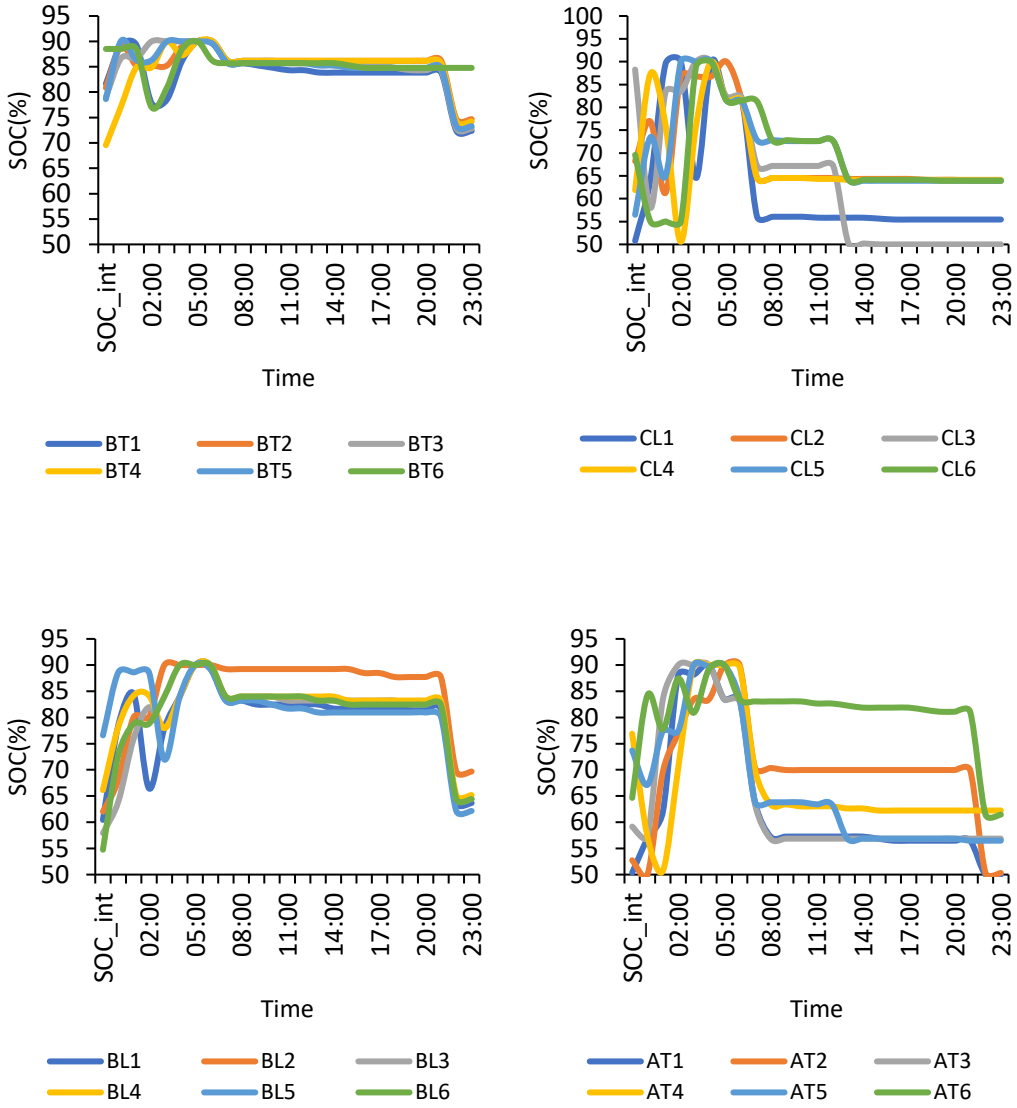

Figure 6-10 EGSE SOC in February.

Moreover, the results show that some of the EGSE charge while others discharge during valley time to keep the minimum load constant. In constraint, the discharging process mainly occurs during the SDR peak load period between 6:00–9:00. In the

second case, the optimisation model is applied during SDR airport off-peak load in September. Figure 6-11 shows the SDR airport optimised curve during September.

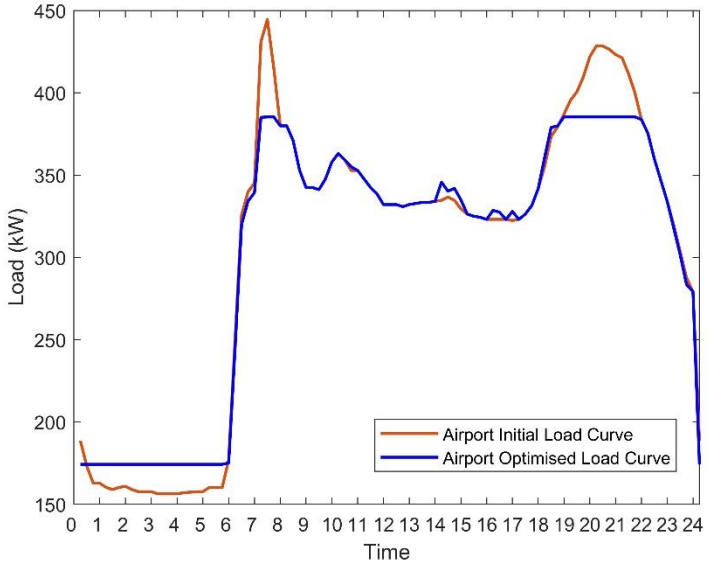

Figure 6-11 Airport power consumption in September.

The results clearly show that EGSE provide sufficient energy to cut the morning peak from about 450kW to 385kW and the evening peak from around 430kW to 385kW. The valley load increases to around 174kW, compared to around 156kW before optimisation. The proposed optimisation model prevents a new peak from happening in both cases, as seen in Figures 6-8 and 6-11. The share of charged and discharged energy by each EGSE type in September is presented in Figure 6-12.

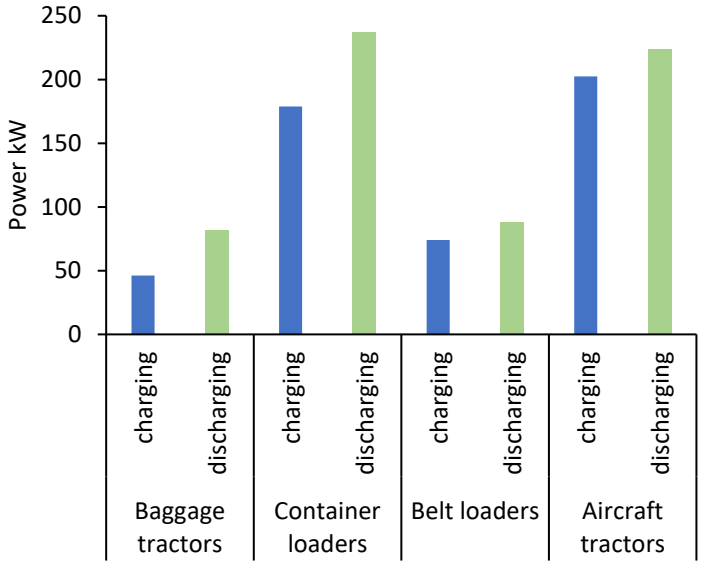

Figure 6-12 EGSE total charging and discharging by type in September.

The highest discharged energy comes from container loaders and aircraft tractors, which are about 240kW and 220kW, respectively. In addition, baggage tractors and belt loaders discharge around 170kW. The total discharged energy is higher than the charged energy in all types compared to the last case where belt loaders charged energy was higher.

Furthermore, Figure 6-13 shows the hourly SOC of the EGSE fleet in September. The SOC stays within the limit, but more than 50% of the EGSE fleet finishes the day with less than 60% SOC. All container loaders final SOC is equal to the minimum specified SOC. The result also revealed that almost half of the EGSE fleet discharged at the beginning and then charged to maximum capacity to fill the valley period. Two discharge cycles are taking place during SDR airport peak load time, when all connected V2B discharge energy in order to shave the peak load.

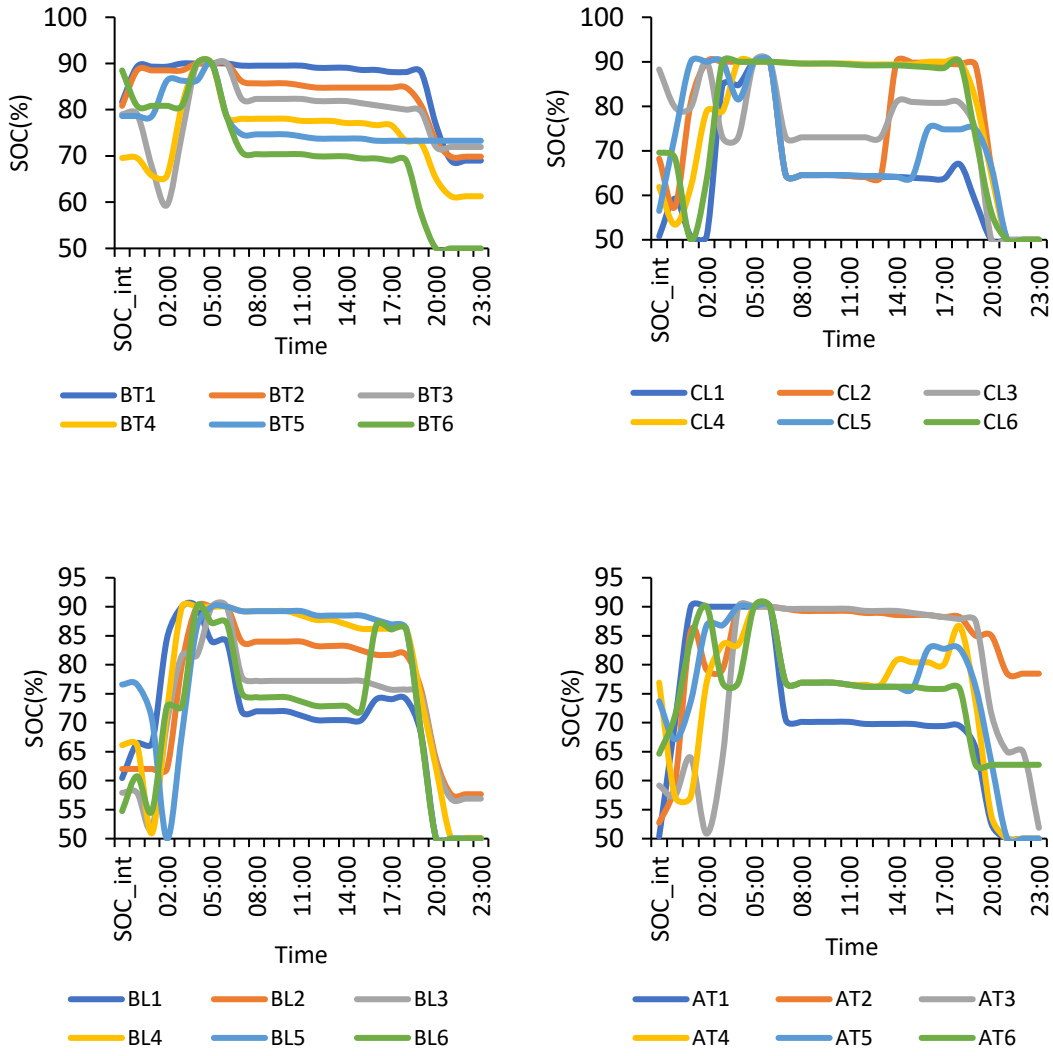

Figure 6-13 EGSE SOC in September.

The proposed optimisation model performance is compared to the base case as presented in Table 6-1 through the previously mentioned indicators.

Table 6-1 Performance evaluation of optimised and baseload curves of SDR airport.

Indicator	February		September	
	Optimised	***Base***	***Optimised***	***Base***
LF	73.2%	64.4%	79.1%	68.8%
PLR	12.1%	-	13.3%	-
VFP	9.1%	-	11.4	-
V/P	38.4%	30.9%	45.2%	35.1%

Indicators show improvement when the peak shaving and valley filling optimisation model is applied, which demonstrate clear benefits. The load curve improves during both simulated airport peak and off-peak days. Figures 6-14 and 6-15 show the optimised load *RoC* during February and September, respectively. The baseload curve is taken as a reference and has a value of 1 *RoC.* The demonstrated *RoC* gives a clear view of charging time, which mainly happens during SDR airport closing hours on both days. While discharging is mainly taking place during SDR airport morning and evening peaks.

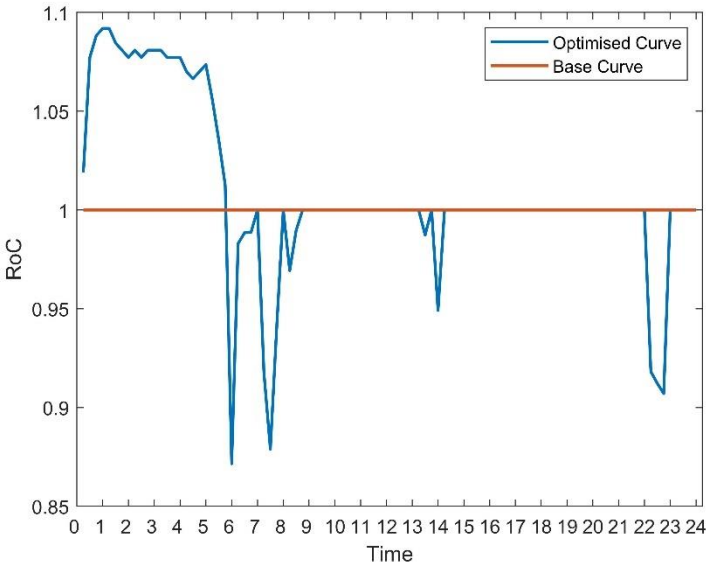

Figure 6-14 Optimised curve RoC in February.

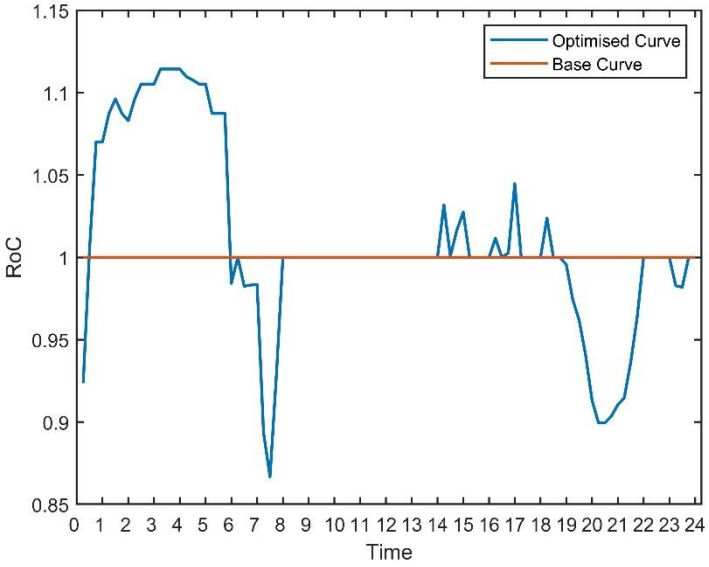

Figure 6-15 Optimised curve RoC in September.

6.7 Discussion

The presented analysis concerning airport activities for load flattening using EGSE offers insightful results, demonstrating a clear potential for enhancing energy management within airport operations. In general, the outcomes of this chapter underscore the potential of EGSE fleets as effective tools for flattening load profiles in airports. The results reveal the significant contribution of certain types of EGSE, namely container loaders and aircraft tractors, in supporting the load flattening process. Equipped with larger battery capacities and higher charging and discharging power, these units exceed other EGSE types in their ability to moderate airport power demand.

The findings also show that it is possible to maintain the SOC of EGSE within defined limits even after they provide peak shaving and valley filling services. This suggests that effective energy management and operational readiness of ground support equipment are not mutually exclusive, and a balance can be struck between the two with careful planning and control. However, some types of EGSE ended the day with minimum SOC, which puts potential constraints on their availability for further airport operations. As such, scope may exist for refining the charging and discharging control strategy to better manage EGSE SOCs while maintaining load flattening objectives.

The results gleaned from this chapter offer valuable insights for airports and policymakers seeking to reduce energy consumption and promote sustainability. The strategic deployment of EGSE for load flattening could significantly contribute to

airport efficiency and the broader goal of greenhouse gas reduction. However, these results are based on specific airport characteristics and theoretical calculations and assumptions, indicating a need for validation with actual operational data. Future investigations could enhance the optimisation model and its applicability in different airport contexts, potentially contributing to more sustainable airport operations on a global scale. Furthermore, findings from this chapter can help formulate effective strategies and recommendations for airports to reduce demand, ensure better energy management, and contribute to a more sustainable aviation sector.

6.8 Summary of Key Findings

This chapter has explored the potential opportunity of the V2B concept to enhance airport power consumption profiles with the aim of reducing airport peak loads and filling valleys by using EGSE. Airport load consumption and flight schedule real-world data were employed to test the proposed optimal peak shaving and valley filling MILP optimisation model. The EGSE charging and discharging power to flatten the airport power profile was modelled in CVX and solved using the GUROBI solver. The primary findings are as follows:

i- In general, using the EGSE fleet in V2B mode can lead to a reduction in peak loads at airports while increasing valleys.

ii- The proposed model can enhance the load shape, including load factor, peak load reduction, and valley to peak ratio.

iii- iii- The charging of the EGSE fleet at airports may occur during shutdown hours or may extend to afternoon hours, depending on the time of year and other factors. For instance, in the February scenario, EGSE fleet charging only took place during shutdown hours, while in the September scenario, charging occurred during both shutdown and afternoon hours.

iv- The peak power reduction is not linearly dependent on the number of available EGSE. Given that the peak power reduction is observed during the morning hours but remains at high levels during the afternoon hours.

v- Electric ground support equipment with larger battery capacities and higher charger power ratings has a higher contribution to reducing peak loads at airports, making it more effective at reducing peak loads than other equipment or vehicles at the airport.

The findings reached were based on specific single-day model runs for various combinations of demand load and flight schedules and a fixed total number of EGSE. In general, using EGSE to flatten the load led to an improvement in the electricity load profile of the airport, which can be beneficial for airport operators. However, future studies may involve running the model for longer periods and incorporating a wider range of EGSE, as well as considering technical constraints.

Chapter 7
Ancillary Services Opportunities at Airports Using Electrified Ground Support Equipment

7.1 Introduction

This chapter focuses on exploring opportunities for the provision of ancillary services to the grid by the aggregation of EGSE vehicles. The developed model is used to investigate the feasibility of EGSE providing frequency regulation services during idle periods between flights. A mixed-integer linear programming optimisation model is introduced to maximise the profits of the EGSE aggregator by controlling EGSE fleet charging and discharging. A commercial optimisation solver package is used to solve the optimisation problem using actual frequency response service data from the Belgian market. This model uses Belgium market data due to its availability but is readily adaptable to other frequency regulation markets.

7.2 Methodology for EGSE Frequency Regulating Provision

The primary aim of this work is to develop a methodology for using EGSE to participate in a day-ahead frequency regulation market through an aggregator based on the flight schedule of an airport. The flowchart of the proposed methodology for participation in ancillary services is shown in Figure 7-1.

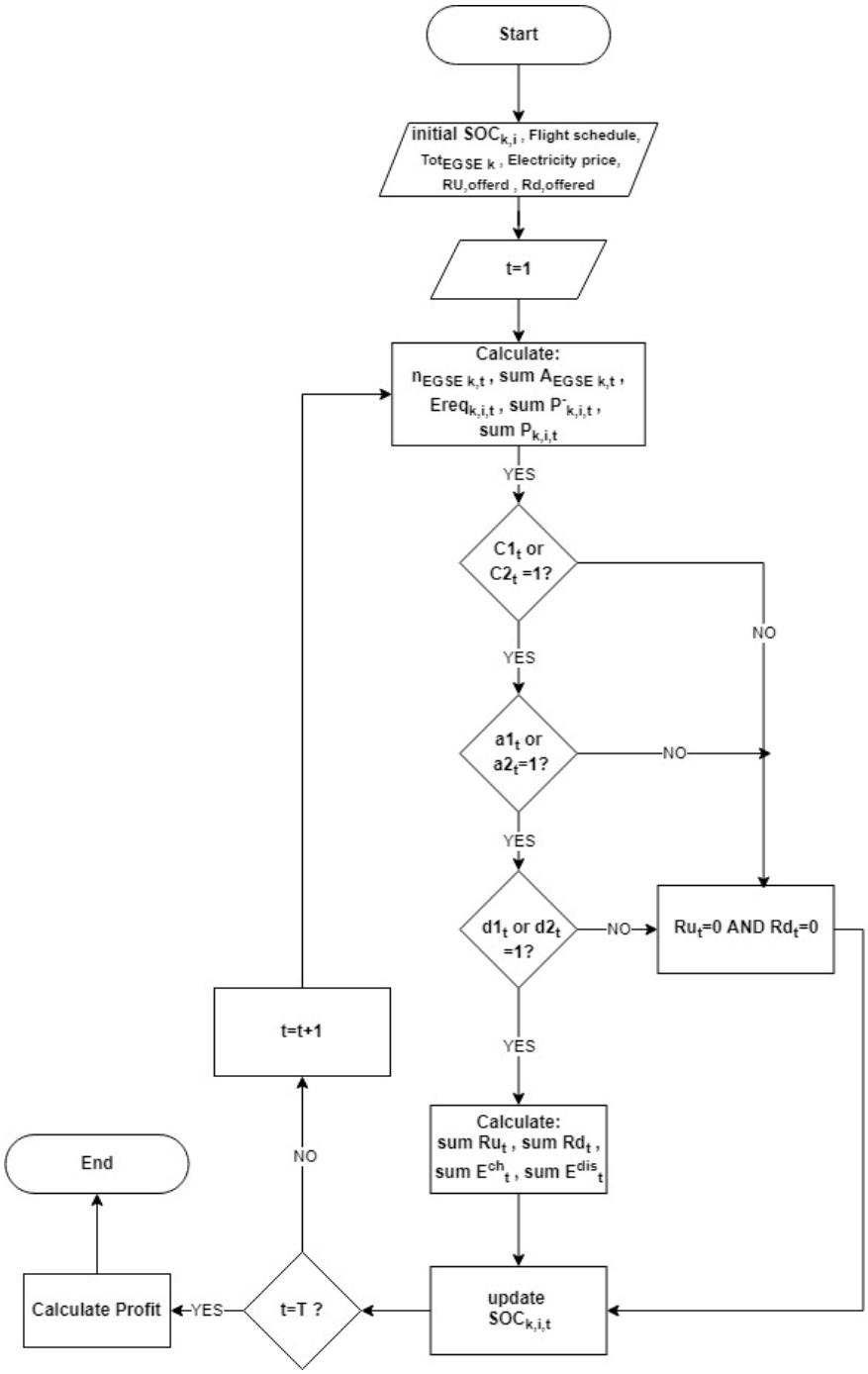

Figure 7-1 Proposed ancillary services flowchart.

The primary function of the proposed EGSE aggregator is to maximise profit, which is based on an optimisation problem subjected to various constraints. The EGSE aggregator profits are like any other investment where the revenue and cost functions are formulated. The EGSE aggregator profit is given in Equation (7.1), where *Rev* is the EGSE aggregator sources of revenue in $ and *C* is the EGSE aggregator total cost in $.

$$Pro = Rev - C \tag{7.1}$$

The EGSE aggregator sources of revenue *Rev* are capacity payment and energy payment. The capacity payment represents the payment for the contracted capacity of the regulation up and down, regardless of whether this capacity is used or not. This is only paid if the EGSE is plugged in and available for the contracted hour. The energy payment is the result of selling energy to the EGSE owner to charge the EGSE fleet and selling energy back to the grid. The revenue is expressed as Equation (7.2).

$$Rev = \sum_{t}[Ru_t \cdot pu_t + Rd_t \cdot pd_t] \cdot \Delta_t + \sum_{k,i,t}[E^{ch}_{k,i,t} \cdot p_t] + \sum_{k,i,t}[E^{dis}_{k,i,t} \cdot pdis_t] \quad (7.2)$$

where Ru_t is available capacity of the regulation up at time *t* in kW, and Rd_t is available capacity of regulation down at time *t* in kW. $E^{ch}_{i,t}$ and $E^{dis}_{i,t}$ are regulation down and up dispatched energy in kWh, respectively. pu_t is the capacity price of regulation up at time *t* in $/kW-h, and pd_t is the capacity price of regulation down at time *t* in $/kW-h. Note that the capacity price for regulation up and down ($/kW-h) means $ per kW available for regulation up or down whether used or not for the hour *t*. p_t is energy tariff at time *t* in $/kWh, $pdis_t$ is the selling energy back price at time *t* in $/kWh, and Δ_t is the time interval. The first part in Equation (7.2) represents the capacity payment revenue, while the second and third parts represent the energy payment that results from either charging or discharging EGSE. The EGSE aggregator total cost is given in Equation (7.3) which includes the cost of energy to charge EGSE and the cost of battery degradation, which is related to discharging the EGSE battery in the V2G mode. It is assumed that the cost of battery degradation is considered only for the discharging cycle because it is a cost borne by the aggregator when using the EGSE battery.

$$C = C_{ch} + C_{deg} \quad (7.3)$$

where C_{ch} is the cost of energy in $ that is needed to charge all the EGSE. This cost is paid by the aggregator to the utility. C_{deg} is the cost of battery degradation in $ which is associated from discharging the EGSE battery in the V2G mode. The cost of energy and degradation are represented in Equations (7.4), and (7.5), respectively.

$$C_{ch} = \sum_{i,t} E^{ch}_{i,t} \cdot \beta_t \quad (7.4)$$

$$C_{deg} = \sum_{i,t} E^{dis}_{i,t} \cdot \varphi \quad (7.5)$$

Equation (7.4) illustrates the positive energy draw $E_{i,t}^{ch}$ by i^{th} EGSE at time *t* to charge it in kWh. It multiplies by the energy price β_t in $/kWh at time *t*. Equation (7.5) shows the degradation cost of the i^{th} EGSE at time *t* that is resulted from discharging the energy E^{dis} to the utility grid in kWh. This cost is paid by the aggregator to the EGSE owner when the EGSE supply the grid by discharging the EGSE battery. φ is the degradation cost in $/kWh. The revenue and cost both depend on the EGSE status; whether it is charging or discharging so, the aggregator must take the i^{th} EGSE availability into account. Airport electric ground vehicles equipment availability is mainly dependant on the flight schedule. The flight schedule is already known in advance which reduces the uncertainty associated with unexpected departures of EGSE. The EGSE fleet availability based on the flight schedule is presented in chapter 6 (Equations 6.1–6.6).

The maximum power that each EGSE can provide for regulation down or up in case of charging or discharging is limited by the stored energy in the battery and the required time to respond for regulation service. The maximum power that EGSE can provide for regulation up to time *t* is calculated using Equation (7.6). The maximum power that EGSE can provide for regulation down at time *t* is given by Equation (7.7).

$$P_{k,i,t}^{-} = (Es_{k,i,t} - SOC_{k,i,t}^{min}) * t_{du} \tag{7.6}$$

$$P_{k,i,t} = (SOC_{k,i,t}^{max} - Es_{k,i,t}) * t_{dw} \tag{7.7}$$

where $P_{k,i,t}^{-}$ is the maximum discharge power in kW, and $P_{k,i,t}$ is the maximum charge power in kW. $Es_{k,i,t}$ is the stored energy in kWh, $SOC_{k,i,t}^{min}$, is the EGSE preferred minimum state of charge in kWh, and $SOC_{k,i,t}^{max}$ is the EGSE preferred maximum state of charge in kWh. t_{du} and t_{dw} are the time needed to dispatch the required energy in hours to response to a regulation up and down, respectively. The required dispatch time depends on the use of bidirectional charger technology. The aggregator offered capacity for regulation up or down at time *t* is the sum of the maximum power of all EGSE for regulation up or down.

The actual energy draw of EGSE for regulation up and down is not known because the aggregator optimises the EGSE fleet in advance. The expected drawn energy of EGSE is consequently described as a fraction of the total contracted capacity for regulation

services. The predicted dispatch energy ratios for regulation up and regulation down are given in Equations (7.8), and (7.9), respectively [162].

$$E_{k,i,t}^{dis} = P_{k,i,t}^{-} \times t_p \times \alpha_{u_{k,i,t}} \tag{7.8}$$

$$E_{k,i,t}^{ch} = P_{k,i,t} \times t_p \times \alpha_{w_{k,i,t}} \tag{7.9}$$

where $\alpha_{u_{k,i,t}}$ and $\alpha_{w_{k,i,t}}$ are the average dispatched to contract ratio for regulation up and down, respectively. t_p indicates the time in hours that EGSE is plugged in and available. The optimisation model is formulated to maximise the profits by participating in the frequency regulation market. The objective function is given in Equation (7.10).

$$Maximise: Pro = Rev - C \tag{7.10}$$

The objective function is subjected to constraints in Equations (7.11) to (7.29).

$$SOC_{k,i,t}^{min} \leq SOC_{k,i,t} \leq SOC_{k,i,t}^{max} \tag{7.11}$$

$$SOC_{k,i,t} = SOC_{k,i,t-1} + \left(E_{k,i,t}^{ch} - E_{k,i,t}^{dis}\right) - Er_{k,i,t} * (1 - ava_{k,i,t}) \tag{7.12}$$

$$P_{k,i,t}^{-} \leq PR_{k,i,t}^{-} \tag{7.13}$$

$$0 \leq P_{k,i,t}^{-} \leq Pdis_m * ava_{k,i,t} \tag{7.14}$$

$$PR_{k,i,t}^{-} - P_{k,i,t}^{-} \leq \left(1 - ava_{k,i,t}\right) * Pdis_m \tag{7.15}$$

$$P_{k,i,t} \leq PR_{k,i,t} \tag{7.16}$$

$$0 \leq P_{k,i,t} \leq Pch_m * ava_{k,i,t} \tag{7.17}$$

$$PR_{k,i,t} - P_{k,i,t} \leq \left(1 - ava_{k,i,t}\right) * Pch_m \tag{7.18}$$

$$Em_{k,i,t} * Pch_l \leq P_{k,i,t}^{-} \leq Pch_m * Em_{k,i,t} \tag{7.19}$$

$$\left(1 - Em_{k,i,t}\right) * Pdis_l \leq P_{k,i,t} \leq Pdis_m * (1 - Em_{k,i,t}) \tag{7.20}$$

$$\sum_{k,i,t} ava_{k,i,t} = AE_{k,t} \tag{7.21}$$

$$d1_t * Ru_{od\,t} \leq Ru_t \leq d1_t * \sum_{k,i,t} P_{k,i,t}^{-} \tag{7.22}$$

$$d2_t * Rd_{od\,t} \leq Rd_t \leq d2_t * \sum_{k,i,t} P_{k,i,t} \tag{7.23}$$

$$C1_t = \begin{cases} 1, & if \ \ Ru_{od\,t} > 0 \\ 0, & Otherwise \end{cases} \tag{7.24}$$

$$a1_t = \begin{cases} 1, & if \ \ Ru_{od\,t} \leq \sum_{k,i,t} P^{-}_{k,i,t} \\ 0, & Otherwise \end{cases} \tag{7.25}$$

$$d1_t = \begin{cases} 1, & if \ \ C1_t + a1_t > 1 \\ 0, & Otherwise \end{cases} \tag{7.26}$$

$$C1_t = \begin{cases} 1, & if \ \ Rd_{od\,t} > 0 \\ 0, & Otherwise \end{cases} \tag{7.27}$$

$$a2_t = \begin{cases} 1, & if \ \ Rd_{od\,t} \leq \sum_{k,i,t} P_{k,i,t} \\ 0, & Otherwise \end{cases} \tag{7.28}$$

$$d2_t = \begin{cases} 1, & if \ \ C2_t + a2_t > 1 \\ 0, & Otherwise \end{cases} \tag{7.29}$$

where $SOC^{max}_{k,i,t}$ is the maximum state of charge in %, $SOC^{min}_{k,i,t}$ is the minimum state of charge in %, $Er_{k,i,t}$ is the required energy to perform a turnaround event in kWh, and $AE_{k,t}$ is the total available EGSE of each type *k*. Additionally, $Pdis_m$ is the maximum discharging power rate in kW, $Pdis_l$ is the minimum discharging power rate in kW, Pch_m is the maximum charging power rate in kW, and Pch_l is the minimum charging power rate in kW. $PR^{-}_{k,i,t}$ is the predicted regulation down capacity in kW, $PR_{k,i,t}$ is the predicted regulation up capacity in kW, $P^{-}_{k,i,t}$ is the maximum discharge power in kW, $P_{k,i,t}$ is the maximum charge power in kW, $Rd_{od\,t}$ is the available regulation down capacity in the market in kW, $Ru_{od\,t}$ is the available regulation up capacity in the market in kW, Ru_t is the available capacity of the regulation up in kW, and Rd_t is available capacity of regulation down in kW. The binary variables $ava_{k,i,t}$ and $Em_{k,i,t}$ indicate the EGSE availability status and whether the EGSE is assigned for up or down regulation, respectively. $d1_t$, $d2_t$, $C1_t$, $C2_t$, $a1_t$, and $a2_t$ are binary indicator variables.

Equations (7.11) and (7.12) are used for the control the state of charge (SOC) of each EGSE to ensure that SOC stays within its assigned limits. Constraints (7.13) to (7.18) are used to determine the fleet total available power capacity for regulation up and down. $ava_{k,i,t}$ is a binary variable that represents the availability state of EGSE. It equals 1 when EGSE is available and not in use to serve an aircraft, while its value is zero when EGSE is being used to serve an aircraft and not available for providing

frequency regulation. Binary variable $Em_{k,i,t}$ in Equations (7.19) and (7.20) is used to guarantee that each vehicle is only providing regulation up or down at the same time. Moreover, Equation (7.21) is used to ensure that the number of available EGSE of the same type at time t is equal to the number of available EGSE of each class which is calculated based on the flight schedule by using Equations (6.1) to (6.6) presented in chapter 6.

Constraints (7.22) and (7.23) are used to guarantee that the bid capacity for regulation up and down is between the fleet's available power capacity for regulation and the offered regulation capacity by the system operator. Indicator Constraints (7.24) to (7.29) are used to ensure regulation bids occur when the offered regulation is larger than zero and the EGSE total capacity for regulation is larger than the offered regulation. This depends on the market policy in which EGSE is participating, where a minimum capacity should be reserved to perform regulation up or down. For example, if the minimum required regulation capacity is 1MW, the aggregator can only make a bid at time t if the total fleet available capacity at the same time t is 1MW or more. If the total available capacity is lower than 1MW, the aggregator cannot make a bid.

7.3 Case Study: Ostend–Bruges Airport

The aircraft push-back, baggage tractor, belt loader, and container loader EGSE are used to demonstrate the performance of the optimisation model. These types of EGSE are selected because they are the most used in airports and because they are mature technologies that already have an electric model available on the market [256]. The specification data of EGSE used in the analysis are shown in Table 2-3 presented in chapter 2 [257].

The case study is considering Ostend–Bruges airport with a pre-COVID-19 flight schedule in August 2019. The Ostend–Bruges airport is considered because of the data availability for the frequency response service that is offered on the Belgian market. In most cases, the flight schedule is fixed and has only minor changes from year to year if a new route is added or an old route is cancelled.

There are 17 aircraft stands for commercial flights located in Ostend–Bruges airport [258], and each aircraft stand is assumed to have baggage tractors, belt loaders, aircraft push-back tractors, and container loaders [246]. It is consequently assumed that EGSE types *k* and *i* are equal to 4 and 17, respectively. The regulation data and energy prices

from Elia Group are used to validate the model [259]. Elia Group is responsible for operating the Belgian grid and controlling the frequency. They publish data on submitted and awarded bids in local balancing auctions. The 1MW minimum volume offered is required, but for the scale-down of the case study, the minimum threshold is reduced to 0.5MW. The regulation data provided by Elia Group, used as input to the optimisation model for validation, is available online [259]. However, the generalised form of the model allows for changes based on market and airport data.

The 15 min data of upward secondary reserve, which is used in this model, is shown in Figure 7-2. The 15 min data for downward secondary reserve used in this model are shown in Figure 7-3. The regulation prices for both regulations up and down are shown in Figure 7-4.

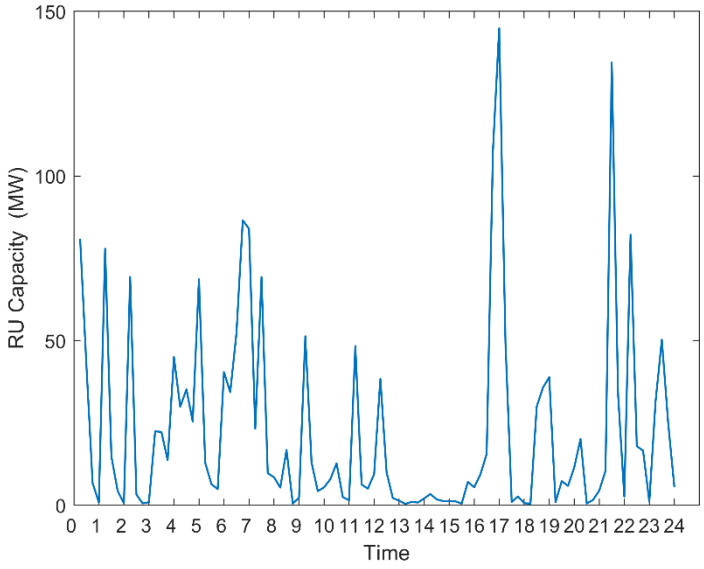

Figure 7-2 Regulation up capacity.

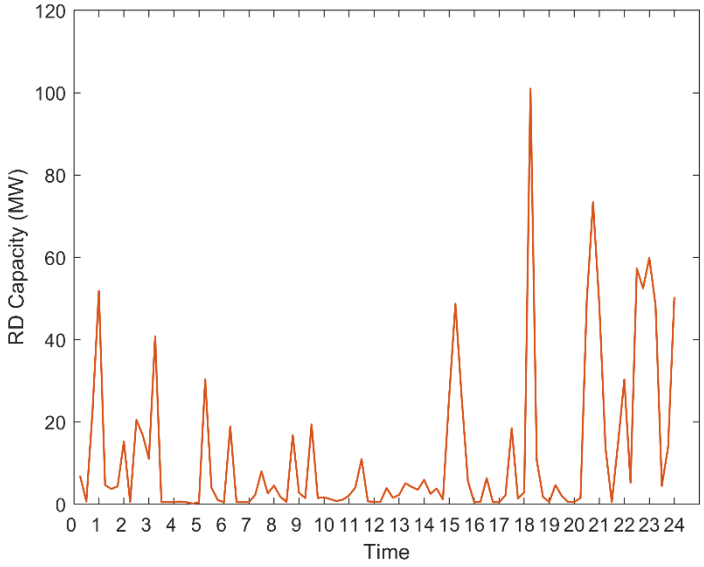

Figure 7-3 Regulation down capacity.

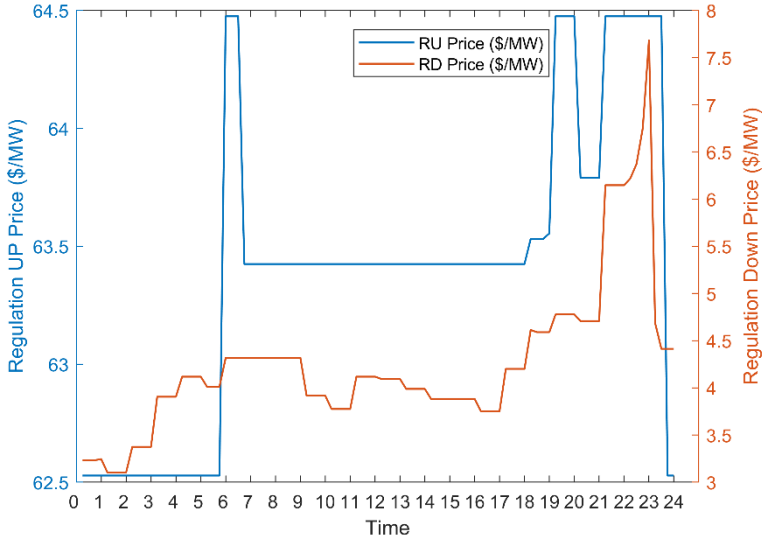

Figure 7-4 Regulation prices.

The expected dispatch ratios used in the modelling study are 0.028 for regulation up and 0.1 for regulation down, based on the average ratio of the actual activated data for the same day that is considered for offering regulation capacity data. The optimisation model was solved using GUROBI optimisation solver Version 9.5 [216] on a desktop computer with a 64-bit Windows 10 operating system, an Intel® Core™ i7 CPU @ 3.4GHz, and 16 GB of RAM. The time horizon for optimisation is 24 h. It is assumed that the initial SOC of EGSE is 50% of the battery capacity at the beginning of the day since the actual data on EGSE SOC is not available and to have enough capacity to perform tasks.

7.4 Results and Analysis

First, Equations (6.1)–(6.6) in chapter 6 are used to calculate the total available EGSE for 24 h. The reserved time factor Res is assumed to be 0.75, which means 15 min each hour is reserved for each EGSE for the driver change, plugging or unplugging the charger, and time delay that might occur [253]. The number of available EGSE of each hour is shown in Figure 7-5.

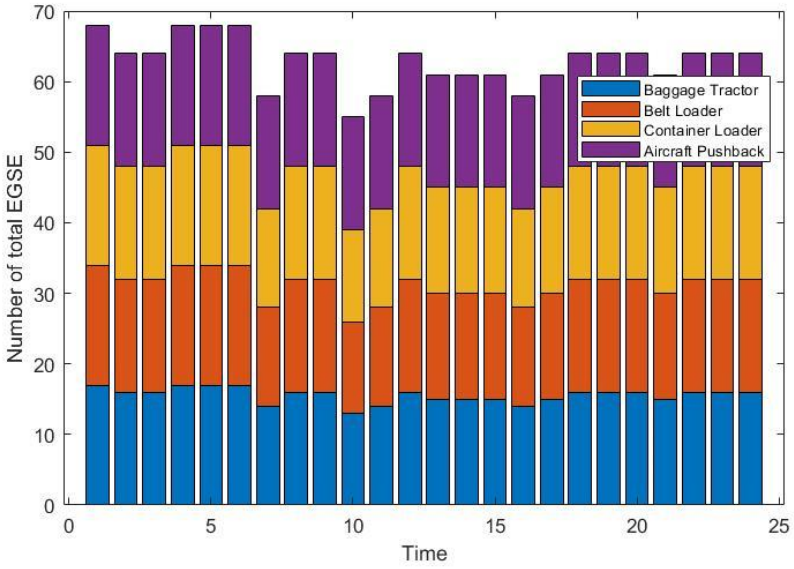

Figure 7-5 Total number of available EGSE.

The optimisation simulation results of regulation up are shown in Figure 7-6. The results show that the aggregator was able to offer a bid for all the considered timeframes and successfully submit the minimum required capacity. The maximum bids are during the airport's off-peak hours, when the number of flights is low.

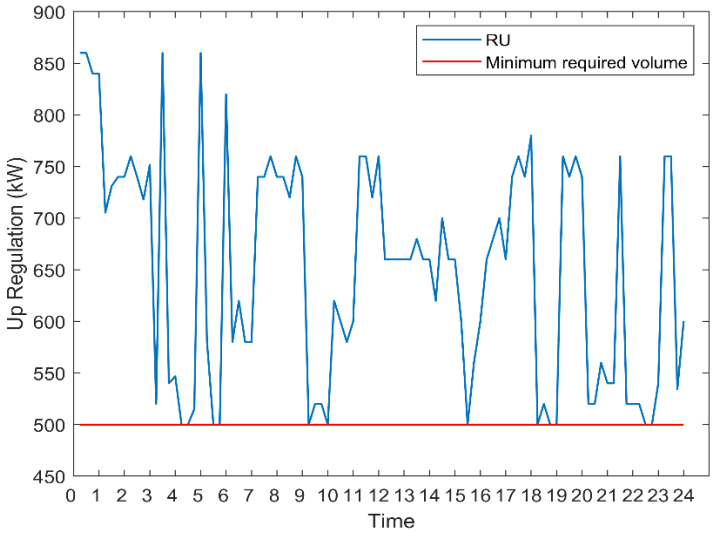

Figure 7-6 Regulation up awarded bids.

Figure 7-7 illustrates the hourly regulation down capacity. The results show that the EGSE aggregator successfully achieves the minimum capacity of bid requirements. It is also noted that regulation down, which corresponds to adjusting the charging rate, occurs during airport off-peak times, when most EGSE are available. The aggregator participates in both regulations up and down at the same time because of EGSE availability, which is based on the flight schedule, which has been considered, and which increased the plugged-in time certainty. This means that some of the total EGSE is used to provide regulation up, and the rest is selected to participate in regulation down.

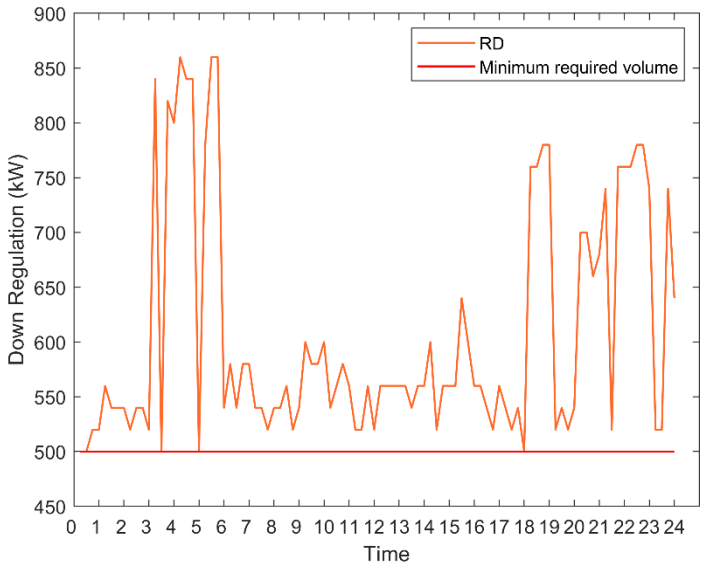

Figure 7-7 Regulation down awarded bids.

The EGSE state of charge was considered to make sure that all EGSE operate within the acceptable SOC limits. Figures 7-8 to 7-11 represent the used EGSE fleet state of charge for the studied period. Equation (7.12) is used to calculate the SOC of each EGSE after each time step to update the SOC to be considered in the next time step. The results show that all EGSE has not violated the maximum or minimum SOC because it is assumed that each EGSE is plugged in during the availability time and provides either regulation up or regulation down. As a result, each EGSE has access to a charging point all the time.

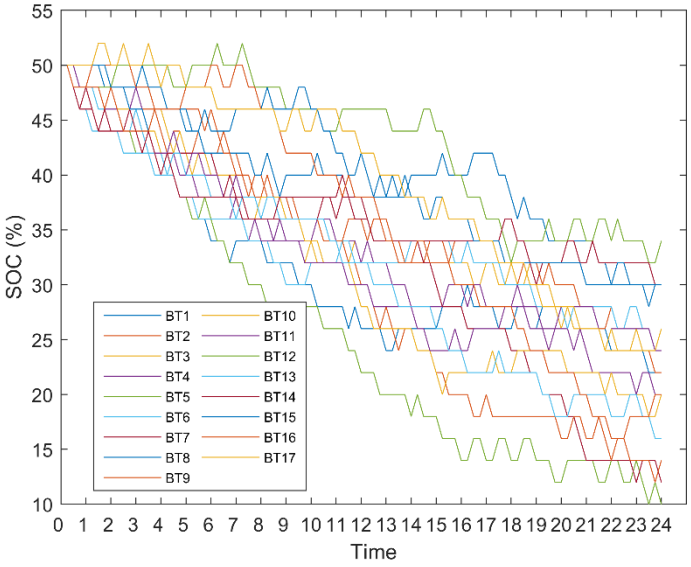

Figure 7-8 Baggage tractors SOC.

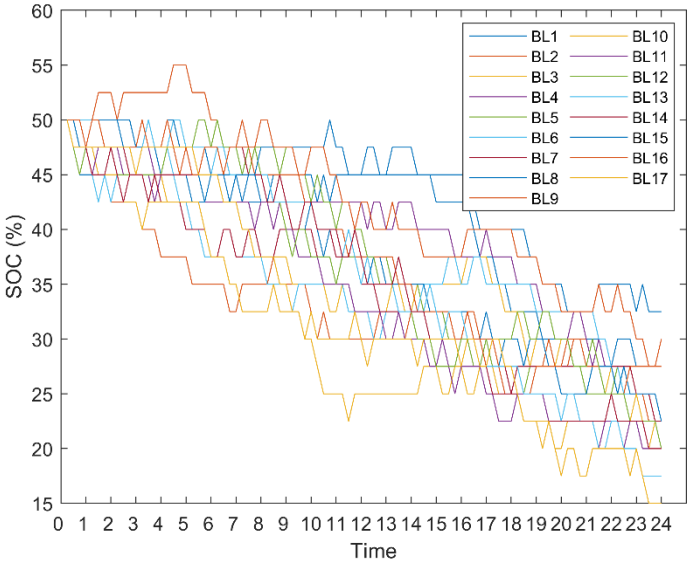

Figure 7-9 Belt loaders SOC.

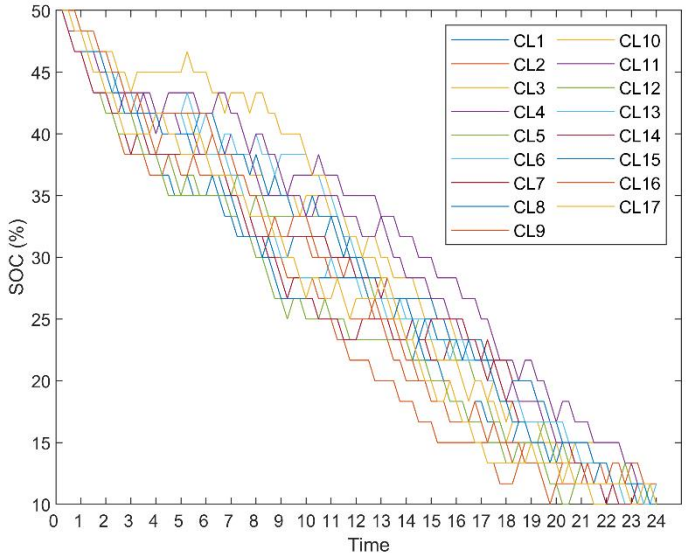

Figure 7-10 Container loaders SOC.

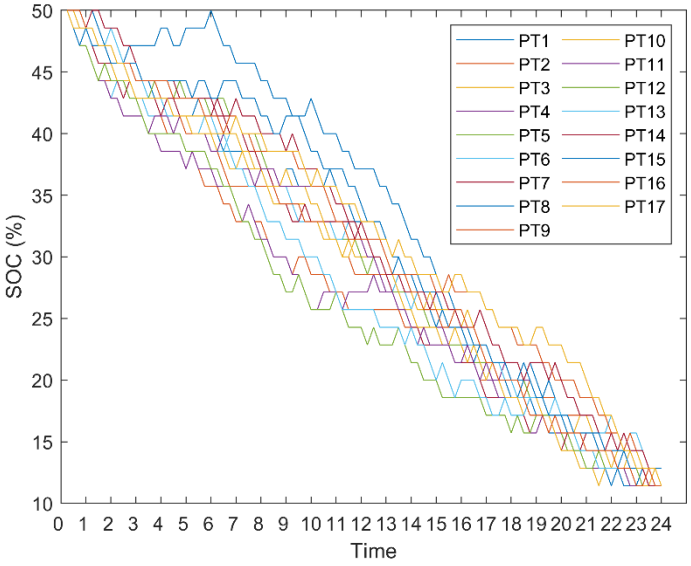

Figure 7-11 Push-back tractors SOC.

The aggregator's total profit from participating in the selected day's ancillary service market is shown in Table 7-1.

Table 7-1 Aggregator revenue and cost.

Revenue and cost breakdown	$/day
Regulation Down Revenue	236
Regulation Up Revenue	3,891
Total Revenue	4,826
Charging Cost	59
Degradation Cost	77
Total Profit	4690

Table 7-1 breaks down the incomes and expenses of participating in the regulation market. The aggregator's net revenue is $4,826/day, which includes the income from providing regulation services and selling the required charging energy to the EGSE fleet. The highest source of income is frequency regulation, which results in over $3,800 in profits. The regulation up revenue share is around 80% of the total revenue. The average committed regulation up capacity and price are 650kW and 0.061$/kW-h, respectively. Moreover, the remaining 20% of earnings come from selling energy to the EGSE fleet for charging and regulation, which are $698/day and $236/day, respectively.

The average committed regulation down capacity and price are 606kW and 0.0038$/kW-h, respectively. The average expected dispatched energy for regulation up is 182kW at an average price of 0.029$/kW. While for regulation down, the average expected dispatched energy is 60kW at an average price of 0.023$/kW. However, the aggregator's total daily cost is $136, which includes the charging and degradation costs. The cost of purchasing energy from the utility, which is the daily required EGSE energy to serve aeroplanes, is $59/day. At the same time, the associated cost of discharging EGSE fleet batteries is $77/day. The net profit that the aggregator can earn from participating in the ancillary market is around $4,700/day over the study period. This demonstrates a clear financial incentive for airports to promote the electrification of their ground support equipment.

7.5 Discussion

The benefit of considering the flight schedule is clearly seen where the aggregator effectively manages the EGSE fleet's participation in the frequency regulation ancillary service market. Besides the positive impact on the environment, electrifying the GSE fleet is a profitable business that can accelerate aviation sector electrification. The calculation results show that the aggregator's primary profitable source is regulation up. This is evident in the significant revenue generated from regulation up, which was higher due to greater capacity prices compared to regulation down prices. The regulation up prices are about 59$/MW while regulation down prices lay around 5$/MW. Moreover, the capacity of available power that an aggregator can control is high because the uncertainty of EGSE availability is very low. It is assumed that all the offered bids by the aggregator are winning bids, so the capacity payment is

guaranteed. The number of EGSE compared to the number of flights is also an advantage because most of the EGSE are always available.

However, the cost only includes both the charging and degradation costs. The charging cost and cost of battery degradation are low since EGSE is charging and discharging in a controllable manner based on fixed usage. The charge and discharged power are a small percentage of the total contracted capacity for regulation down and regulation up, so increasing this percentage will reduce the total revenue. Moreover, the regulation up price, which is the cost of supplying energy to the grid, is much higher than the regulation down price; thus, the aggregator income is high. The EGSE availability certainty level has clearly increased profits where aggregators successfully submitted regulations bids for the whole time. Comparing EGSE with on-road EVs, EGSE proves to be a more confident source of providing frequency regulation services and could be more beneficial because EGSE operates in a closed operation environment. These are off-road vehicles operating in a controlled environment where travel distance is scheduled in advance and speed is controlled, which precludes traffic congestion and guarantees EGSE availability.

Despite the promising results, the study is subject to some limitations. These include the assumption that all bids made for ancillary services are successful, which may not always be the case given the competitive nature of the market. The analysis is based on a one-day horizon, which does not consider variations in the cost of providing these services, potential maintenance costs, or changes in regulations or market prices over longer periods. Additionally, the generalisation of results to other airports might be constrained due to differences in operational patterns and airport configurations.

7.6 Summary of Key Findings

In this chapter, the economic opportunity of the frequency regulation provision provided by EGSE through an aggregator was investigated. A MILP model to help aggregators utilise the EGSE to participate in the frequency regulation market was developed. The monetary benefits of deploying EGSE into the ancillary services market were simulated using frequency regulation up and down and energy price data from the Belgian TSO Elia group. The Ostend–Bruges airport flight schedule for 2019 was adopted to coordinate EGSE availability. From the simulation results, the primary findings are as follows:

i- Overall, the EGSE idle time could be beneficial where the aggregator could make profit by participating in the frequency regulation ancillary services market.

ii- The regulation up market proves more profitable compared to the regulation down market due to the considerably higher prices for regulation up. In particular, the revenues for regulation up and regulation down were $3,900 and $240, respectively.

iii- The average committed regulation was higher than the average expected dispatched energy for regulation up and down, which resulted in higher revenue than costs.

iv- Electric ground support equipment batteries are predominantly charged during late-night hours to participate in the regulation down market, despite having a higher capacity for regulation up. The charged energy is utilised to participate in the regulation up market when prices are higher and perform tasks during airport busy times.

The conclusions were drawn from running specific day data of the day-ahead electricity and frequency regulation market and flight schedule. However, future studies may involve running the model for longer periods and at different airport locations, as well as improving the model to include real-time market data.

Chapter 8
A Study of Transformer Dynamic Loading at an Airport in the Context of a Microgrid with Distributed Energy Resources

8.1 Introduction

The approach of dynamic loading a distribution transformer supplying an airport with considerable EGSE uptake is discussed in this chapter. Transformers are a very expensive line item for an airport. They are critical components in the distribution networks, which are designed to deliver electricity to end-users. This chapter aims to investigate to what extent the additional load of EGSE increases the transformer loading condition and presents a method of adapting the additional load to defer the transformer upgrade, which therefore adds additional monetary value for the grid. The transformer's thermal characteristics have been considered to load the transformer based on changing conditions rather than a fixed condition. A mixed-integer non-linear programming optimisation model is introduced to minimise the impact of EGSE on transformers using an existing open-source software package and solver. This modelling uses the data of a civilian airport and EGSE fleet presented in chapter 5 as a case study but is readily adaptable to other airport locations and different EGSE types.

8.2 Methodology for Transformer Dynamic Loading

This study is proposing a smart charging model that optimises the transformer lifetime with the presence of EGSE. The objective of the model is to minimise the transformer loss of life $L_{(n)}$ over the considered period. Figure 8-1 shows the transformer dynamic loading optimisation algorithm. The proposed methodology is shown in Figure 8-2.

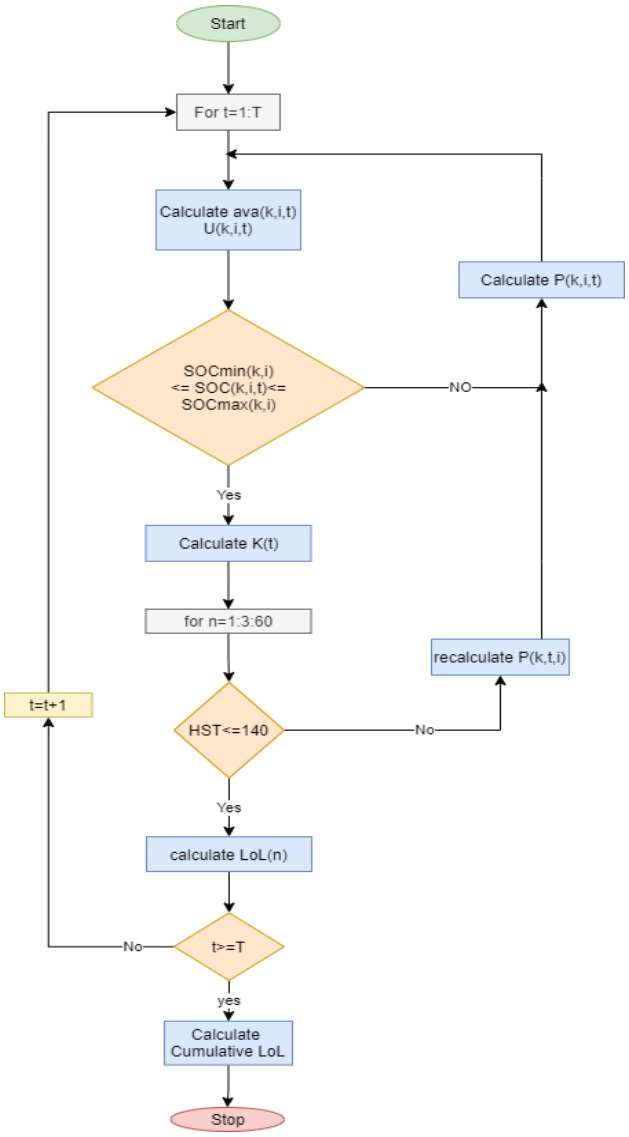

Figure 8-1 Dynamic loading algorithm of the distribution transformer.

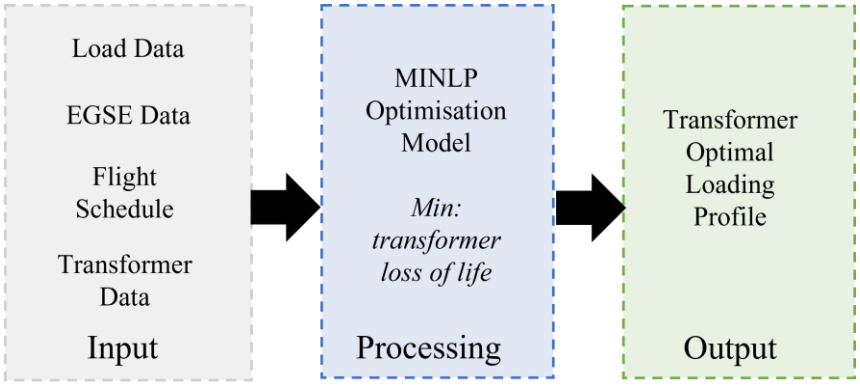

Figure 8-2 Flowchart of dynamic loading methodology.

The electric ground support equipment SOC is also considered to ensure all EGSE have specified SOC based on the operator requirements. The transformer dynamic loading (DL) is formulated as non-linear mixed-integer programming. The objective

function is given in Equation (8.1), where $L_{(n)}$ is the transformer total loss of life at the n^{th} time step in minutes.

$$\min \sum_{n} L_{(n)} \tag{8.1}$$

As mentioned earlier in section 2.11.1, $L_{(n)}$ is very sensitive to hot-spot temperature, which also depends on the load factor K. The load factor K at time *t* is calculated using Equation (8.2).

$$K_t = \frac{Z_t + P_t^{tch}}{P_{rated}} \tag{8.2}$$

where Z_t is the airport load at time *t* in kW, P_t^{tch} is the total charging load at time *t* of EGSE fleet in kW, and P_{rated} is the transformer rated load in in kVA. Decision binary variables Ava and U are introduced to represent the EGSE states whether it is plugged in to charge or to serve an aeroplane. $Ava = 1$ and $U = 0$ when the EGSE is plugged in. Whereas, when the EGSE is serving an aircraft, the decision variables $Ava = 0$ and $U = 1$. The EGSE battery SOC is calculated for each hour as expressed in Equation (8.3).

$$SOC_{k,i,t} = SOC_{k,i,t-1} + E_{k,i,t}^{ch} \times Ava_{k,i,t} - Er_{k,i,t} \times U_{k,i,t} \tag{8.3}$$

where $SOC_{k,i,t}$ is the state of charge of vehicle *i* of type *k* at time *t* in kWh. $P^{ch}{}_{k,i,t}$ is the battery charged energy of vehicle *i* of type *k* at time *t* in kWh, and $Er_{k,i,t}$ is the consumed energy of vehicle *i* of type *k* at time *t* to perform turnaround events in kWh. $Ava_{k,i,t}$ and $U_{k,i,t}$ are the decision binary variables of vehicle *i* of type *k* at time *t*. The total charging power of EGSE fleet at time *t* is given in Equation (8.4), where $P^{ch}{}_{k,i,t}$ is the charging power of vehicle *i* of type *k* at time *t*.

$$P_t^{tch} = \sum_{k,i,t} P_{k,i,t}^{ch} \times Ava_{k,i,t} \tag{8.4}$$

The objective function is subjected to constraints in Equations (8.5) to (8.11).

$$\theta_{h(n)} \leq 140°\text{C} \tag{8.5}$$

$$\sum_{k,i,t} Ava_{k,i,t} = AE_{k,t} \tag{8.6}$$

$$\sum_{k,i,t} U_{k,i,t} = NO_{k,t} \tag{8.7}$$

$$Ava_{k,i,t} + U_{k,i,t} \leq 1 \quad (8.8)$$

$$SOC_{k,i}^{min} \leq SOC_{k,i,t} \leq SOC_{k,i}^{max} \quad (8.9)$$

$$Ava_{k,i,t} \; and \; U_{k,i,t} \in \{0,1\} \quad (8.10)$$

$$P_{k,i,t}^{min} \leq P^{ch}{}_{k,i,t} \leq P_{k,i,t}^{max} \quad (8.11)$$

where $\theta_{h(n)}$ is the transformer hot-spot temperature in °C, $AE_{k,t}$ is the total available number of EGSE of each type, and $NO_{k,t}$ is the required number of EGSE to serve aircrafts. Additionally, $SOC_{k,i}^{min}$ is the EGSE minimum preferred SOC in %, $SOC_{k,i}^{max}$ is the EGSE maximum preferred SOC in %, $P_{k,i,t}^{min}$ is the minimum charging rate in kW, and $P_{k,i,t}^{max}$ is the maximum charging rate in kW.

To prevent gas bubbles, which could reduce the dielectric strength, the hot-spot temperature is limited to under 140°C in Equation (8.5). The constraint in Equation (8.6) is used to ensure that the total number of available EGSE of each type *k* is equal to the calculated available number based on the flight schedule. Whereas Equation (8.7) is used to guarantee the sum of the EGSE that serve aeroplanes is equal to the required number of electric ground support equipment of each type *k* to serve all flights at time *t*. The constraint in Equation (8.8) ensures each EGSE is only available for either charging or serving an aircraft at time *t*. Equation (8.9) limits the EGSE battery state of charge to be within the allocated limits. The constraint in Equation (8.11) limits the charging power to be within the charger's limits.

8.3 Case Study: Seve Ballesteros-Santander Airport

The case study considers Seve Ballesteros–Santander airport in Spain, presented in chapter 6, with power load, flight schedule, and ambient temperature data from 2015. Usually, the yearly flight schedule is constant, with only minor changes happening from time to time due to routes being added or cancelled. Six aircraft stands are used in this chapter with the same EGSE types, which are baggage tractor, belt loader, container loader, and aircraft push-back. The 24h airport load profile and ambient temperature are illustrated in Figure 8-3 [230], [260].

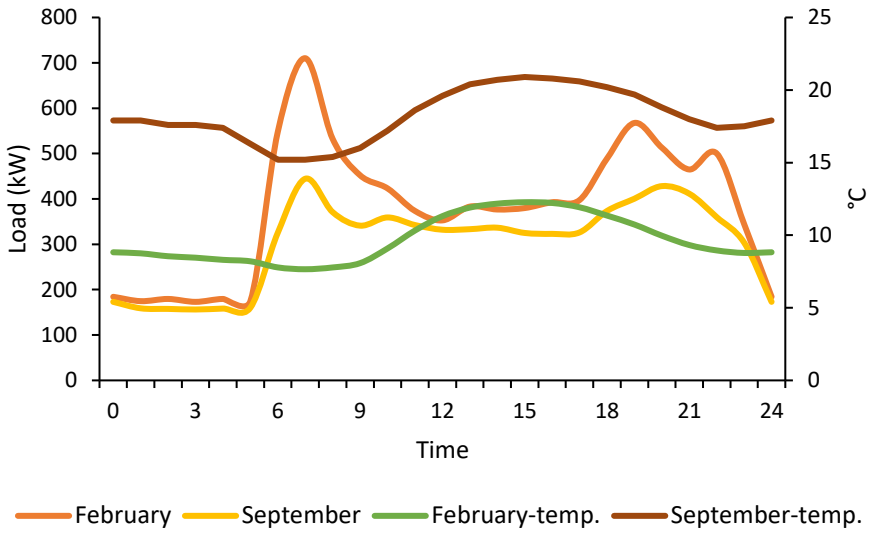

Figure 8-3 SDR airport load profile and ambient temperature.

Note that the airport shutdown time is between 23:30–6:00 and the airport is located in a mild-climate zone. The number of flights, load profile, and ambient temperature are used as inputs to validate the proposed optimisation algorithm. The algorithm has a level of generality and can be used for any chosen airport location. It is assumed that the installed distribution transformer capacity is 750kVA. The oil-immersed distribution transformer's thermal characteristics are shown in Table 8-1 [203].

Table 8-1 Transformer thermal characteristics.

Component	Value
y	1.6
x	0.8
k_{11}	1
k_{21}	1
k_{22}	2
τ_o	180 (min)
τ_w	4 (min)
Rx	65 (K)
R	5
Hr	35 (K)

Existing commercial EGSE is considered in the analysis. Battery specifications for each type are shown in Tables 2-3 as presented in chapter 2. The maximum SOC is set to 90% of the battery size, the minimum SOC is set to 10% of the battery size, and the initial SOC is set to the minimum SOC to examine the maximum possible impact on the transformer lifetime due to EGSE charging.

The optimised transformer dynamic loading is modelled using OpenSolver Version 2.9 [261], [262] and solved using COIN-OR Couenne solver Version 1.0 [217] on a desktop computer with a 64-bit Windows 10 operating system, an Intel® Core™ i7 CPU @ 3.4 GHz, and 16 GB of RAM. The OpenSolver package is an open-source Excel add-in that is compatible with different solvers to solve linear and non-linear mixed-integer optimisation problems.

The primary aim of this chapter is to introduce a smart charging model that reduces transformer degradation. The transformer thermal behaviour is studied in the presence of EGSE charging, considering both cases with and without a dynamic loading model to compare the performance of the proposed algorithm. Load profiles from two representative days have been modelled to investigate extreme cases, including demand peaks and off-peaks, which can be used as a point of comparison to better understand typical cases. The SOC of the EGSE fleet is set to maximum at the end of simulated days to examine the maximum possible impact on transformer age due to EGSE charging. The following scenarios are investigated to evaluate the transformer's loss of life:

Scenario 1: Airport peak load day in February 2015, considering the following case studies:

- Base_NoEGSE represents the current situation without EGSE implementation.
- Without_DL represents the uncontrolled charging to meet the maximum SOC at the end of the day.
- With_DL represents the proposed dynamic loading (DL) charging model to meet maximum SOC at the end of the day.

Scenario 2: Airport off-peak load day in September 2015 considering the following case studies:

- Base_NoEGSE represents the current situation without EGSE implementation.
- Without_DL represents the uncontrolled charging to meet the maximum SOC at the end of the day.
- With_DL represents the proposed DL charging model to meet maximum SOC at the end of the day.

8.4 Results and Analysis

The EGSE availability based on the flight schedule is obtained by using the equations described in chapter 6 (Equations 6.1–6.6). The total available number of EGSE units for scenarios 1 and 2 are shown in Figures 6-6 and 6-7, respectively. Figure 8-4 shows the transformer loading demand of the three modelled case studies for scenario 1.

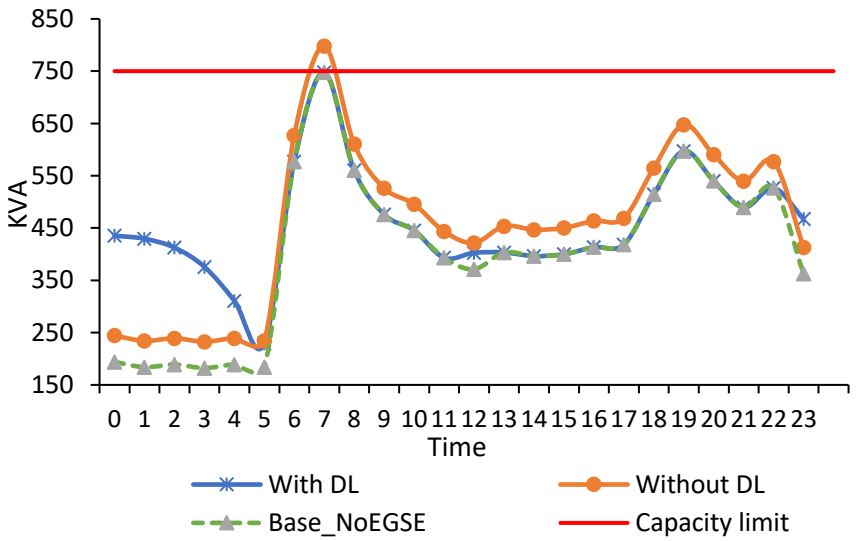

Figure 8-4 Transformer loading profile for scenario 1.

In the case of Base_NoEGSE, the load demand does not exceed the transformer limit. The transformer has a surplus capacity over the entire day except during peak hours, when demand is about 747kVA. Whereas, in the case of uncontrolled charging, the transformer loading increased by an average of 15% over the day. The load demand exceeds the transformer limit by 6% compared to the base case for a short period of time during peak demand hours. In contrast, the proposed DL algorithm increases load demand during the first 6 h and the last hour to meet charging requirements by the end of the day. In the same case with DL, the transformer loading profile does not exceed the transformer capacity limit, as seen in Figure 8-4. Figure 8-5 shows the transformer loading factor of the three simulated case studies for scenario 1.

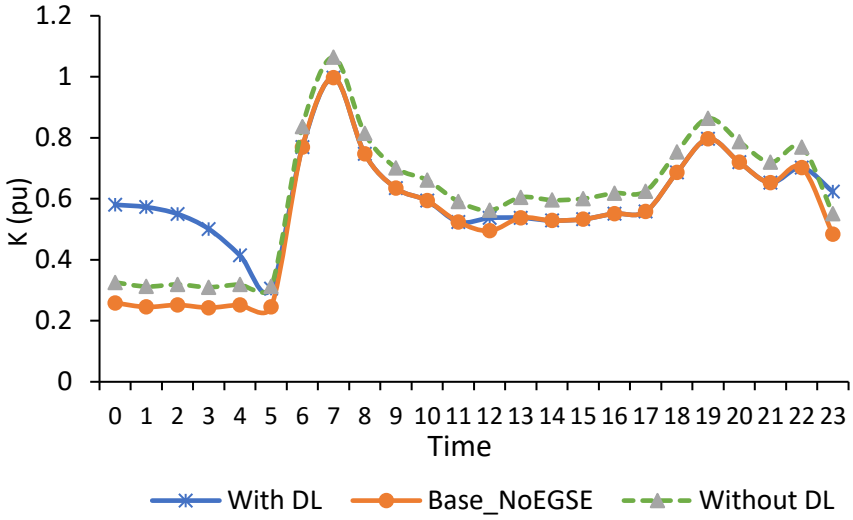

Figure 8-5 Transformer load factor for scenario 1.

The transformer loading factor is about 0.24 during airport shutdown time and increases above 0.8 between 6:00–8:00 before EGSE implantation. Moreover, the transformer loading factor has a maximum of 0.99 loading for only 1h at 7:00 and decreases to an average of 0.6 loading from 8:00–23:00. Uncontrolled charging loading factors increase over the day, and the maximum load factor rises to 1.1 and exceeds the capacity limit for 1h. Conversely, when DL is applied, the transformer loading factor rises in the first 6h and maintains the same peak load factor at 0.99 as compared to the base case. The transformer thermal performance relating to scenario 1 is illustrated in Figure 8-6.

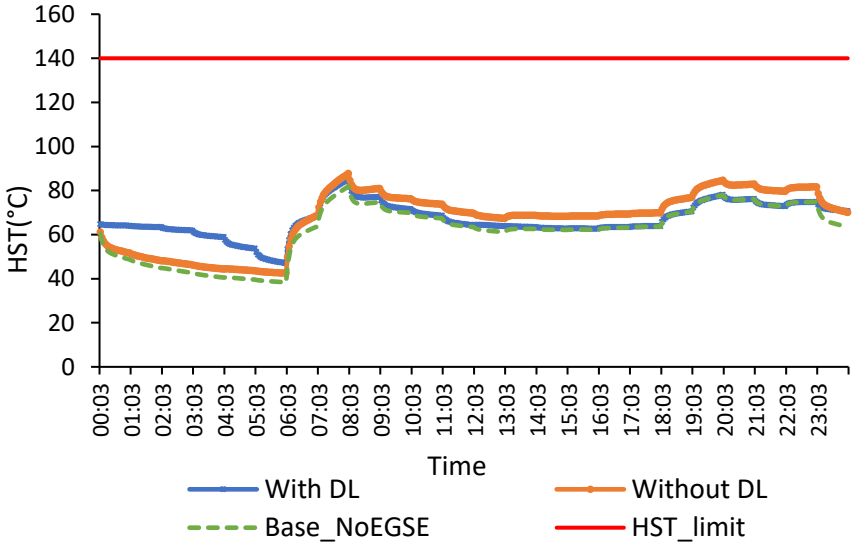

Figure 8-6 Transformer hot-spot temperature for scenario 1.

Transformer hot-spot temperature (HST) is shown because it has a direct influence on transformer ageing rate. The hot-spot temperature is below the maximum permissible 140°C temperature in the three analysed loading situations. The hot-spot temperature is lower than the reference ageing rate temperature of 110°C; the maximum HST over the simulated period is about 90°C for all conditions of scenario 1. The HST in the case of Without_DL has small differences from 10:00–23:00 compared to Base_NoEGSE. Whereas in the case of With_DL HST, there is a notable variance between 00:00–6:00 as compared with other transformer loading situations. Figure 8-7 shows the transformer loss of life (LOL) over 24h for scenario 1.

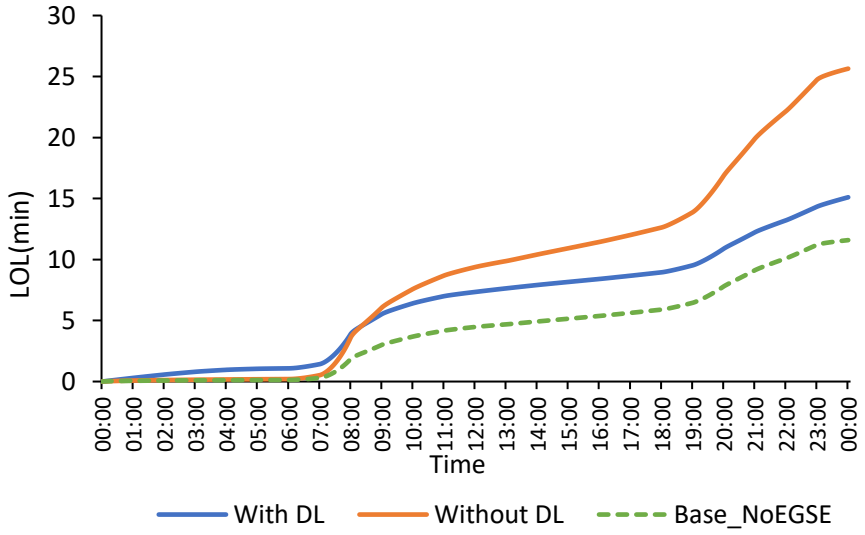

Figure 8-7 Transformer loss of life for scenario 1.

The transformer LOL gradually increases to reach 12min cumulative daily LOL in the base case before EGSE deployment. Moreover, in Without_DL case, the cumulative LOL rapidly increases from 20:00 and reaches about 26min. In contrast, the transformer LOL grow on steady pace which by the end of the day results in around 15min cumulative LOL in case of With_DL. Figure 8-8 shows the load demand of the airport for scenario 2.

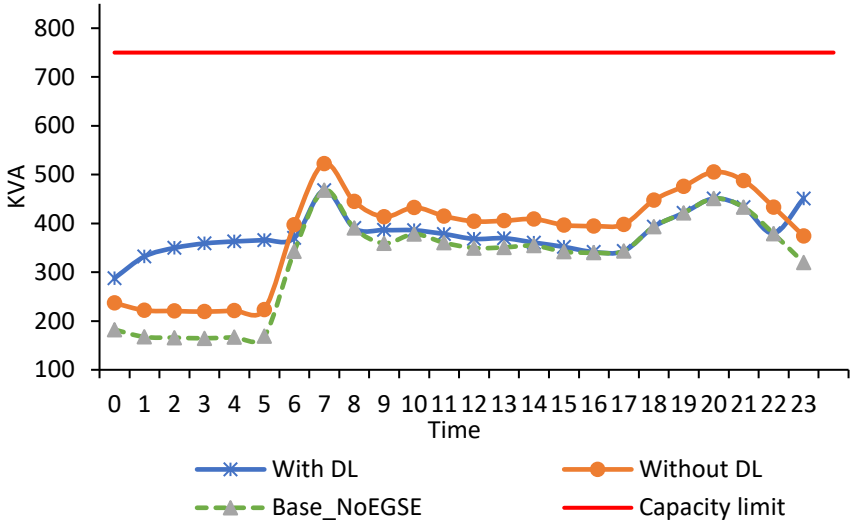

Figure 8-8 Transformer loading profile for scenario 2.

In the base case, the transformer is loaded well below its rated capacity. The transformer peak load is about 470kVA, which corresponds to airport opening times between 6:30–7:30 and a night peak at 20:00, whereas the transformer's maximum load increases to about 500kVA at 7:00 and 20:00 in the case of uncontrolled charging. In the case of With_DL, the transformer loading is almost constant, and peak load is maintained the same as in the base case. The EGSE charging process occurs almost throughout the day, except during peak demand hours. The transformer loading factor *K* of the three investigated cases for scenario 2 is shown in Figure 8-9.

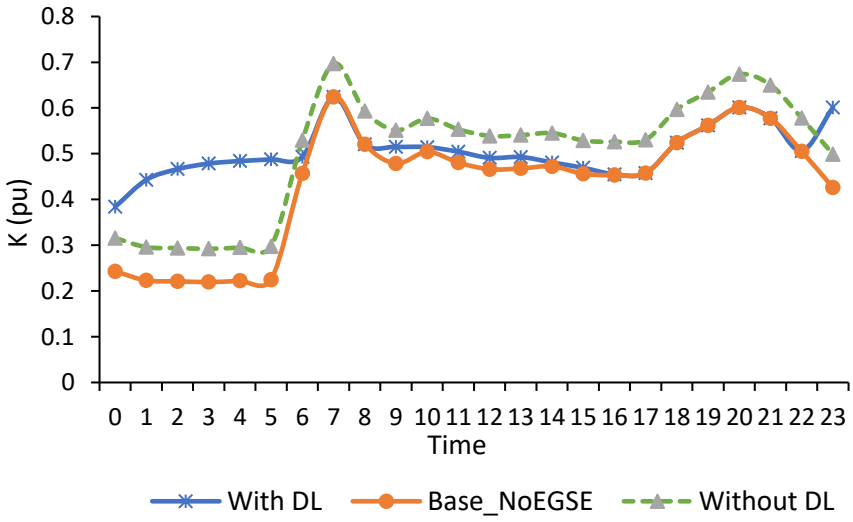

Figure 8-9 Transformer load for scenario 2.

The loading factor in the base case is about 0.21 and 0.6 for base load and maximum load, respectively. The transformer loading factor increases to around 0.3 and 0.7 to meet the base load and maximum load, respectively, in the case of Without_DL compared with the base case. In the case of With_DL, the transformer loading factor stabilised at around 0.5 for most of the time when compared to other cases. In the same simulated case, the maximum load factor remains unchanged compared to the base case. The transformer HST that corresponds to scenario 2 is presented in Figure 8-10.

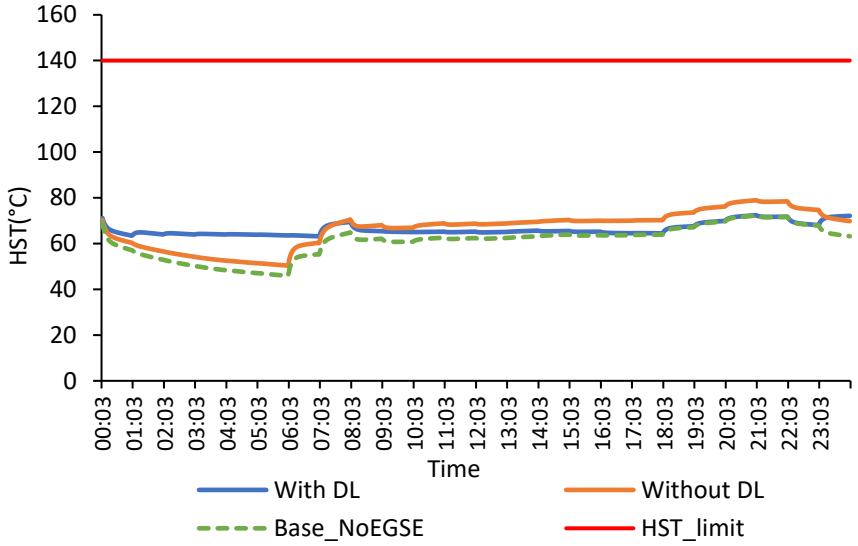

Figure 8-10 Transformer hot-spot temperature for scenario 2.

The HST in all three simulated case studies in scenario 2 is below 110°C which is the corresponding temperature of the relative ageing rate. The transformer is thermally underloaded in all the investigated cases. In addition, the HST is well below the maximum allowed temperature of 140°C in all cases. In both base and without_DL cases, the HST is steadily decreasing from 00:00–6:30 and then increasing until the end of the day. In contrast, in the case of With_DL, the HST is almost constant at around 60°C over the simulated period. Figure 8-11 shows the transformer cumulative LOL in each case for scenario 2.

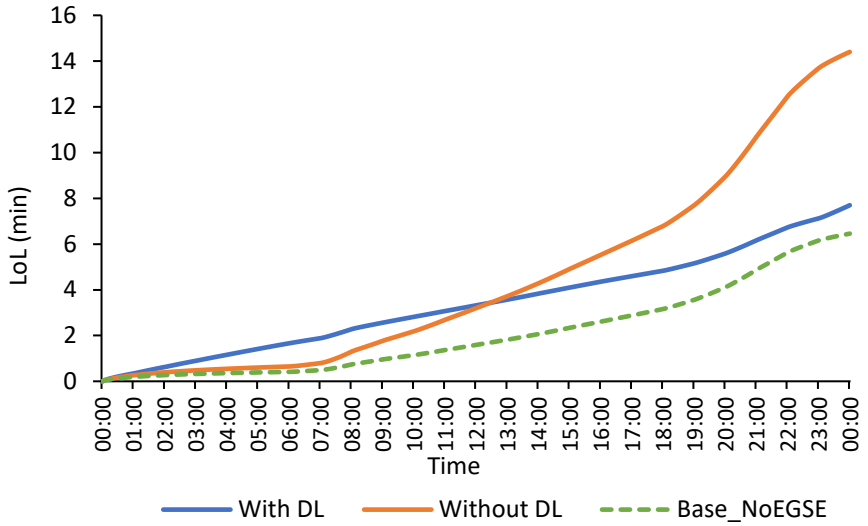

Figure 8-11 Transformer loss of life for scenario 2.

Base case corresponding cumulative LOL is about 6 min, whereas uncontrolled charging cumulative LOL is about 14min. By applying DL, the effect of EGSE deployment on the transformer's cumulative LOL is reduced from 14min to about 7min. As seen in Figure 8-11, the transformer LOL is gradually increasing in all three cases. Furthermore, the developed dynamic loading model controls the EGSE battery SOC to be within the pre-defined limits. Equation (8.3) is used to calculate the SOC of each EGSE after each hour and update the SOC to be considered in the next hour. Electric ground support equipment battery SOCs of each type are demonstrated in Figures 8-12 to 8-15.

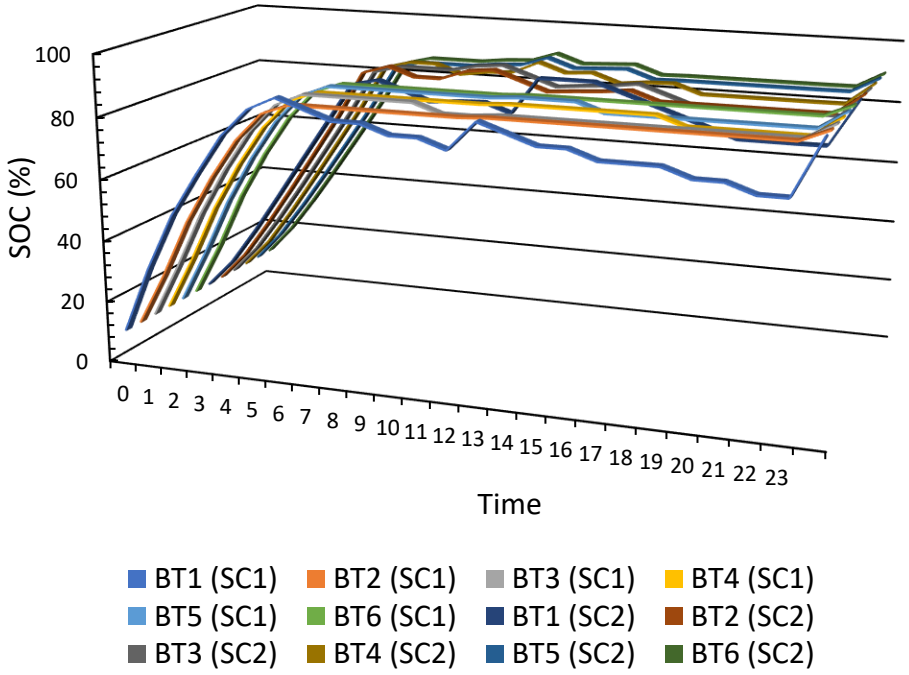

Figure 8-12 SOC of baggage tractors.

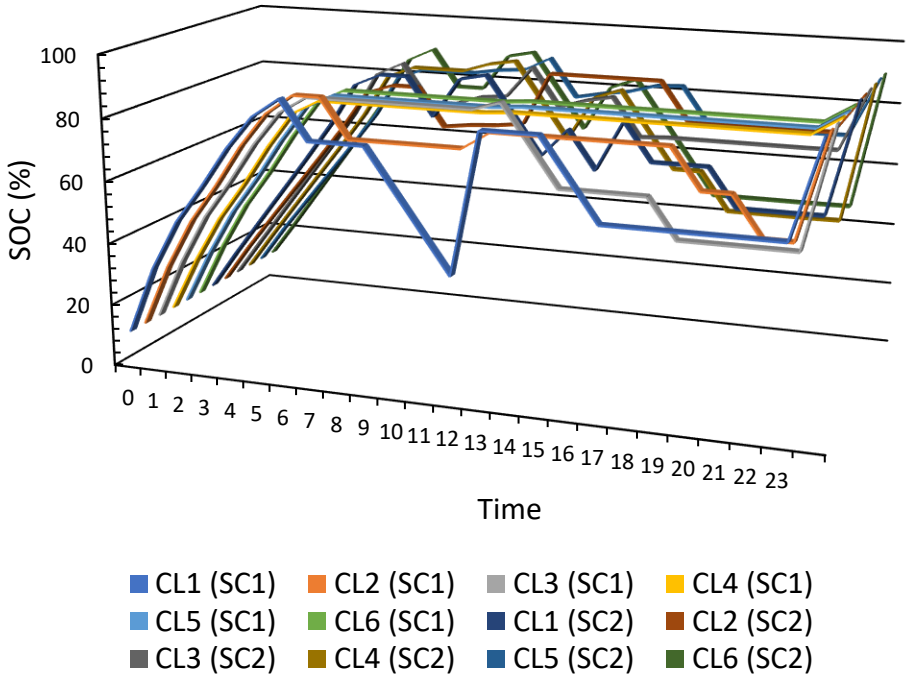

Figure 8-13 SOC of container loaders.

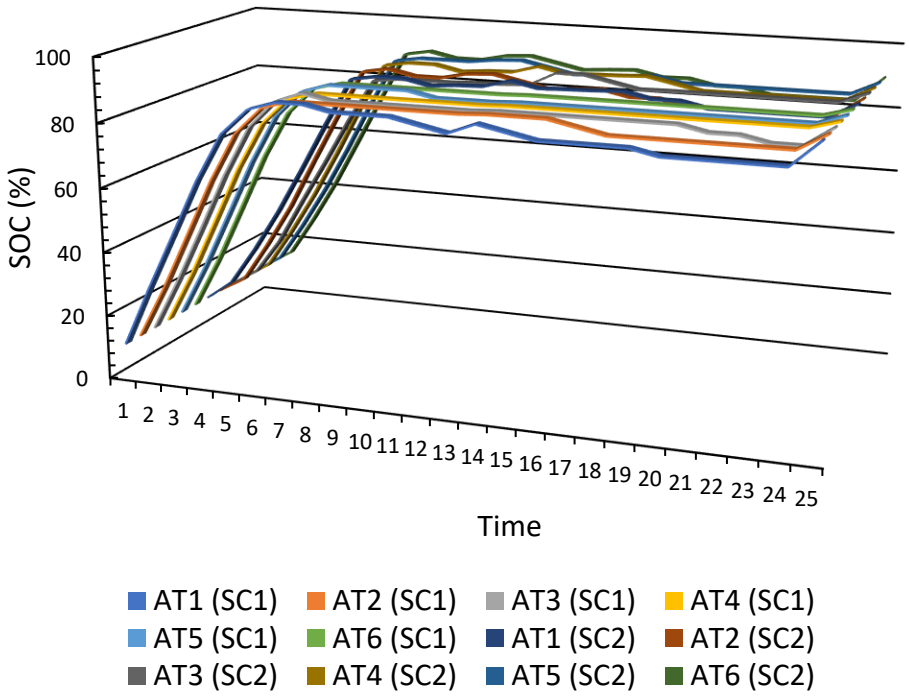

Figure 8-14 SOC of aircraft push-back tractors.

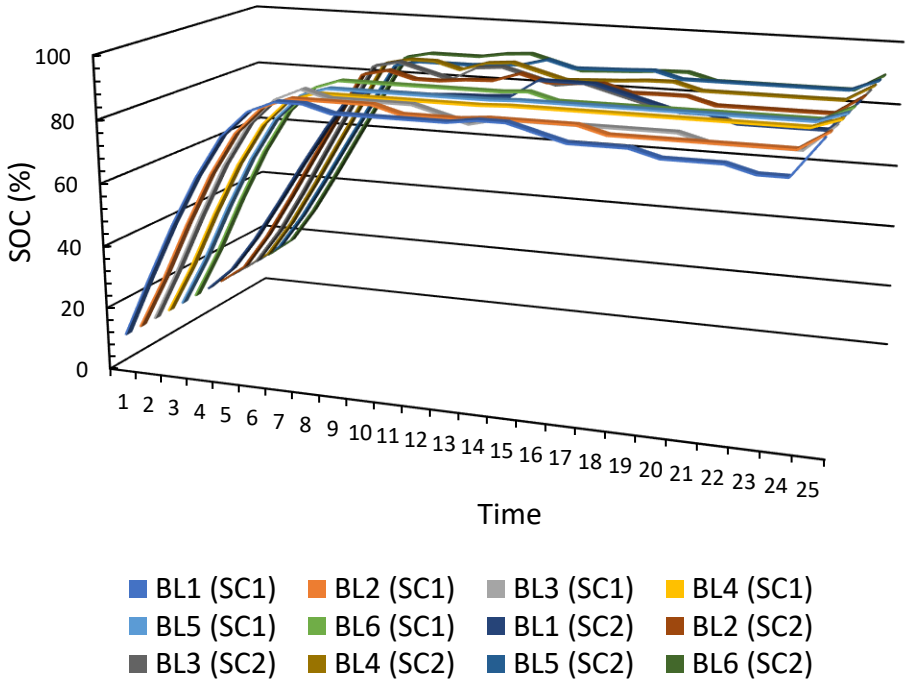

Figure 8-15 SOC of belt loaders.

It can be seen that the battery SOC is kept within the limits for baggage tractors, container loaders, belt loaders, and aircraft push-back tractors. The charging process mainly occurs between the first 6h and the last hour, which are airport closing and low

ambient temperature times. The total required charging energy is equally distributed over the day in the case of uncontrolled charging.

8.5 Discussion

The objective of the recommended dynamic loading model is to minimise the effect of the EGSE charging process on the distribution transformer while ensuring continuous fleet operation. The comparison of results presented in Table 8-2 shows the benefits of deploying the dynamic loading model to reduce the ageing rate.

Table 8-2 Comparison of simulation results.

	Base_NoEGSE		**Without Dynamic Loading**		**With Dynamic Loading**	
	Scen. 1	***Scen. 2***	***Scen. 1***	***Scen. 2***	***Scen. 1***	***Scen. 2***
Maximum load factor	0.99	0.62	1.1	0.7	0.99	0.62
Maximum HST (°C)	82	72	88	79	85	72
Yearly LOL (day)	3	1.5	6.4	3.7	3.8	1.8

In the Base_NoEGSE case study, the transformer ends the year losing about 3 and 1.5 days of its expected lifetime before EGSE deployment under the simulated operation conditions of February and September, respectively. This low LOL result is because the airport distribution transformer is not overloaded and the airport is located in a mild-climate region. If the EGSE were deployed without considering DL, the transformer would lose about 6.4 days and 3.7 days of its yearly lifetime, respectively, considering February and September loading conditions. DL implementation reduces the effect of EGSE deployment on transformer LOL from 6.4 days under the February loading condition to about 3.8 days. Considering the September condition, the DL model successfully reduces the effect of EGSE deployment on transformer lifetime from transformer losses of 3.8 days by the end of the year to 1.8 days. The proposed DL decreases the effect of EGSE implementation on transformer age, and the results are close to the base case without EGSE.

The transformer dynamic loading model improves the studied airport distribution transformer lifetime. The simulated case study has a small number of EGSE, but in other cases with a larger number of EGSE or a smaller distribution transformer size, the effect of using DL is more beneficial. Benefits could include, for example, the potential deferral of network reinforcement investment. The reinforcement delay

period depends on the load increment rate, which is correlated with the EGSE deployment rate. In larger airports and more electrified types of GSE, using a dynamic loading model to mitigate the effect of a larger load will be beneficial. Moreover, the transformer lifetime improvement will be more significant in extreme climate areas, which is another crucial factor in limiting the number of EGSE charges since the ambient temperature has a reverse effect on the HST.

8.6 Summary of Key Findings

This chapter investigated the dynamic loading of an airport distribution transformer with the aim of containing the possible impact of additional load resulting from EGSE charging without risking the transformer's lifetime. The effect of the controlled and uncontrolled charging processes of the airport EGSE fleet on the distribution power transformer was simulated for two scenarios using representative days of airport peak and off-peak load. The following conclusions were drawn from the findings:

i- The transformer dynamic loading model has the potential to reduce transformer loss of life due to EGSE implementation and enhance distribution transformer lifetime. This additional flexibility in the power system can potentially defer any required transformer reinforcement.

ii- The dynamic loading model effectively controls factors that can risk the transformer's lifetime, such as hot-spot temperature.

iii- The dynamic loading model effectively controls charging sessions to occur during transformer minimal loading.

iv- A comparison of the transformer under dynamic loading and uncontrolled charging shows that the overall effect is to reduce the ageing rate and eliminate new load peaks.

The conclusions were derived by analysing specific data related to a specific airport location, specific transformer characteristics, and a particular day's load profile and temperature. However, more future research is necessary to run the model for longer durations, include different airport locations, and examine various transformer sizes and types.

Chapter 9
Overall Conclusion and Discussion

9.1 Fulfilling the Aim of the Study

The primary aim of this thesis has been to promote green energy technologies in airports to reduce direct and indirect emissions and evaluate the feasibility of implementing economically viable green energy solutions to achieve carbon neutrality, aligning with airport sustainability initiatives.

The reviewed literature revealed that GHG emissions related to airport energy consumption and ground operation handling account for the largest portion of emissions. The adoption rate of green technologies, such as renewable DER and EGSE, lags well behind other sectors. The following solutions have been proposed in this thesis to promote renewable energy resources and GSE electrification:

i- The use of microgrids within airport premises to reduce reliance on fossil fuel-produced electricity and enhance resilience was investigated. A hybrid renewable energy system was economically analysed to reduce electricity purchasing, which reduces airport electricity costs and indirect emissions (chapter 4). A grid-connected microgrid was developed to increase the airport's power resilience and offer cost savings in line with direct and indirect airport emissions reduction (chapter 5).

ii- Electric ground support equipment promotion through smart charging techniques was developed. A robust optimisation algorithm for airport peak load shaving and valley filling using an EGSE fleet was developed and simulated using airport demand shape (chapter 6). An optimisation model was developed to aggregate an EGSE fleet for participating in ancillary services market via an EGSE aggregator (chapter 7). Finally, a dynamic loading model for an airport transformer hosting EGSE was developed and tested on an airport transformer (chapter 8).

Section 2 has provided a broad overview of the green energy solutions response to the interest in sustainable airports, and a review of the global literature relating to green energy technologies associated with airports transition to sustainability was performed. It was found that solutions proposed to cut direct and indirect airport emissions include only solar PV in most cases. It was demonstrated that solutions to the issues introduced

by the transition to sustainable airports must be based on the implementation of renewable distributed energy resources and microgrids, as well as the electrification of ground support equipment. Airport microgrid implementation within airport ecosystems is an underutilised solution identified as key to providing clean, reliable, and resilient electricity. However, various factors, including airport size, location, available resources, energy demand, technology type, and local energy regulations, influence the decision.

The electrification of GSE will pose various potential benefits and challenges at different levels of the power grid. The flexibility and ancillary service opportunities that EGSE can provide would help attract decision-makers to boost the electrification of current conventional GSE fleets. The electrification of GSE fleets will increase airports electricity demand to a level that will exceed the rating of existing electrical system components such as transformers. The key findings of section 2 are listed as follows:

- The process of electrification, with an emphasis on renewable energy and electric ground support equipment utilisation, holds significant potential for carbon reduction within airports.
- Microgrids present an underutilised opportunity within the airport ecosystem, offering an efficient solution for decentralised energy generation and improved resilience.
- The incorporation of wind turbines in proximity to airports presents challenges, primarily due to potential interferences with radar systems and aviation routes.
- An in-depth examination of the benefits conferred by EGSE fleets, extending beyond emission mitigation and operational cost reduction, could accelerate their adoption within the aviation sector. Conversely, the implications of EGSE charging on power system components need rigorous analysis, thereby necessitating the formulation of comprehensive EGSE management strategies.

Section 3 has provided a review and assessment of various modelling methods and tools aimed at promoting the integration of distributed energy resources and airport microgrids. It was identified that although the use of binary integers in optimisation problem formulation may increase computational time, it is indispensable for articulating the EGSE availability status. Microgrid modelling tools will be particularly useful in contexts that require economic analysis; however, the

incorporation of multiple tools, especially power analysis tools, will be mandatory to provide a near-realistic vision. The key findings of section 3 are listed as follows:

- Modelling tools for distributed energy resources and microgrids are essential for economic analysis. However, in some cases, careful planning may be required depending on the desired analysis and the types of distributed energy resources involved.
- Ancillary services and EV charging modelling are not widely included in distributed energy resources and microgrid modelling tools.

In section 4, a techno-economic assessment was conducted to evaluate the feasibility of implementing an on-site grid-connected hybrid renewable energy system (HRES) for a medium-sized civilian airport. This assessment involved the simulation and evaluation of the renewable-based hybrid system using load, weather, and irradiance data from 2015. The evaluated system consisted of solar PV, a power-to-hydrogen-to-power system (P2H2P), and stationary battery storage. The total savings from this system were compared using the standard financial tools of net present cost, levelised cost of energy, and payback. Notably, the hydrogen produced on site was generated using surplus solar energy, ensuring a sustainable and environmentally friendly production process. This work stands out, as it employs HOMER Pro for the techno-economic analysis of airport HRES, a methodology not used in any existing studies.

The results of this modelling indicated that the HRES for airports is beneficial in terms of lowering costs, reducing indirect emissions, and supplying energy needs. For the simulated airport, HRES provided an economic saving of about **$800,000** over the 25 yr project lifetime. The installed P2H2P system permitted surplus renewable energy to be stored during periods of maximum solar PV output and then used later at peak times. As the size of the solar PV system and P2H2P system increased, the economic feasibility of producing a larger quantity of green hydrogen became less advantageous. A substantial reduction of around **35%** in emissions was achieved by the implementation of HRES, resulting in potential annual savings of approximately **$19,570** through the European Union Emissions Trading System (EU ETS). The HRES achieved the minimum NPC of **$6.20 million** and the lowest LCOE of **$0.1479** in the case of costs of system components decreasing by 50%. Conversely, in the case of a 75% increase in energy prices, the NPC and LCOE rose to **$9.45 million** and **$0.226**, respectively. Green hydrogen production still faces some barriers to

widespread implementation, mainly due to high capital costs and the short lifetime of the P2H2P system. The conclusion reached is that implementing supportive industry and policy changes, such as incentives and funding mechanisms, to attract investors for installing green technologies is crucial for accelerating the adoption of sustainable solutions and achieving the net-zero transformation of the aviation sector. The key findings of section 4 are listed as follows:

- The implementation of HRES can offer environmental and economic benefits, underscoring sustainability by reducing costs and cutting emissions without compromising economic viability in airports.
- Despite the high costs of green hydrogen production, its combination with small-scale fuel cells can improve the approach to energy use and cost-efficiency in airports.
- The viability of HRES in meeting national emission targets hinges on policy measures that balance component costs and energy market stability, by focusing on cost reduction and price stability promotion.

In section 5, the technical and economic assessment of an airport grid-connected microgrid to improve airport power resilience under various power interruption scenarios was developed. The proposed system to enhance airport power resilience includes solar PV, an energy storage system, and a diesel generator. A MILP optimisation model was modified to minimise the total annual operating cost of the proposed resilient system. The model was implemented in XENDEE with airport electrical load profiles, solar irradiance data, EGSE daily charging requirements, and time-of-use tariffs to find optimal resilient microgrid sizing and dispatching. The use of the modelling tool XENDEE and the consideration of the EGSE fleet are novel aspects, as they have not been addressed before in the limited number of studies conducted on airport microgrids in the existing literature. Three power interruption situations were examined and compared with business as usual to verify the role of microgrids in enhancing resilience, including the following:

i- **Various outages criteria:** This scenario was modelled to evaluate different power interruption starting times, critical load levels, and interruption durations.

ii- **Changes in solar PV performance**: This scenario was modelled since solar PV is dependent on solar irradiance, which is very likely to be affected during natural catastrophes.

iii- **Load management**: This scenario investigated the different levels of value of lost loads.

The results showed that the proposed microgrid can achieve an annual operational cost reduction while ensuring a continuous power supply for all considered outage scenarios. The annual operational cost savings are between **20%** and **22%**. The proposed resilient microgrid's optimal sizing and dispatching are highly impacted by the duration of the outage and critical load level. For short and less critical load levels, diesel generators are an uneconomical choice. In addition, the energy storage system was found to highly contribute to demand savings when utility tariffs are high during microgrid normal operation. The energy storage system is the preferable choice over diesel generators during all simulated outages for saving value during normal operation. The key findings of section 5 are listed as follows:

- Airport microgrids demonstrate the potential for self-sustainability in electricity supply, particularly during power interruptions, and contribute to lower operational costs, thus aiding the move towards a net-zero aviation industry.
- The ability of renewable energy sources to supply critical loads during short-term interruptions underlines the significant role of renewable energy in reducing operational costs and emissions.

In section 6, a robust optimisation algorithm was devolved to coordinate the charging and discharging of an EGSE fleet at airport premises based on the passenger flight schedule. The objective of the proposed optimisation model was to flatten the airport demand curve through peak shaving and valley filling by using the EGSE fleet, a concept that has not been previously presented in the literature. The proposed MILP optimisation algorithm minimises the difference between the demand peak and minimum using civilian medium-sized airport load profiles and flight schedule data for peak and off-peak days. First, the required number of EGSE of each type and its required energy per hour were calculated using the turnaround event characteristic. The calculated hourly required energy and required number are fed to the optimisation model in order to improve airport terminal electrical load shape. The load factor (*LF*), peak load reduction (*PLR*), valley filling promotion (*VFP*), valley-peak ratio (*V/P*), and load rate of change (*RoC*) indicators are used to evaluate the suggested model's

performance. The optimisation approach was modelled in the MATLAB CVX package and solved using the GUROBI solver.

It was found that in the case of peak load days, the EGSE fleet prefers to charge when the airport is closed, which matches the valley time and results in about a **9%** minimum load increment. In addition, the EGSE fleet contributed to decreasing the load at various times during the day, but the primary discharge process was seen in the morning, which was following the airport opening time. The peak load reduction was about **11.9%**. The load factor and valley-peak ratio were improved by about **14%** and **24%**, respectively. In the second case study of an off-peak load day, the EGSE fleet increased the airport minimum load to nearly **11.5%**. Furthermore, the EGSE fleet was able to minimise morning and evening peak demand. The simulation results show that the model performance during off-peak days is higher than peak days, even during peak load days when more EGSE are available. This is because load during peak days is about one and a half times higher than off-peak days and EGSE fleet charging and discharging rates. Finally, it was found that the proposed model is more effective in reducing the peak load than valley filling in both simulated cases. The key findings of section 6 are listed as follows:

- The use of EGSE fleet with V2B mode enhances energy efficiency at airports, contributing to emission reduction and sustainability goals.
- The peak power reduction is not linearly dependent on the number of available EGSE emphasising the need for a complementary energy management scheme in airports to optimise energy consumption and contribute to emissions reduction.

In section 7, an optimisation algorithm to manage an airport EGSE fleet to participate in the electricity ancillary services was developed using day-ahead electricity market data, ancillary service prices, and passenger flight schedules. The proposed optimisation model allows EGSE to participate in the frequency regulation ancillary services through an aggregator, a novel work not been previously discussed in the literature. The simulated airport EGSE fleet provided the secondary frequency regulation ancillary service through an aggregator. The proposed MILP optimisation algorithm maximises the aggregator's profits while satisfying the EGSE fleet's daily energy needs. The efficiency of the optimisation algorithm was simulated using quarter-hourly data of upward and downward secondary frequency regulation capacity

and prices of the Belgian electricity market and the hourly flight schedule of a Belgian civilian airport. The optimisation algorithm was solved using the GUROBI solver.

It was found that the aggregated EGSE fleet could earn a sufficient amount of profit during idle time of about **$4,700** per day. The primary source of profit was frequency regulation, where the EGSE aggregator received the most offers. This is because the frequency regulation up prices are higher than the frequency regulation down prices. The total number of flights is low because the majority of EGSE fleet vehicles participated in frequency regulation service during the simulated day. The key findings of section 7 are listed as follows:

- The potential profits from EGSE by participating in the ancillary services need to be properly examined and rewarded by system operators which can promote sustainable practices in airports.
- The variation in global ancillary services market structures and prices can introduce risks for investors in EGSE aggregation.

In section 8, an optimisation algorithm was developed to dynamically manage an airport distribution transformer's loading. The proposed algorithm aims to minimise the impact of EGSE deployment on the airport distribution transformer lifetime, a concept that has not been previously introduced in the literature and defers the necessity to upgrade or replace the transformer. A mixed-integer non-linear programming optimisation model was presented to minimise the transformer's total loss of life. The formulated transformer dynamic loading model is based on transformer thermal characteristics established in the IEC 60076-7 standard. The proposed model was simulated using civilian medium-sized airport load profiles, ambient temperature, and flight schedule data from February and September 2015. The transformer thermal limit, EGSE hourly availability, and EGSE battery SOC are used to constrain the dynamic loading optimisation model, ensuring that the transformer loss of life and EGSE energy needs are met. The OpenSolver software tool is used to simulate the optimisation model, which was then solved using the COIN-OR Couenne solver.

The findings revealed that the proposed dynamic loading model reduced the transformer accumulative loss of life due to EGSE implementation nearly to the base case (without EGSE consideration), compared to the case of EGSE uncontrolled charging. The proposed dynamic loading reduced the yearly lifetime loss of the

transformer by about **42%** and **53%**, respectively, in the loading conditions of February and September 2015. The key findings of section 8 are listed as follows:

- The implementation of EGSE can influence the performance of electrical system components, most notably affecting the lifespan of transformers due to the substantial energy requirements associated with charging the EGSE fleet.
- The implementation of a transformer dynamic loading model, controlling factors such as hot-spot temperature and ensuring charging sessions occur during minimal transformer loading periods, reflects advancements in energy management that can enhance equipment longevity, reduce costs, and contribute to achieving sustainability targets in airports.

9.2 Thesis Contributions

The contributions of this thesis are summarised as:

1- A grid-connected hybrid renewable energy-based system, including on-site green power to green hydrogen to power system, was proposed to boost the implementation of renewable DERs within civilian airports, which is consistent with aviation sustainability trends. This is a contribution, as it addresses the pressing global demand for sustainable airports and aviation solutions, paving the way for the deployment of green hydrogen in airports. The proposed hybrid renewable system can be beneficial for airport operators through the deployment of microgrids and green hydrogen into future sustainable airport planning designs.

2- An optimal economic dispatch of an airport grid-connected microgrid, including an EGSE fleet, was proposed to leverage power resilience benefits. The motivation behind this contribution is to provide robust, sustainable energy solutions to airports that can withstand potential disruptions. This proposition can be employed by decision-makers in their sustainability plans to improve energy resilience.

3- A novel algorithm was developed for airport peak demand reduction and valley filling using the EGSE fleet that was coordinated based on the passenger flight schedule. The motivation behind this contribution is to underscore the distinctive benefits of EGSE, showcasing its efficiency and sustainability compared to conventional GSE, which can drive the transformation towards cleaner airport operations. This algorithm provides a practical tool for airport

operators, allowing them to efficiently manage and reduce electricity purchasing costs.

4- An optimisation algorithm was developed for frequency regulation provision using the EGSE fleet via an EGSE aggregator, which benefits from passenger flight schedules to define the hourly availability of the EGSE fleet. This model contributes by providing an opportunity for EGSE owners to play a role in the modern structure of energy markets. The presented model can be adopted by airport operators, airline companies, or third-party ground handling companies to enhance the economic viability of GSE electrification for more sustainable airports.

5- A dynamic loading model of an airport distribution transformer under various operation and climate temperature conditions to reduce EGSE charging impact was developed. The proposed model is readily adaptable to other airports in different regions. The model can be useful as it offers a tool for DNOs for efficient operation and planning, providing reliable energy, and helping to defer costs associated with network reinforcement.

9.3 Future Work Suggestions

The possible future study directions following the examination of the simulated findings in this PhD thesis are as follows:

1- In the work presented in chapter 4 regarding hybrid renewable-based energy systems, the on-site-produced green hydrogen is used to supply airport electricity loads only. As such, the work can be extended with consideration of producing green hydrogen to supply fuel cell GSE and hydrogen fuel-based aircraft, as these technologies could be part of the sustainable aviation sector in the next few decades. The resulting oxygen from the water electrolysis process can be included to add additional economic and environmental benefits.

2- The resilient microgrid presented in chapter 5 was evaluated from an economic dispatch perspective. Future work could consequently be extended to include various operational constraints and power flow analysis, resulting in a more realistic case study since these data are held by certain engineering organisations and were not available when conducting this study. Future work

could examine the economic benefits of using resilient microgrids to provide various ancillary services, as presented in chapter 7.

3- The simplified EGSE fleet aggregation model used in chapters 6–8 can be improved to include aircraft sizes, an aspect not included in the current model due to insufficient datasets used in the modelling, which mostly have a direct influence on EGSE availability.

4- The optimisation algorithm to flatten the airport demand curve using EGSE presented in chapter 6 could be extended to evaluate the economic benefits, including EGSE's battery degradation cost, since EGSE is mostly owned by airlines and third-party companies. An economic feasibility comparison could be conducted to include the usage of second-hand stationary battery storage along with the EGSE fleet to demonstrate the economic importance of load balancing for large energy consumers.

5- The EGSE fleet participating in frequency regulation ancillary services via an aggregator investigated in chapter 7 used day-ahead market data, which assumed that all submitted bids were winning bids. As such, future work could further develop the model to involve real-time electricity market data, various types of ancillary services, and infrastructure costs to give more realistic and reliable results for decision-makers. The work could be expanded to include the aggregation of more than one airport EGSE fleet to provide various ancillary services at a wider national level to create a more profitable business.

6- The transformer dynamic loading model presented in chapter 8 was modelled to limit the impact of part of the GSE fleet's future electrification due to restricted dataset availability. The consideration of the additional load of a fully electrified GSE fleet and electric aeroplanes and the potential impact of renewable energy resources should consequently be included in the study to further the work and provide a more comprehensive assessment of future sustainable airports.

References

[1] International Air Transport Association (IATA), "Airports." https://www.iata.org/en/youandiata/airports/#tab-1 (accessed Feb. 15, 2022).

[2] Statista, "Number of scheduled passengers boarded by the global airline industry from 2004 to 2022." https://www.statista.com/statistics/564717/airline-industry-passenger-traffic-globally/ (accessed Feb. 15, 2022).

[3] Statista, "Worldwide air cargo traffic 2004-2022 ." https://www.statista.com/statistics/564668/worldwide-air-cargo-traffic/ (accessed Feb. 15, 2022).

[4] Air Transport Action Group (ATAG), "Aviation: Benefits Beyond Borders," Geneva, Switzerland, Aug. 2018. Accessed: Jun. 04, 2022. [Online]. Available: https://www.atag.org/our-publications/latest-publications.html

[5] International Energy Agency (IEA), "Aviation," *IEA, Paris*, 2021, [Online]. Available: https://www.iea.org/reports/aviation

[6] International Air Transport Association (IATA), "Press Release No: 62," Oct. 24, 2018. https://www.iata.org/en/pressroom/pr/2018-10-24-02/ (accessed Feb. 17, 2022).

[7] International Council on Clean Transportation, "Aviation." https://theicct.org/aviation (accessed Sep. 14, 2021).

[8] The United States Environmental Protection Agency (USEPA), "Inventory of U.S. greenhouse gas emissions and sinks: 1990-2018," 2020. [Online]. Available: https://www.epa.gov/ghgemissions/inventory-us-greenhouse-gas-emissions-and-sinks-1990-2018

[9] Climate Change Committee (CCC), "The Sixth Carbon Budget-Aviation," 2020. [Online]. Available: https://www.theccc.org.uk/wp-content/uploads/2020/12/Sector-summary-Aviation.pdf

[10] David Hirst, "Aviation, decarbonisation and climate change," Sep. 2021. Accessed: Feb. 14, 2022. [Online]. Available: https://commonslibrary.parliament.uk/research-briefings/cbp-8826/

[11] B. Graver, D. Rutherford, and Sola Zheng, "CO2 emissions from commercial aviation: 2013, 2018, and 2019," International Council on Clean Transportation, Washington, DC, 2020. [Online]. Available: https://theicct.org/publications/co2-emissions-commercial-aviation-2020

[12] International Civil Aviation Organization (ICAO), "ICAO global environmental trends – Present and future aircraft noise and emissions (A40-WP/54)," 2019. [Online]. Available: https://www.icao.int/Meetings/A40/Documents/WP/wp_054_en.pdf

[13] International Air Transport Association (IATA), "Carbon Offset Program." https://www.iata.org/en/programs/environment/carbon-offset/ (accessed Feb. 14, 2022).

[14] International Civil Aviation Organization (ICAO), "CORSIA Eligible Emissions Units." https://www.icao.int/environmental-protection/CORSIA/Pages/CORSIA-Emissions-Units.aspx (accessed Feb. 14, 2022).

[15] International Air Transport Association (IATA), "ACE - Aviation Carbon Exchange." https://www.iata.org/en/programs/environment/ace/ (accessed Feb. 14, 2022).

[16] European Commission, "EU Emissions Trading System (EU ETS)." https://ec.europa.eu/clima/policies/ets_en#Main_legislation (accessed Sep. 14,

2021).
[17] International Carbon Action Partnership, “Korea Emissions Trading Scheme,” 2016. [Online]. Available: https://icapcarbonaction.com/en/ets
[18] Air Transport Action Group (ATAG), “Offsetting emissions (CORSIA).” https://aviationbenefits.org/environmental-efficiency/climate-action/offsetting-emissions-corsia/ (accessed Oct. 18, 2021).
[19] Sustainable Aviation, “Decarbonisation Road-Map: A Path to Net Zero.,” 2020. [Online]. Available: https://www.sustainableaviation.co.uk/wp-content/uploads/2020/02/SustainableAviation_CarbonReport_20200203.pdf
[20] European Commission Directorate-General for Mobility and Transport Directorate-General for Research and Innovation, “Flightpath 2050-Europe’s vision for aviation : maintaining global leadership and serving society’s needs,” 2011. doi: 10.2777/50266.
[21] Eviation, “Aircraft – Alice.” https://www.eviation.co/aircraft/#Alice (accessed Feb. 14, 2022).
[22] Rolls-Royce, “Rolls-Royce’s all-electric ‘Spirit of Innovation’ takes to the skies for the first time,” *Press release*, Sep. 15, 2021. https://www.rolls-royce.com/media/press-releases/2021/15-09-2021-rr-all-electric-spirit-of-innovation-takes-to-the-skies-for-the-first-time.aspx (accessed Feb. 14, 2022).
[23] Airbus, “ZEROe concept aircraft.” https://www.airbus.com/en/innovation/zero-emission/hydrogen/zeroe (accessed Feb. 14, 2022).
[24] Airports Council International Europe, “Airport Carbon Accreditation Application Manual,” Issue. 12, 2020. [Online]. Available: https://www.airportcarbonaccreditation.org/airport/technical-documents.html
[25] International Civil Aviation Organization (ICAO), “Annex 14 Aerodromes Design and Operations,” *8th Edition*, Jul. 2018. https://store.icao.int/en/annex-14-aerodromes (accessed Feb. 15, 2022).
[26] European Union, “Commission Implementing Regulation (EU) 2017/373,” Mar. 2017. Accessed: Feb. 15, 2022. [Online]. Available: https://eur-lex.europa.eu/legal-content/EN/TXT/?uri=CELEX%3A32017R0373
[27] International Organization for Standardization (ISO), “ISO 14001:2015 - Environmental management systems,” *3rd Edition*, Sep. 2015. https://www.iso.org/standard/60857.html (accessed Feb. 15, 2022).
[28] Airports Council International, “Airport Industry Connectivity Report 2022,” 2022. [Online]. Available: https://www.aci-europe.org/air-connectivity.html
[29] Federal Aviation Administration (FAA), “Airport Categories,” 2022. https://www.faa.gov/airports/planning_capacity/categories
[30] N. Ashford, S. A. Mumayiz, and P. H. Wright, *Airport engineering : design, planning, and development of 21st century airports*, 4th ed. Wiley, 2011.
[31] O. F. Yildiz, M. Yilmaz, and A. Celik, “Reduction of energy consumption and CO2 emissions of HVAC system in airport terminal buildings,” *Build. Environ.*, vol. 208, p. 108632, Jan. 2022, doi: 10.1016/j.buildenv.2021.108632.
[32] A. Kazda and R. E. Caves, *Airport Design and Operation*. Bingley, United Kingdom: Emerald Publishing Limited, 2015.
[33] International Civil Aviation Organization (ICAO), “Ground Support Equipment (GSE).” https://www.icao.int/cybersecurity/Lists/Glossary/DispForm.aspx?ID=111 (accessed Feb. 15, 2021).
[34] Allied Market Research, “Ground Support Equipment Market ,” Apr. 2020. https://www.alliedmarketresearch.com/ground-support-equipment-market

(accessed Feb. 16, 2022).
[35] National Academies of Sciences Engineering and Medicine, *Airport Ground Support Equipment (GSE): Emission Reduction Strategies, Inventory, and Tutorial*. Washington, D.C.: Transportation Research Board, 2012. doi: 10.17226/22681.
[36] National Renewable Energy Laboratory (NREL), "Electric Ground Support Equipment at Airports," Golden, CO, 2017. [Online]. Available: https://afdc.energy.gov/files/u/publication/egse_airports.pdf
[37] Delta Airlines, "Airline's other fleet: Science behind ground equipment," Jan. 06, 2016. https://news.delta.com/airlines-other-fleet-science-behind-ground-equipment (accessed Feb. 16, 2022).
[38] National Academies of Sciences Engineering and Medicine, *Improving Ground Support Equipment Operational Data for Airport Emissions Modeling*. Washington, D.C.: Transportation Research Board, 2015. doi: 10.17226/22084.
[39] John Bean Technologies (JPT) AeroTech, "Ranger^{TM}15E Electric Cargo Loader." https://www.jbtc.com/aerotech/products-and-services/ground-support-equipment/cargo-loaders/ranger-15e-electric-cargo-loader/ (accessed Apr. 26, 2023).
[40] John Bean Technologies (JPT) AeroTech, "Commander® 15i E Electric Cargo Loader." https://www.jbtc.com/aerotech/products-and-services/ground-support-equipment/cargo-loaders/commander-15i-e-electric-cargo-loader/ (accessed Apr. 26, 2023).
[41] Teleflex Lionel Dupont (TLD), "JET-16." https://www.tld-group.com/products/baggage-tractors/jet-16/ (accessed Apr. 26, 2023).
[42] Vestergaard Company, "Vestergaard Company introduces revolutionary plug-in hybrid deicer ." https://vestergaardcompany.com/press-release-vestergaard-company-introduces-revolutionary-plug-in-hybrid-deicer/ (accessed Apr. 26, 2023).
[43] A. Shetty, B. G. Fernandes, J. O. Ojo, and J. A. Ferreira, "Three Phase PWM Rectifier with Integrated Battery for Automotive Applications," in *2018 IEEE Industry Applications Society Annual Meeting (IAS)*, Sep. 2018, pp. 1–6. doi: 10.1109/IAS.2018.8544681.
[44] John Bean Technologies (JPT) AeroTech, "LEKTRO 89 Tow Tractors." https://www.jbtc.com/aerotech/products-and-services/ground-support-equipment/lektro-tow-vehicles/lektro-89/ (accessed Apr. 26, 2023).
[45] Vollk Fahrzeugbau, "HFZ 40 N." [Online]. Available: https://www.behrend-sgt.de/volk-zugmaschinen-hybrid/
[46] Aero Specialties, "AERO JetGo 800AL-RJ." https://www.aerospecialties.com/aviation-ground-support-equipment-gse-products/aircraft-ground-power-units/28-volt-dc-gpu/diesel-generators-dc/aero-jetgo-800al-rj-28v-dc-diesel-hybrid-ground-power-unit/ (accessed Apr. 26, 2023).
[47] B. G. Pollet, I. Staffell, and J. L. Shang, "Current status of hybrid, battery and fuel cell electric vehicles: From electrochemistry to market prospects," *Electrochim. Acta*, vol. 84, pp. 235–249, Dec. 2012, doi: 10.1016/j.electacta.2012.03.172.
[48] Mulag Fahrzeugwerk, "Comet Airport Towing Tractors." [Online]. Available: https://www.mulag.de/fileadmin/content/media/01_flughafenfahrzeuge/produkte/flughafenschlepper/mulag_gse_comet_product_overview_dok0822_464en_web.pdf
[49] D. Alonso Tabares and F. Mora-Camino, "Aircraft ground operations: steps

towards automation," *CEAS Aeronaut. J.*, vol. 10, no. 3, pp. 965–974, Sep. 2019, doi: 10.1007/s13272-019-00390-5.
[50] Electric Power Research Institute (EPRI) and Southern Company, "Electrification of an Airport Lower Deck Container Loader," 2009. https://www.epri.com/research/products/000000000001020484 (accessed Jan. 19, 2022).
[51] Trepel Airport Equipment, "Manufacturer of cargo high loaders and aircraft tractors." https://trepel.com/ (accessed Jan. 19, 2022).
[52] S. Liu, "Sustainability," in *Bioprocess Engineering*, Elsevier, 2017, pp. 829–870. doi: 10.1016/B978-0-444-63783-3.00014-9.
[53] Sustainable Aviation, "Goals." https://www.sustainableaviation.co.uk/goals/ (accessed Mar. 04, 2022).
[54] Air British Petroleum, "What is sustainable aviation fuel (SAF) and why is it important?" https://www.bp.com/en/global/air-bp/news-and-views/views/what-is-sustainable-aviation-fuel-saf-and-why-is-it-important.html (accessed Mar. 04, 2022).
[55] Federal Aviation Administration (FAA), "Airport Sustainability." https://www.faa.gov/airports/environmental/sustainability/ (accessed Mar. 04, 2022).
[56] Heathrow Airport, "Heathrow's Net Zero Plan," Feb., 2022. [Online]. Available: https://www.heathrow.com/content/dam/heathrow/web/common/documents/company/heathrow-2-0-sustainability/futher-reading/Heathrow Net Zero Plan FINAL.pdf
[57] Denver International Airport, "2020 Annual Environmental Performance Report," 2020. [Online]. Available: https://www.flydenver.com/sites/default/files/environmental/enviro_2020_Annual_Performance_Report.pdf
[58] San Francisco International Airport, "Zero-Emission Vehicle Readiness Roadmap & Intermodal Electrification Strategic Plan," 2020. [Online]. Available: https://www.flysfo.com/sites/default/files/ZEVR_Summary.pdf
[59] San Francisco International Airport, "Zero Net Energy at SFO," 2020. [Online]. Available: https://www.flysfo.com/sites/default/files/SFO_ZERO_Annual Report_2020.pdf
[60] Swissport International, "Sustainability Report," 2020. [Online]. Available: https://www.swissport.com/en/media/files/company-publications/2020-sustainability-report
[61] Dnata, "Environment." https://www.dnata.com/en/about/environment (accessed Mar. 08, 2022).
[62] Menzies, "Corporate responsibility & sustainability ." https://menziesaviation.com/about-overview/corporate-responsibility-and-sustainability/ (accessed Mar. 08, 2022).
[63] Menzies, "Menzies Aviation provides Ryanair with fully electric turns at airports across Europe ," Oct. 27, 2021. https://menziesaviation.com/news/menzies-aviation-provides-ryanair-with-fully-electric-turns-at-airports-across-europe/ (accessed Mar. 08, 2022).
[64] Office of Energy Efficiency & Renewable Energy, "Energy Efficiency." https://www.energy.gov/eere/energy-efficiency (accessed May 22, 2023).
[65] The Manchester Airports Group, "Airfield re-designation scheme is launched," Dec. 19, 2019. https://mediacentre.manchesterairport.co.uk/airfield-re-designation-scheme-is-launched/ (accessed May 22, 2023).
[66] N. Réhault, F. Ohr, and R. Maier, "Online Survey on European Airports Energy

Operation," 2012. [Online]. Available: https://www.researchgate.net/publication/326347096_Report_on_Online_Survey_on_European_Airports_Energy_Operation
[67] Distributed Utility Associates, "Using Distributed Energy Resources, A How-To Guide for Federal Facility Managers," 2002, [Online]. Available: https://www.osti.gov/biblio/15000472
[68] S. Chowdhury, S. P. Chowdhury, and P. Crossley, *Microgrids and Active Distribution Networks*. Institution of Engineering and Technology, 2009. doi: 10.1049/PBRN006E.
[69] International Renewable Energy Agency (IRENA), "World Energy Transitions Outlook: 1.5°C Pathway," Abu Dhabi, Jun. 2021. Accessed: Feb. 17, 2022. [Online]. Available: https://irena.org/publications/2021/Jun/World-Energy-Transitions-Outlook
[70] Federal Aviation Administration (FAA), "Obstruction Evaluation / Airport Airspace Analysis (OE/AAA)," 2022. [Online]. Available: https://oeaaa.faa.gov/oeaaa/external/portal.jsp
[71] B. Karlson, B. Miller, and J. Biddle, "Wind Turbine/Radar Interference: Offshore Test Options," Albuquerque, NM, and Livermore, CA, Sep. 2014. doi: 10.2172/1762101.
[72] S. B. Barrett, P. M. DeVita, and J. R. Lambert, *Guidebook for Energy Facilities Compatibility with Airports and Airspace*. Washington, D.C.: Transportation Research Board, 2014. doi: 10.17226/22399.
[73] Office of Energy Efficiency & Renewable Energy, "How Does Solar Work?" https://www.energy.gov/eere/solar/how-does-solar-work#:~:text=There are two main types,-thermal power (CSP). (accessed May 17, 2023).
[74] National Renewable Energy Laboratory (NREL), "Solar Energy Basics." https://www.nrel.gov/research/re-solar.html (accessed May 17, 2023).
[75] S. S. Kim, "Essays on U.S. Renewable Energy and Local Sustainability Policy," The Florida State University, 2019. [Online]. Available: https://www.proquest.com/docview/2273201707/452A6BDC721B4087PQ/1?accountid=9883#
[76] Federal Aviation Administration (FAA), "Voluntary Airport Low Emissions Program (VALE)." https://www.faa.gov/airports/environmental/vale/ (accessed Feb. 17, 2022).
[77] A. Tunnicliffe, "Solar power: the future of airport infrastructure," *Airpt. Ind. Rev.*, no. 61, Nov. 2020, Accessed: Nov. 09, 2021. [Online]. Available: https://airport.nridigital.com/air_nov20/solar_power_airports
[78] Cenin, "Cardiff International Airport: Solar PV Project," 2022. [Online]. Available: https://cenin.co.uk/wp-content/uploads/2022/02/CENIN-@-Cardiff-Airport-FINAL1.pdf
[79] S. Sukumaran and K. Sudhakar, "Fully solar powered airport: A case study of Cochin International airport," *J. Air Transp. Manag.*, vol. 62, pp. 176–188, Jul. 2017, doi: 10.1016/j.jairtraman.2017.04.004.
[80] S. Sukumaran and K. Sudhakar, "Fully solar powered Raja Bhoj International Airport: A feasibility study," *Resour. Technol.*, vol. 3, no. 3, pp. 309–316, Sep. 2017, doi: 10.1016/j.reffit.2017.02.001.
[81] Homer Energy, "HOMER Pro. (version 3.14.5)." 2021. Accessed: Nov. 03, 2021. [Online]. Available: https://www.homerenergy.com/products/pro/docs/index.html
[82] A. Dobos, "PVWatts Version 5 Manual," Golden, CO, Sep. 2014. doi: 10.2172/1158421.

[83] F. Dawood, G. Shafiullah, and M. Anda, “Stand-Alone Microgrid with 100% Renewable Energy: A Case Study with Hybrid Solar PV-Battery-Hydrogen,” *Sustainability*, vol. 12, no. 5, p. 2047, Mar. 2020, doi: 10.3390/su12052047.
[84] M. Paidar, V. Fateev, and K. Bouzek, “Membrane electrolysis—History, current status and perspective,” *Electrochim. Acta*, vol. 209, pp. 737–756, Aug. 2016, doi: 10.1016/j.electacta.2016.05.209.
[85] Hydrogen and Fuel Cell Technologies Office, “Comparison of Fuel Cell Technologies,” U.S. Department of Energy, 2016. [Online]. Available: https://www.energy.gov/sites/default/files/2016/06/f32/fcto_fuel_cells_comparison_chart_apr2016.pdf
[86] S. Hamidi, S. Haghighi, and K. Askari, “PEM Fuel Cell Dataset (Proton Exchange Membrane (PEM) Fuel Cell Dataset).” https://paperswithcode.com/dataset/pem-fuel-cell-dataset (accessed Mar. 16, 2022).
[87] A. Z. Weber, S. Balasubramanian, and P. K. Das, “Proton Exchange Membrane Fuel Cells,” 2012, pp. 65–144. doi: 10.1016/B978-0-12-386874-9.00003-8.
[88] Hydrogen and Fuel Cell Technologies Office, “Hydrogen Production: Electrolysis,” *U.S. Department of Energy*. https://www.energy.gov/eere/fuelcells/hydrogen-production-electrolysis (accessed Mar. 16, 2022).
[89] F. Odoi-Yorke and A. Woenagnon, “Techno-economic assessment of solar PV/fuel cell hybrid power system for telecom base stations in Ghana,” *Cogent Eng.*, vol. 8, no. 1, p. 1911285, Jan. 2021, doi: 10.1080/23311916.2021.1911285.
[90] R. Moradi and K. M. Groth, “Hydrogen storage and delivery: Review of the state of the art technologies and risk and reliability analysis,” *Int. J. Hydrogen Energy*, vol. 44, no. 23, pp. 12254–12269, May 2019, doi: 10.1016/j.ijhydene.2019.03.041.
[91] The United States Environmental Protection Agency (USEPA), “Distributed Generation of Electricity and its Environmental Impacts.” https://www.epa.gov/energy/distributed-generation-electricity-and-its-environmental-impacts (accessed Feb. 22, 2022).
[92] G. Brunekreeft, J. Kusznir, R. Meyer, M. Sawabe, and T. Hattori, “Incentive regulation of electricity networks under large penetration of distributed energy resources-selected issues,” No. 33. Bremen Energy Working Papers, 2020.
[93] L. Tricarico, “Community Energy Enterprises in the Distributed Energy Geography,” *Int. J. Sustain. Energy Plan. Manag.*, vol. 18, pp. 81–94, Dec. 2018, doi: 10.5278/IJSEPM.2018.18.6.
[94] N. Bilakanti, F. Lambert, and D. Divan, “Integration of Distributed Energy Resources and Microgrids - Utility Challenges,” in *2018 IEEE Electronic Power Grid (eGrid)*, Nov. 2018, pp. 1–6. doi: 10.1109/eGRID.2018.8598678.
[95] North American Electric Reliability Corporation (NERC), “Distributed Energy Resources: Connection Modeling and Reliability Considerations,” Feb., 2017. [Online]. Available: https://www.nerc.com/comm/Other/essntlrlbltysrvcstskfrcDL/Distributed_Energy_Resources_Report.pdf
[96] Institute of Electrical and Electronic Engineers (IEEE), *IEEE Guide for Design, Operation, and Integration of Distributed Resource Island Systems with Electric Power Systems*. IEEE Standard1547.4-2011, 2011.
[97] Guidehouse, “Global Microgrid Capacity Is Expected to Experience a Compound Annual Growth Rate of 21% Over the Next Decade,” Nov. 14, 2019.

https://guidehouseinsights.com/news-and-views/global-microgrid-capacity-is-expected-to-experience-a-compound-annual-growth-rate-of-21-over-the-nex (accessed Feb. 23, 2022).
[98] Elisa Wood, "Will a Single Utility, PG&E, Boost the 2020 Microgrid Market by $1 Billion?," Feb. 24, 2020. https://microgridknowledge.com/pge-microgrids-1-billion/ (accessed Feb. 23, 2022).
[99] R. H. and E. Mannarino, *Microgrids and Their Application for Airports and Public Transit*. Washington, D.C.: Transportation Research Board, 2018. doi: 10.17226/25233.
[100] Allegheny County Airport Authority, "Pittsburgh International Airport Goes Live with First-of-Its-Kind Microgrid Powering Entire Facility with Natural Gas and Solar Energy," Jul. 14, 2021. https://flypittsburgh.com/acaa-corporate/newsroom/news-releases/pittsburgh-international-airport-goes-live-with-first-of-its-kind-microgrid-powering-entire-facility-with-natural-gas-and-solar-energy/ (accessed Feb. 23, 2022).
[101] B. Cao, W. Dong, Z. Lv, Y. Gu, S. Singh, and P. Kumar, "Hybrid Microgrid Many-Objective Sizing Optimization With Fuzzy Decision," *IEEE Trans. Fuzzy Syst.*, vol. 28, no. 11, pp. 2702–2710, Nov. 2020, doi: 10.1109/TFUZZ.2020.3026140.
[102] P. Ray and M. Biswal, Eds., *Microgrid: Operation, Control, Monitoring and Protection*, vol. 625. Singapore: Springer Singapore, 2020. doi: 10.1007/978-981-15-1781-5.
[103] P. Tozzi and J. H. Jo, "A comparative analysis of renewable energy simulation tools: Performance simulation model vs. system optimization," *Renew. Sustain. Energy Rev.*, vol. 80, pp. 390–398, Dec. 2017, doi: 10.1016/j.rser.2017.05.153.
[104] A. L. Bukar, C. W. Tan, and K. Y. Lau, "Optimal sizing of an autonomous photovoltaic/wind/battery/diesel generator microgrid using grasshopper optimization algorithm," *Sol. Energy*, vol. 188, pp. 685–696, Aug. 2019, doi: 10.1016/j.solener.2019.06.050.
[105] A. Singh, P. Baredar, and B. Gupta, "Techno-economic feasibility analysis of hydrogen fuel cell and solar photovoltaic hybrid renewable energy system for academic research building," *Energy Convers. Manag.*, vol. 145, pp. 398–414, Aug. 2017, doi: 10.1016/j.enconman.2017.05.014.
[106] S. Vendoti, M. Muralidhar, and R. Kiranmayi, "Techno-economic analysis of off-grid solar/wind/biogas/biomass/fuel cell/battery system for electrification in a cluster of villages by HOMER software," *Environ. Dev. Sustain.*, vol. 23, no. 1, pp. 351–372, Jan. 2021, doi: 10.1007/s10668-019-00583-2.
[107] B. Dursun, "Determination of the optimum hybrid renewable power generating systems for Kavakli campus of Kirklareli University, Turkey," *Renew. Sustain. Energy Rev.*, vol. 16, no. 8, pp. 6183–6190, Oct. 2012, doi: 10.1016/j.rser.2012.07.017.
[108] M. Neil, "A market analysis of customer-connected mass energy storage," Queen's University Belfast, 2022. Accessed: May 16, 2023. [Online]. Available: https://pure.qub.ac.uk/en/studentTheses/a-market-analysis-of-customer-connected-mass-energy-storage
[109] Z. K. Pecenak, M. Stadler, P. Mathiesen, K. Fahy, and J. Kleissl, "Robust design of microgrids using a hybrid minimum investment optimization," *Appl. Energy*, vol. 276, no. August, p. 115400, Oct. 2020, doi: 10.1016/j.apenergy.2020.115400.
[110] Z. K. Pecenak *et al.*, "The impact of project financing in optimizing microgrid design," *J. Renew. Sustain. Energy*, vol. 12, no. 6, p. 065301, Nov. 2020, doi:

10.1063/5.0026187.
[111] A. Cosic, M. Stadler, M. Mansoor, and M. Zellinger, “Mixed-integer linear programming based optimization strategies for renewable energy communities,” *Energy*, vol. 237, p. 121559, Dec. 2021, doi: 10.1016/j.energy.2021.121559.
[112] A. Klauber *et al.*, *Airport Microgrid Implementation Toolkit*. Washington, D.C.: Transportation Research Board, 2021. doi: 10.17226/26165.
[113] Airport Cooperative Research Program, “Airport Microgrid Implemntation Toolkit.” https://acrpmicrogridtoolkit.xendee.com/ (accessed May 06, 2023).
[114] Y. Xiang, H. Cai, J. Liu, and X. Zhang, “Techno-economic design of energy systems for airport electrification: A hydrogen-solar-storage integrated microgrid solution,” *Appl. Energy*, vol. 283, no. January, p. 116374, Feb. 2021, doi: 10.1016/j.apenergy.2020.116374.
[115] M. Wang, Y. Liu, J. Liu, Y. Tao, W. Xu, and J. Gou, “Mobile Energy Storage Scheduling for AC-DC Microgrids Enabling Low-carbon Airport,” in *2019 IEEE PES Asia-Pacific Power and Energy Engineering Conference (APPEEC)*, Dec. 2019, pp. 1–5. doi: 10.1109/APPEEC45492.2019.8994604.
[116] Energy Research Partnership, “Future Resilience of the UK Electricity System,” Nov. 2018. Accessed: Feb. 25, 2022. [Online]. Available: https://erpuk.org/project/future-resilience-of-the-uk-electricity-system/
[117] International Civil Aviation Organization (ICAO), “A Focus on the production of renewable energy at the Airport site,” 2017. Accessed: Oct. 29, 2021. [Online]. Available: https://www.icao.int/environmental-protection/Documents/Energy at Airports.pdf
[118] European Commission, “CASCADE: reducing energy use by airports,” 2014. Accessed: Nov. 01, 2021. [Online]. Available: https://digital-strategy.ec.europa.eu/en/news/cascade-reducing-energy-use-airports
[119] The Ohio State University, “Is our energy grid ready for the future? Nope.,” Jul. 2021. https://si.osu.edu/news/our-energy-grid-ready-future-nope (accessed Apr. 09, 2022).
[120] M. H. Amirioun, F. Aminifar, H. Lesani, and M. Shahidehpour, “Metrics and quantitative framework for assessing microgrid resilience against windstorms,” *Int. J. Electr. Power Energy Syst.*, vol. 104, pp. 716–723, Jan. 2019, doi: 10.1016/j.ijepes.2018.07.025.
[121] Z. Li, M. Shahidehpour, F. Aminifar, A. Alabdulwahab, and Y. Al-Turki, “Networked Microgrids for Enhancing the Power System Resilience,” *Proc. IEEE*, vol. 105, no. 7, pp. 1289–1310, Jul. 2017, doi: 10.1109/JPROC.2017.2685558.
[122] M. Yadav, N. Pal, and D. K. Saini, “Microgrid Control, Storage, and Communication Strategies to Enhance Resiliency for Survival of Critical Load,” *IEEE Access*, vol. 8, pp. 169047–169069, 2020, doi: 10.1109/ACCESS.2020.3023087.
[123] N. Bhusal, M. Abdelmalak, M. Kamruzzaman, and M. Benidris, “Power System Resilience: Current Practices, Challenges, and Future Directions,” *IEEE Access*, vol. 8, pp. 18064–18086, 2020, doi: 10.1109/ACCESS.2020.2968586.
[124] Office of the Press Secretary, “Critical Infrastructure Security and Resilience,” *The White House*, Feb. 13, 2013. https://obamawhitehouse.archives.gov/the-press-office/2013/02/12/presidential-policy-directive-critical-infrastructure-security-and-resil (accessed Feb. 25, 2022).
[125] Science and Technology Committee, “The Resilience of the Electricity System ,” *House of Lords*, Feb. 24, 2015. https://publications.parliament.uk/pa/ld201415/ldselect/ldsctech/121/12102.ht

m (accessed Feb. 25, 2022).
[126] A. Gholami, F. Aminifar, and M. Shahidehpour, “Front Lines Against the Darkness: Enhancing the Resilience of the Electricity Grid Through Microgrid Facilities,” *IEEE Electrif. Mag.*, vol. 4, no. 1, pp. 18–24, Mar. 2016, doi: 10.1109/MELE.2015.2509879.
[127] G. Kandaperumal and A. K. Srivastava, “Resilience of the electric distribution systems: concepts, classification, assessment, challenges, and research needs,” *IET Smart Grid*, vol. 3, no. 2, pp. 133–143, Apr. 2020, doi: 10.1049/iet-stg.2019.0176.
[128] The U.S. Department of State and the U.S. Department of Homeland Security’s (DHS) Cybersecurity and Infrastructure Security Agency (CISA), “A Guide to Critical Infrastructure Security and Resilience,” November 2019. [Online]. Available: https://www.cisa.gov/sites/default/files/publications/Guide-Critical-Infrastructure-Security-Resilience-110819-508v2.pdf
[129] C. Grosse, “Airports as Critical Infrastructure: The Role of the Transportation-by-Air System for Regional Development and Crisis Management,” in *2019 IEEE International Conference on Industrial Engineering and Engineering Management (IEEM)*, Dec. 2019, pp. 440–444. doi: 10.1109/IEEM44572.2019.8978905.
[130] National Renewable Energy Laboratory (NREL), “Distributed solar PV for electricity system resiliency: Policy and regulatory considerations,” 2014. [Online]. Available: https://www.nrel.gov/docs/fy15osti/62631.pdf
[131] A. Kenward and U. Raja, “Blackout: Extreme Weather , Climate Change and Power Outages,” *Clim. Cent.*, p. 23, 2014, [Online]. Available: http://assets.climatecentral.org/pdfs/PowerOutages.pdf
[132] A. Hussain, V.-H. Bui, and H.-M. Kim, “Microgrids as a resilience resource and strategies used by microgrids for enhancing resilience,” *Appl. Energy*, vol. 240, pp. 56–72, Apr. 2019, doi: 10.1016/j.apenergy.2019.02.055.
[133] K. Anderson, N. DiOrio, D. Cutler, R. Butt, and A. Richards, “Increasing Resiliency Through Renewable Energy Microgrids,” *Int. J. Energy Sect. Manag.*, vol. 2, no. 2, 2017, [Online]. Available: https://www.osti.gov/biblio/1389210
[134] A. Younesi, H. Shayeghi, P. Siano, A. Safari, and H. H. Alhelou, “Enhancing the Resilience of Operational Microgrids Through a Two-Stage Scheduling Strategy Considering the Impact of Uncertainties,” *IEEE Access*, vol. 9, pp. 18454–18464, 2021, doi: 10.1109/ACCESS.2021.3053390.
[135] E. Rosales-Asensio, M. de Simón-Martín, A. E. Rosales, and A. Colmenar-Santos, “Solar-plus-storage benefits for end-users placed at radial and meshed grids: An economic and resiliency analysis,” *Int. J. Electr. Power Energy Syst.*, vol. 128, no. November 2020, 2021, doi: 10.1016/j.ijepes.2020.106675.
[136] M. Ganji, “Airport microgrids: Transportation energy as a service,” *IEEE Electrif. Mag.*, vol. 8, no. 4, pp. 121–122, 2020, doi: 10.1109/MELE.2020.3026512.
[137] G. Emanuella, O. Jon, P. Madison, and Z. Christina, “Atlanta’s Hartsfield-Jackson airport restores power after crippling outage,” *CNN*. https://edition.cnn.com/2017/12/17/us/atlanta-airport-power-outage/index.html (accessed Jan. 11, 2022).
[138] J. Mullen, C. Isidore, and J. Wattles, “Delta’s big headache - Day 2,” *CNN*, 2016. https://money.cnn.com/2016/08/09/news/companies/delta-flights-system-outage-delays-cancellations/index.html?iid=EL (accessed Jan. 11, 2022).

[139] C. Isidore, “Delta: 5-hour computer outage cost us $150 million,” *CNN*, 2016. https://money.cnn.com/2016/09/07/technology/delta-computer-outage-cost (accessed Jan. 11, 2022).
[140] M. Panteli, P. Mancarella, D. N. Trakas, E. Kyriakides, and N. D. Hatziargyriou, “Metrics and Quantification of Operational and Infrastructure Resilience in Power Systems,” *IEEE Trans. Power Syst.*, vol. 32, no. 6, pp. 4732–4742, Nov. 2017, doi: 10.1109/TPWRS.2017.2664141.
[141] S. Mousavizadeh, M.-R. Haghifam, and M.-H. Shariatkhah, “A linear two-stage method for resiliency analysis in distribution systems considering renewable energy and demand response resources,” *Appl. Energy*, vol. 211, pp. 443–460, Feb. 2018, doi: 10.1016/j.apenergy.2017.11.067.
[142] M. Panteli, C. Pickering, S. Wilkinson, R. Dawson, and P. Mancarella, “Power System Resilience to Extreme Weather: Fragility Modeling, Probabilistic Impact Assessment, and Adaptation Measures,” *IEEE Trans. Power Syst.*, vol. 32, no. 5, pp. 3747–3757, Sep. 2017, doi: 10.1109/TPWRS.2016.2641463.
[143] Y. Wang, C. Chen, J. Wang, and R. Baldick, “Research on Resilience of Power Systems Under Natural Disasters—A Review,” *IEEE Trans. Power Syst.*, vol. 31, no. 2, pp. 1604–1613, Mar. 2016, doi: 10.1109/TPWRS.2015.2429656.
[144] M. M. Sellberg, P. Ryan, S. T. Borgström, A. V. Norström, and G. D. Peterson, “From resilience thinking to Resilience Planning: Lessons from practice,” *J. Environ. Manage.*, vol. 217, pp. 906–918, Jul. 2018, doi: 10.1016/j.jenvman.2018.04.012.
[145] J. Najafi, A. Peiravi, and J. M. Guerrero, “Power distribution system improvement planning under hurricanes based on a new resilience index,” *Sustain. Cities Soc.*, vol. 39, pp. 592–604, May 2018, doi: 10.1016/j.scs.2018.03.022.
[146] M. R. Elkadeem, S. Wang, A. M. Azmy, E. G. Atiya, Z. Ullah, and S. W. Sharshir, “A systematic decision-making approach for planning and assessment of hybrid renewable energy-based microgrid with techno-economic optimization: A case study on an urban community in Egypt,” *Sustain. Cities Soc.*, vol. 54, p. 102013, Mar. 2020, doi: 10.1016/j.scs.2019.102013.
[147] G. Veilleux *et al.*, “Techno-economic analysis of microgrid projects for rural electrification: A systematic approach to the redesign of Koh Jik off-grid case study,” *Energy Sustain. Dev.*, vol. 54, pp. 1–13, Feb. 2020, doi: 10.1016/j.esd.2019.09.007.
[148] S. D. Nazemi, K. Mahani, A. Ghofrani, M. Amini, B. E. Kose, and M. A. Jafari, “Techno-Economic Analysis and Optimization of a Microgrid Considering Demand-Side Management,” in *2020 IEEE Texas Power and Energy Conference (TPEC)*, Feb. 2020, pp. 1–6. doi: 10.1109/TPEC48276.2020.9042562.
[149] N. I. Nwulu and X. Xia, “Optimal dispatch for a microgrid incorporating renewables and demand response,” *Renew. Energy*, vol. 101, pp. 16–28, Feb. 2017, doi: 10.1016/j.renene.2016.08.026.
[150] C. Gamarra and J. M. Guerrero, “Computational optimization techniques applied to microgrids planning: A review,” *Renew. Sustain. Energy Rev.*, vol. 48, pp. 413–424, Aug. 2015, doi: 10.1016/j.rser.2015.04.025.
[151] A. Micallef, J. M. Guerrero, and J. C. Vasquez, “New Horizons for Microgrids: From Rural Electrification to Space Applications,” *Energies*, vol. 16, no. 4, p. 1966, Feb. 2023, doi: 10.3390/en16041966.
[152] H. Masrur, A. Sharifi, M. R. Islam, M. A. Hossain, and T. Senjyu, “Optimal and economic operation of microgrids to leverage resilience benefits during grid

outages," *Int. J. Electr. Power Energy Syst.*, vol. 132, no. November 2020, p. 107137, 2021, doi: 10.1016/j.ijepes.2021.107137.
[153] S. Gaikwad and H. Mehta, "Investigation of effects of increasing EV penetration on distribution transformers in Modi Ganpati Area, Pune," in *2020 IEEE Electric Power and Energy Conference (EPEC)*, Nov. 2020, pp. 1–5. doi: 10.1109/EPEC48502.2020.9319915.
[154] C. Marmaras, "Charging of electric vehicles at commercial buildings," Cardiff University, 2017.
[155] International Renewable Energy Agency (IRENA), "Innovation landscape brief: Electric-vehicle smart charging," Abu Dhabi, 2019.
[156] F. Un-Noor, S. Padmanaban, L. Mihet-Popa, M. Mollah, and E. Hossain, "A Comprehensive Study of Key Electric Vehicle (EV) Components, Technologies, Challenges, Impacts, and Future Direction of Development," *Energies*, vol. 10, no. 8, p. 1217, Aug. 2017, doi: 10.3390/en10081217.
[157] M. Behrangrad, "A review of demand side management business models in the electricity market," *Renew. Sustain. Energy Rev.*, vol. 47, pp. 270–283, Jul. 2015, doi: 10.1016/j.rser.2015.03.033.
[158] A. Ford, A. Gillich, and P. Mirzania, "Sustainable Energy and Energy Efficient Technologies," in *Future Energy*, Elsevier, 2020, pp. 611–630. doi: 10.1016/B978-0-08-102886-5.00028-1.
[159] F. Shariatzadeh, P. Mandal, and A. K. Srivastava, "Demand response for sustainable energy systems: A review, application and implementation strategy," *Renew. Sustain. Energy Rev.*, vol. 45, pp. 343–350, May 2015, doi: 10.1016/j.rser.2015.01.062.
[160] Western Power Distribution, "Flexibility Services," 2018. [Online]. Available: https://www.nationalgrid.co.uk/downloads/4099/7-flexibility-services.pdf
[161] E. Sortomme and M. A. El-Sharkawi, "Optimal scheduling of vehicle-to-grid energy and ancillary services," *IEEE Trans. Smart Grid*, vol. 3, no. 1, pp. 351–359, 2012, doi: 10.1109/TSG.2011.2164099.
[162] W. Kempton and J. Tomić, "Vehicle-to-grid power fundamentals: Calculating capacity and net revenue," *J. Power Sources*, vol. 144, no. 1, pp. 268–279, 2005, doi: 10.1016/j.jpowsour.2004.12.025.
[163] A. Aldik and T. Khatib, "EV aggregators and energy storage units scheduling into ancillary services markets: The concept and recommended practice," *World Electr. Veh. J.*, vol. 11, no. 1, 2020, doi: 10.3390/WEVJ11010008.
[164] Z. Luo *et al.*, "Economic analyses of plug-in electric vehicle battery providing ancillary services," *2012 IEEE Int. Electr. Veh. Conf. IEVC 2012*, pp. 1–5, 2012, doi: 10.1109/IEVC.2012.6183272.
[165] K. Oureilidis *et al.*, "Ancillary Services Market Design in Distribution Networks: Review and Identification of Barriers," *Energies*, vol. 13, no. 4, p. 917, Feb. 2020, doi: 10.3390/en13040917.
[166] New York Independent System Operator (NYISO), "Ancillary Services." https://www.nyiso.com/ancillary-services (accessed Mar. 02, 2022).
[167] National Grid Electricity System Operator, "Balancing Services." https://www.nationalgrideso.com/industry-information/balancing-services (accessed Mar. 02, 2022).
[168] Elia, "Flexible Demand Management Products," 2017. [Online]. Available: https://www.elia.be/-/media/project/elia/elia-site/electricity-market-and-system---document-library/balancing---balancing-services-and-bsp/2017/2017-brochure-flexible-demand-management-products_en.pdf
[169] U. Helman, H. Singh, and P. Sotkiewicz, *RTOs, Regional Electricity Markets,*

and Climate Policy, 1st ed. Elsevier Inc., 2010. doi: 10.1016/B978-1-85617-655-2.00019-5.
[170] A. Kaushal and D. Van Hertem, "An overview of Ancillary Services and HVDC systems in European Context," *Energies*, vol. 12, no. 18, p. 3481, Sep. 2019, doi: 10.3390/en12183481.
[171] TenneT Transmission System Operator (TSO), "Dutch Ancillary Services." https://www.tennet.eu/electricity-market/dutch-ancillary-services/ (accessed Mar. 28, 2022).
[172] Pennsylvania-New Jersey-Maryland Regional Transmission Organization (PJMRTO), "Ancillary Services." https://www.pjm.com/markets-and-operations/ancillary-services (accessed Mar. 30, 2022).
[173] J. M. Clairand, "Participation of electric vehicle aggregators in ancillary services considering users' preferences," *Sustain.*, vol. 12, no. 1, pp. 1–17, 2020, doi: 10.3390/SU12010008.
[174] A. Gómez Expósito, A. J. Conejo, and C. Cañizares, "Frequency and Voltage Control," in *Electric Energy Systems*, 2nd ed., Chapter 9: CRC Press, 2018, pp. 373–434. doi: 10.1201/9781315192246-9.
[175] Pennsylvania-New Jersey-Maryland Regional Transmission Organization (PJMRTO), "Ancillary Services Market." https://learn.pjm.com/three-priorities/buying-and-selling-energy/ancillary-services-market.aspx (accessed Mar. 30, 2022).
[176] California Independent System Operator (CAISO), "Market processes and products." http://www.caiso.com/market/Pages/MarketProcesses.aspx (accessed Mar. 30, 2022).
[177] Australian Energy Market Operator (AEMO), "Settlements Guide to Ancillary Services Payment and Recovery," 2020. [Online]. Available: https://aemo.com.au/-/media/files/electricity/nem/data/ancillary_services/2020/settlements-guide-to-ancillary-services-payment-and-recovery.pdf?la=en
[178] European Commission, "Establishing a guideline on electricity balancing," Nov. 2017. Accessed: Mar. 30, 2022. [Online]. Available: https://eur-lex.europa.eu/legal-content/EN/TXT/?uri=uriserv:OJ.L_.2017.312.01.0006.01.ENG&toc=OJ:L:2017:312:TOC
[179] D. Lamont, "Flexible power balancing on the Elia grid," Jun. 11, 2020. https://www.egssis.com/flexible-power-balancing-on-elia-grid/ (accessed Mar. 30, 2022).
[180] A. Janjic, L. Velimirovic, M. Stankovic, and A. Petrusic, "Commercial electric vehicle fleet scheduling for secondary frequency control," *Electr. Power Syst. Res.*, vol. 147, pp. 31–41, Jun. 2017, doi: 10.1016/j.epsr.2017.02.019.
[181] F. Teng, M. Aunedi, D. Pudjianto, and G. Strbac, "Benefits of Demand-Side Response in Providing Frequency Response Service in the Future GB Power System," *Front. Energy Res.*, vol. 3, Aug. 2015, doi: 10.3389/fenrg.2015.00036.
[182] C. Guille and G. Gross, "A conceptual framework for the vehicle-to-grid (V2G) implementation," *Energy Policy*, vol. 37, no. 11, pp. 4379–4390, 2009, doi: https://doi.org/10.1016/j.enpol.2009.05.053.
[183] X. Ke, D. Wu, and N. Lu, "A Real-Time Greedy-Index Dispatching Policy for Using PEVs to Provide Frequency Regulation Service," *IEEE Trans. Smart Grid*, vol. 10, no. 1, pp. 864–877, 2019, doi: 10.1109/TSG.2017.2754241.
[184] N. DeForest, J. S. MacDonald, and D. R. Black, "Day ahead optimization of an electric vehicle fleet providing ancillary services in the Los Angeles Air Force

Base vehicle-to-grid demonstration," *Appl. Energy*, vol. 210, pp. 987–1001, 2018, doi: 10.1016/j.apenergy.2017.07.069.
[185] C. Pang, P. Dutta, and M. Kezunovic, "BEVs/PHEVs as Dispersed Energy Storage for V2B Uses in the Smart Grid," *IEEE Trans. Smart Grid*, vol. 3, no. 1, pp. 473–482, Mar. 2012, doi: 10.1109/TSG.2011.2172228.
[186] The Alliance Center, "Living Laboratory: Pilot Innovative Building Solutions." https://www.thealliancecenter.org/livinglaboratory/ (accessed Mar. 03, 2022).
[187] A. Tchagang and Y. Yoo, "V2B/V2G on Energy Cost and Battery Degradation under Different Driving Scenarios, Peak Shaving, and Frequency Regulations," *World Electr. Veh. J.*, vol. 11, no. 1, p. 14, Jan. 2020, doi: 10.3390/wevj11010014.
[188] D. Borge-Diez, D. Icaza, E. Açıkkalp, and H. Amaris, "Combined vehicle to building (V2B) and vehicle to home (V2H) strategy to increase electric vehicle market share," *Energy*, vol. 237, p. 121608, Dec. 2021, doi: 10.1016/j.energy.2021.121608.
[189] Peak Drive, "V2B Technology ." https://www.peakdriveenergy.com/v2b-technology (accessed Mar. 03, 2022).
[190] A. Ouammi, "Peak load reduction with a solar PV-based smart microgrid and vehicle-to-building (V2B) concept," *Sustain. Energy Technol. Assessments*, vol. 44, p. 101027, Apr. 2021, doi: 10.1016/j.seta.2021.101027.
[191] B. Li, W. Zhang, J. Wang, J. Xu, and J. Su, "Research and Analysis on Energy Consumption Features of Civil Airports," *IOP Conf. Ser. Earth Environ. Sci.*, vol. 94, p. 12134, 2017, doi: 10.1088/1755-1315/94/1/012134.
[192] International Energy Agency (IEA), "Spain 2021," *IEA, Paris*, 2021, [Online]. Available: https://www.iea.org/reports/spain-2021
[193] Spanish Airports and Air Navigation (AENA), "Environmental sustainability report," 2019. [Online]. Available: https://www.aena.es/en/corporative/environment-sustainability/sustainability/sustainability-strategy.html
[194] U. Datta, A. Kalam, and J. Shi, "The Strategies of EV Charge/Discharge Management in Smart Grid Vehicle-to-Everything (V2X) Communication Networks," in *Advanced Communication and Control Methods for Future Smartgrids*, IntechOpen, 2019. doi: 10.5772/intechopen.85385.
[195] S. M. S. Sadati and K. S. Cetin, "Data-Driven Method to Study the Impact of Utilizing Electric Ground Power Systems on Airport Electricity Demand Profile," *Transp. Res. Rec.*, vol. 2674, no. 4, pp. 261–271, 2020, doi: 10.1177/0361198120911051.
[196] M. Maigha and M. L. Crow, "A Transactive Operating Model for Smart Airport Parking Lots," *IEEE Power Energy Technol. Syst. J.*, vol. 5, no. 4, pp. 157–166, Dec. 2018, doi: 10.1109/JPETS.2018.2876453.
[197] B. Hou, S. Bose, L. Marla, and K. Haran, "Impact of Aviation Electrification on Airports: Flight Scheduling and Charging," pp. 1–19, 2021, [Online]. Available: http://arxiv.org/abs/2108.08963
[198] M. Kang, M. Bergés, and B. Akinci, "Forecasting airport building electricity demand on the basis of flight schedule information for demand response applications," *Transp. Res. Rec.*, vol. 2603, pp. 29–38, 2017, doi: 10.3141/2603-04.
[199] R. Godina, N. G. Paterakis, O. Erdinc, E. M. G. Rodrigues, and J. P. S. Catalao, "Electric vehicles home charging impact on a distribution transformer in a Portuguese Island," *Proc. - 2015 Int. Symp. Smart Electr. Distrib. Syst. Technol. EDST 2015*, no. September, pp. 74–79, 2015, doi:

10.1109/SEDST.2015.7315186.
[200] T. Antić, T. Capuder, and M. Bolfek, “A Comprehensive Analysis of the Voltage Unbalance Factor in PV and EV Rich Non-Synthetic Low Voltage Distribution Networks,” *Energies*, vol. 14, no. 1, p. 117, Dec. 2020, doi: 10.3390/en14010117.
[201] J. Then, A. P. Agalgaonkar, and K. M. Muttaqi, “Coordination of Spatially Distributed Electric Vehicle Charging for Voltage Rise and Voltage Unbalance Mitigation in Networks with Solar Penetration,” in *2021 IEEE Texas Power and Energy Conference (TPEC)*, Feb. 2021, pp. 1–6. doi: 10.1109/TPEC51183.2021.9384960.
[202] M. R. Islam, H. Lu, J. Hossain, M. R. Islam, and L. Li, “Multiobjective Optimization Technique for Mitigating Unbalance and Improving Voltage Considering Higher Penetration of Electric Vehicles and Distributed Generation,” *IEEE Syst. J.*, vol. 14, no. 3, pp. 3676–3686, Sep. 2020, doi: 10.1109/JSYST.2020.2967752.
[203] International Electrotechnical Commission (IEC), *IEC 60076-7:2018 Power transformers Part 7: Loading guide for oil-immersed power transformers*, 2nd ed.
[204] C. L. Su, C. N. Lu, K. E. Zheng, J. H. Teng, R. C. Leou, and K. F. Huang, “Analysis of PEV charging impact on distribution transformer aging for charging station transformer design,” *2014 IEEE Ind. Appl. Soc. Annu. Meet. IAS 2014*, pp. 1–8, 2014, doi: 10.1109/IAS.2014.6978491.
[205] R. O. Oliyide, “Load Management of Electric Vehicles and Heat Pumps in Emerging Electricity System,” Cardiff University, 2019. [Online]. Available: https://orca.cardiff.ac.uk/122249/
[206] A. D. Hilshey, P. D. H. Hines, P. Rezaei, and J. R. Dowds, “Estimating the impact of electric vehicle smart charging on distribution transformer aging,” *IEEE Trans. Smart Grid*, vol. 4, no. 2, pp. 905–913, 2013, doi: 10.1109/TSG.2012.2217385.
[207] Scottish Power Energy Networks, “Methodology & Learning Report Work Package 2.1: Dynamic thermal rating of assets – Primary Transformers,” 2015. [Online]. Available: https://www.spenergynetworks.co.uk/userfiles/file/Dynamic thermal rating of assets.pdf
[208] Y. Gao, “Thermal Monitoring and Thermodynamic Modelling of Distribution Transformers,” The University of Manchester, 2016. [Online]. Available: https://www.enwl.co.uk/globalassets/innovation/enwl002-thermal-modelling/enwl002-closedown/enwl002-appendix-1---thermal-monitoring-of-distribution-transformers.pdf
[209] H. Taha, *Operations Research: An Introduction*, 10th ed. Pearson, 2016.
[210] R. C. Bansal, “Optimization Methods for Electric Power Systems: An Overview,” *Int. J. Emerg. Electr. Power Syst.*, vol. 2, no. 1, Mar. 2005, doi: 10.2202/1553-779X.1021.
[211] A. Swarnkar and A. Swarnkar, “Artificial Intelligence Based Optimization Techniques: A Review,” 2020, pp. 95–103. doi: 10.1007/978-981-15-0214-9_12.
[212] D. Chen, R. G. Batson, and Y. Dang, *Applied Integer Programming : Modeling and Solution*, 1st ed. Wiley, 2011.
[213] J. N. Hooker, “Operations Research Methods in Constraint Programming,” 2006, pp. 527–570. doi: 10.1016/S1574-6526(06)80019-2.
[214] U. Klanšek, “A comparison between MILP and MINLP approaches to optimal

solution of Nonlinear Discrete Transportation Problem," *Transport*, vol. 30, no. 2, pp. 135–144, Jun. 2015, doi: 10.3846/16484142.2014.933361.
[215] R. Anand, D. Aggarwal, and V. Kumar, "A comparative analysis of optimization solvers," *J. Stat. Manag. Syst.*, vol. 20, no. 4, pp. 623–635, Jul. 2017, doi: 10.1080/09720510.2017.1395182.
[216] Gurobi Optimization LLC, "Gurobi Optimizer Reference Manual.," 2021. https://www.gurobi.com
[217] R. Lougee-Heimer, "The Common Optimization INterface for Operations Research: Promoting open-source software in the operations research community," *IBM J. Res. Dev.*, vol. 47, no. 1, pp. 57–66, Jan. 2003, doi: 10.1147/rd.471.0057.
[218] S. Hossain-McKenzie, M. Reno, J. Eddy, and K. Schneider, "Assessment of Existing Capabilities and Future Needs for Designing Networked Microgrids," United States, Feb. 2019. doi: 10.2172/1761847.
[219] XENDEE Inc, "Microgrid Design and Decision Support Platform." Accessed: Jan. 16, 2022. [Online]. Available: https://xendee.com/
[220] P. Gilman, N. Blair, M. Mehos, C. Christensen, S. Janzou, and C. Cameron, "Solar Advisor Model User Guide for Version 2.0," Golden, CO, Aug. 2008. doi: 10.2172/937349.
[221] S. Mishra *et al.*, "Computational framework for behind-the-meter DER techno-economic modeling and optimization: REopt Lite," *Energy Syst.*, vol. 13, no. 2, pp. 509–537, May 2022, doi: 10.1007/s12667-021-00446-8.
[222] Electric Power Research Institute (EPRI), "DER-VET User Guide: User Guide and Technical Documentation for the Distributed Energy Resources Value Estimation Tool (DER-VET^{TM}).," Palo Alto, CA, 2020. [Online]. Available: https://www.der-vet.com/files/DER-VET_User_Guide_v0.1.1.pdf
[223] B. Dursun and E. Aykut, "An investigation on wind/PV/fuel cell/battery hybrid renewable energy system for nursing home in Istanbul," *Proc. Inst. Mech. Eng. Part A J. Power Energy*, vol. 233, no. 5, pp. 616–625, Aug. 2019, doi: 10.1177/0957650919840519.
[224] J. D. D. Niyonteze, F. Zou, G. Asemota, S. Bimenyimana, and G. Shyirambere, "Key technology development needs and applicability analysis of renewable energy hybrid technologies in off-grid areas for the Rwanda power sector," *Heliyon*, vol. 6, no. 1, p. e03300, Jan. 2020, doi: 10.1016/j.heliyon.2020.e03300.
[225] P. Mathiesen, M. Stadler, J. Kleissl, and Z. Pecenak, "Techno-economic optimization of islanded microgrids considering intra-hour variability," *Appl. Energy*, vol. 304, p. 117777, Dec. 2021, doi: 10.1016/j.apenergy.2021.117777.
[226] M. Stadler, Z. Pecenak, P. Mathiesen, K. Fahy, and J. Kleissl, "Performance Comparison between Two Established Microgrid Planning MILP Methodologies Tested On 13 Microgrid Projects," *Energies*, vol. 13, no. 17, p. 4460, Aug. 2020, doi: 10.3390/en13174460.
[227] XENDEE Inc, "US Army Garrison Bavaria Selects XENDEE for Design of Resilient Microgrids in Garmisch," 2019. https://xendee.com/2019/12/18/us-army-garrison-bavaria/ (accessed Jan. 16, 2022).
[228] XENDEE Inc, "Recent Project Portfolio." https://xendee.com/projects/ (accessed Jan. 16, 2022).
[229] Spanish Airports and Air Navigation (AENA), "Air traffic statistics." https://www.aena.es/es/estadisticas/inicio.html (accessed Jan. 16, 2022).
[230] S. Ortega Alba and M. Manana, "Characterization and Analysis of Energy Demand Patterns in Airports," *Energies*, vol. 10, no. 1, pp. 1–35, Jan. 2017, doi: 10.3390/en10010119.

[231] Endesa Energía SA, "Electricity rates," 2021. https://www.endesa.com/en/companies/electricity?filter=6000-36000 (accessed Nov. 04, 2021).
[232] J. Ortiz, A. Fonseca i Casas, J. Salom, N. Garrido Soriano, and P. Fonseca i Casas, "Cost-effective analysis for selecting energy efficiency measures for refurbishment of residential buildings in Catalonia," *Energy Build.*, vol. 128, pp. 442–457, Sep. 2016, doi: 10.1016/j.enbuild.2016.06.059.
[233] A. Acakpovi, P. Adjei, N. Nwulu, and N. Y. Asabere, "Optimal Hybrid Renewable Energy System: A Comparative Study of Wind/Hydrogen/Fuel-Cell and Wind/Battery Storage," *J. Electr. Comput. Eng.*, vol. 2020, pp. 1–15, Dec. 2020, doi: 10.1155/2020/1756503.
[234] Red Eléctrica de España, "CO2 emissions of electricity generation in Spain," pp. 1–9, 2021.
[235] Electricity Maps, "Climate Impact by Area." https://app.electricitymaps.com/map (accessed May 18, 2023).
[236] Statista, "European Union Emission Trading System (EU-ETS) carbon pricing from January 2022 to May 2023," *Ember*, 2023. https://www.statista.com/statistics/1322214/carbon-prices-european-union-emission-trading-scheme/ (accessed May 29, 2023).
[237] N. Farrell, "Policy design for green hydrogen," *Renew. Sustain. Energy Rev.*, vol. 178, p. 113216, May 2023, doi: 10.1016/j.rser.2023.113216.
[238] I. Surwillo, "Reflections on the energy crisis in Europe," DIIS: Dansk Institut for Internationale Studier, Feb. 2023. Accessed: May 31, 2023. [Online]. Available: https://policycommons.net/artifacts/3446983/reflections-on-the-energy-crisis-in-europe/4247121/
[239] Z. K. Pecenak, M. Stadler, and K. Fahy, "Efficient multi-year economic energy planning in microgrids," *Appl. Energy*, vol. 255, no. April 2019, p. 113771, 2019, doi: 10.1016/j.apenergy.2019.113771.
[240] T. Schittekatte, M. Stadler, G. Cardoso, S. Mashayekh, and N. Sankar, "The impact of short-term stochastic variability in solar irradiance on optimal microgrid design," *IEEE Trans. Smart Grid*, vol. 9, no. 3, pp. 1647–1656, 2018, doi: 10.1109/TSG.2016.2596709.
[241] S. Mashayekh, M. Stadler, G. Cardoso, and M. Heleno, "A mixed integer linear programming approach for optimal DER portfolio, sizing, and placement in multi-energy microgrids," *Appl. Energy*, vol. 187, pp. 154–168, 2017, doi: 10.1016/j.apenergy.2016.11.020.
[242] Endesa Energía SA, "Óptima Rate for companies." https://www.endesa.com/en/companies/electricity/optimum-rate (accessed Jan. 17, 2022).
[243] Spanish Airports and Air Navigation (AENA), "Seve Ballesteros-Santander." https://www.aena.es/en/seve-ballesteros-santander.html (accessed Jan. 19, 2022).
[244] M. Sullivan, M. T. Collins, J. Schellenberg, and P. H. Larsen, "Estimating Power System Interruption Costs: A Guidebook for Electric Utilities," E-Scholarship Repository, Berkeley, CA, May 2018. doi: 10.2172/1462980.
[245] S. Baik, A. H. Sanstad, N. Hanus, J. H. Eto, and P. H. Larsen, "A hybrid approach to estimating the economic value of power system resilience," *Electr. J.*, vol. 34, no. 8, p. 107013, Oct. 2021, doi: 10.1016/j.tej.2021.107013.
[246] Electric Power Research Institute (EPRI), "Electric Ground Support And Gate Electrification Equipment For Airports," Oct. 2020. [Online]. Available: https://www.epri.com/research/products/000000003002018326

[247] S. Mishra and P. Palanisamy, “Efficient Power Flow Management and Peak Shaving in a Microgrid-PV System,” in *2018 IEEE Energy Conversion Congress and Exposition (ECCE)*, Sep. 2018, pp. 3792–3798. doi: 10.1109/ECCE.2018.8558312.
[248] M. Aziz and T. Oda, “Load Leveling Utilizing Electric Vehicles and their Used Batteries,” in *Modeling and Simulation for Electric Vehicle Applications*, InTech, 2016. doi: 10.5772/64432.
[249] M. Uddin, M. F. Romlie, M. F. Abdullah, S. Abd Halim, A. H. Abu Bakar, and T. Chia Kwang, “A review on peak load shaving strategies,” *Renew. Sustain. Energy Rev.*, vol. 82, no. November 2017, pp. 3323–3332, 2018, doi: 10.1016/j.rser.2017.10.056.
[250] S. O. Alba and M. Manana, “Energy research in airports: A review,” *Energies*, vol. 9, no. 5, pp. 1–19, 2016, doi: 10.3390/en9050349.
[251] Michael Grant and Stephen Boyd, “CVX: Matlab software for disciplined convex programming, version 2.1,” 2014. http://cvxr.com/cvx
[252] M. C. Grant and S. P. Boyd, “Graph Implementations for Nonsmooth Convex Programs,” in *Recent Advances in Learning and Control*, Springer, 2008, pp. 95–110. doi: 10.1007/978-1-84800-155-8_7.
[253] F. Jarnehammar, “Asset management of electrical transportation systems using alternative charging technologies : case study Stockholm Arlanda Airport Asset management of electrical transportation systems using alternative charging,” KTH Royal institute of technology, 2018.
[254] London City Airport, “Noise pollution: Airport operating hours.” https://www.londoncityairport.com/corporate/noise-and-track-keeping-system/Airport-operating-hours (accessed Oct. 02, 2021).
[255] Spanish Association for Slot Coordination and Facilitation (AECFA), “Horarios Operativos (UTC),” 2021 [Online]. Available: https://www.slotcoordination.es/csee/Satellite?blobcol=urldata&blobheader=application%2Fpdf&blobkey=id&blobtable=MungoBlobs&blobwhere=1445426450281&ssbinary=true&blobheadername1=Content-disposition&blobheadervalue1=attachment; filename=Estatutos-AECFA.pdf
[256] Electric Power Research Institute (EPRI), “Austin-Bergstrom International Airport Electrification: Landside Vehicle and Airside Equipment Operations,” Palo Alto, CA, 2011. [Online]. Available: https://www.epri.com/research/products/000000000001023202
[257] Trepel Airport Equipment, “Trepel Airport Equepment: Product overview.” [Online]. Available: https://trepel.com/download/trepel-products.pdf
[258] Ostend-Bruges International Airport, “Ostend-Bruges International Airport Flight Schedule.” https://www.ostendbruges-airport.com/flightdates/ (accessed Sep. 15, 2021).
[259] Elia Group, “Data Download.” https://www.elia.be/en/grid-data/data-download-page
[260] State Meteorological Agency (AEMET), “Weather: Santander (Cantabria).” http://www.aemet.es/en/eltiempo/prediccion/municipios/santander-id39075 (accessed Sep. 17, 2021).
[261] A. J. Mason, “OpenSolver - An Open Source Add-in to Solve Linear and Integer Progammes in Excel,” in *Operations Research Proceedings 2011*, D. Klatte, H.-J. Lüthi, and K. Schmedders, Eds. Berlin, Heidelberg: Springer Berlin Heidelberg, 2012, pp. 401–406. doi: 10.1007/978-3-642-29210-1_64.
[262] OpenSolver, “OpenSolver for Excel.” opensolver.org (accessed Sep. 16, 2021).

Appendix A

Scripts used in this work.

----------Load Flatting Model (Ch.6) ----------

```
close all;
clear all;
clc;

%%_____________________Data_____________________________
z=xlsread('data.xlsx','sheet1','F1:F24');
avail1=xlsread('data.xlsx','sheet2','A1:A24');
avail2=xlsread('data.xlsx','sheet2','B1:B24');
avail3=xlsread('data.xlsx','sheet2','C1:C24');
avail4=xlsread('data.xlsx','sheet2','D1:D24');

%%_____________________ Variables & Parameters_________________

cvx_begin
cvx_precision( 0.01 )
i=6;
t=24;
s=4;
variable x1(t,i);
variable x2(t,i);
variable x3(t,i);
variable x4(t,i);
variable grid_s(t);

variable f1(t,i) binary;
variable f2(t,i) binary;
variable f3(t,i) binary;
variable f4(t,i) binary;

variable xd1(t,i);
variable xd2(t,i);
variable xd3(t,i);
variable xd4(t,i);

variable fu1(t,i) binary;
variable fu2(t,i) binary;
variable fu3(t,i) binary;
variable fu4(t,i) binary;

variable x1_f1(t,i);
variable x2_f2(t,i);
variable x3_f3(t,i);
variable x4_f4(t,i);

variable xd1_f1(t,i);
variable xd2_f2(t,i);
variable xd3_f3(t,i);
variable xd4_f4(t,i);

variable EM1(t,i) binary;
variable EM2(t,i) binary;
variable EM3(t,i) binary;
variable EM4(t,i) binary;



x1ch=x1_f1(:,1)+x1_f1(:,2)+x1_f1(:,3)+x1_f1(:,4)+x1_f1(:,5)+x1_f1(:,6);

x2ch=x2_f2(:,1)+x2_f2(:,2)+x2_f2(:,3)+x2_f2(:,4)+x2_f2(:,5)+x2_f2(:,6);
```

```
x3ch=x3_f3(:,1)+x3_f3(:,2)+x3_f3(:,3)+x3_f3(:,4)+x3_f3(:,5)+x3_f3(:,6);

x4ch=x4_f4(:,1)+x4_f4(:,2)+x4_f4(:,3)+x4_f4(:,4)+x4_f4(:,5)+x4_f4(:,6);

xd1dis=xd1_f1(:,1)+xd1_f1(:,2)+xd1_f1(:,3)+xd1_f1(:,4)+xd1_f1(:,5)+xd1_f1(:,
6);

xd2dis=xd2_f2(:,1)+xd2_f2(:,2)+xd2_f2(:,3)+xd2_f2(:,4)+xd2_f2(:,5)+xd2_f2(:,
6);

xd3dis=xd3_f3(:,1)+xd3_f3(:,2)+xd3_f3(:,3)+xd3_f3(:,4)+xd3_f3(:,5)+xd3_f3(:,
6);

xd4dis=xd4_f4(:,1)+xd4_f4(:,2)+xd4_f4(:,3)+xd4_f4(:,4)+xd4_f4(:,5)+xd4_f4(:,
6);


x1chplot=[x1ch(1,:),x1ch(2,:),x1ch(3,:),x1ch(4,:),x1ch(5,:),x1ch(6,:),x1ch(7
,:),x1ch(8,:),x1ch(9,:)...

,x1ch(10,:),x1ch(11,:),x1ch(12,:),x1ch(13,:),x1ch(14,:),x1ch(15,:),x1ch(16,:
),x1ch(17,:)...

,x1ch(18,:),x1ch(19,:),x1ch(20,:),x1ch(21,:),x1ch(22,:),x1ch(23,:),x1ch(24,:
)];


x2chplot=[x2ch(1,:),x2ch(2,:),x2ch(3,:),x2ch(4,:),x2ch(5,:),x2ch(6,:),x2ch(7
,:),x2ch(8,:),x2ch(9,:)...

,x2ch(10,:),x2ch(11,:),x2ch(12,:),x2ch(13,:),x2ch(14,:),x2ch(15,:),x2ch(16,:
),x2ch(17,:)...

,x2ch(18,:),x2ch(19,:),x2ch(20,:),x2ch(21,:),x2ch(22,:),x2ch(23,:),x2ch(24,:
)];

x3chplot=[x3ch(1,:),x3ch(2,:),x3ch(3,:),x3ch(4,:),x3ch(5,:),x3ch(6,:),x3ch(7
,:),x3ch(8,:),x3ch(9,:)...

,x3ch(10,:),x3ch(11,:),x3ch(12,:),x3ch(13,:),x3ch(14,:),x3ch(15,:),x3ch(16,:
),x3ch(17,:)...

,x3ch(18,:),x3ch(19,:),x3ch(20,:),x3ch(21,:),x3ch(22,:),x3ch(23,:),x3ch(24,:
)];

x4chplot=[x4ch(1,:),x4ch(2,:),x4ch(3,:),x4ch(4,:),x4ch(5,:),x4ch(6,:),x4ch(7
,:),x4ch(8,:),x4ch(9,:)...

,x4ch(10,:),x4ch(11,:),x4ch(12,:),x4ch(13,:),x4ch(14,:),x4ch(15,:),x4ch(16,:
),x4ch(17,:)...

,x4ch(18,:),x4ch(19,:),x4ch(20,:),x4ch(21,:),x4ch(22,:),x4ch(23,:),x4ch(24,:
)];


xd1disdisplot=[xd1dis(1,:),xd1dis(2,:),xd1dis(3,:),xd1dis(4,:),xd1dis(5,:),x
d1dis(6,:),xd1dis(7,:),xd1dis(8,:),xd1dis(9,:)...

,xd1dis(10,:),xd1dis(11,:),xd1dis(12,:),xd1dis(13,:),xd1dis(14,:),xd1dis(15,
:),xd1dis(16,:),xd1dis(17,:)...

,xd1dis(18,:),xd1dis(19,:),xd1dis(20,:),xd1dis(21,:),xd1dis(22,:),xd1dis(23,
:),xd1dis(24,:)];

xd2disdisplot=[xd2dis(1,:),xd2dis(2,:),xd2dis(3,:),xd2dis(4,:),xd2dis(5,:),x
d2dis(6,:),xd2dis(7,:),xd2dis(8,:),xd2dis(9,:)...

,xd2dis(10,:),xd2dis(11,:),xd2dis(12,:),xd2dis(13,:),xd2dis(14,:),xd2dis(15,
:),xd2dis(16,:),xd2dis(17,:)...
```

```
,xd2dis(18,:),xd2dis(19,:),xd2dis(20,:),xd2dis(21,:),xd2dis(22,:),xd2dis(23,
:),xd2dis(24,:)];

xd3disdisplot=[xd3dis(1,:),xd3dis(2,:),xd3dis(3,:),xd3dis(4,:),xd3dis(5,:),x
d3dis(6,:),xd3dis(7,:),xd3dis(8,:),xd3dis(9,:)...

,xd3dis(10,:),xd3dis(11,:),xd3dis(12,:),xd3dis(13,:),xd3dis(14,:),xd3dis(15,
:),xd3dis(16,:),xd3dis(17,:)...

,xd3dis(18,:),xd3dis(19,:),xd3dis(20,:),xd3dis(21,:),xd3dis(22,:),xd3dis(23,
:),xd3dis(24,:)];

xd4disdisplot=[xd4dis(1,:),xd4dis(2,:),xd4dis(3,:),xd4dis(4,:),xd4dis(5,:),x
d4dis(6,:),xd4dis(7,:),xd4dis(8,:),xd4dis(9,:)...

,xd4dis(10,:),xd4dis(11,:),xd4dis(12,:),xd4dis(13,:),xd4dis(14,:),xd4dis(15,
:),xd4dis(16,:),xd4dis(17,:)...

,xd4dis(18,:),xd4dis(19,:),xd4dis(20,:),xd4dis(21,:),xd4dis(22,:),xd4dis(23,
:),xd4dis(24,:)];

totalcharging=x1chplot(:)+x2chplot(:)+x3chplot(:)+x4chplot(:);
totaldis=xd1disdisplot(:)+xd2disdisplot(:)+xd3disdisplot(:)+xd4disdisplot(:)
;
totalload=z(:)+totalcharging(:)-totaldis(:);

tariff=[0.1485,0.1485,0.1485,0.1485,0.1485,0.1485,0.1485,0.1694,
0.1902,0.1902,...

0.1902,0.1902,0.1902,0.1694,0.1694,0.1694,0.1694,0.1902,0.1902,0.1902,0.1902
,0.1902...
    0.1485,0.1485];
Obj=max(totalload(:)) - min(totalload(:));  %Objective

minimize Obj;

subject to

%%_____________________ availability Cons._________________

for t=1:t
sum(f1(t,:),2)==avail1(t);
sum(f2(t,:),2)==avail2(t);
sum(f3(t,:),2)==avail3(t);
sum(f4(t,:),2)==avail4(t);

sum(fu1(t,:),2)==6-avail1(t);
sum(fu2(t,:),2)==6-avail2(t);
sum(fu3(t,:),2)==6-avail3(t);
sum(fu4(t,:),2)==6-avail4(t);
end

%%_____________________ V2B model_________________

for t=1:t

0<= x1(t,:);
0<= x2(t,:);
0<= x3(t,:);
0<= x4(t,:);

x1(t,:)<=7.6;
x2(t,:)<=22;
x3(t,:)<=7.6;
x4(t,:)<=22;

0<= xd1(t,:);
0<= xd2(t,:);
0<= xd3(t,:);
```

```
0<= xd4(t,:);

xd1(t,:)<=7.6;
xd2(t,:)<=22;
xd3(t,:)<=7.6;
xd4(t,:)<=22;

0<= x1_f1(t,:);
0<= x2_f2(t,:);
0<= x3_f3(t,:);
0<= x4_f4(t,:);

x1_f1(t,:)<=7.6;
x2_f2(t,:)<=22;
x3_f3(t,:)<=7.6;
x4_f4(t,:)<=22;

0<= xd1_f1(t,:);
0<= xd2_f2(t,:);
0<= xd3_f3(t,:);
0<= xd4_f4(t,:);

xd1_f1(t,:)<=7.6;
xd2_f2(t,:)<=22;
xd3_f3(t,:)<=7.6;
xd4_f4(t,:)<=22;

x1_f1(t,:) <= x1(t,:);
x2_f2(t,:) <= x2(t,:);
x3_f3(t,:) <= x3(t,:);
x4_f4(t,:) <= x4(t,:);

xd1_f1(t,:) <= xd1(t,:);
xd2_f2(t,:) <= xd2(t,:);
xd3_f3(t,:) <= xd3(t,:);
xd4_f4(t,:) <= xd4(t,:);

    end

for t=1:24
    for i=1:6
x1_f1(t,i) <= 7.6*f1(t,i);
x2_f2(t,i) <= 22*f2(t,i);
x3_f3(t,i) <= 7.6*f3(t,i);
x4_f4(t,i) <= 22*f4(t,i);

x1(t,i)- x1_f1(t,i) <= (1-f1(t,i))*7.6;
x2(t,i)- x2_f2(t,i) <= (1-f2(t,i))*22;
x3(t,i)- x3_f3(t,i) <= (1-f3(t,i))*7.6;
x4(t,i)- x4_f4(t,i) <= (1-f4(t,i))*22;

xd1_f1(t,i) <= 7.6*f1(t,i);
xd2_f2(t,i) <= 22*f2(t,i);
xd3_f3(t,i) <= 7.6*f3(t,i);
xd4_f4(t,i) <= 22*f4(t,i);

xd1(t,i)- xd1_f1(t,i) <= (1-f1(t,i))*7.6;
xd2(t,i)- xd2_f2(t,i) <= (1-f2(t,i))*22;
xd3(t,i)- xd3_f3(t,i) <= (1-f3(t,i))*7.6;
xd4(t,i)- xd4_f4(t,i) <= (1-f4(t,i))*22;

EM1(t,i)*0<= x1(t,i) ;
EM2(t,i)*0<= x2(t,i) ;
EM3(t,i)*0<= x3(t,i) ;
EM4(t,i)*0<= x4(t,i) ;

x1(t,i)<= EM1(t,i)*7.6;
x2(t,i)<= EM2(t,i)*22;
x3(t,i)<= EM3(t,i)*7.6;
x4(t,i)<= EM4(t,i)*22;
```

```
(1-EM1(t,i))*0<= xd1(t,i) ;
(1-EM2(t,i))*0<= xd2(t,i) ;
(1-EM3(t,i))*0<= xd3(t,i) ;
(1-EM4(t,i))*0<= xd4(t,i) ;

xd1(t,i)<= (1-EM1(t,i))*7.6;
xd2(t,i)<= (1-EM2(t,i))*22;
xd3(t,i)<= (1-EM3(t,i))*7.6;
xd4(t,i)<= (1-EM4(t,i))*22;

f1(t,i)+fu1(t,i)<=1;
f2(t,i)+fu2(t,i)<=1;
f3(t,i)+fu3(t,i)<=1;
f4(t,i)+fu4(t,i)<=1;

    end
end

%%_____________________ SOC Cons._________________

SOC1in = 49.6*0.5 + (49.6*0.9-49.6*0.5).*rand(6,1)';
SOC2in = 64.8*0.5 + (64.8*0.9-64.8*0.5).*rand(6,1)';
SOC3in = 31.6*0.5 + (31.6*0.9-31.6*0.5).*rand(6,1)';
SOC4in = 84*0.5 + (84*0.9-84*0.5).*rand(6,1)';


for t=1
   for i=1:6
      SOC1(t,i)=SOC1in(t,i)+sum(x1_f1(t,i)-xd1_f1(t,i))-0.9*fu1(t,i);
      SOC2(t,i)=SOC2in(t,i)+sum(x2_f2(t,i)-xd2_f2(t,i))-4*fu2(t,i);
      SOC3(t,i)=SOC3in(t,i)+sum(x3_f3(t,i)-xd3_f3(t,i))-1.2*fu3(t,i);
      SOC4(t,i)=SOC4in(t,i)+sum(x4_f4(t,i)-xd4_f4(t,i))-1.5*fu4(t,i);

   end
end
for t=2:24
   for i=1:6
      SOC1(t,i)=SOC1(t-1,i)+sum(x1_f1(t,i)-xd1_f1(t,i))-0.9*fu1(t,i);
      SOC2(t,i)=SOC2(t-1,i)+sum(x2_f2(t,i)-xd2_f2(t,i))-4*fu2(t,i);
      SOC3(t,i)=SOC3(t-1,i)+sum(x3_f3(t,i)-xd3_f3(t,i))-1.2*fu3(t,i);
      SOC4(t,i)=SOC4(t-1,i)+sum(x4_f4(t,i)-xd4_f4(t,i))-1.5*fu4(t,i);
   end
end


for t=1:24
SOC1(t,:)<=49.6*0.9;
SOC2(t,:)<=64.8*0.9;
SOC3(t,:)<=31.6*0.9;
SOC4(t,:)<=84*0.9;

49.6*0.5<=SOC1(t,:);
64.8*0.5<=SOC2(t,:);
31.6*0.5<=SOC3(t,:);
84*0.5<=SOC4(t,:);
end


 cvx_end

%%_____________________PLOT_________________

plot(z,'k','LineWidth',1);
hold on
plot(totalload,'b','LineWidth',1);
```

----------Frequency Regulation Model (Ch.7) ----------

```
import pulp
import pandas as pd
from matplotlib import pyplot as plt

solver = pulp.GUROBI(timeLimit = 60*60*2 , gapRel= 1)

phi = 0.035
bet = 0.0802
activated = pd.read_excel("data.xlsx" , "Activated")
Ava_data = pd.read_excel("data.xlsx" , "AVA Data")
Ava_data = Ava_data.rename(columns = {'AVA(C )' : "AVA(C)"})
list(Ava_data)
soc_data = pd.read_excel("data.xlsx" , "Soc Pu data")
Time = activated["Time"].to_list()
typ = ["A" , "B" , "C" , "D"]
seg = range(1 , 18)
model = pulp.LpProblem("me", pulp.LpMaximize)
pu = {}
pu_availabe = {}
for n in typ:
    pu[n] = {}
    pu_availabe[n] = {}
    for i in seg:
        pu[n][i] = {}
        pu_availabe[n][i] = {}
        for t in Time :
            pu[n][i][t] =  pulp.LpVariable('pu ' + str(n) + " i= " + str(i)
+ " t =  " + str(t), lowBound=0, cat="Continuous")
            pu_availabe[n][i][t] =  pulp.LpVariable('pu_availabe ' + str(n)
+ " i= " + str(i) + " t =  " + str(t), lowBound=0, cat="Continuous")

pdu = {}
pdu_availabe = {}
for n in typ:
    pdu[n] = {}
    pdu_availabe[n] = {}
    for i in seg:
        pdu[n][i] = {}
        pdu_availabe[n][i] = {}
        for t in Time :
            pdu[n][i][t] =  pulp.LpVariable('pdu ' + str(n) + " i= " +
str(i) + " t =  " + str(t), lowBound=0, cat="Continuous")
            pdu_availabe[n][i][t] =  pulp.LpVariable('pdu_availabe ' +
str(n) + " i= " + str(i) + " t =  " + str(t), lowBound=0, cat="Continuous")

availabe = {}
itspu = {}
for n in typ:
    availabe[n] = {}
    itspu[n] = {}
    for i in seg:
        availabe[n][i] = {}
        itspu[n][i] = {}
        for t in Time :
            availabe[n][i][t] =  pulp.LpVariable('availabe ' + str(n) + " i=
" + str(i) + " t =  " + str(t),  cat="Binary")
            itspu[n][i][t] =  pulp.LpVariable('itspu ' + str(n) + " i= " +
str(i) + " t =  " + str(t),  cat="Binary")
"""
Y =xb

Y <= X
Y <= Xmax * b
X-Y <= (1-b)Xmax

"""
```

```
for n in typ:
    for i in seg:
        for t in Time :
            model += pu_availabe[n][i][t] <= pu[n][i][t]
            model += pu_availabe[n][i][t] <= soc_data[soc_data["n"] ==
"Pumax"][n].values[0] * availabe[n][i][t]
            model += pu[n][i][t] - pu_availabe[n][i][t] <= ( 1 -
availabe[n][i][t] )* soc_data[soc_data["n"] == "Pumax"][n].values[0]

            model += pdu_availabe[n][i][t] <= pdu[n][i][t]
            model += pdu_availabe[n][i][t] <= soc_data[soc_data["n"] ==
"Pdmax"][n].values[0] * availabe[n][i][t]
            model += pdu[n][i][t] - pdu_availabe[n][i][t] <= ( 1 -
availabe[n][i][t] ) * soc_data[soc_data["n"] == "Pdmax"][n].values[0]

            model += pu[n][i][t]  <= ( itspu[n][i][t] ) *
soc_data[soc_data["n"] == "Pumax"][n].values[0]
            model += pu[n][i][t]  >= ( itspu[n][i][t] ) *
soc_data[soc_data["n"] == "Pumin"][n].values[0]

            model += pdu[n][i][t]  <= ( 1-itspu[n][i][t] ) *
soc_data[soc_data["n"] == "Pdmax"][n].values[0]
            model += pdu[n][i][t]  >= (1- itspu[n][i][t] ) *
soc_data[soc_data["n"] == "Pdmin"][n].values[0]

Ru = {}
Rd = {}
for t in Time :
    Ru[t] = sum ( sum( pu_availabe[n][i][t]      for i in seg ) for n in typ
)
    Rd[t] = sum ( sum( pdu_availabe[n][i][t]      for i in seg ) for n in
typ   )

soc = {}
for n in typ:
    soc[n] = {}
    for i in seg:
        soc[n][i] = {}
        for t in Time :
            if t == Time[0] :
                soc[n][i][t] = int(soc_data[soc_data["n"] == "SOC
intial"][n].values[0])
            else :
                soc[n][i][t] =  soc[n][i][Time[Time.index(t) - 1 ]] -
pu_availabe[n][i][t] + pdu_availabe[n][i][t] - \
                    (1-availabe[n][i][t]) *  soc_data[soc_data["n"] ==
""][n].values[0]
                model += soc[n][i][t] <= soc_data[soc_data["n"] ==
"SOCmax"][n].values[0]
                model += soc[n][i][t] >= soc_data[soc_data["n"] ==
"SOCmin"][n].values[0]

for n in typ:
    for t in Time:
        model += sum( availabe[n][i][t]  for i in seg) ==
Ava_data[Ava_data["Hour"] == int(t[:2])]["AVA(" +  n  + ")"].values[0]

for t in Time:
    model += Ru[t]  == activated[activated["Time"] == t]["
RU_offerd"].values[0]
    model += Rd[t] == activated[activated["Time"] ==
t]["RD_offerd"].values[0]

C_ch = sum( bet   *  Rd[t] * 0.062           for t in Time)
C_deg = sum( phi   *  Ru[t] * 0.033           for t in Time)

Rev = sum (   Ru[t] * activated[activated["Time"] == t]['R+
Prrice($/MWh)'].values[0]  + \
```

```
           +\
                activated[activated["Time"] == t][''].values[0] *Rd[t]
*0.062   +\
                    activated[activated["Time"] == t][''].values[0]
*Ru[t]*0.033  for t in Time )

# Objective function
model +=  Rev - (C_ch + C_deg)
print("ready to solve ")
model.solve(solver)
print(pulp.LpStatus[model.status])
print(pulp.value(    model.objective  ))
print("C_ch =  " , pulp.value(C_ch))
print("C_deg =  " , pulp.value(C_deg))
print("Rev =  " , pulp.value(Rev))

"""
##################plot
t = '00:00 -> 00:15'
n = "A"
plt.xlabel('segment')
plt.ylabel('pu')
plt.title('pu in T = ' + t + " for the type " + n)
plt.plot([pulp.value(pu[n][i][t])  for i in seg])

######################plot
"""
df_available  = {}
df_available["availabe"] = pd.DataFrame()
for n in typ :
    df_available["availabe"][n] = [ " ".join([str(int(
pulp.value(availabe[n][i][t] )) ) for i in seg])             for t in Time]
df_available["pu"] = pd.DataFrame()
for n in typ :
    df_available["pu"][n] = [ " ".join([str(int( pulp.value(pu[n][i][t] )) )
for i in seg])             for t in Time]
df_available["pd"] = pd.DataFrame()
for n in typ :
    df_available["pd"][n] = [ " ".join([str(int( pulp.value(pdu[n][i][t] ))
) for i in seg])             for t in Time]
df_available["pu  availabe"] = pd.DataFrame()
for n in typ :
   df_available["pu  availabe"][n] = [ " ".join([str(int(
pulp.value(pu_availabe[n][i][t] )) ) for i in seg])             for t in
Time]

df_available["pd   availabe"] = pd.DataFrame()
for n in typ :
    df_available["pd   availabe"][n] = [ " ".join([str(int(
pulp.value(pdu_availabe[n][i][t] )) ) for i in seg])             for t in
Time]

df_available["Ru and Rd"] = pd.DataFrame()

df_available["Ru and Rd"]["Ru"] = [    pulp.value(Ru[t] )      for t in
Time]
df_available["Ru and Rd"]["Rd"] = [    pulp.value(Rd[t] )      for t in
Time]


df_available["soc"] = pd.DataFrame()
for n in typ :
    df_available["soc"][n] = [ " ".join([str(int( pulp.value(soc[n][i][t] ))
) for i in seg])             for t in Time]

writer = pd.ExcelWriter('result obj = ' + str(pulp.value(    model.objective
) )+ '.xlsx', engine='xlsxwriter')
for e in df_available:
    df_available[e]["Time"] = Time
```

```
    df_available[e].set_index("Time").to_excel(writer, sheet_name=e
,index=True)

writer.save()
```

----------Dynamic Loading Model Screenshots (Ch.8) ----------

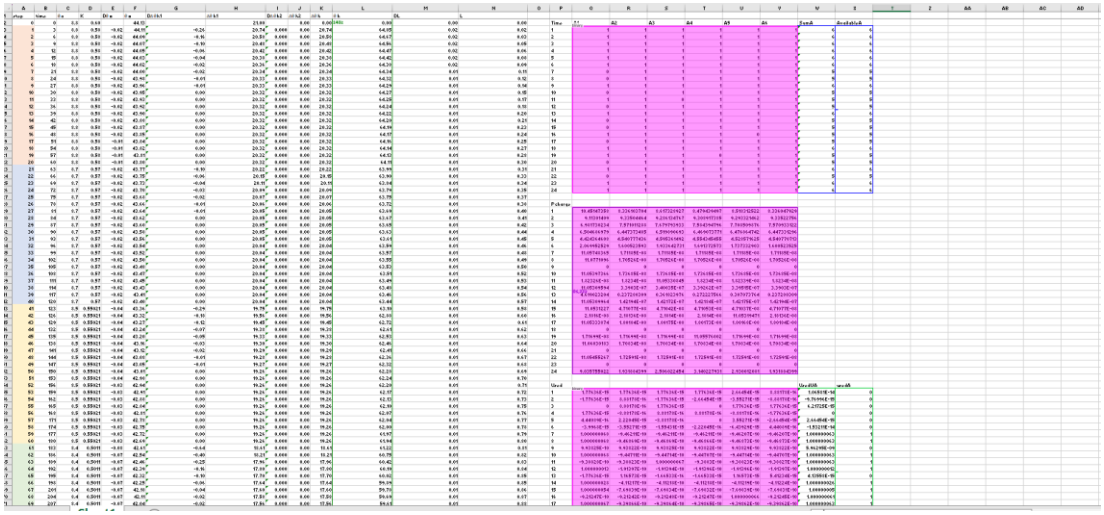

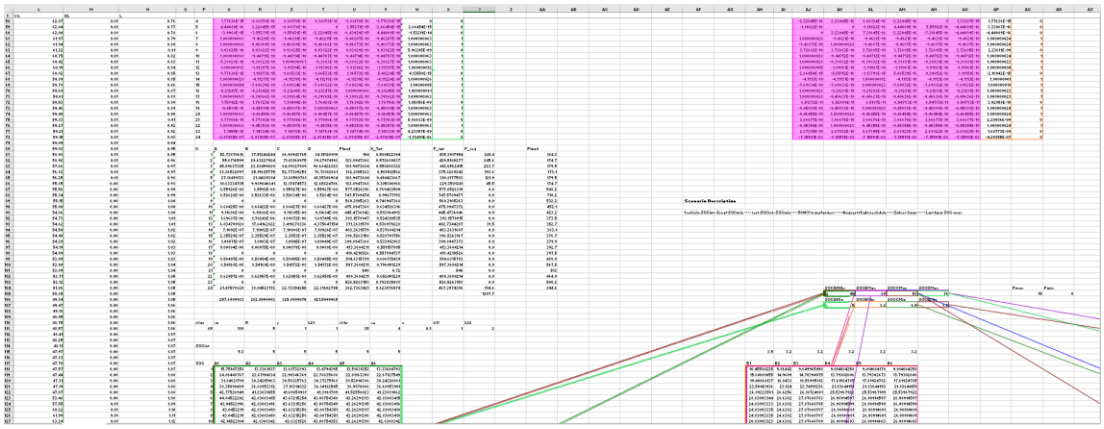

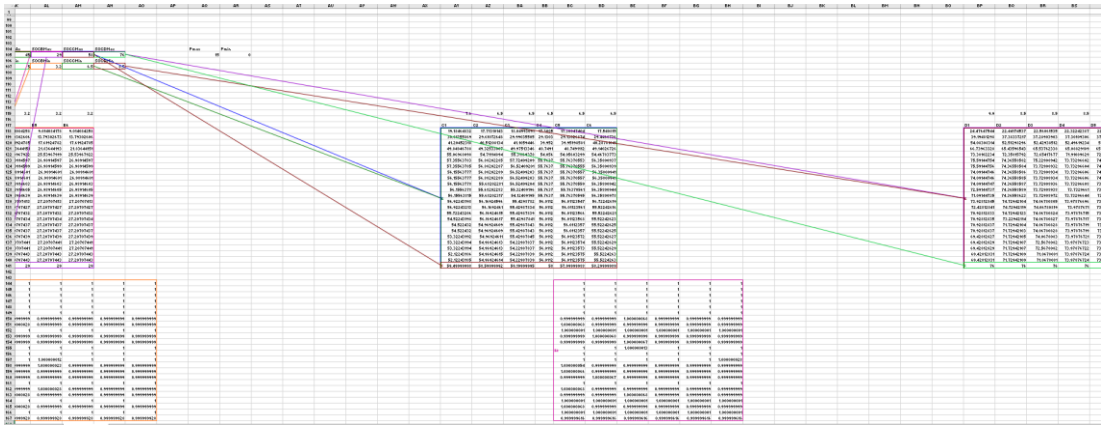

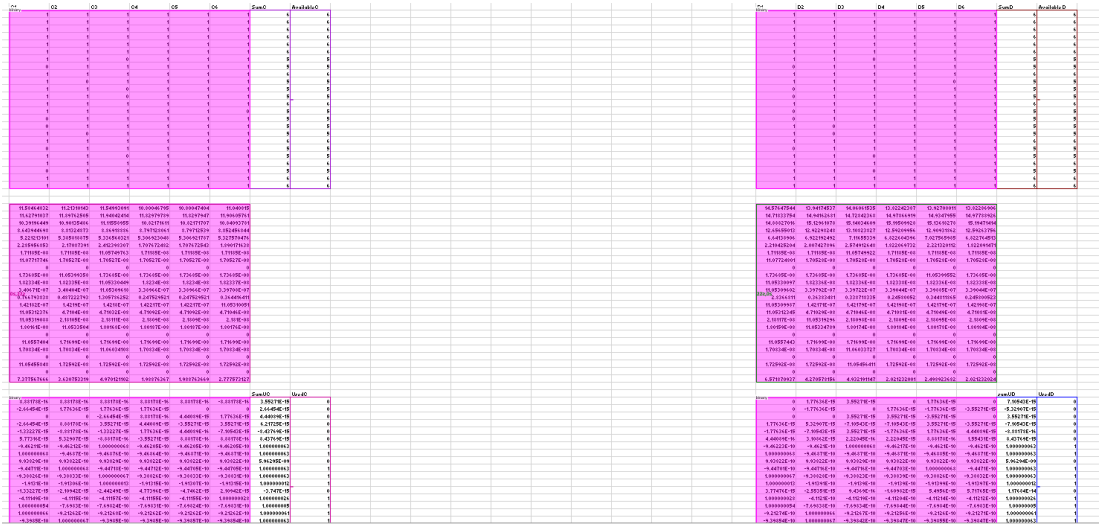

	A	B	C	D	E	F	G	H	I	J	K	L	M	N	O	P
1	step	time	θa	K	Dθ a	θ a	Δθ h1		Δθ h2	Δθ h2	Δθ h	θ h	DL	L		
419	417	1251	9.9	0.72	0.04	50.92	0.00	25.20	0.000	0.00	25.20	76.12	0.07	12.03		
420	418	1254	9.9	0.72	0.03	50.96	0.00	25.20	0.000	0.00	25.20	76.16	0.07	12.10		
421	419	1257	9.9	0.72	0.03	50.99	0.00	25.20	0.000	0.00	25.20	76.19	0.07	12.17		
422	420	1260	9.9	0.72	0.03	51.03	0.00	25.20	0.000	0.00	25.20	76.23	0.07	12.24		
423	421	1263	9.3	0.65249	-0.05	50.97	-0.89	24.31	0.000	0.00	24.31	75.29	0.06	12.30		
424	422	1266	9.3	0.65249	-0.05	50.92	-0.55	23.76	0.000	0.00	23.76	74.68	0.06	12.35		
425	423	1269	9.3	0.65249	-0.05	50.87	-0.35	23.41	0.000	0.00	23.41	74.29	0.05	12.41		
426	424	1272	9.3	0.65249	-0.05	50.82	-0.22	23.20	0.000	0.00	23.20	74.02	0.05	12.46		
427	425	1275	9.3	0.65249	-0.05	50.77	-0.14	23.06	0.000	0.00	23.06	73.84	0.05	12.51		
428	426	1278	9.3	0.65249	-0.05	50.73	-0.08	22.98	0.000	0.00	22.98	73.71	0.05	12.56		
429	427	1281	9.3	0.65249	-0.05	50.68	-0.05	22.93	0.000	0.00	22.93	73.61	0.05	12.61		
430	428	1284	9.3	0.65249	-0.05	50.63	-0.03	22.89	0.000	0.00	22.89	73.53	0.05	12.66		
431	429	1287	9.3	0.65249	-0.05	50.59	-0.02	22.87	0.000	0.00	22.87	73.46	0.05	12.70		
432	430	1290	9.3	0.65249	-0.04	50.54	-0.01	22.86	0.000	0.00	22.86	73.40	0.05	12.75		
433	431	1293	9.3	0.65249	-0.04	50.50	-0.01	22.85	0.000	0.00	22.85	73.35	0.05	12.80		
434	432	1296	9.3	0.65249	-0.04	50.46	-0.01	22.85	0.000	0.00	22.85	73.30	0.05	12.85		
435	433	1299	9.3	0.65249	-0.04	50.41	0.00	22.84	0.000	0.00	22.84	73.26	0.05	12.89		
436	434	1302	9.3	0.65249	-0.04	50.37	0.00	22.84	0.000	0.00	22.84	73.21	0.05	12.94		
437	435	1305	9.3	0.65249	-0.04	50.33	0.00	22.84	0.000	0.00	22.84	73.17	0.05	12.99		
438	436	1308	9.3	0.65249	-0.04	50.29	0.00	22.84	0.000	0.00	22.84	73.13	0.05	13.03		
439	437	1311	9.3	0.65249	-0.04	50.25	0.00	22.84	0.000	0.00	22.84	73.09	0.05	13.08		
440	438	1314	9.3	0.65249	-0.04	50.21	0.00	22.84	0.000	0.00	22.84	73.05	0.05	13.13		
441	439	1317	9.3	0.65249	-0.04	50.17	0.00	22.84	0.000	0.00	22.84	73.01	0.05	13.17		
442	440	1320	9.3	0.65249	-0.04	50.14	0.00	22.84	0.000	0.00	22.84	72.97	0.05	13.22		
443	441	1323	8.9	0.70204	0.01	50.15	0.65	23.49	0.000	0.00	23.49	73.63	0.05	13.27		
444	442	1326	8.9	0.70204	0.01	50.16	0.41	23.89	0.000	0.00	23.89	74.05	0.05	13.32		
445	443	1329	8.9	0.70204	0.01	50.17	0.25	24.15	0.000	0.00	24.15	74.32	0.05	13.37		
446	444	1332	8.9	0.70204	0.01	50.18	0.16	24.31	0.000	0.00	24.31	74.49	0.05	13.43		
447	445	1335	8.9	0.70204	0.01	50.19	0.10	24.41	0.000	0.00	24.41	74.59	0.06	13.48		
448	446	1338	8.9	0.70204	0.01	50.20	0.06	24.47	0.000	0.00	24.47	74.67	0.06	13.54		
449	447	1341	8.9	0.70204	0.01	50.21	0.04	24.51	0.000	0.00	24.51	74.72	0.06	13.59		
450	448	1344	8.9	0.70204	0.01	50.22	0.02	24.53	0.000	0.00	24.53	74.75	0.06	13.65		
451	449	1347	8.9	0.70204	0.01	50.23	0.02	24.55	0.000	0.00	24.55	74.77	0.06	13.71		
452	450	1350	8.9	0.70204	0.01	50.24	0.01	24.56	0.000	0.00	24.56	74.79	0.06	13.76		
453	451	1353	8.9	0.70204	0.01	50.25	0.01	24.56	0.000	0.00	24.56	74.81	0.06	13.82		
454	452	1356	8.9	0.70204	0.01	50.26	0.00	24.57	0.000	0.00	24.57	74.82	0.06	13.88		
455	453	1359	8.9	0.70204	0.01	50.26	0.00	24.57	0.000	0.00	24.57	74.83	0.06	13.94		
456	454	1362	8.9	0.70204	0.01	50.27	0.00	24.57	0.000	0.00	24.57	74.84	0.06	13.99		
457	455	1365	8.9	0.70204	0.01	50.28	0.00	24.57	0.000	0.00	24.57	74.85	0.06	14.05		
458	456	1368	8.9	0.70204	0.01	50.29	0.00	24.57	0.000	0.00	24.57	74.86	0.06	14.11		
459	457	1371	8.9	0.70204	0.01	50.30	0.00	24.57	0.000	0.00	24.57	74.87	0.06	14.17		
460	458	1374	8.9	0.70204	0.01	50.31	0.00	24.57	0.000	0.00	24.57	74.88	0.06	14.22		
461	459	1377	8.9	0.70204	0.01	50.31	0.00	24.57	0.000	0.00	24.57	74.89	0.06	14.28		
462	460	1380	8.9	0.70204	0.01	50.32	0.00	24.57	0.000	0.00	24.57	74.89	0.06	14.34		
463	461	1383	8.7	0.62308	-0.08	50.24	-1.04	23.53	0.000	0.00	23.53	73.78	0.05	14.39		
464	462	1386	8.7	0.62308	-0.08	50.16	-0.65	22.89	0.000	0.00	22.89	73.05	0.05	14.43		
465	463	1389	8.7	0.62308	-0.08	50.08	-0.40	22.48	0.000	0.00	22.48	72.56	0.04	14.48		
466	464	1392	8.7	0.62308	-0.08	50.00	-0.25	22.23	0.000	0.00	22.23	72.23	0.04	14.52		
467	465	1395	8.7	0.62308	-0.08	49.93	-0.16	22.07	0.000	0.00	22.07	72.00	0.04	14.56		
468	466	1398	8.7	0.62308	-0.07	49.85	-0.10	21.97	0.000	0.00	21.97	71.83	0.04	14.60		
469	467	1401	8.7	0.62308	-0.07	49.78	-0.06	21.91	0.000	0.00	21.91	71.69	0.04	14.64		
470	468	1404	8.7	0.62308	-0.07	49.71	-0.04	21.87	0.000	0.00	21.87	71.58	0.04	14.67		
471	469	1407	8.7	0.62308	-0.07	49.64	-0.02	21.85	0.000	0.00	21.85	71.49	0.04	14.71		
472	470	1410	8.7	0.62308	-0.07	49.57	-0.02	21.83	0.000	0.00	21.83	71.40	0.04	14.75		
473	471	1413	8.7	0.62308	-0.07	49.50	-0.01	21.82	0.000	0.00	21.82	71.32	0.04	14.79		
474	472	1416	8.7	0.62308	-0.07	49.43	-0.01	21.82	0.000	0.00	21.82	71.25	0.04	14.82		
475	473	1419	8.7	0.62308	-0.07	49.36	0.00	21.81	0.000	0.00	21.81	71.18	0.04	14.86		
476	474	1422	8.7	0.62308	-0.07	49.30	0.00	21.81	0.000	0.00	21.81	71.11	0.04	14.89		
477	475	1425	8.7	0.62308	-0.06	49.24	0.00	21.81	0.000	0.00	21.81	71.05	0.04	14.93		
478	476	1428	8.7	0.62308	-0.06	49.17	0.00	21.81	0.000	0.00	21.81	70.98	0.04	14.97		
479	477	1431	8.7	0.62308	-0.06	49.11	0.00	21.81	0.000	0.00	21.81	70.92	0.04	15.00		
480	478	1434	8.7	0.62308	-0.06	49.05	0.00	21.81	0.000	0.00	21.81	70.86	0.03	15.04		
481	479	1437	8.7	0.62308	-0.06	48.99	0.00	21.81	0.000	0.00	21.81	70.80	0.03	15.07		
482	480	1440	8.7	0.62308	-0.06	48.93	0.00	21.81	0.000	0.00	21.81	70.74	0.03	15.10		Obj
483																